ANALYTICA CHIMICA ACTA

International monthly devoted to all branches of analytical chemistry
Revue mensuelle internationale consacrée à tous les domaines de la chimie analytique
Internationale Monatsschrift für alle Gebiete der analytischen Chemie

ELSEVIER PUBLISHING COMPANY
AMSTERDAM

Anal. Chim. Acta, Vol. 48, No. 2, 197–452, December 1969
Published monthly
Completing Volume 48

Publication Schedule for 1969

In the interests of rapid publication it has been found necessary to schedule 5 volumes for appearance in 1969. Since monthly publication will be maintained, this implies that 2 of the volumes will each consist of three issues, while 3 of the volumes will each consist of only 2 issues. The following provisional schedule applies:

Vol. **44**, No. **1**	January 1969	
Vol. **44**, No. **2**	February 1969	**(completing Vol. 44)**
Vol. **45**, No. **1**	March 1969	
Vol. **45**, No. **2**	April 1969	
Vol. **45**, No. **3**	May 1969	**(completing Vol. 45)**
Vol. **46**, No. **1**	June 1969	
Vol. **46**, No. **2**	July 1969	**(completing Vol. 46)**
Vol. **47**, No. **1**	August 1969	
Vol. **47**, No. **2**	September 1969	
Vol. **47**, No. **3**	October 1969	**(completing Vol. 47)**
Vol. **48**, No. **1**	November 1969	
Vol. **48**, No. **2**	December 1969	**(completing Vol. 48)**

Subscription price: $ 17.50 or Dfl. 63.— per volume plus postage. Total subscription price for 1969: $ 87.50 or Dfl. 315.— plus postage. Additional cost for copies by airmail available on request. For subscribers in the U.S.A. and Canada, 2nd class postage paid at Jamaica, N.Y. For advertising rates apply to the publishers.

Subscriptions should be sent to:

ELSEVIER PUBLISHING COMPANY P.O. Box 211, Amsterdam, The Netherlands

---

GENERAL INFORMATION

Languages

Papers will be published in English, French or German.

Submission of papers

Papers should be sent to:

Prof. Philip W. West,
Coates Chemical Laboratories,
College of Chemistry and Physics,
Louisiana State University,
Baton Rouge 3,
La. 70803 (U.S.A.)

or to:

Dr. A. M. G. Macdonald,
Department of Chemistry,
The University,
P.O. Box 363
Birmingham 15 (Great Britain)

Reprints

Fifty reprints will be supplied free of charge. Additional reprints (minimum 100) can be ordered at quoted prices. They must be ordered on order forms which are sent together with the proofs.

SUMMARIES OF PAPERS PUBLISHED IN ANALYTICA CHIMICA ACTA

Vol. 48, No. 2, December 1969

A NEW, SIMPLE ATOM RESERVOIR FOR ATOMIC FLUORESCENCE SPECTROMETRY

The disadvantages of flames as atomizers are summarized, and a new, simple and efficient means of atomization of samples is proposed. The solution on a platinum loop is vaporized by electrical heating into an argon stream. Limits of detection were 10^{-14} g for cadmium, 10^{-8} g for mercury, and 10^{-7} g for gallium. Linear calibration graphs were obtained over 3 or 4 orders of magnitude. Of the various sheathing gases studied, argon was most efficient. The method is relatively insensitive to matrix effects.

M. P. BRATZEL, JR., R. M. DAGNALL AND J. D. WINEFORDNER,
Anal. Chim. Acta, 48 (1969) 197–203

ATOMIC ABSORPTION DETERMINATION OF MICROGRAM QUANTITIES OF MOLYBDENUM IN LAKE WATERS

The extraction of molybdenum by various complexing agents was studied and their atomic absorption sensitivity compared. Oxine and dithiol are among the most sensitive. Optimum conditions for extraction of molybdenum with oxine at microgram levels and the interference of certain elements in atomic absorption were investigated. Molybdenum was extracted directly from 100 ml of water by oxine in MIBK and determined by atomic absorption spectroscopy with a nitrous oxide–acetylene flame. The coefficient of variation for spiked lake water and natural lake water containing 20 μg Mo/l and 5.56 μg Mo/l were found to be 1.8% and 4.0% respectively. The sensitivity of the method was 1 p.p.b.

Y. K. CHAU AND K. LUM-SHUE-CHAN,
Anal. Chim. Acta, 48 (1969) 205–212

SEPARATION AND DETERMINATION BY NEUTRON ACTIVATION OF TRACES OF HAFNIUM IN SCANDIUM

(in French)

A method is proposed for the separation and determination of traces of hafnium ($\geqq 1$ p.p.m.) in scandium metal. The metals, as sulfate complexes, are separated by anion exchange in sulfuric acid medium. Analysis by thermal neutron activation is based on the formation of 179m-hafnium ($T_{\frac{1}{2}} = 19$ sec) and 46m-scandium ($T_{\frac{1}{2}} =$ 19.5 sec). The complete separation and determination requires only 1 h.

L. BALSENC, W. HAERDI AND D. MONNIER,
Anal. Chim. Acta, 48 (1969) 213–218

SPOT TESTS IN ORGANIC ANALYSIS

Seventh English Edition, completely revised and enlarged

by FRITZ FEIGL in collaboration with VINZENZ ANGER

6 x 9", xxiii + 772 pages, 19 tables, over 2000 lit.refs., 1966, Dfl. 85.00, £10.0.0.

This 7th edition has involved complete revision and reorganisation of the subject in order to present a still clearer picture of the multitudinous applications open to organic spot test analysis. The amount of new work which is appearing has certainly necessitated expansion, but the author has kept this to a minimum by omitting the chapter on spot test techniques (which are covered in the companion volume *Spot Tests in Inorganic Analysis*) and by limiting the number of tables and structural formulae.
Comparison with the 6th edition reveals the following differences:

	Number in 6th Edn.	 7th Edn.
Preliminary tests	32	45
Functional group tests	70	109
Individual compound tests	133	148
Detection of particular structures and types of compounds	0	74
Differentiation of isomers etc.	0	54
Applications in the testing of materials etc.	111	131

In total the book now gives in 561 sections information on more than 900 tests compared with 600 tests in 346 sections in the preceding edition.

An important feature is the inclusion of a large number of recently developed tests and comments which have not hitherto been published in any form.

It is the author's hope that this work will help to correct the widespread impression that physical instrumentation is always superior to chemical methods for solving analytical problems. Each of the chapters presents instances of problems for which no solutions by physical means have yet been developed, or for which the rapid spot tests are equal or superior to the expensive instrumental procedure.

CONTENTS: 1. Development, present state and prospects of organic spot test analysis. 2. Preliminary (exploratory) tests. 3. Detection of characteristic functional groups in organic compounds. 4. Detection of structures and certain types of organic compounds. 5. Identification of individual organic compounds. 6. Application of spot tests in the differentiation of isomers and homologous compounds. Determination of constitutions. 7. Application of spot reactions in the testing of materials, examinations of purity, characterization of pharmaceutical products, etc... Appendix: Individual compounds and products examined. Author index. Subject index.

FROM REVIEWS OF THE NEW EDITION

... As we have come to expect, Professor FEIGL has once more provided an outstanding service to the chemical community ...

Analytica Chimica Acta

... C'est pourquoi le livre du professeur FEIGL est extrêmement précieux pour le chimiste comme le montre la succession des éditions ...

Bulletin de la Société Chimique de France

... This volume, together with its companion on "Spot Tests in Inorganic Analysis" (5th ed., 1958), is a useful and authoritative source of information not only to analytical chemists but also to organic chemists, pharmaceutical chemists, and biochemists. Advanced students and research workers in analytical chemistry will find these two volumes stimulating and helpful ...

Analytical Chemistry

... As each successive edition of this book appeared, it was greeted with ever increasing praise. It is difficult, therefore, to find adequate superlatives to describe this new, completely revised edition ...
... The astonishing range of applications of the tests makes this book essential for every chemist concerned with organic compounds ...

Chemistry in Britain

Elsevier
Publishing
Company AMSTERDAM LONDON NEW YORK

147E

THE DETERMINATION OF IMPURITIES IN ZINC BY NEUTRON ACTIVATION

PART II. THE DETERMINATION OF GERMANIUM

(in French)

After separation of germanium and zinc on a Dowex 50 resin at pH 1.42, germanium is precipitated as GeS_2, and the ^{71}Ge X-ray activity is counted by scintillation. The chemical yield is determined by classical polarography. Before zone refining, the germanium concentration in zinc was found to be 0.109 ± 0.024 p.p.m.; after zone refining, the content decreased to 0.049 ± 0.014 p.p.m.

R. Machiroux and F. Mousty,
Anal. Chim. Acta, 48 (1969) 219–226

FLUORESCENCE AND METALLIC VALENCY STATES

PART III. DETERMINATION OF TIN

Tin is selectively and simply determined in aqueous solution by measuring the fluorescence produced with oxine-5-sulphonic acid at a pH of 4–5.2; intensities are linear from 5 p.p.b. to 0.25 p.p.m. The fluorescence intensity attains a maximum after 10 min and is constant for hours. Few ions interfere and less than 1 p.p.b. can be determined in alcoholic solutions. Fluorescence spectra and intensities are independent of the valence state of the metal.

B. K. Pal and D. E. Ryan,
Anal. Chim. Acta, 48 (1969) 227–231

ION EXCHANGE, EXTRACTION SEPARATION AND RADIOCHEMICAL DETERMINATION OF NEPTUNIUM-237 IN PLUTONIUM-238

Neptunium-237 in concentrations of 10 p.p.m. can be isolated from 10-mg quantities of plutonium-238, with sufficient purity to allow its determination by direct α-counting. After suitable treatment of the sample in hydrobromic acid medium, neptunium(V) is separated from the bulk of plutonium by cation exchange. The neptunium eluate is then treated with tin(II) chloride, and neptunium(IV) is extracted into TTA–xylene, leaving the last amount of plutonium in the aqueous phase. Uranium causes no problem and can be determined simultaneously in the same sample.

J. Bubernak, M. S. Lew and G. M. Matlack,
Anal. Chim. Acta, 48 (1969) 233–241

CHLOROFORM EXTRACTION AND POLYMERIZATION OF TETRAPHENYLARSONIUM CHLORIDE

Measurements of the distribution of tetraphenylarsonium chloride between aqueous sodium chloride solutions and chloroform give an ionization constant, K^0, $=0.079$ and a partition constant ($CHCl_3/H_2O$), P^0, $=3.3$ for monomeric $(C_6H_5)_4AsCl$ at 25°. Distribution measurements at higher tetraphenylarsonium chloride concentrations show that polymerization occurs in chloroform. A system consisting of monomer, dimer and tetramer best represents the extraction data, which furnish the polymerization constants $\beta_2 = 163 \pm 16$, $\beta_4 = 4.5 \cdot 10^5 \pm 0.9 \cdot 10^5$. Vapor pressure measurements of dry chloroform solutions give the values $\beta_2 = 72 \pm 14$, $\beta_4 = 4.0 \cdot 10^5 \pm 0.7 \cdot 10^5$ (25°).

J. S. Fok, Z Z. Hugus and E. B. Sandell,
Anal. Chim. Acta, 48 (1969) 243–249

ADHESION AND ADHESIVES

2nd, completely revised, edition

edited by R. Houwink and G. Salomon

Volume 1

Adhesives

7 × 10″, xvi + 548 pages, 72 tables, 150 illus., 1965, £ 8.0.0, Dfl. 67.50

The introductory chapter of this first volume is a concise guide to the scientific background of all adhesive processes. Surface science and bulk properties of solids, as related to adhesive bonding, are discussed and illustrated by recent examples from the technology of metals, glass, rubber and plastics. An annotated bibliography is provided for the reader who wants access to more highly specialized works. The further nine chapters, making up the volume, cover the basic materials used in adhesion technology. Greatest attention is paid to synthetic adhesives, especially the classical thermohardening and the new epoxy resins. Fields previously examined in the first edition have been extended, and a brief contribution added on the adhesion of glass and on glass-to-metal bonding.

CONTENTS:

1. Adhesion. 2. Animal glue and related protein adhesives. 3. Vegetable adhesives. 4. Synthetic organic adhesives. 5. Bituminous binders and coatings. 6. Rubbers. 7. Glass, enamels and ceramics. 8. Inorganic adhesives and cements. Part A: Soluble silicates. 9. Inorganic adhesives and cements. Part B: Miscellaneous inorganic materials. 10. Metallic adhesives. Appendix: Historical table. Subject index.

Volume 2

Applications

7 × 10″, xiv + 590 pages, 21 tables, 300 illus., 1967 £ 8.0.0, Dfl. 67.50

In this second volume the main trends i industrial application are outlined by sixtee specialists. Assessment of surface geome try, choice of surface treatment, and selec tion of the most economical bonding proces — the correct decision in each case is th basis for any successful engineering process The introductory chapter deals with thi general background; it links the two volume and extends the annotated bibliography t 1966. Two compact "adhesives charts' facilitate the choice of a candidate adhesiv and of processing methods. The work als contains a Subject Index to Volume 2 and a Author Index to both volumes.

CONTENTS:

Introduction. 11. Surface texture. 12. Surface treatme of adherends. 13. Adhesive bonding processes. 1 Wood, reconstituted wood and glued laminated struc tures. 15. Adhesive-bonded metal structures. 16. Bonde composite structures. 17. Pressure-sensitive adhesiv tapes. 18. Rubber-textile structures. 19. The tack printing inks. 20. Adhesion in paint technology. 2 Miscellaneous applications. 22. Testing of adhesive 23. Mechanical testing of bonded joints. Append Adhesives charts. Subject index. Author index Volumes 1 and 2.

Elsevier
Publishing
Company

Amsterdam London New York

194E

SELENAZONE: THE SELENIUM ANALOGUE OF DITHIZONE

The selenium analogue of dithizone has been synthesised by treating 3-nitro-1,5-diphenylformazan or 3-methylmercapto-1,5-diphenylformazan with ammonia and hydrogen selenide in oxygen-free ethanol. The new reagent "selenazone" exists as tautomeric forms analogous to the thiol and thione forms of dithizone and is readily oxidised to a diselenide, $C_{26}H_{22}N_8Se_2$, from which the parent selenazone is recoverable by reduction with alkaline dextrose, sulphurous acid or hypophosphorous acid. The spectra of selenazone and the diselenide in a variety of organic solvents are reported and compared with similar data for dithizone itself.

Selenazone forms a range of brilliantly coloured metallic complexes which are soluble in organic solvents. It thus permits of the solvent extraction of the ions Ag^+, Mn^{2+}, Fe^{2+}, Co^{2+}, Ni^{2+}, Cu^{2+}, Zn^{2+}, Cd^{2+}, Hg^{2+}, Pb^{2+}, Ti^+ and Bi^{3+} from aqueous solution, the percentage extraction being governed by the pH. The diselenide also forms extractable coloured complexes; it is more selective than selenazone or dithizone, for the behaviour appears to be limited to Ag^+, Hg^{2+}, Ni^{2+} and Pd^{2+}.

R. S. RAMAKRISHNA AND H. M. N. H. IRVING,
Anal. Chim. Acta, 48 (1969) 251–266

THE EXTRACTION OF SILVER(I) FROM HYDROCHLORIC ACID BY SOLUTIONS OF TRI-*n*-HEXYLAMMONIUM AND TETRA-*n*-HEXYLAMMONIUM CHLORIDE IN ORGANIC SOLVENTS

Silver(I) is very readily extracted from hydrochloric acid by solutions of tetrahexylammonium chloride (NR_4Cl) in 1,2-dichloroethane as the ion-pair $NR_4^+AgCl_2^-$. Solutions of tri-*n*-hexylammonium chloride in nitrobenzene extract silver(I) as $NR_3H^+AgCl_2^-$ but with solutions in *m*-xylene the species $(NR_3H^+)_2AgCl_3^{2-}$ (or the quadrupole $(NR_3H^+)(AgCl_2^-)(NR_3H^+)(Cl^-)$) is favoured. In each case the distribution ratio decreases with increase in chloride ion concentration. Hydrochloric acid itself is extracted more effectively by the quaternary liquid exchanger.

H. M. N. H. IRVING AND A. D. DAMODARAN,
Anal. Chim. Acta, 48 (1969) 267–272

SELECTIVITY IN FOAM SEPARATION BY CONTROL OF CHARGE ON THE EXTRACTING SOLUTE: METAL CHLORO COMPLEXES

The application of selective concentration by foam separation of trace species via control of charge on these species has been investigated. The removal of anionic chloro complexes of iron(III), mercury(II), and cobalt(II) has been examined. Distribution factors, Γ/C, as a function of hydrochloric acid concentration have been measured with the cationic surfactant, hexadecyltrimethylammonium bromide; the trends have been found to be similar to those obtained in ion-exchange measurements, with an anionic exchanger. In the case of iron(III), Γ/C has also been measured as a function of surfactant concentration, initial $FeCl_3$ concentration, and % ethanol in water. Total reflux foam separation measurements were performed for selective removal. It was found that 10^{-7} *M* $FeCl_3$ could be selectively removed in the presence of a 100-fold excess of $HgCl_2$. Further, $HgCl_2$ could be selectively concentrated at 1 *M* hydrochloric acid and 10^{-7} *M* in the presence of $CoCl_2$. A model based on a mobile ion-exchanger surface is presented to explain qualitatively the trends observed.

B. L. KARGER AND M. W. MILLER,
Anal. Chim. Acta, 48 (1969) 273–290

Photoluminescence of Solutions

With Applications to Photochemistry and Analytical Chemistry

by C. A. Parker, Royal Naval Scientific Service, Head of Chemistry Division of the Admiralty Materials Laboratory, Holton Heath, Poole, Dorset, England

6 × 9", xvi + 544 pages, 53 tables, 188 illus., 443 lit. refs., 1968, Dfl. 85.00, £11.10.0.

Contents: Basic principles, definitions and kinectics of fluorescence, phosphorescence and delayed fluorescence; polarisation; light scattering; monochromators; light sources; filters; photodetectors; actinometry; recording systems; inner filter effects; specimen compartments; correction of spectra; measurement of photoluminescence efficiency and lifetime; purity of materials; parameters of singlet and triplet states; equilibria in the excited state; excited dimers; solvent effects; fluorescence and phosphorescence analysis.

Comprehensive Analytical Chemistry

edited by C. L. Wilson, Professor of Inorganic and Analytical Chemistry, University of Belfast (Northern Ireland)
and D. W. Wilson, Head of the Chemistry Department, Sir John Cass College, London (England)

VOLUME IIB: Physical Separation Methods

6 × 9", xvi + 445 pages, 30 tables, 116 illus., 897 lit.refs., 1968, Dfl. 70.00, £8.10.0.

Volume Two, Part B is devoted to physical separation methods. After an account of the theory and practise of liquid chromatography in columns, the volume continues with a lengthy treatment of gas chromatography.
The next chapter, on ion exchangers, is notable for the account it gives of analytical applications, while distillation (theory and technique) is the last topic to be treated in the present volume.

Contents: I. *Liquid Chromatography in Columns*. 1. Introduction. 2. Theory. 3. Apparatus and operation. II. *Gas Chromatography*. 1. Introduction and general principles. 2. Theoretical aspects. 3. Apparatus. 4. The partitioning phases. 5. Absorbents and gas-solid chromatography. 6. Gas-liquid chromatography. 7. Analytical methods. 8. Applications. III. *Ion Exchangers*. 1. Foreword. 2. Introduction. 3. The constitution of ion exchangers. 4. The mechanism of ion exchange. 5. Technique. 6. Analytical applications. Appendix 1: Ion-exchanger data. Appendix 2: Methods of testing ion exchangers. Appendix 3: Bibliography. IV. *Distillation*. 1. Introduction. 2. Theoretical background. 3. Experimental techniques.

Atomic-Absorption Spectroscopy

and Analysis by Atomic-Absorption Flame Photometry

by J. Ramírez-Muñoz, Principal Applications Chemist at Beckman Instruments Inc. and Scientific Research Collaborator of the C.S.I.C., Spain

6 × 9", xii + 493 pages, 23 tables, 156 illus., 950 lit. refs., 1968, Dfl. 80.00, £9.15.0.

Contents: *Part I: Fundamentals*. 1. Origins of the method and nomenclature. 2. General principles and characteristics. 3. Absorption and emission. 4. The literature of atomic-absorption spectroscopy. 5. Theory. *Part II: Instrumental Systems*. 6. Instrumental systems. 7. Emission systems. 8. Absorption system. 9. Selection system. 10. Photometric system. 11. Instruments. *Part III: Range and Limitations of Atomic Absorption Methods*. 12. Determinable elements. Choice of lines. 13. Sensitivity. 14. Limitations in atomic absorption. *Part IV: Experimental Methods*. 15. Experimental process. 16. Standard solutions. 17. Preparation of the sample. 18. Experimental measurements and calibration. *Part V: Applications*. 19. Applications. Appendix. Bibliography.

Elsevier
Publishing
Company Amsterdam London New York

THE SOLUTION CHEMISTRY OF ETHYLMETHYLGLYOXIME

PART II. THE NICKEL COMPLEX

The following properties of the two modifications of nickel ethylmethylglyoxime have been examined: X-ray powder diffraction patterns, u.v.–vis.–i.r. solid state spectra, solubility products and intrinsic solubilities. In addition, the complex formation and chloroform distribution constants have been measured as well as the u.v.–vis. chloroform solution spectra. Differentiating properties are summarized and compared with those of nickel dimethylglyoxime. The influence of the crystal structures on the intrinsic solubilities is discussed and the distribution constants and solubilities of other nickel dialkylglyoximes are predicted.

B. Egneus,

Anal. Chim. Acta, 48 (1969) 291–307

THE RELATIVE ACIDITIES OF PHENOLS AND BENZOIC ACIDS IN DIMETHYLSULFOXIDE

An attempt is made to correlate the relative acidities of phenols and benzoic acids in dimethylsulfoxide and water. Mathematical expressions relating the acidity of the acids in the two solvents are presented and the data show that phenols display a greater increase in their relative acidity in dimethylsulfoxide than do benzoic acids. Differentiating titrations are presented and such titrations are feasible where the acids differ by 140 mV in their half-neutralization potentials. Comparative data are presented for the pyridine solvent system.

R. Morales,
Anal. Chim. Acta, 48 (1969) 309–314

LOW-TEMPERATURE PRECIPITATION TITRATION OF PERCHLORATE AND TETRAFLUOROBORATE WITH TETRAPHENYLARSONIUM CHLORIDE AND ION-SELECTIVE ELECTRODES

Perchlorate and tetrafluoroborate have been determined at low concentrations by precipitation titration with tetraphenylarsonium chloride, the appropriate anion-selective electrodes being used to follow the course of the titration potentiometrically. A low temperature, 2°, was employed to sharpen the titration curves, thus resulting in greater accuracy and lower limits of analysis. As little as 0.05 mmol of perchlorate and 0.25 mmol of tetrafluoroborate have been determined to within 1% relative accuracy. These limits could easily be extended by a factor of 10 by using a miniaturized titration apparatus.

M. J. Smith and S. E. Manahan,
Anal. Chim. Acta, 48 (1968) 315–319

AN INDIRECT POTENTIOMETRIC DETERMINATION OF CHLORIDE IN CLEANING SOLUTIONS FOR POWER PLANT BOILERS

The potentiometric determination of chloride in cleaning solutions for power plant boilers is described. The procedure is based on a potentiometric sensing of excess added silver reagent. Curves prepared from data taken on an expanded scale pH meter can subsequently be used as reference curves for data taken on less precise pH meters.

J. G. Frost,
Anal. Chim. Acta, 48 (1969) 321–328

A New Important Encyclopaedic Work of Reference

COMPREHENSIVE CHEMICAL KINETICS

edited by C.H. BAMFORD F.R.S.,
and C.F.H. TIPPER

The aim of this series is to cover in a critical way the practice and theory of kinetics and the kinetics of inorganic and organic reactions in the gas and condensed phases or at interfaces.
Each chapter is written by an expert in the field so that the series as a whole will serve as a direct source of reference and information over the whole range of kinetics.
The vast amount of material scattered through the literature has never before been gathered together and presented in this accessible form.

Subscribers who place a standing order for the whole series before December 15, 1969 will be entitled to an overall 15% discount.

Elsevier
Publishing
Company

P.O. BOX 211,
AMSTERDAM, THE NETHERLANDS
402E

Volume 1. The Practice of Kinetics

1. Experimental methods for the study of slow reactions (L. Batt)
2. Experimental methods for the study of fast reactions (D.N. Hague)
3. Experimental methods for the study of heterogeneous reactions (D. Shooter)
4. The detection and estimation of intermediates (R.P. Wayne)
5. The treatment of experimental data (D. Margerison)

7 x 10″, xiii + 450 pages, 32 tables, 161 illus., 1174 lit. refs., 1969, Dfl. 95.00, £10.15.0
SBN 444-40673-5

Volume 2. The Theory of Kinetics

1. Kinetic characterization of complex reaction systems (Z.G. Szabó)
2. Chain reactions (V.N. Kondratiev)
3. Theory of the kinetics of elementary gas phase reactions (R.P. Wayne)
4. Theory of elementary reactions in solution (I.D. Clark and R.P. Wayne)
5. Theory of solid phase kinetics (L.G. Harrison)

7 x 10″, xiii + 462 pages + index, 16 tables, 77 illus., 794 lit. refs., 1969
SBN 444-40674-3

Volume 3. Formation and Decay of Excited Species

1. Effect of low energy radiation (C.S. Burton and W.A. Noyes, Jr.)
2. Effect of high energy radiation (G. Hughes)
3. The chemical production of excited states (T. Carrington and D. Garvin)
4. The transfer of energy between chemical species (A.B. Callear and J.D. Lambert)

7 x 10″, 1969, in preparation
SBN 444-40676-x

The series as a whole will comprise about 25 volumes divided into a number of sections:

Section 1. The practice and theory of kinetics (3 volumes)
Section 2. Decomposition and isomerisation reactions (2 volumes)
Section 3. Inorganic reactions (2 volumes)
Section 4. Organic reactions (6 volumes)
Section 5. Polymerization reactions (2 volumes)
Section 6. Oxidation and combustion reactions (2 volumes)
Section 7. Selected elementary reactions (2 volumes)

Other sections are planned on heterogeneous reactions, solid state reactions, and kinetics and technological processes.

INVESTIGATION OF SOME CONTINUOUS VOLTAMMETRIC SENSORS FOR THE DETERMINATION OF CALCIUM IN THE PRESENCE OF MAGNESIUM

Several types of voltammetric sensor have been studied for the continuous sensing of complexones in a flowing stream. The determination of calcium and magnesium has been based on the automation of two manual polarographic procedures. In the first the sum of calcium and magnesium is determined from the decrease in the height of the anodic wave of EDTA. The calcium concentration is then determined in a similar manner with ethyleneglycol-bis(β-aminoethyl ether)-N,N,N′,N′-tetraacetic acid (EGTA).

M. D. Booth, B. Fleet, Soe Win and T. S. West,
Anal. Chim. Acta, 48 (1969) 329–337

SPECTROPOLARIMETRIC TITRIMETRY

Because of the recent development of high-precision photoelectric spectropolarimeters, it is possible to purchase or construct instruments which will permit the rapid determination of optical rotation at various wavelengths. The method of spectropolarimetric titrimetry previously described for strong acids and bases is extended to include optically inactive weak acids and bases as well as optically active weak acids and bases. In the former cases an asymmetric substance which acts as an indicator is added to the material being titrated, whereas in the latter cases, the optically active acids or bases serve as self-indicators. Extensions of this spectropolarimetric titrimetric technique to the determination of metal ions, both optically active and optically inactive ligands, and the ratio of ligands to metal in a complex ion in solution are described.

K. H. Pearson and S. Kirschner,
Anal. Chim. Acta, 48 (1969) 339–348

SPECTROPHOTOMETRIC DETERMINATION OF TRACE AMOUNTS OF TITANIUM(IV), ZIRCONIUM(IV) AND THORIUM(IV) WITH MOLYBDOPHOSPHORIC ACID SOLUTION

Trace amounts of titanium(IV), zirconium(IV) and thorium(IV) ions were determined spectrophotometrically with molybdophosphoric acid solution. The method is based on the formation of the ternary heteropoly complex by reaction of the metal ion with molybdophosphoric acid, and the elimination of unreacted molybdophosphoric acid by extraction with *n*-butyl acetate. Beer's law was obeyed over the range 1–7 p.p.m. of metal ion. These ternary heteropoly complexes have the composition of Me:P:Mo = 1:1:12. The formation constants increase in the order, molybdotitanophosphate, molybdothorophosphate, and molybdozirconophosphate.

Katsuo Murata, Yu Yokoyama and Shigero Ikeda,
Anal. Chim. Acta, 48 (1969) 349–356

EXTRACTION AND SPECTROPHOTOMETRIC DETERMINATION OF TIN, ARSENIC AND GERMANIUM AS THEIR IODIDES

Tin(IV), arsenic(III) and germanium(IV) can be extracted quantitatively into cyclohexane from solutions containing sulfuric acid and sodium iodide. The extracted iodides have characteristic absorbance spectra in the ultraviolet region. When the measurements are made at 364 nm for tin, at 282 nm for arsenic and at 360 nm for germanium, the respective absorption maxima, the calibration graphs are linear and the molar absorptivities are 8700, 9700 and 6600, respectively. Arsenic(III) can be extracted mainly as its iodide from hydrochloric acid solutions containing sodium iodide, the molar absorptivity at 282 nm being also 9700. Recommended procedures are given for the determination of tin in juice, tin and arsenic in steels (simultaneously), and germanium in its concentrates.

K. Tanaka and N. Takagi,
Anal. Chim. Acta, 48 (1969) 357–366

THE MEASUREMENT OF SMALL DEVIATIONS FROM STOICHIOMETRY OF URANIUM DIOXIDE

(in French)

The measurement of deviations from stoichiometry x of uranium dioxide UO_{2+x} has been investigated in the particular case of x less than 0.01. The powdered sample is dissolved in concentrated phosphoric acid. Uranium(VI) is measured by coulometric reduction at controlled potential; uranium(IV) is oxidised by a standard solution of potassium dichromate. It is shown that the uncertainty in x is essentially due to the lack of reproducibility of the initial dissolution. With the described operating method, values of x equal to 0.0005 have been determined with a relative reproducibility of 20%.

J. C. Viguie and J. P. Chabert,
Anal. Chim. Acta, 48 (1969) 367–380

AUTOMATIC METHOD FOR THE RAPID MICRODETERMINATION OF CARBON AND HYDROGEN

(in German)

A fully automatic method for the rapid microdeterminaiton of carbon and hydrogen is described. The sample is covered with manganese dioxide and burnt in a stream of oxygen in a vertical silica tube; the products of combustion are led over copper oxide to ensure complete oxidation. The apparatus is flushed with nitrogen; water is frozen out, and carbon dioxide is absorbed in a titration cell containing an amine in dimethylformamide. The carbon dioxide is titrated automatically with standard tributylmethylammonium hydroxide, with colorimetric end-point determination, the volume of titrant being displayed digitally and printed out. Water is vapourized in a stream of nitrogen and passed over carbon at 1120° to form carbon monoxide, which is then oxidized with copper oxide to carbon dioxide; this is absorbed and titrated as just described. The whole cycle is controlled automatically by time switches. By using duplicate freezing traps and titration cells, water from a previous combustion can be determined at the same time as carbon dioxide. The analysis time for both carbon and hydrogen is then 8 min.

W. Merz,
Anal. Chim. Acta, 48 (1969) 381–390

COORDINATION CHEMISTRY REVIEWS

Editor: A.B.P. LEVER (Downsview, Ont., Canada)

This international journal offers rapid publication of relatively short review articles in the field of coordination chemistry. The term "coordination chemistry" is interpreted broadly, but does not include "organometallic chemistry". In general the reviews published fall into the following categories:

- surveys of developments in a particular area during the last few years
- surveys and/or discussions of the results obtained with a particular technique during the last few years
- general or philosophical discussions of some specific aspects of coordination chemistry

Articles dealing with the application of physical techniques are also included, as well as those on the theory or practice of the coordination chemistry of transition or non-transition metals. The main language of the journal is English, although reviews in French or German are also published.

CONTENTS Volume 4, No. 1, February 1969

Divalent transition metal β-keto-enolate complexes as Lewis acids - D.P. Graddon (Kensington, N.S.W., Australia)
Metal-halogen stretching vibrations in coordination complexes of gallium, indium and thallium - A.J. Carty (Waterloo, Ont., Canada)
Reactions involving metal complexes of sulphur ligands - L.F. Lindoy (Kensington, N.S.W., Australia)
Electronic spectra of quadrate chromium(III) complexes - J.R. Perumareddi (Pittsburgh, Pa., U.S.A.)
The effect of axial ligand fields on ground state properties of complexes with orbitally degenerate ground terms - G.A. Webb (Guildford, England)

CONTENTS Volume 4, No. 2, April 1969

Carbonato complexes of cobalt(III) - C.R. Piriz Mac-Coll (Montevideo, Uruguay)
Some aspects of the chemistry of manganese(III) in aqueous solution - G. Davies (Waltham, Mass., U.S.A.)
Carbon-bonded beta-diketone complexes - D. Gibson (Manchester, Great Britain)

Publication is in one volume of four issues per year. Subscription price for 1969 is Dfl. 70.00 plus Dfl. 3.50 postage or equivalent (US$19.50 plus US$1.00). A free specimen copy will be sent on request.
Vol. 1 (1966), Vol. 2 (1967); Vol. 3 (1968); Vol. 4 (1969).

Please send your order to your usual supplier or to the publisher.

Elsevier

P.O. Box 211
Amsterdam - The Netherlands

ULTRAVIOLET EMISSION AND ABSORPTION SPECTRA PRODUCED BY ORGANIC COMPOUNDS IN OXYHYDROGEN FLAMES

PART I. EMISSION SPECTRA

Ultraviolet emission spectra produced by aspirating organic compounds into oxyhydrogen flames have been investigated. Spectra are presented and compared. The prominent bands observed are listed by wavelength and species emitting. Flame emission profiles for organic and inorganic fragments are presented. Maximum emission by organic fragments occurred in the reaction zone of the flame. Emission by OH and fragments containing phosphorus or sulfur was intense above and within the reaction zone of the flame. Spectra obtained by varying the hydrogen-to-oxygen ratio in the flame and by aspirating with hydrogen instead of oxygen reflected the different sizes of the resulting flames. The bands observed were similar. Estimates of detection limits obtained for pyridine and ethanol by measuring the intensities of emission from NH and CH fragments were $\geq 2\%$ pyridine in ethanol and $\geq 5\%$ ethanol in water.

V. J. Smith and J. W. Robinson,
Anal. Chim. Acta, 48 (1969) 391–403

AN ANALYSIS OF THE THERMAL DECOMPOSITION OF TETRAETHOXYSILANE BY GAS CHROMATOGRAPHY

The principle products of the thermal decomposition of tetraethoxysilane in a flowing system are acetaldehyde, ethanol, ethylene, and ethane. Acetal is found as a secondary reaction product formed by the addition of collected ethanol to acetaldehyde. Although the same products are produced by the thermal decomposition of diethyl ether at the same temperature, no ether has been found in the reaction products of the silane compound. The products are probably derived directly from the silane molecule.

G. W. Heunisch,
Anal. Chim. Acta, 48 (1969) 405–409

MODIFIED WINKLER DETERMINATION OF OXYGEN IN DIMETHYLFORMAMIDE: OXYGEN SOLUBILITY AS A FUNCTION OF PARTIAL PRESSURE

Dissolved oxygen concentrations in dimethylformamide were determined by a modified Winkler method with small sample sizes and no special control of ambient temperature and pressure. The concentrations measured covered a range 0.008–2.59 mM with a relative deviation of less than 1%. Both the oxygen concentrations determined by this method and polarographic diffusion currents were linear functions of the mole fraction of oxygen; therefore a polarographic reduction of oxygen can be used for rapid determination of oxygen in this solvent.

H. J. James and R. F. Broman,
Anal. Chim. Acta, 48 (1969) 411–417

A RAPID METHOD FOR THE ANALYSIS OF TOTAL AND ORGANIC CARBON IN SHALE WITH A HIGH-FREQUENCY COMBUSTION FURNACE

(Short Communication)

J. W. Wimberley,
Anal. Chim. Acta, 48 (1969) 419–422

Inorganic Macromolecules Reviews

The Chemistry, Physics and Technology of Macromolecular Inorganic Compounds and Materials

Editors: F.G.R. Gimblett (London, Great Britain)
K.A. Hodd (London, Great Britain)

The principal aim of the journal is to contribute actively to the study and exploitation of inorganic macromolecules by providing a review periodical which covers all aspects of their science and technology.

Inorganic macromolecules will be interpreted broadly to embrace both natural and synthetic systems. The Reviews thus will help bridge the gap existing between organic polymer science, glasses and ceramics and should be of interest to chemists, physicists, polymer scientists, materials scientists and materials engineers working in this field. Reviews will be published in English, French or German, though preferably in English.

The first two issues will contain the proceedings of the International Symposium on Inorganic Polymers held April 9, 10 and 11, 1969 at the Northern Polytechnic, London.

Some forthcoming papers:

Polymer chemistry of boron cluster compounds
H.A. Schroeder (Connecticut, U.S.A.)

Nitrogen-sulphur compounds
M. Becke-Goehring (Heidelberg, Germany)

Polyelementorganosiloxane formation
K.A. Andrianov (Moscow, U.S.S.R.)

Viscoelasticity in inorganic polymers
A. Eisenberg (Montreal, Canada)

Inorganic Polymers
L. Holliday (London, Great Britain)

Approximately one volume of four issues will be published per year. Subscription price is Dfl. 90.00 plus Dfl. 3.00 postage or equivalent (US$25.00 plus US$0.85 or £10.9.6. plus 7s. at April 1, 1969). The first issue is scheduled for publication in mid-1969.

Further information, specimen copies and hints to authors will be sent by the publisher on request. Subscription orders may be placed with your usual supplier or with the publisher

Elsevier

P.O. Box 211
Amsterdam - The Netherlands

THE DETERMINATION OF FREE ALCOHOLS IN ALCOHOL ETHOXYLATES BY PROGRAMMED-TEMPERATURE GAS CHROMATOGRAPHY

(Short Communication)

J. W. Wimberley,
Anal. Chim. Acta, 48 (1969) 423–425

THE SPECTROPHOTOMETRIC DETERMINATION OF CERIUM WITH METHYLENE BLUE

(Short Communication)

F. Vernon,
Anal. Chim. Acta, 48 (1969) 425–427

RAPID POLAROGRAPHY OF URANIUM IN 1 *M* HYDROFLUORIC ACID WITH A VERTICAL-ORIFICE POLYTETRAFLUOROETHYLENE DROPPING-MERCURY ELECTRODE

(Short Communication)

H. P. Raaen,
Anal. Chim. Acta, 48 (1969) 427–430

THE SPECTROPHOTOMETRIC DETERMINATION OF COPPER IN SEA WATER WITH QUINOLINE-2-ALDEHYDE-2-QUINOLYLHYDRAZONE

(Short Communications)

J. Abraham, M. Winpe and D. E. Ryan,
Anal. Chim. Acta, 48 (1969) 431–432

A NEW REFERENCE ELECTRODE FOR ELECTROCHEMISTRY IN PYRIDINE

(Short Communication)

J. Broadhead and P. J. Elving,
Anal. Chim. Acta, 48 (1969) 433–434

ERRORS IN THE USE OF VOLUMETRIC FLASKS FOR EXTRACTION IN ATOMIC ABSORPTION SPECTROSCOPY

(Short Communication)

Y. K. Chau and K. Lum-Shue-Chan,
Anal. Chim. Acta, 48 (1969) 434–437

SOLVENTS FOR LOW-TEMPERATURE PHOSPHORIMETRY OF NYLON

(Short Communication)

L. D. Johnson,
Anal. Chim. Acta, 48 (1969) 437–438

SELECTIVITY IN THE SYNERGETIC EXTRACTION OF COBALT(II) AND NICKEL(II) WITH A MIXTURE OF 2-THENOYLTRIFLUOROACETONE AND PYRIDINE BASES

(Short Communication)

H. Akaiwa and H. Kawamoto,
Anal. Chim. Acta, 48 (1969) 438–441

Announcing a NEW Journal

thermo-chimica acta

Editor-in-Chief:
W. W. Wendlandt (Houston, Texas, U.S.A.)

THERMOCHIMICA ACTA is concerned with the broader aspects of thermochemistry and its applications to chemical problems. It will publish original research contributions in the field of thermochemistry and chemical thermodynamics.

Specific areas involved are static calorimetry of all types, dynamic calorimetry of all types, including differential scanning calorimetry, specific heat calorimetry and other types of calorimetric measurements, high temperature chemical thermodynamic studies, the thermochemistry of high temperature reactions and thermoanalytical studies of all kinds.

The main field of science to be covered will be the chemical research areas of inorganic, organic, physical and analytical chemistry. However thermochemical studies in other areas such as biochemistry, geochemistry, metallurgy, soil science, geology and ceramic science may also be included.

THERMOCHIMICA ACTA will be published in yearly volumes of six bimonthly issues. The subscription price per volume will be approximately Dfl. 81.00 plus Dfl. 5.40 postage or, equivalent (US$22.50 plus US$1.50 or £9.8.0 plus 13s. as of August 15, 1969). The first issue is scheduled for publication in early 1970.

A notice to Authors and a free specimen copy are available from the publisher at the address below. Subscription orders may be placed with your usual supplier or direct with Elsevier Publishing Company, P.O. Box 211, Amsterdam, The Netherlands.

Elsevier

P.O. Box 211
AMSTERDAM - The Netherlands

436 E

Analytica Chimica Acta
Elsevier Publishing Company, Amsterdam
Printed in The Netherlands

A NEW, SIMPLE ATOM RESERVOIR FOR ATOMIC FLUORESCENCE SPECTROMETRY

M. P. BRATZEL, JR., R. M. DAGNALL* AND J. D. WINEFORDNER
Department of Chemistry, University of Florida, Gainesville, Fla. 32601 (U.S.A)
(Received July 4th, 1969)

Premixed and turbulent flames produced by means of direct nebulizer-burners (total consumption) and indirect nebulizer-burners (chamber type) are efficient atomizers of most of the volatile elements that are present as relatively volatile compounds at low concentrations in solution. Most previous analytical studies in atomic fluorescence spectrometry have employed such flames as atomizers[1-3]. Nebulizer-burners provide simple, rapid, precise, and accurate means of introducing analyte solution into the flame atomizer.

However, the flame as an atomizer possesses several serious disadvantages, which are summarized below.

(i) Because a flame is a dynamic system, solutions at high concentrations of the analyte or at high concentrations of the other components in the sample matrix may undergo incomplete solute vaporization (aspiration efficiency, ε, less than unity) because of the short transit time of any solute particle within the flame gases[4]. Recent work on flames has been directed toward improved nebulization to produce a finer aerosol; *e.g.*, use of heated chambers, ultrasonic nebulizers, etc.

(ii) All analytical flames possess sufficient concentrations of flame gas radicals, such as O, OH, etc., to combine with an appreciable fraction of many elements producing stable monoxides, monohydroxides, etc. This results in a degree of atomization (the free atom fraction, β) being less than unity[5]. Recent work has been directed toward the use of high-temperature, fuel-rich flames to minimize this problem.

(iii) Flames also contain appreciable concentrations of molecular quenchers, *e.g.*, N_2, CO_2, CO, etc., which efficiently quench a large fraction of the radiationally excited atoms[6-8]. The decrease in fluorescence quantum efficiency results in a decreased fluorescence signal and signal-to-noise ratio.

(iv) Flames in certain wavelength regions have considerable background with its concomitant background flicker noise which limits the signal-to-noise ratio in nearly all cases. The more analytically useful flames, *e.g.*, acetylene/nitrous oxide and acetylene/oxygen, have considerable background in the analytically useful wavelength range (2000–8000 Å). At wavelengths below 2000 Å, considerable reduction in intensity results owing to absorption or radiation by flame gas products. By making fluorescence measurements in the non-luminous portion of the flame, background noise can be reduced[9].

(v) Flames produce appreciable thermal excitation of elements having reso-

---

[*] On leave from Imperial College, London S. W. 7 (England).

nance lines at wavelengths greater than about 3000 Å. By means of synchronous methods, such emission signals can be minimized[10].

(vi) At high concentrations of analyte and/or other components and at high solution transport rates (particularly into direct nebulizer-burners), scattering of exciting radiation by solute particles can be considerable[11].

The above disadvantages can be minimized by using certain non-flame type atom reservoirs. MASSMANN[12] used an electrically heated graphite cell for atomic absorption and atomic fluorescence measurements. His samples were syringed into a graphite cup with slits in opposite sides. A current of about 400 A or less was passed through the cup, producing a temperature of about 2900°K or less. The resulting atomic vapor was excited by means of high-intensity, hollow-cathode lamps. To minimize the signal caused by a large blackbody continuum from the heated graphite cell, a modulated source with frequency selection rectification was used. His limits of detection were: $4 \cdot 10^{-14}$ g for zinc; $2.5 \cdot 10^{-13}$ g for cadmium; $2.5 \cdot 10^{-12}$ g for silver; $2 \cdot 10^{-10}$ g for antimony; $3 \cdot 10^{-9}$ g for iron; $2 \cdot 10^{-9}$ g for thallium; $3.5 \cdot 10^{-11}$ g for lead; $3.5 \cdot 10^{-12}$ g for magnesium; and $4.5 \cdot 10^{-10}$ g for copper. The relative standard deviation of measuring the above metals in 30 μl or smaller samples was between 4 and 12%. The accuracy of analysis was similar to the precision when the signal was integrated.

WEST AND WILLIAMS[13] devised a highly efficient carbon filament reservoir for use in atomic absorption and atomic fluorescence spectroscopy. Small volumes (5 μl or less) of analyte solution were placed on the filament (1–2 mm diameter) and atomized by means of passing a 100-A current through the filament (in an argon atmosphere). Analyses were complete in 5 sec. The limits of detection for silver and magnesium were 10^{-15} g and $3 \cdot 10^{-11}$ g, respectively. However, the precision of measurement was only 30%.

The above graphite cell furnaces are based upon the L'vov[14] modification of the King furnace. Other means (used only in atomic absorption spectrometry) of non-flame atomization of samples include: cathodic sputtering of metals used as cathodes in hollow-cathode discharge tubes[15]; laser shot vaporization of small surface areas[16]; and flash lamp vaporizations of thin films of materials within a silica chamber[17]. Most non-flame cells used so far in atomic absorption and atomic fluorescence studies have been rather complex, inaccurate, and non-reproducible. In addition, sampling difficulties have been a major draw-back in most previous systems.

In this paper, a new, simple, and efficient means is described for the atomization of samples containing volatile elements (non-volatile elements have not yet been studied). In this device, the analyte solution is placed on a platinum loop which is electrically heated to vaporize the analyte into an argon stream. This system is sufficiently compact to fit into the burner mount of any flame spectrometer. The device is shown to be an efficient atomizer for cadmium, gallium and mercury in a variety of matrices.

EXPERIMENTAL

Apparatus

The experimental setup was identical to that previously described[9] except for the atomizer, position of focus of the source image, and the d.c. electrometer. The nebulizer-burner was replaced by a platinum loop (optimum size: 30 gauge wire—1/32 in i.d.) held in place by two clips connected to a step-down a.c. transformer with a variac input. Solutions were placed on the platinum loop by simply dipping the loop into the solution (average percent standard deviation of about 8%) or placing a small sample (about 1 μl) on the loop with a hypodermic syringe (percent standard deviation of about 5%). The platinum loop was then heated to an orange glow by passing current through the wire. This resulted in vaporization of the analyte into a sheath gas stream flowing past the loop. The resulting vapor was excited with appropriate electrodeless discharge tube line sources[18].

A schematic diagram of the platinum loop, sheath gas inlet, and optical system is given in Fig. 1. The source of excitation was imaged at the intersection of the optical axes rather than slightly beyond as in a flame cell[1,2]. The loop was positioned at the lower end of the source image.

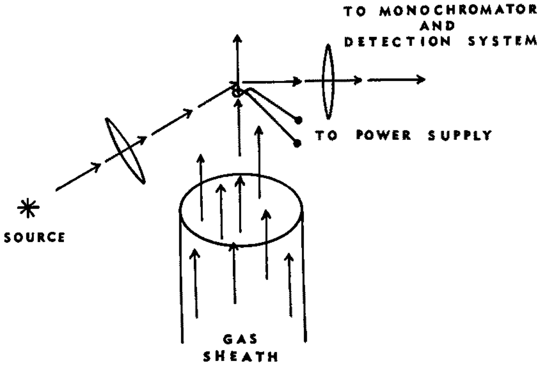

Fig. 1. Schematic diagram of platinum loop atomizer and instrumental system for atomic fluorescence studies.

The current measurement system was a d.c. electrometer[19] with a 1 mA (0.3-sec full-scale response) recording galvanometer (Rectimeter Rectilinear Milliameter, Texas Instruments, Inc., Houston, Texas 77006).

Loops (platinum wire 30 gauge) with a diameter larger than 1/32 in resulted in exploding films upon heating, with a scattering spike and a reduced fluorescence signal. Loops with a diameter smaller than 1/32 in resulted in reduced sensitivity, and the loops were more difficult to fabricate. The optimum horizontal position of the loop was at the intersection of the monochromator and source–lens optical axes, and the optimum vertical position was at a height of about 1.5 cm below the center of the entrance slit of the monochromator. By positioning the loop at an approximately 45° angle between the monochromator and source–lens optical axes, reflection of incident radiation into the monochromator was negligible.

Other sampling devices than the platinum loop were also used but with considerably less success. A platinum boat—fabricated by flattening and indenting a piece of 30-gauge platinum wire—was used but much poorer limits of detection resulted with the boat than with the loop. Various shapes of platinum spirals and helices were also studied but sampling was difficult and non-reproducible. In addition, the sample was present on the spiral or helix as a droplet rather than as a film. Moreover, higher detection limits for cadmium were obtained than with the simple platinum loop system.

The sheathing gas flowed through a 10-mm i.d. tube placed directly under the loop. The sheath tube was placed about 2.5 cm below the loop, and a gas flow of about 3 l min^{-1} was employed. At low inert gas flow rates (argon sheath), the signal was small, but as the gas flow rate increased up to 3 l min^{-1}, the peak fluorescence signal reached a plateau. At very high gas flow rates, the signal became erratic owing to cooling of the loop by the gas.

Procedure

The analyte solution was applied to the loop as described above. By passing a low current through the platinum loop (no visible glow), solvent (water in all our cases) was completely vaporized in several seconds without vaporization of the sample salt. By passing a higher current through the loop (dull red glow), the analyte vaporized from the loop and atomized into the argon stream flowing past the loop. The atomization of analyte required about 2 sec for cadmium chloride, gallium chloride, and mercury(II) chloride. Under the same power, gallium began atomizing almost instantaneously, whereas cadmium and mercury required about 1.0 and 0.5 sec respectively to begin atomizing. All fluorescence signals were recorded as a function of time and only peak signals were measured although peak areas probably are less sensitive to experimental conditions.

RESULTS AND DISCUSSION

Limits of detection

The absolute limits of detection for cadmium, mercury, and gallium (sample size of 1 μl) were 10^{-14} g, 10^{-8} g, and 10^{-7} g, respectively. More intense light sources should lower the limits of detection almost inversely with the increase in intensity since light scatter noise was negligible[20]. The limits of detection were essentially independent of sample size over the range 0.1–3.0 μl. The limits of detection (assuming a 1.0-ml sample in flame spectrometry) for cadmium and mercury in optimized flames[1,2] were about the same as with the platinum loop, but for gallium the optimum flame resulted in a 10-fold lower limit of detection. This was certainly a result of the sluggish reponse of the electronic system used for measuring transient signals. With an electronic system capable of responding to the transient signals, the results for cadmium, mercury and especially gallium should be improved considerably. Such a system is currently being investigated.

Analytical curves

Analytical curves were linear (for peak heights) from the limit of detection to about 10^{-9} g for cadmium and 10^{-5} g for mercury. Greater linearity of analytical curves should result with peak areas, since higher concentrations of analyte resulted in irregular spikes on the time-dependent fluorescence signal. Also large sample volumes (greater than about 3 μl) regardless of concentration resulted in irregular spikes.

Interference for cadmium

The influence of several anionic species—carbonate, silicate, sulfate, and phosphate at a 1000-fold excess compared to the analyte (0.1 μg/ml Cd)—on the peak transient response was studied. Carbonate and silicate produced no significant change in peak height whereas sulfate and phosphate produced enhancements. The enhanced signals (peak heights) were probably due to a reduced rate of vaporization in the presence of the interference, producing a more sluggish signal capable of being tracked by the measurement system used.

Sheathing gas

Several sheathing gases were studied: Ar, N_2, CO_2, N_2O, O_2, air (passing through the sheath), and static air (atmosphere). Hydrogen could not be studied because of the catalytic effect of platinum resulting in spontaneous ignition even at room temperature. Helium could not be studied because of its great cooling effect upon the platinum loop. The influence of sheath gas upon the fluorescence signal (peak height) of cadmium (2288 Å), mercury (2537 Å), and gallium (4033 Å) is given in Table I. The results are proportional to $\varepsilon\beta Y$, where ε is the degree of solute vaporization, β is the degree of atomization (free atom fraction) and Y is the quantum yield.

TABLE I

INFLUENCE OF SHEATH GAS UPON THE PEAK FLUORESCENCE SIGNALS FOR Cd 2288 Å, Hg 2537 Å, AND Ga 4033 Å AND 4172 Å LINES

Element	*Sheath gas*	*Peak signal relative to Ar*[d]
Cd	Ar[a]	1.00
	N_2[a]	0.68
	CO_2[a]	0.24
	Air[a]	0.28
	O_2[b]	0.06
	N_2O[c]	0.18
Hg	Ar[a]	1.00
	N_2[a]	0.81
	CO_2[a]	0.34
	Air[a]	0.02
	O_2[a]	0.00
	N_2O[a]	0.00
Ga	Ar[b]	1.00 (1.00)[e]
	N_2[b]	0.83 (0.96)[e]
	CO_2[b]	1.18 (1.09)[e]
	Air[b]	0.83 (0.85)[e]
	O_2[b]	0.85 (1.08)[e]
	N_2O[b]	0.93 (1.29)[e]

[a] Sheath gas flow rate of 3.2 l mm^{-1}.
[b] Sheath gas flow rate of 2.0 l mm^{-1}.
[c] Sheath gas flow rate of 2.6 l mm^{-1}.
[d] Sample size is same for any element in all sheath gases.
[e] Value outside parentheses for 4033 Å; value inside parentheses for 4172 Å.

If the analyte is completely atomized into the argon stream ($\varepsilon\beta = 1$ for argon sheath), then the peak signals for any gas other than argon should be approximately proportional to Y in that sheath gas. Since Y for many lines of many elements[6–8] in nitrogen, carbon dioxide, etc. is about 0.1, the results in Table I indicate that the argon stream contains sufficient nitrogen and oxygen from the air to reduce $\varepsilon\beta Y$ for argon. Even so, the peak signals for cadmium and mercury are greatest in argon, indicating more efficient atomization and less efficient quenching of excited atoms. For gallium, the sheath gas appears to have little influence. The authors are currently redesigning the instrumental system to exclude atmospheric air—yet provide simple sample introduction—as well as to allow rapid integration of peak areas.

Uses of the platinum loop

The platinum loop atomization method is a simple, efficient means of atomizing volatile elements. In addition, no scatter signal comparable to those in flames[1,2] results. By improvement in the atomizer design and by repetitive sampling, precision comparable to that obtained in a flame should be obtainable. The method also appears to be relatively insensitive to the matrix and at least in theory should be independent of the matrix if integral techniques are used. Therefore, this atomization method would appear to have considerable advantage for trace metal analysis of small quantities of biological materials as well as for trace metal analyses where sample size is not a limitation, *e.g.*, trace wear metals in lubricating oils. However, prior to any applications, other volatile elements and especially nonvolatile metals should and are being studied.

Other studies in progress or to be carried out include: measurement of quantum efficiencies of various lines of various elements in different gases and estimation of quenching cross sections; study of rates of vaporization of various species in various compounds into different gases; and study of thermal stability of compounds. For some of these studies, a tungsten loop, rather than a platinum loop, will be used to enable higher temperatures to be achieved.

This work was supported by AROSR(SRC)-OAR, U.S.A.F. AF-AFOSR-69-1685.

SUMMARY

The disadvantages of flames as atomizers are summarized, and a new, simple and efficient means of atomization of samples is proposed. The solution on a platinum loop is vaporized by electrical heating into an argon stream. Limits of detection were 10^{-14} g for cadmium, 10^{-8} g for mercury, and 10^{-7} g for gallium. Linear calibration graphs were obtained over 3 or 4 orders of magnitude. Of the various sheathing gases studied, argon was most efficient. The method is relatively insensitive to matrix effects.

RÉSUMÉ

Les inconvénients de flammes comme atomiseurs sont résumés et un nouveau système d'atomisation d'échantillons, simple et efficace, est proposé. La solution sur une boucle de platine est vaporisée par chauffage électrique dans un courant d'argon. Les limites de détection sont: 10^{-14} g pour le cadmium, 10^{-8} g pour le mercure et 10^{-7} g pour le gallium. Parmi divers gaz examinés, c'est l'argon qui a fourni les meilleurs résultats. La méthode est relativement insensible aux influences de la matrice.

ZUSAMMENFASSUNG

Es werden die Nachteile von Flammen als Atomisierer bei der Atomabsorptionsanalyse zusammengefasst und ein neues, einfaches und wirksames Mittel zur Atomisation der Proben vorgeschlagen. Die Lösung wird von einer Platinschleife durch elektrische Heizung in einem Argonstrom verdampft. Die Nachweisgrenzen betragen 10^{-14} g für Cadmium, 10^{-8} g für Quecksilber und 10^{-7} g für Gallium. Lineare Eichkurven wurden über 3 oder 4 Grössenordnungen erhalten. Von den verschiedenen Gasen, die untersucht wurden, war Argon am wirksamsten. Die Methode ist gegenüber Matrixeffekten relativ unempfindlich.

REFERENCES

1 M. P. Bratzel, Jr., R. M. Dagnall and J. D. Winefordner, *Anal. Chem.*, 41 (1969) 713.
2 M. P. Bratzel, Jr., R. M. Dagnall and J. D. Winefordner, *Anal. Chem.*, 41 (1969) 1529.
3 R. M. Dagnall, K. C. Thompson and T. S. West, *Anal. Chim. Acta*, 36 (1966) 269.
4 J. D. Winefordner, C. T. Mansfield and T. J. Vickers, *Anal. Chem.*, 35 (1963) 1607.
5 L. De Galan and J. D. Winefordner, *J. Quant. Spectry. Radiative Transfer*, 7 (1967) 251.
6 H. P. Hooymayers and C. T. J. Alkemade, *J. Quant. Spectry. Radiative Transfer*, 6 (1966) 501.
7 H. P. Hooymayers and C. T. J. Alkemade, *J. Quant. Spectry. Radiative Transfer*, 6 (1966) 847.
8 D. R. Jenkins, *Spectrochim. Acta*, 23B (1967) 167.
9 J. M. Mansfield, Jr., J. D. Winefordner and C. Veillon, *Anal. Chem.*, 37 (1965) 1049.
10 R. Herrmann and C. T. J. Alkemade, *Flame Photometry*, 2nd Edn., Springer, Berlin, 1960; translated into English by P. T. Gilbert, Jr.: *Chemical Analysis by Flame Photometry*, Interscience, New York, 1963.
11 R. Smith, R. Elser and J. D. Winefordner, *Anal. Chim. Acta*, 48 (1969) 35.
12 H. Massmann, *Spectrochim. Acta*, 23B (1968) 215.
13 T. S. West and X. K. Williams, *Anal. Chim. Acta*, 45 (1969) 27.
14 B. V. L'vov, *Spectrochim. Acta*, 17 (1961) 761.
15 B. M. Gatehouse and A. Walsh, *Spectrochim. Acta*, 16 (1960) 602.
16 V. G. Mossotti, K. Laqua and W. D. Hagenah, *Spectrochim. Acta*, 23B (1968) 197.
17 L. S. Nelson and N. A. Kuebler, *Spectrochim. Acta*, 19 (1963) 781.
18 K. E. Zacha, M. P. Bratzel, Jr., J. D. Winefordner and J. M. Mansfield, Jr., *Anal. Chem.*, 40 (1968) 1733.
19 T. C. O'Haver and J. D. Winefordner, *J. Chem. Educ.*, 46 (1968) 241.
20 J. D. Winefordner, M. L. Parsons, J. M. Mansfield and W. J. McCarthy, *Anal. Chem.*, 39 (1967) 436.

Analytica Chimica Acta
Elsevier Publishing Company, Amsterdam
Printed in The Netherlands

ATOMIC ABSORPTION DETERMINATION OF MICROGRAM QUANTITIES OF MOLYBDENUM IN LAKE WATERS

Y. K. CHAU AND K. LUM-SHUE-CHAN*
Canada Centre for Inland Waters, Burlington, Ontario (Canada)

(Received August 4th, 1969)

The determination of certain trace elements in lake water and sediments has become significant in the studies of the geochemical, biochemical and industrial processes in the Great Lakes. Among these, molybdenum as a biologically active element for growth[1,2] and as a micronutrient in the aquatic environment in lakes[3] is under investigation. A considerable amount of literature is available on the determination of molybdenum in natural waters and sea water[4-6] in the range of 0.5–16 μg/l. All these methods require a preliminary concentration step either by coprecipitation with a hydrous metallic oxide or by cocrystallization with an organic reagent or by the combination of both before the determination by either spectrophotometric or spectrographic methods. A sample of 500–1000 ml is generally required. Despite the high sensitivity achieved, all these methods are quite laborious. BROOKS[7], using liquid–liquid countercurrent extraction with 1% oxine in chloroform in connection with a d.c. arc spectrograph was able to determine 0.2–1.5 μg Mo/l in sea water on an 8-l sample. The method, however, is not conveniently applicable to analyses of multiple samples. A simple, sensitive and accurate technique has always been in demand for trace element analysis on a routine basis. To accomplish this, complexation and solvent extraction followed by atomic absorption spectroscopy provides an attractive combination.

Many studies have been made on the determination of molybdenum by atomic absorption spectroscopy. DAVID[8] studied fully the parameters affecting the sensitivity of molybdenum absorption and achieved a detection limit of 0.5 p.p.m. in aqueous solution with a luminous air–acetylene flame. The sensitivity was later improved by BUTLER AND MATTHEWS[9] who used an ammonium pyrrolidine dithiocarbamate–methyl isobutyl ketone (APDC–MIBK) extraction system in studies of molybdenum in waters, plants and silicate samples. Sensitivity was enhanced to reach 2 p.p.b. for water by including a concentration factor of 50 involving both evaporation and extraction. The preliminary evaporation is time-consuming and not very suitable for routine practice. DELAUGHTER[10] used dithiol and MIBK to extract molybdenum from 800 g of brine, and claimed a sensitivity of 1 p.p.b. with reference to the weight of brine. All these methods employed a luminous air–acetylene flame for atomic absorption work.

For the determination of elements which easily form refractory oxides in the flame, nitrous oxide has been proved more suitable as a supporting gas than air in providing a non-oxidizing flame of high temperature. Better sensitivity has been

---

* Student assistant from Chemistry Department, McMaster University, Hamilton, Ontario, Canada.

reported[11] by using such a flame mixture for atomic absorption of molybdenum. With such a flame, KIRKBRIGHT *et al.*[12] determined molybdenum in niobium and tantalum in the range of 60–600 p.p.m. after extraction of the molybdenum with oxine in butanol.

The present study describes the atomic absorption sensitivity of several molybdenum complexes, and the development of a simple and sensitive method for the determination of molybdenum at p.p.b. levels.

Extraction of molybdenum complexes

The transfer of a metal ion from aqueous solution into an organic phase through complexation and extraction has been widely used for enhancement of sensitivity in atomic absorption spectroscopy. To select a suitable chelate extraction system, several chelating agents were investigated and their absorption intensity compared. Experiments were carried out on 20-ml aliquots of molybdenum-free lake water spiked with 100 μg of molybdenum. The solution was adjusted to pH 2–3 with dilute sulfuric acid and placed in a 60-ml separatory funnel, and 5 ml of the chelating solution was added. After mixing, 10 ml of MIBK was introduced and the mixture was equilibrated in a mechanical shaker for 5 min. The organic phase was separated and sprayed into the flame to measure its absorption intensity. These tests indicated (Table I) that oxine, cupferron, acetylacetone and dithiol showed the best absorption sensitivity.

TABLE I

ATOMIC ABSORPTION INTENSITY OF SOME MOLYBDENUM COMPLEXES

(100 ml of lake water containing 100 μg Mo, extracted in 10 ml of MIBK)

Complexing agent	*Reagent soln.*	*Absorption (%A)*[a]
Ammonium pyrrolidine dithiocarbamate	1% in water	20
Thenoyltrifluoroacetone	0.1 *M* in acetone	5
Diethylammonium diethyldithiocarbamate	1% in MIBK	3
Oxine	1% in acetone	43
Cupferron	1% in acetone	44
Sodium diethyldithiocarbamate	1% in water	33
Acetylacetone (0.2 *N* H_2SO_4 medium)	3 ml	35
α-Benzoinoxime (1 *N* HCl medium)	1% in MIBK	23
Dithiol (4 *N* HCl medium)	1% in MIBK	50
Dithiol (0.01 *N* HCl medium)	1% in MIBK	15

[a] Absorption taken at 1 × scale.

Further experiments at lower concentration levels were carried out with these four chelating agents; 100-ml aliquots of molybdenum-free lake water were spiked with 0.5, 1.0 and 3.0 μg of molybdenum respectively, and extracted with the same amount of chelating agent but with 5 ml of MIBK. The results (Table II) showed that at these levels, only dithiol and oxine were suitable for extraction of molybdenum. Cupferron and acetylacetone gave low absorption signals, probably owing to their poor extraction efficiency for low concentrations of molybdenum.

The use of dithiol in the spectrophotometric determination of molybdenum has been reported by several workers[5,10,13] because of its high sensitivity. Quantitative formation of the complex, according to SANDELL[13], occurs in concentrated

TABLE II

EXTRACTION OF MOLYBDENUM AT p.p.b. LEVEL

(100 ml of lake water, spiked with 0.5, 1, 3 μg Mo; 5 ml of MIBK)

Complexing agent[a]	*Absorption (%A)*[b]		
	0.5 μg	*1 μg*	*3 μg*
Cupferron	5	13	42
Oxine	12	24	72
Acetylacetone	0	3	14
Dithiol (4 *M* HCl medium)	13	27	90

[a] For concentration of chelating agent, see Table I.

[b] Absorption taken at 10× scale.

acid medium ranging from 6 to 14 *N* in sulfuric acid or 4 *M* in hydrochloric acid[14]; the high acidity is necessary to convert molybdenum from the anionic molybdate form to a cationic species suitable for dithiol extraction. CHAN AND RILEY[5] found that 5 ml of hydrochloric acid was necessary to provide optimal extraction conditions for 10 μg of molybdenum from 20 ml of solution. Experiments indicated that extraction of 1 μg of molybdenum from 100 ml of distilled water increased with increasing acidity. Absorption signals of 10% and 21% were obtained respectively for 0.01 *N* and 0.1 *N* acidity of the medium. When the acidity was raised to 4 *N*, the signal increased to 38%. The introduction of a large quantity of acid into the sample is one of the objections to the dithiol method. In the course of the experiments, it was also noted that the dithiol reagent was unstable even when its stable form diacetyldithiol was used in alkaline solution. For these reasons the molybdenum dithiolate complex was not investigated further.

Extraction of molybdenum oxinate for atomic absorption

The extraction of molybdenum(VI) with oxine has been studied extensively by STARÝ[15]. At macro concentrations, molybdenum is quantitatively extractable by 0.01 *M* oxine in chloroform at pH 1–5. The oxine-extractable form of molybdenum is molybdenic acid (H_2MoO_4) which is the predominant form at pH 1–2. KIRKBRIGHT *et al.*[12] also reported the quantitative extraction of molybdenum oxinate into butanol in the pH range 2–5. Because of its high extraction capability, wide pH range of operation and high absorption sensitivity of the molybdenum complex, the oxinate was chosen for further study.

The extraction of molybdenum at microgram levels and its pH dependence were investigated by using 100 ml of lake water to which 2 μg of molybdenum had been added; the solutions were adjusted to a range of pH values with sulfuric acid or ammonium hydroxide. The solution was shaken for 10 min with 5 ml of 1% oxine in MIBK. The results (Fig. 1) showed that the pH range for optimum extraction was 1.8–2.6. At pH 3–5, a 5% decrease in absorption signal was observed and beyond pH 5 the extraction dropped off rapidly. The maximum extraction at pH 1.8–2.6 is probably due to the presence of the extractable species of molybdenum (H_2MoO_4) at this range. The decrease in extraction at higher pH values is caused by the decrease of equilibrium concentration of H_2MoO_4[15]. Extraction of molybdenum at higher pH values could be made possible by using higher oxine concentrations, but such solutions were unsuitable for subsequent aspiration in atomic absorption measurements. Extraction for all investigations was therefore made at pH 2–2.4.

The oxinate of molybdenum was found to be very stable in MIBK solvent. No change in absorption intensity was observed up to a storage period of two weeks.

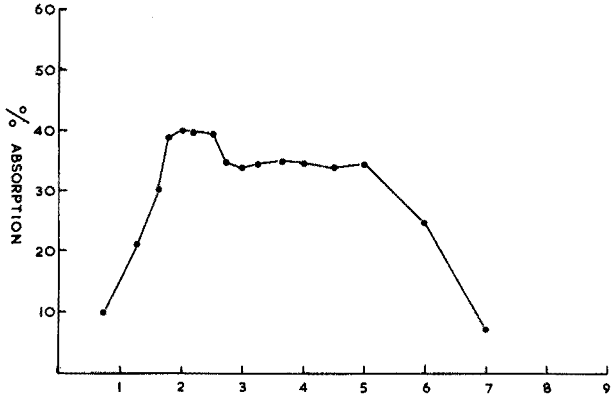

Fig. 1. Extraction efficiency of molybdenum oxinate at various pH values.

Concentration of oxine and equilibrium time

After the working pH had been established, similar experiments were conducted to determine the optimum quantity of oxine to bring about maximum absorption. The absorption signal was independent of oxine concentration over the range 0.6–3.5% in MIBK. Higher concentrations of oxine reduced the absorption signal, owing to the clogging of the burner slit which affected aspiration. A 1% solution of oxine was found satisfactory in extraction and in the flame.

According to STARÝ[15], extraction equilibrium is attained at high pH values for high oxine concentrations within a few minutes, but at low pH and low oxine concentrations the extraction rate is small. For the present concentration range, experiments carried out with all other parameters set at their optimal values, indicated that 10 min was the minimum time to attain extraction equilibrium. No further increase in the absorption of the organic phase was observed by shaking up to a period of 60 min.

Solvent effect

The effect of solvent in atomic absorption sensitivity is well known. The degree of enhancement of sensitivity depends on the extraction efficiency of the metal and the aspiration rate of the solvent. Table III summarized the investigation of the effect of a number of solvents. In these tests the oxine was added to 100 ml of lake water in acetone medium and 5 ml of each solvent was used for extraction. After separation of the organic phase in a 5-ml volumetric flask, the volume was made up to the mark with the respective solvent to eliminate the effect of solubility differences. Both MIBK and butyl acetate were found suitable for extraction of molybdenum oxinate. MIBK is more soluble than butyl acetate, but the volume is quite reproducible under normal laboratory conditions. Since the absorption signal

TABLE III

EFFECT OF SOLVENTS ON EXTRACTION OF MO-OXINATE

(100 ml lake water, spiked with 2 µg Mo; 5 ml of final solvent volume)

Solvent	*Absorption intensity (%A)*
Ethyl acetate	5
Butyl acetate	20
Amyl acetate	16
Isoamyl alcohol	5
n-Decyl alcohol	2
Methyl amyl ketone	14
Methyl hexyl ketone	10
Methyl isobutyl ketone	24

of the molybdenum complex was higher in MIBK than in butyl acetate, the former solvent was chosen for extraction work.

Interference studies

Many metals are known to form oxinates and are extractable into organic solvents. With the present extraction and atomic absorption procedure, no interference was observed in the determination of 2 µg of molybdenum from 100 ml of lake water in the presence of 1000 µg of each of the following ions: Na, Ca, Mg, Cu(II), Ni, Al, Cr(III), Mn(II), Co(II), Cl^-, SO_4^{2-}, NO_3^-, OAc^- and PO_4^{3-}. Vanadium(V) and iron(III) were found to enhance absorption and chromium(VI) and tungsten(VI) to suppress it. All these interferences were eliminated by the reducing action of ascorbic acid. With 5 ml of 1% ascorbic acid added to the sample before extraction, up to 5000 µg of iron(III), 100 µg of vanadium(V), and 1000 µg of chromium(VI) or tungsten(VI) could be tolerated. The above limits are not likely to be exceeded in the analyses of natural waters.

EXPERIMENTAL

Instrumentation

A Jarrell-Ash atomic absorption spectrophotometer model 82-528 was used. The burner was a "tri-flame" type fitted with a 5-cm nitrous oxide burner head. The nitrous oxide supply was operated at 30 psi and acetylene at 15 psi. Entrance and exit slits were 100 µ and 150 µ, respectively. The resonance source was a Westinghouse high-intensity molybdenum hollow-cathode lamp operated at 15 mA. The 3133 Å line was used. The instrument was operated in the concentration mode with signals given in a linear percentage scale presented on a 10-inch strip chart recorder (Leeds and Northrup).

Reagents

Molybdenum standard solution. Dissolve 0.0750 g of dried molybdenum trioxide in 5–10 ml of 0.1 *N* sodium hydroxide, dilute with water to *ca.* 100 ml, make slightly acidic with hydrochloric acid and make up to 500 ml. This solution contains 100 µg Mo/ml. Prepare daily a working solution containing 1 µg Mo/ml by subsequent dilution of this stock solution.

Oxine solution. 1% in MIBK, stable for at least one week.

Methyl isobutyl ketone. Refined by distillation. Reagent-grade solvent generally contains impurities giving flickers in the flame.

Molybdenum-free lake water. Adjust filtered lake water to pH 5±0.2 and pass it through a 120×15-mm glass column packed with Chelex-100 at the rate of *ca.* 5 ml/min. The resin is prepared[16] by washing with 2 *N* nitric acid, and then with distilled water until the washing has a pH of 4–5.

Atomic absorption procedure

Set the nitrous oxide flow at 11 SCFH (flow meter reading) and increase the acetylene slowly until the characteristic "red feather" is about 2 in long and the flame is just about to become luminous.

The Jarrell-Ash instrument has a continuous scale expansion feature in the concentration mode achieved with a logarithmic amplifier which gives signals linear in concentration. It normally requires a standard solution to set the range of the instrument. It was found possible to preset the amplifier to a definite scale expansion by introducing an electronic signal through the zero adjustment. The instrument was set to 10× expansion.

It was found useful to prepare a solution of molybdenum in MIBK (*ca.* 0.4 p.p.m. in MIBK) and use it as a reference standard to standardize the instrument for optimum conditions of flame and burner positions. All absorption measurements are made against a solvent blank.

Determination of molybdenum in lake water

Filter the sample through a millipore membrane (0.5 μ) immediately after collection and acidify to pH 2 with nitric acid. To 100 ml of sample in a 150-ml separatory funnel, add 5 ml of 1% (w/v) ascorbic acid and carefully adjust the pH to 2–2.4. If the molybdenum content is below 3 p.p.b., proportionately more sample up to 200 ml can be used. Add 5 ml of 1% oxine in MIBK and equilibrate it in a mechanical shaker for 15 min. If the sample is increased to 200 ml, 7 ml of oxine solution should be added to maintain the oxine concentration and to compensate for the solubility of MIBK. Separate the organic phase and aspirate directly into the flame. Determine the reagent blank by carrying out the extraction with 100 ml of molybdenum-free water. Calibrate the method by adding 0.5 and 1 μg of molybdenum to 100 ml of molybdenum-free lake water and taking the solutions through the entire procedure.

RESULTS

The recovery of the method was evaluated by analyzing a series of molybdenum-free lake water samples spiked with known amounts of molybdenum. The

TABLE IV

RECOVERY OF MOLYBDENUM FROM 100 ml OF LAKE WATER

Mo added (μg)	0	0.5	1.0	1.5	2.0	2.5	3.0	4.0
Mo found (μg)	0	0.49	0.98	1.48	1.98	2.55	3.06	4.00
% Recovery	0	98	98	99	99	102	102	100

results obtained (Table IV) indicated that the accuracy of the described method was satisfactory. The calibration curve was linear up to at least 5 μg of molybdenum in 100 ml of sample (0–50 p.p.b.), and passed through the origin. Concentrations above 50 p.p.b. gave sufficient signals to be measured in the normal scale without the use of expansion. For each 0.5-μg increment of molybdenum in the sample (5 p.p.b.), the average absorption intensity increment was 11%. The sensitivity was calculated to be 1 p.p.b. for a 2% absorption signal.

The precision of the method was tested by replicate analyses of a lake water sample and spiked molybdenum-free water. Analyses (10) of 100-ml aliquots of spiked water with 2 μg of molybdenum gave a coefficient of variation of 1.8%. Other analyses (10) on a surface sample taken from the western basin of Lake Ontario gave an average content of 5.65 ± 0.22 μg Mo/l with a coefficient of variation of 4.0%.

SUMMARY

The extraction of molybdenum by various complexing agents was studied and their atomic absorption sensitivity compared. Oxine and dithiol are among the most sensitive. Optimum conditions for extraction of molybdenum with oxine at microgram levels and the interference of certain elements in atomic absorption were investigated. Molybdenum was extracted directly from 100 ml of water by oxine in MIBK and determined by atomic absorption spectroscopy with a nitrous oxide–acetylene flame. The coefficient of variation for spiked lake water and natural lake water containing 20 μg Mo/l and 5.56 μg Mo/l were found to be 1.8% and 4.0% respectively. The sensitivity of the method was 1 p.p.b.

RÉSUMÉ

On étudie l'extraction du molybdène par divers agents complexants et on compare leur sensibilité d'absorption atomique. L'oxine et le dithiol sont parmi les plus sensibles. Les conditions optima d'extraction du molybdène avec l'oxine à l'échelle micro sont examinées, de même que l'influence de certains éléments. Le molybdène est extrait directement de 100 ml d'eau par l'oxine et dosé par spectroscopie par absorption atomique avec une flamme oxyde nitreux–acétylène. La sensibilité de la méthode est 1 p.p.b.

ZUSAMMENFASSUNG

Es wurde die Extraktion von Molybdän durch zahlreiche Komplexbildner untersucht und die Atomabsorptionsempfindlichkeiten verglichen. Oxin und Dithiol sind die empfindlichsten. Es wurden die optimalen Bedingungen für die Extraktion von Molybdän mit Oxin im Mikrogrammbereich und die Störungen gewisser Elemente bei der Atomabsorption festgestellt. Molybdän wurde direkt aus 100 ml Wasser durch Oxin in Methylisobutylketon extrahiert und mit der Atomabsorptionsspektroskopie unter Verwendung einer Stickstoffoxid–Acetylen-Flamme bestimmt. Der Variationskoeffizient für Binnenwässer verschiedener Herkunft mit 20 μg Mo/l und 5.56 μg Mo/l betrug 1.8 bzw. 4.0%. Die Empfindlichkeit der Methode beträgt 1 p.p.b.

REFERENCES

1 D. J. Arnon and P. R. Stout, *Plant Physiol.*, 14 (1939) 599.
2 J. B. Walker, *Arch. Biochem. Biophys.*, 46 (1953) 1.
3 C. R. Goldman, *Science*, 132 (1960) 106.
4 J. P. Riley, in *Chemical Oceanography*, Vol. 2, Academic Press, New York, 1965, pp. 353–354.
5 K. M. Chan and J. P. Riley, *Anal. Chim. Acta*, 36 (1966) 220.
6 Y. S. Kim and H. Zeitlin, *Limnol. Oceanog.*, 13 (1968) 534.
7 R. R. Brooks, *Geochim. Cosmochim. Acta*, 29 (1965) 1369.
8 D. J. David, *Analyst*, 86 (1961) 730.
9 L. R. P. Butler and P. M. Matthews, *Anal. Chim. Acta*, 36 (1966) 319.
10 B. DeLaughter, *Atomic Absorption Newsletter*, 4 (1965) 273.
11 G. F. Kirkbright, A. M. Smith and T. S. West, *Analyst*, 91 (1966) 705.
12 G. F. Kirkbright, M. K. Peters and T. S. West, *Analyst*, 91 (1966) 705.
13 E. B. Sandell, *Colorimetric Determination of Trace Metals*, 3rd Edn., Interscience, New York, 1964.
14 J. Starý, *The Solvent Extraction of Metal Chelates*, Pergamon Press, Oxford, 1964.
15 J. Starý, *Anal. Chim. Acta*, 28 (1963) 132.
16 J. P. Riley and D. Taylor, *Anal. Chim. Acta*, 41 (1968) 175.

Analytica Chimica Acta
Elsevier Publishing Company, Amsterdam
Printed in The Netherlands

SEPARATION ET DOSAGE PAR ACTIVATION NEUTRONIQUE DE TRACES D'HAFNIUM DANS LE SCANDIUM

L. BALSENC, W. HAERDI ET D. MONNIER
Institut de Chimie Analytique et Minérale de l'Université, 1211 Genève 4 (Suisse)

(Reçu le 20 août, 1969)

Le problème du dosage de traces d'hafnium dans le scandium s'est posé il y a un an environ, lorsque des alliages de ces métaux ont été expérimentés avec succès en astronautique.

Nous avons alors mis au point une méthode rapide de dosage en séries de l'hafnium en présence de grandes quantités de scandium.

Une analyse non-destructive basée sur la formation de l'isotope radioactif 179m-hafnium ($T_{\frac{1}{2}}=19$ sec; $E_\gamma=0.16$ MeV) ne peut s'appliquer dans le cas présent en raison de la formation simultanée de 46m-scandium ($T_{\frac{1}{2}}=19.5$ sec; $E_\gamma=0.15$ MeV), qui interfère. C'est pourquoi nous avons eu recours à une séparation chimique préalable des deux éléments.

Nous avons choisi la séparation par échangeur d'ions sur colonne. Cette méthode, d'un rendement satisfaisant et demandant peu de manipulations, présente une sélectivité élevée et peut être facilement automatisée.

Le procédé utilise le partage des complexes sulfate anioniques d'hafnium et de scandium entre une résine échangeur d'anions chargée d'ions sulfate et une solution sulfurique. Une étude analytique théorique, qui fera l'objet d'une communication ultérieure, a montré que les coefficients de partage à l'équilibre sont suffisamment différents pour permettre une bonne séparation.

ÉTUDE ANALYTIQUE

Bien qu'un certain nombre d'auteurs aient étudié la fixation de l'hafnium sur les échangeurs d'anions[1-7], la littérature ne propose, à notre connaissance, que peu de méthodes pratiques pour la séparation hafnium–scandium.

Notre méthode s'apparente à celle d'HAMAGUCHI *et al.*[6] concernant la séparation de l'uranium, de l'yttrium et du zirconium sur résine à groupements fortement basiques en milieu sulfurique.

Pour l'adapter à la fixation simultanée de l'hafnium et du scandium, nous avons apporté des modifications qui portent essentiellement sur la quantité de résine utilisée, la longueur et le diamètre de la colonne, le mode de fixation, la nature de l'influent et de l'éluant et la vitesse d'élution.

Choix de la résine

Pour séparer un certain nombre de métaux les uns des autres, les résines anioniques se révèlent souvent plus efficaces que les résines cationiques, les constantes des complexes formés par divers métaux avec un même anion étant généralement très différentes.

Cette méthode semble être la plus favorable pour la fixation des éléments du groupe IV B, qui doivent être complexés pour se maintenir en solution. Nous avons choisi, pour notre travail, une résine aminoquaternaire du type Dowex 1-X8.

Choix du ligand, du groupe actif de la résine et de l'éluant

L'anion SO_4^{2-} formant des complexes très stables avec l'hafnium(IV) a été choisi comme ligand. Ce choix a été motivé également par le fait qu'un grand nombre de cations en solution acide sulfurique diluée ne se fixent pas sur les résines anioniques.

C'est également le groupement sulfate qui a été choisi comme groupe actif de la résine, afin de ne pas introduire dans le milieu un ion étranger susceptible de former des complexes avec l'hafnium.

Finalement, nous avons choisi comme éluant l'acide sulfurique qui, contrairement à l'ion fluor ou à l'ion chlore préconisés dans la plupart des méthodes de la littérature, ne s'active pas lors d'une irradiation rapide.

PARTIE EXPÉRIMENTALE

Conditions expérimentales

Préparation de la résine. La résine a été préparée selon la méthode mise au point par HAMAGUCHI *et al.*[6].

Colonnes d'échange. Des colonnes de verre classiques de 0.65 cm de diamètre et de 13 cm de longueur ont été utilisées. La hauteur du lit de résine est de 9 cm.

Réactifs. Solution de sulfate d'ammonium Merck pro anal 10^{-1} *M* (soln. 1). Solution aqueuse d'acide sulfurique Merck (p.a.) $2.5 \cdot 10^{-2}$ *M* (soln. 2). Solution de base: mélange à volumes égaux des solutions 1 et 2.

Eluant. Acide sulfurique 2 *M* (40 ml).

Solution standard. Hafnium(IV), renfermant ^{181}Hf comme traceur, en solution dans l'acide sulfurique $2 \cdot 10^{-1}$ *M* (concentration de l'hafnium $5 \cdot 10^{-3}$ g/ml).

Les essais de séparation se font sur des parties aliquotes de solution standard diluée à 5 ml avec l'acide sulfurique $2 \cdot 10^{-1}$ *M* +5 ml de solution de sulfate d'ammonium 10^{-1} *M*.

Adsorption de l'hafnium

Nous avons fait passer sur l'échangeur Dowex 1-X8 forme sulfate, des solutions d'hafnium de concentrations différentes. Pour chacune d'elles, partant de la solution standard, nous avons préparé trois mêmes dilutions dont nous avons mesuré la proportion d'hafnium fixé et élué. Les résultats sont donnés dans le Tableau I.

Ayant observé, lors de travaux antérieurs, que certains complexes deviennent très difficiles à éluer lorsqu'ils se trouvent en faible concentration dans la résine, nous avons déterminé la masse minimum d'hafnium à traiter dont l'élution est encore quantitative et reproductible.

Nous avons constaté que pour des masses d'hafnium inférieures à un microgramme, il est très difficile d'obtenir une élution quantitative (v. Tableau I).

Les différences constatées entre la détermination des quantités d'hafnium ajoutées et mesurées proviennent des erreurs de comptage du traceur radioactif. En

TABLEAU I

ADSORPTION DE L'HAFNIUM

Hf ajouté (g)	*Hf retrouvé (g)*		
	I	*II*	*III*
$1.0 \cdot 10^{-2}$	$0.97 \cdot 10^{-2}$	$0.99 \cdot 10^{-2}$	$0.99 \cdot 10^{-2}$
$1.0 \cdot 10^{-3}$	$0.98 \cdot 10^{-3}$	$1.01 \cdot 10^{-3}$	$1.10 \cdot 10^{-3}$
$1.0 \cdot 10^{-4}$	$1.03 \cdot 10^{-4}$	$0.95 \cdot 10^{-4}$	$0.98 \cdot 10^{-4}$
$1.0 \cdot 10^{-5}$	$0.97 \cdot 10^{-5}$	$0.97 \cdot 10^{-5}$	$0.97 \cdot 10^{-5}$
$1.0 \cdot 10^{-6}$	$0.89 \cdot 10^{-6}$	$0.94 \cdot 10^{-6}$	$0.90 \cdot 10^{-6}$
$1.0 \cdot 10^{-7}$	$0.72 \cdot 10^{-7}$	$0.70 \cdot 10^{-7}$	$0.74 \cdot 10^{-7}$

outre, nous avons observé qu'une certaine quantité d'hafnium, que nous avons mesurée, se trouve fixée irréversiblement sur la résine. Cette quantité reste constante quelle que soit la masse d'hafnium mise en jeu. Il est évident que l'erreur qui en résulte est proportionnellement plus importante sur les petites quantités que sur les grandes.

Fraction d'hafnium retrouvé après élution (F)

Si nous donnons la valeur 100% à la masse d'hafnium versée au sommet de la colonne, nous définirons la fraction F comme étant le rapport:

$$F = \frac{\%\ \text{d'Hf retrouvé après élution}}{\%\ \text{d'Hf versé au sommet de la colonne}}$$

Si l'on trace la courbe donnant F en fonction de la quantité de l'hafnium ajoutée, on s'aperçoit que celle-ci decroît très rapidement pour des masses d'hafnium égales ou inférieures à 1 µg, donc dans nos conditions de travail, la méthode n'est valable que pour des masses d'hafnium supérieures.

Séparations hafnium–scandium

Pour la séparation de traces d'hafnium en présence de quantités importantes de scandium, nous avons mis au point deux méthodes très voisines. Le choix de l'une ou de l'autre dépend de la nature de l'échantillon et des conditions de l'analyse.

Dans la première, les éléments sont séparés par élutions successives avec 3 éluants différents; c'est celle que nous avons adoptée pour nos analyses, ce qui nous a permis de recueillir 3 fractions successives dans lesquelles nous trouvons: le manganèse et le vanadium (1ère fraction), le scandium (2ème fraction) et l'hafnium (3ème fraction).

Si l'on désire doser l'hafnium seul, à l'exclusion de tout autre élément présent dans le milieu, on utilise de préférence le second procédé ("filtration sur colonne") qui est un peu plus rapide.

Mode opératoire

Solutions standard. Hafnium(IV) en solution dans l'acide sulfurique $2 \cdot 10^{-1}$ *M*. Conc. $5 \cdot 10^{-4}$ g/ml. Scandium(III) en solution dans l'acide sulfurique.

Méthodes analytiques. Hafnium: Traceur radioactif ^{181}Hf. Scandium: (*a*) titration par EDTA. Indicateur: Xylenol orange; (*b*) traceur radioactif ^{46}Sc.

Méthode A. Les deux éléments en solution dans l'acide sulfurique 0.1 *M*

(5 ml) sont introduits avec 5 ml d'une solution de sulfate d'ammonium 0.1 M au sommet de la colonne de résine, celle-ci étant prééquilibrée par lavage avec 20 ml de la solution de base.

On fait passer le mélange à séparer à travers la colonne; la vitesse d'écoulement est fixée à 1 ml par min. L'hafnium et le scandium sont quantitativement retenus. On lave avec 20 ml de la solution de base.

Le scandium est élué avec 20 ml d'une solution 0.4 M d'acide sulfurique. On recueille la totalité du scandium fixé (10^{-2} à 1 g; 99%); l'hafnium reste adsorbé. Le passage de 40 ml d'acide sulfurique 2 M, à raison de 2 ml par min, entraîne l'élution de l'hafnium fixé (10^{-4} g) (v. Fig. 1).

L'opération (fixation et élution) demande environ une heure.

Cette méthode est utilisable pour séparer 10^{-2} à 10^{-5} g d'hafnium de 1 g de scandium.

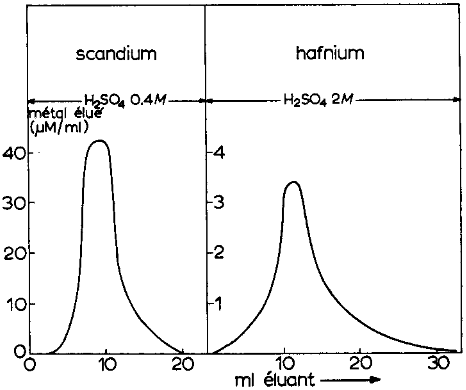

Fig. 1. Elution d'un mélange hafnium–scandium par l'acide sulfurique.

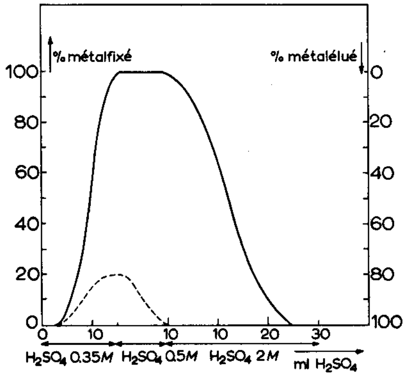

Fig. 2. Fixation et élution hafnium–scandium. (—) Hafnium, (---) scandium.

Méthode B. La solution sulfurique 0.35 M des deux éléments (15 ml) est introduite au sommet de la colonne prééquilibrée par lavage avec la solution de base.

Le mélange s'écoule à travers la colonne à raison de 1 ml par minute; la solution recueillie contient 80% du scandium alors que tout l'hafnium est fixé.

La totalité du scandium restant est éluée par lavage avec 10 ml d'acide sulfurique 0.5 M (Fig. 2).

L'hafnium est ensuite élué à 98% avec 25 ml d'acide sulfurique 2 M.

La durée de la séparation est de 40 min environ.

Résultats

Nous avons composé des mélanges renfermant de l'hafnium et du scandium en proportions variables.

Dans un échantillon de scandium, nous avons pu séparer 1 p.p.m. d'hafnium avec un rendement supérieur à 90% (Tableau II).

Le rendement de l'élution de l'hafnium ne dépend pas du rapport des masses Hf/Sc mais de la quantité absolue d'hafnium traité (v. p. 215).

TABLEAU II

DOSAGE DES MÉLANGES DE L'HAFNIUM ET DU SCANDIUM

Echantillon	*Hafnium*		*Scandium*	
	Ajouté (g)	*Retrouvé (g)*	*Ajouté (g)*	*Retrouvé (g)*
1	$1.0 \cdot 10^{-4}$	$1.07 \cdot 10^{-4}$	$1.0 \cdot 10^{-2}$	$0.96 \cdot 10^{-2}$
2	$1.0 \cdot 10^{-5}$	$0.98 \cdot 10^{-5}$	$1.0 \cdot 10^{-2}$	$0.98 \cdot 10^{-2}$
3	$1.0 \cdot 10^{-6}$	$0.93 \cdot 10^{-6}$	$1.0 \cdot 10^{-2}$	$1.10 \cdot 10^{-2}$
4	$1.0 \cdot 10^{-7}$	$0.80 \cdot 10^{-7}$	$1.0 \cdot 10^{-2}$	$0.99 \cdot 10^{-2}$
5	$1.0 \cdot 10^{-6}$	$0.95 \cdot 10^{-6}$	1.0	0.99

APPLICATION

Nous avons appliqué cette méthode à la détermination de la teneur en hafnium d'un alliage de scandium de composition connue, renfermant 110 p.p.m. d'hafnium ainsi que des quantités plus importantes de manganèse (3100 p.p.m.), de cobalt (7000 p.p.m.) et de vanadium (6800 p.p.m.).

Nous avons fait 4 analyses complètes de l'alliage (Tableau III). La séparation a été faite selon la méthode décrite ci-dessus. Le dosage est basé sur la formation, par activation aux neutrons thermiques, de l'isotope hafnium-179m ($T_{\frac{1}{2}}=19$ sec; $E_{\gamma}=0.160$ MeV).

Conditions expérimentales

Prises = 1 g; t irrad = 60 sec; t accum = 78 sec; flux $\phi=2.5 \cdot 10^{9}$ n cm^{-2} sec^{-1}.

TABLEAU III

ANALYSE DES ALLIAGES DE SCANDIUM

Echantillon 1 Hf trouvé (p.p.m.) = 103
2 = 98
3 = 109
4 = 116
Moyenne: 106 p.p.m.
Erreur relative sur la moyenne = 4%.

CONCLUSION

Le dosage radiochimique de quantités d'hafnium de l'ordre du p.p.m. dans le scandium est possible après séparation. La durée totale de l'analyse est d'une heure environ.

L'erreur relative sur la moyenne pour l'analyse complète n'est pas supérieure à 5% pour des quantités d'hafnium de l'ordre de 100 μg.

La présence de quantités relativement importantes de manganèse (rapport pondéral Hf/Mn = 1/30), de cobalt (1/90) et de vanadium (1/70) n'interfèrent pas dans nos conditions d'expérience.

Nous remercions le Fonds National Suisse qui nous a permis d'entreprendre ce travail.

RÉSUMÉ

Une méthode de séparation et de dosage de traces d'hafnium ($\geqq 1$ p.p.m.) dans le scandium est proposée. Les deux métaux, sous forme de complexes sulfate, sont séparés par échange sur résine anionique en milieu sulfurique. Ils sont ensuite dosés par activation neutronique: l'hafnium sous forme d'hafnium-179m ($T_{\frac{1}{2}}=19$ sec), le scandium sous forme de scandium-46m ($T_{\frac{1}{2}}=19.5$ sec). La durée totale de l'analyse, séparation, activation, et sortie des résultats, n'excède pas une heure.

SUMMARY

A method is proposed for the separation and determination of traces of hafnium($\geqq 1$ p.p.m.) in scandium metal. The metals, as sulfate complexes, are separated by anion exchange in sulfuric acid medium. Analysis by thermal neutron activation is based on the formation of 179m-hafnium ($T_{\frac{1}{2}}=19$ sec) and 46m-scandium ($T_{\frac{1}{2}}=19.5$ sec). The complete separation and determination requires only 1 h.

ZUSAMMENFASSUNG

Es wird eine neutronenaktivierungsanalytische Methode zur Bestimmung von Spuren Hafnium ($\geqq 1$ p.p.m.) in Scandiummetall vorgeschlagen. Die Metalle werden aus schwefelsaurer Lösung am Anionenaustauscher getrennt. Die Bestimmung erfolgt über das ^{179m}Hf ($T_{\frac{1}{2}}=19$ sec) und das ^{46m}Sc ($T_{\frac{1}{2}}=19.5$ sec). Die vollständige Trennung und Bestimmung erfordert nur 1 Stunde.

BIBLIOGRAPHIE

1 K. S. RAJAN ET G. GUPTA, *J. Sci. Ind. Res. India*, 14B (1955) 453.
2 K. S. RAJAN ET G. GUPTA, *J. Sci. Ind. Res. India*, 16B (1957) 459.
3 J. L. HAGUE ET L. A. MACHLAN, *J. Res. Natl. Bur. Std.*, 65A (1961) 75; 66A (1962) 517.
4 C. CORNET, M. THIBAULT, J. HURE ET B. TRÉMILLON, *Bull. Soc. Chim. France*, (1961) 286.
5 D. I. RYABCHIKOV, I. N. MAROV, A. N. ERMAKOV ET V. K. BELYAEVA, *J. Inorg. & Nucl. Chem.*, 26 (1964) 965.
6 H. HAMAGUCHI, A. OHUCHI, T. SHIMIZU, N. ONUMA ET R. KURODA, *Anal. Chem.*, 36 (1964) 2304.
7 F. W. E. STRELOW ET C. J. C. BOTHMA, *Anal. Chem.*, 39 (1967) 595.

Analytica Chimica Acta
Elsevier Publishing Company, Amsterdam
Printed in The Netherlands

DOSAGE DES IMPURETES DANS LE ZINC PAR ACTIVATION NEUTRONIQUE

TOME II. DOSAGE DU GERMANIUM

R. MACHIROUX ET F. MOUSTY
Laboratoires de Chimie Analytique, Université de Liège, Liège (Belgique)

(Reçu le 15 juillet, 1969)

Dans un précédent article[1], nous avons entamé l'exposé des premiers résultats enregistrés dans l'analyse du zinc par activation neutronique. Aux dosages du cobalt et de l'argent, il nous a paru intéressant d'ajouter la détermination quantitative de certains autres éléments.

La présente publication est consacrée à l'application de la technique d'activation au dosage du germanium.

Propriétés nucléaires du germanium

Nous avons déjà exposé les propriétés nucléaires du zinc dans l'article cité plus haut. En ordre principal, cet élément possède deux isotopes, ^{65}Zn et ^{69m}Zn qui confèrent à la matrice irradiée une très forte activité spécifique ($\sim$10–20 mCi/g pour une irradiation de 4 jours dans un flux de $8 \cdot 10^{12}$ n sec^{-1} cm^{-2}).

Le Tableau I[2,3] rassemble les données nucléaires relatives au germanium.

Sur la base de ces données, nous avons décidé d'utiliser, pour nos dosages, l'isotope de masse 71 pour les raisons suivantes:

(*a*) sa période de 11.4 jours nous laisse toute latitude pour effectuer les séparations indispensables.

TABLEAU I

PROPRIÉTÉS NUCLÉAIRES DU GERMANIUM

A	*Abond. isotop. (%)*	σ *(barns)*	*Réactions nucléaires*	$T_{1/2}$	β*(MeV)*	γ*(MeV)*
70	20.55	3.2	^{70}Ge(n,γ)^{71}Ge	11.4 j	—	E.C. (100%)
72	27.37	1.0	^{72}Ge(n,γ)^{73m}Ge	0.53 sec	0.012–0.043 0.053	Ge X rays; 0.054
73	7.67	—	—	Stable	—	—
74	36.7	0.3	^{74}Ge(n,γ)^{75m}Ge	48 sec	0.128–0.138	Ge X rays; 0.139
		0.2	^{74}Ge(n,γ)^{75}Ge	82 min	1.19	0.066–0.199 0.265–0.427– 0.477–0.628
76	7.67	0.1	^{76}Ge(n,γ)^{77m}Ge	53 sec	2.9–0.158– 0.148	0.159–0.215
		0.1	^{76}Ge(n,γ)^{77}Ge	11.3 h	2.2–0.253 0.198	0.21–0.26– 0.37–0.42

(*b*) sa forte section efficace de capture nous permet d'espérer une bonne sensibilité pour le dosage.

Sur le plan des réactions parasites, la seule que nous aurions à prendre en considération serait ^{74}Se(n,α)^{71}Ge si des essais antérieurs ne nous avaient démontré l'absence de quantités mesurables de sélénium.

Conditions de comptage

Pour la mesure du rayonnement-X du ^{71}Ge (X rays de 9.4 keV), nous avons utilisé un cristal mince de NaI(Tl) de 2 × 25.4 mm, recouvert d'une fenêtre de 0.2 mm de béryllium et un spectromètre monocanal Philips. Les isotopes suivants (sources solides minces) nous ont permis d'étalonner la gamme d'énergie comprise entre 4 et 12 keV:

^{55}Fe	5.9 keV
^{65}Zn	7.0 keV
^{75}Se	10.5 keV.

La Fig. 1 montre les spectres et la droite d'étalonnage obtenus.

Au cours des analyses, le choix des conditions de seuil et de fenêtre nous a permis d'éliminer l'influence des rayonnements d'énergie $E > 12$ keV. Ainsi, une source intense de ^{110m}Ag ($\pm 20\ \mu$Ci) placée au voisinage immédiat du compteur ne modifie pas l'activité mesurée d'une preparation-étalon de ^{71}Ge.

Au risque d'anticiper, ajoutons encore que le germanium a été compté sous

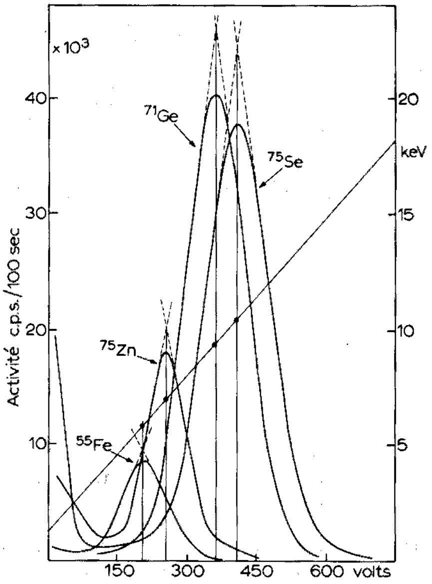

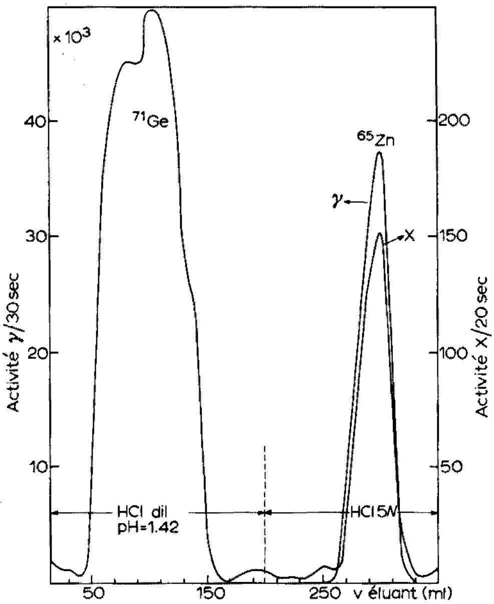

Fig. 1. Spectre X des isotopes suivants: ^{55}Fe (5.9 keV), ^{65}Zn (7.0 keV), ^{71}Ge (9.4 keV), ^{75}Se (10.5 keV). Spectromètre monocanal Philips. Cristal NaI(Tl) 25.4 × 2 mm, fenêtre en Be (0.2 mm). Seuil: 1.65 V. H.T.: 900 V. Fenêtre: 3.60 V.

Fig. 2. Courbe d'élution Ge/Zn. Colonne Dowex 50 W, 100/200 mesh/in, forme Na$^+$, hauteur 25 cm, diam: 2 cm. Eluants: Ge: HCl à pH = 1.42; Zn: HCl 5 *N*. Débit: 0.5 ml cm^{-2} min^{-1}.

forme de précipité de GeS_2 et que, dans un large domaine, la correction d'autoabsorption s'est avérée négligeable.

Méthodes de séparation

Tout comme dans le cas de l'argent et du cobalte, l'activité de la matrice ne nous a pas permis de pratiquer des analyses non destructives.

Dans le choix d'une méthode de séparation, nous nous sommes laissés guider par un certain nombre de considérations. Nous avons écarté, pour des raisons de sécurité, les séparations faisant appel à la distillation ou à l'extraction de $GeCl_4$ par CCl_4. D'autre part, la forte tension de vapeur de $GeCl_4$ (Teb: 83.1°) conduit à de mauvais rendements lors des séparations sur échangeurs anioniques en milieu acide chlorhydrique 5 *M* et ce, à cause de la durée des opérations.

A ces méthodes, nous avons préféré une séparation en trois stades:

(*a*) fixation sur résine Dowex 50 en milieu HNO_3/HF à pH = 1.42 de tous les métaux formant des cations: Zn^{2+}, Co^{2+}, Ni^{2+}, Mn^{2+}, Al^{3+}...,

(*b*) récupération du Ge par lavage de la colonne par l'acide chlorhydrique dilué, pH = 1.42,

(*c*) précipitation du GeS_2 par H_2S en milieu de l'acide sulfurique 6 *N*.

Le principal inconvénient de cette séparation tient au fait que certains éléments (halogènes, S, P, Se, Te, Sb, As...) sont élués en même temps que le germanium. Toutefois, une partie d'entre-eux est éliminée par la précipitation et la technique de comptage supprime l'effet perturbateur des autres.

Nous n'avons pas expérimenté la précipitation directe du germanium (germanomolybdate, tannate ou sulfure) à partir de la solution active pour éviter les risques de contamination des précipités par le ^{65}Zn, émetteur X voisin du germanium (E_X = 7.0 keV).

MÉTHODE DE DOSAGE

Echantillonnage et irradiation

Nous disposions de 4 types d'alliages:

(*a*) zinc à ±500 p.p.m. de Ge (all. synthétique) (série I),
(*b*) zinc à ±5 p.p.m. de Ge (all. synthétique) (serie II),
(*c*) zinc pur non raffiné par zone (série III),
(*d*) zinc hyperpur raffiné par zone (série IV).

Les échantillons sciés ont été irradiés à Saclay {(*a*) et (*b*), 6 jours à $6 \cdot 10^{11}$ n cm^{-2} sec^{-1}} et à Mol {(*c*) et (*d*), 4 jours à $8 \cdot 10^{12}$ n cm^{-2} sec^{-1}}.

Préparation des étalons

Dans chaque irradiation, nous avons inclu trois étalons de GeO_2 spectroscopiquement pur, enfermé dans des tubes de quartz scellés.

Après dissolution des étalons irradiés dans le soude 0.1 *M*, nous avons prélevé trois parties aliquotes de chacun d'eux et nous en avons mesuré l'activité spécifique (précipitation de GeS_2, mesure de l'activité, détermination du rendement de la précipitation).

Pour le calcul des résultats, nous avons appliqué une correction tenant compte de la décroissance de l'activité spécifique de ^{71}Ge ($T_{\frac{1}{2}}$: 11.4 jours).

Mise en solution

Les échantillons irradiés ont été mis en solution par le mélange d'acides suivant: 5 ml HNO_3 14 N, 0.5 ml HF 4 N, 2 gouttes H_2PtCl_6 et 3 ml H_2O, en présence de 10 à 15 mg de germanium élémentaire comme entraîneur.

Isolement du germanium

Séparation sur échangeur d'ions. Dès la fin de la dissolution du zinc, on ajuste le pH de la solution active à 1.42 par NaOH à 400 g/l (pHmètre—électrode combinée verre–calomel) et on transfère cette solution sur une colonne de résine Dowex 50 W (50 g de résine 100/200 mesh/in; 25 × 2 cm) préalablement conditionnée sous forme Na^+ à pH = 1.42. Le germanium est récupéré intégralement par lavage de la colonne au moyen de 175 ml de l'acide chlorhydrique dilué, amené à pH = 1.42. La Fig. 2 montre l'allure d'une courbe d'élution.

Précipitation de GeS_2. On rend alors l'éluat 6 N en l'acide sulfurique par addition d'acide concentré p.a. dans la solution refroidie sous un courant d'eau. On précipite GeS_2 à froid par passage de H_2S gazeux pendant 30 min. On filtre le précipité sur papier serré et on le lave jusqu'à neutralité du filtrat.

Les conditions de température et d'acidité doivent être respectées de manière assez stricte sous peine de redissolution du GeS_2 sous forme de $Ge_2S_5{}^{2-}$ ou de GeO_2.

Mesure des activités

Les filtres humides sont transférés dans des cuvettes en porcelaine et leur activité mesurée dans les conditions spécifiées plus haut.

Chaque valeur d'activité est la moyenne de trois mesures de 1000 sec au moins, encadrées et séparées par des mesures de fond continu de même durée.

Nous avons relevé le spectre X de quelques précipités entre 4 et 15 keV afin d'en contrôler la pureté radiochimique. Dans tous les cas, nous avons enregistré un pic unique et bien symétrique de 9.4 keV d'énergie (Fig. 1).

Les spectres γ et le comptage β ont révélé la présence dans les précipités et dans les filtrats de contaminants dont nous préciserons la nature ultérieurement.

Enfin, nous n'avons pu déceler ni dans les spectres γ, ni dans les spectres X, la présence de ^{65}Zn, même après décroissance complète du ^{71}Ge. Ceci constitue un important critère quant à l'efficacité de la séparation, sur le plan de la décontamination.

Détermination du rendement des séparations

Après le comptage, on redissout le précipité par 5 ml de NaOH 1 M et 1 ml de H_2O_2 à 110 vol. dont on détruit l'excès par une ébullition prolongée. On détermine alors le rendement des séparations par polarographie classique en milieu alcalin[4] entre -1 et -2 V *vs.* S.C.E. ($E_{\frac{1}{2}}$ pour Ge ~ -1.5 V).

RÉSULTATS EXPÉRIMENTAUX

Résultats qualitatifs

L'examen des spectres γ des précipités de GeS_2 des échantillons des séries III et IV a mis en évidence les isotopes suivants: ^{198}Au ($T_{\frac{1}{2}}$: 2.7 jours) et ^{122}Sb ($T_{\frac{1}{2}}$: 2.8 jours). A partir du filtrat de précipitation, nous avons isolé le ^{82}Br et le ^{32}P respectivement par précipitation de AgBr et de NH_4MgPO_4. Le ^{82}Br a été identifié par son spectre γ; le ^{32}P par mesure de l'énergie maximum β par la méthode de Feather.

Dans tous les cas, les mesures spectroscopiques ont été confirmées par la détermination des périodes radioactives.

Résultats quantitatifs

Ceux-ci sont rassemblés dans le Tableau II. Les valeurs relatives aux échantillons 10 et 14 n'ont pas été prises en considération pour le calcul des moyennes et des écarts-types. L'application du test de Fisher nous a permis de les rejeter comme valeurs aberrantes.

TABLEAU II

RÉSULTATS QUANTITATIFS

Séries	*No.*	*Poids échant. (g)*	*Poids entr. (mg)*	*Activ. mesurée /10^3 sec*[a]	*Rendement (%)*	*Poids de Ge (μg)*	*Teneurs (p.p.m.)*
I	1	1.3737	11.25	1,544,131	96.5	578	418
	2	1.4888	11.05	2,314,249	97.4	644	433
	3	1.6200	12.42	1,827,727	95.6	685	423
	4	1.2134	11.39	1,556,731	71.5	541	446
	5	2.0589	7.50	5,451,690	98.2	912	443
Moyenne (p.p.m.) 433							
σ (p.p.m.) ± 12.2							
σ (%) ± 2.8							
II	6	1.0141	9.59	21,198	94.01	4.58	4.52
	7	0.5815	10.41	13,097	93.1	2.53	4.36
	8	1.0410	10.10	20,467	97.6	4.85	4.66
	9	0.7658	3.08	23,484	93.3	3.60	4.71
	10	0.8449	15.10	22,870	96.2	2.81	(3.33)
Moyenne (p.p.m.) 4.56							
σ (p.p.m.) ± 0.16							
σ (%) ± 3.40							
III	11	0.9821	13.69	3,482	89.9	0.106	0.108
	12	1.7189	14.60	9,033	82.3	0.257	0.150
	13	0.9105	12.39	2,030	89.6	0.082	0.090
	14	0.6748	15.38	11,662	96.8	0.174	(0.259)
	15	1.5757	13.90	4,724	87.0	0.146	0.093
	16	1.6933	8.44	4,003	91.5	0.150	0.089
	17	0.9294	8.92	660	19.7	0.115	0.124
Moyenne (p.p.m.) 0.109							
σ (p.p.m.) ± 0.024							
σ (%) ± 22							
IV	18	0.4755	10.44	1,869	96.6	0.028	0.059
	19	0.8898	12.83	1,191	45.4	0.054	0.061
	20	1.1075	12.92	1,656	91.2	0.027	0.025
	21	1.3816	12.93	4,787	97.6	0.074	0.054
	22	1.1049	10.56	2,142	89.3	0.042	0.038
	23	0.9571	10.94	2,378	93.4	0.057	0.060
Moyenne (p.p.m.) 0.049							
σ (p.p.m.) ± 0.014							
σ (%) ± 29							

[a] Pour la comparaison avec les étalons, nous avons corrigé les mesures en fonction de la décroissance du ^{71}Ge et du rendement mesuré.

DISCUSSION

Précision de la méthode

Les valeurs reprises dans le Tableau III montrent que pour des teneurs de 5–500 p.p.m., la précision du dosage peut être estimée à 3–3.5 %; en dessous de 1 p.p.m., l'écart-type est compris entre 20 et 30%. A ce sujet, nous voudrions faire quelques remarques. En premier lieu, quelle que soit la teneur en germanium, toutes les opérations ont été effectuées de manière reproductible. En second lieu, nous avons veillé spécialement à minimiser les erreurs sur les mesures d'activité: (*a*) en assurant la reproductibilité des conditions géométriques; (*b*) en effectuant un minimum de trois mesures par échantillon; (*c*) en adaptant la durée de la mesure à la valeur de l'activité.

TABLEAU III

PRÉCISION DU DOSAGE

Série	*I*	*II*	*III*	*IV*
Moyenne (p.p.m.)	433	4.56	0.109	0.049
σ (%)	2.8	3.4	22	29

Enfin, les activités spécifiques des deux séries d'étalons étant bien groupées ($\sigma = 2.9$ et 2.5%), on peut admettre que les deux séries d'échantillons ont été irradiées dans des flux assez homogènes.

Dans ces conditions, nous pensons pouvoir vraisemblablement imputer la dispersion des séries III et IV à un défaut d'homogénéité de la répartition du Ge dans le zinc. Un effet semblable a déjà été mis en évidence par MOUSTY *et al.*[5] lors du dosage de l'argent dans un zinc du même type.

Sensibilité de la méthode

Dans le cas des séries III et IV, nous avons pu analyser le premier échantillon 48 h après sa sortie du réacteur. Pour le calcul de la sensibilité de la méthode, nous avons appliqué la formule[6]

$$S = \frac{3\sqrt{2\,A_f/t}}{A_S}$$

où S = sensibilité (μg), A_f = activité du fond continu, t = temps de mesure de A_f (min), A_S = activité spécifique de l'élément (c.p.m./μg).

Dans notre cas, $A_f = 24$ c.p.m. et $A_S = 5118$ c.p.m./μg; ces chiffres permettent de calculer $S = 0.004$ μg, ou encore $S = 4$ p.p.b., pour des échantillons d'un poids voisin de 1 g. La valeur de S est tributaire de l'influence d'un certain nombre de facteurs: (*a*) les caractéristiques nucléaires de l'isotope utilisé, (*b*) l'efficacité du dispositif de mesure, (*c*) le bruit de fond de l'installation, (*d*) le rendement des séparations chimiques, (*e*) le facteur de décontamination, (*f*) la durée et le flux d'irradiation.

Nous pensons bien avoir réalisé, entre ces différents facteurs, un compromis favorable qui nous a permis d'atteindre une sensibilité relativement élevée par rapport aux valeurs généralement citées dans la littérature[7–9], valeurs qui oscillent entre 1 et 0.1 p.p.m.

D'autre part, nous avons pu comparer nos résultats avec ceux de LANFRANCO ET BIANCHINI[10]. Après des précipitations répétées du tannate de germanium et une distillation de $GeCl_4$, ces deux chercheurs isolent le germanium sous forme de GeO_2 dont ils mesurent l'activité au moyen d'un tube G-M usuel (isotope: ^{71}Ge). La méthode par précipitation nous paraît passablement délicate et très susceptible d'occasionner des contaminations du précipité par le ^{65}Zn. Enfin, le mode de comptage adopté nous paraît manquer d'efficacité pour un rayonnement électromagnétique. Ceci pourrait expliquer la faible sensibilité dont font état ces deux auteurs (S = 0.1 p.p.m.). Par contre, leur technique de séparation s'avère nettement plus sélective que l'élution que nous avons pratiquée.

Possibilités de la méthode

Comme nous l'avons déjà signalé, le germanium est accompagné, lors de l'élution, par un certain nombre d'éléments (Au, P, Sb, Br) qui pourraient être dosés sans complication exagérée. En outre, il est possible d'envisager soit d'éluer sélectivement les cations fixés sur la colonne, soit de les récupérer par passage sur la colonne d'une solution d'acide chlorhydrique concentré et d'effectuer une séparation sur colonne anionique.

Nous disposons donc là des données suffisantes pour envisager un schéma élargi d'analyse du zinc par activation neutronique.

C'est un agréable devoir pour nous de témoigner à Monsieur le Professeur G. DUYCKAERTS notre sincère gratitude pour la sollicitude et l'intérêt constants qu'il a bien voulu nous manifester pendant l'accomplissement de ce travail. Nous tenons également à remercier l'Institut Interuniversitaire des Sciences Nucléaires qui a subsidié une partie de ce travail. Nous remercions vivement Monsieur G. SEMPELS, Directeur des Recherches à la Vieille Montagne qui nous a fourni les échantillons de zinc.

RÉSUMÉ

Après séparation préalable du germanium et du zinc sur une colonne de résine Dowex 50, à pH = 1.42, le germanium est précipité sous forme de GeS_2 et l'activité X du ^{71}Ge est comptée par scintillation. Le rendement des séparations a été déterminé par polarographie classique. Avant raffinage par zone, la teneur en germanium s'élève à 0.109 ± 0.024 p.p.m.; après raffinage, elle descend à 0.049 ± 0.014 p.p.m.

SUMMARY

After separation of germanium and zinc on a Dowex 50 resin at pH 1.42, germanium is precipitated as GeS_2 and the ^{71}Ge X-ray activity is counted by scintillation. The chemical yield is determined by classical polarography. Before zone refining, the germanium concentration in zinc was found to be 0.109 ± 0.024 p.p.m.; after zone refining, the content decreased to 0.049 ± 0.014 p.p.m.

BIBLIOGRAPHIE

1 R. MACHIROUX ET F. MOUSTY, *Anal. Chim. Acta*, 42 (1968) 371.
2 R. C. KOCH, *Activation Analysis Handbook*, Academic Press, New York and London, 1960.

3 M. Lederer, J. M. Hollander et I. Perlman, *Table of Isotopes*, 6th Edn., John Wiley, New York, 1967.
4 Gh. Sauvenier et G. Duyckaerts, *Anal. Chim. Acta*, 13 (1955) 396.
5 J. Fouarge, F. Mousty et G. Duyckaerts, *Anal. Chim. Acta*, 36 (1966) 478.
6 F. Girardi, G. Guzzi et J. Pauly, *Data Handbook for Sensitivity Calculations in Neutron Activation Analysis*, EUR 1898, 1965.
7 D. F. C. Morris et J. S. P. Batchelor, *Geochim. Cosmochim. Acta*, 30 (1966) 737.
8 H. P. Yule, *Anal. Chem.*, 38 (1968) 818.
9 J. T. Wasson et J. Kimberlin, *Radiochim. Acta*, 5, 3 (1966) 170.
10 G. Lanfranco et A. Bianchini, *Chim. Ind. (Milan)*, 50 (1968) 332.

Analytica Chimica Acta
Elsevier Publishing Company, Amsterdam
Printed in The Netherlands

FLUORESCENCE AND METALLIC VALENCY STATES

PART III. DETERMINATION OF TIN

B. K. PAL AND D. E. RYAN
Department of Chemistry, Dalhousie University, Halifax, Nova Scotia (Canada)
(Received July 22nd, 1969)

Few fluorimetric methods have been recommended for tin; none has been reported as effective for both tin(II) and tin(IV). A number of compounds[1-6], which are reduced to fluorescent products by tin(II), have been used for the detection of tin. The reaction of flavanol with tin(IV)[7] permits 0.1 p.p.m. to be determined and only phosphate, fluoride, hafnium and zirconium interfere; close control of dimethylformamide concentration is necessary and satisfactory results are not obtained in the presence of chloride ion. Oxine[8] has also been used but the method is not particularly sensitive (2 p.p.m.); STEVENS has suggested, after a study of oxine–metal complexes[9], that metals with variable valence would show, at best, only weak fluorescence.

During recent investigations[10,11] it was observed that oxine-5-sulphonic acid produced a much stronger fluorescence than oxine with tin; similar observations have been reported for substituted oxines with a number of metal ions[12-17]. The present paper describes the use of oxine-5-sulphonic acid for determining parts per billion of tin; equal fluorescence intensity is developed for the same concentrations of tin(II) and tin(IV) and large amounts of chloride ion do not interfere.

EXPERIMENTAL

Apparatus, reagents and solutions

An Aminco Bowman Spectrophotofluorimeter was used for recording excitation and emission spectra. A Bausch and Lomb Spectronic 505 recording spectrophotometer was employed to record absorption spectra.

8-Hydroxyquinoline-5-sulphonic acid was recrystallized several times from water and dried at 110°; the melting point was 320–323° with decomposition. Reagent solutions ($10^{-3}F$) were freshly prepared in doubly distilled water.

Stock tin(IV) solutions were prepared by dissolving 500 mg of tin foil in 20 ml of aqua regia and diluting to 250 ml. Tin(II) solutions were similarly prepared in hydrochloric acid or were obtained from standard tin(IV) solutions by reduction with sodium hydrosulphite (1% in water) or thioglycollic acid (1:5).

Acetate–acetic acid buffers (4.0–5.2) were prepared in the usual manner[18].

Procedure

To 1 ml of neutral solution containing 0.05–2.5 μg of tin(II) or tin(IV), add 2–3 ml of acetate–acetic acid buffer and a 125–250 molar excess of oxine-5-sulphonic acid. Dilute to 10 ml in a volumetric flask and measure the fluorescence intensity at 510–515 nm after 10 min; the excitation wavelength is 360 nm. A reagent blank should be run concurrently.

Typical results are shown in Fig. 1. Excitation and emission spectra are shown in Fig. 2.

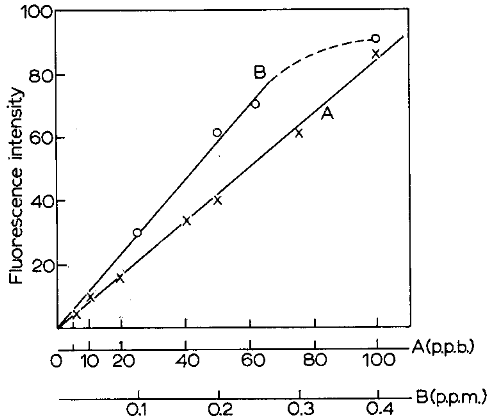

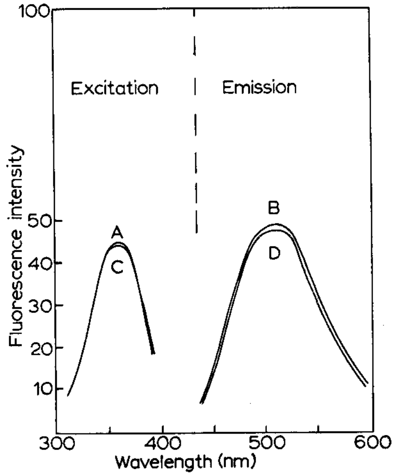

Fig. 1. Calibration curves. (A) Meter multiplier (MM) setting 0.003 and sensitivity (S) 25; (B) MM 0.01 and S 30.

Fig. 2. Fluorescence spectra, MM 0.003 and S 0. (A) and (B) are excitation and emission spectra for tin(II) (0.1 p.p.m.)–oxine sulphonic acid complex; (C) and (D) are similar spectra for tin(IV) (0.1 p.p.m.)

RESULTS AND DISCUSSION

Factors affecting fluorescence intensity

The fluorescence intensity was maximum and constant when the molar ratio of reagent to tin was 125–250:1. For 0.1 p.p.m. of tin the relative intensity was 14 for a reagent-to-metal ratio of 10:1, 70 for 100:1, 83±0.5 for 125, 150, 200 and 250:1, and 75 for 300:1 at the same instrument setting.

Constant maximum intensity was obtained in the pH range 4.0–5.2. The intensity decreased at lower and higher pH values; for 0.1 p.p.m. of tin the fluorescence intensity was 66 at pH 3.5, 82 at pH 4.0, 4.5 or 5.2, and 50 at pH 5.8.

The fluorescence intensity reached a maximum after 10 min and remained constant for hours; at the same instrument setting the fluorescence intensity was 36 after 5 min, 39 after 10, 30, 60 and 180 min and 38 after 28 h.

Ethanol, methanol, *p*-dioxane and dimethylformamide increased the fluorescence intensity but for consistent results close control of their concentration was necessary; on increasing the % methanol from 50 to 80%, the intensity increased by a factor of 3.5. Less than 1 p.p.b. of tin could be determined in ethanol, methanol or *p*-dioxane solutions.

Results and interferences

Plots of fluorescence intensity against metal concentration are linear through the origin from 5 p.p.b. to 0.25 p.p.m. (Fig. 1). Ten samples, each containing 0.1 p.p.m. of tin, were analyzed by the above procedure; the percent standard deviation was 1.4.

Tin (0.1 p.p.m.) was accurately determined in the presence of 1000 p.p.m. of Ba^{2+}, Ca^{2+}, Mn^{2+}, Sr^{2+}; 300 p.p.m. Fe^{2+}; 200 p.p.m. Be^{2+}, Ce^{3+}, La^{3+}, Pb^{2+}, Tl^{+}; 100 p.p.m. Li^{+}; 50 p.p.m. Mg^{2+}; 25 p.p.m. Cd^{2+}, Th^{4+}; 20 p.p.m. Co^{2+}. Large amounts (10,000 p.p.m.) of sodium, potassium, ammonium, acetate, chloride, chlorate, perchlorate, cyanate, thiocyanate, nitrate, phthalate, sulphate, thiosulphate, hydrosulphite, hydroxylamine hydrochloride, thioglycollic acid and 2000 p.p.m. of persulphate had no effect on the results obtained. Although iron(III), copper(II) and mercury(II) quench the fluorescence in the normal procedure, 300 p.p.m. of iron(III), 75 p.p.m. of copper(II) and 100 p.p.m. of mercury(II) do not interfere in the determination of 0.1 p.p.m. of tin in the presence of hydroxylamine hydrochloride or thioglycollic acid (for iron), sodium thiosulphate (for copper) or chloride ions (for mercury).

Small amounts of fluoride (5 p.p.m.) and EDTA (2.5 p.p.m.) quench the fluorescence of 0.1 p.p.m. of tin; relatively large amounts (500 p.p.m.) of citrate, oxalate, or

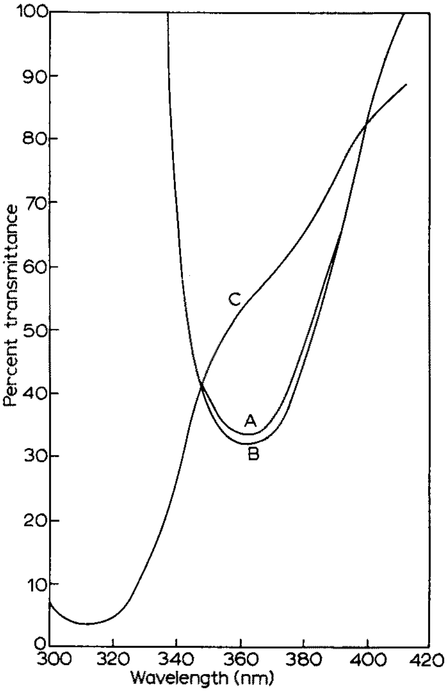

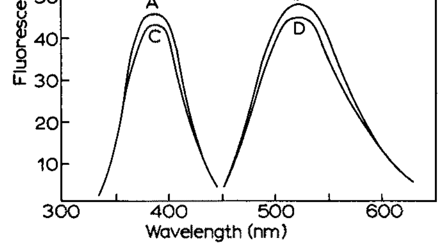

Fig. 3. Absorption spectra. (A) Tin(II)–oxine sulphonic acid *vs.* reagent blank; (B) tin(IV)–oxine sulphonic acid *vs.* reagent blank; (C) reagent *vs.* water blank. Solutions were prepared by mixing 0.05 ml of $1.8 \cdot 10^{-2}$ *F* tin solutions with 0.25 ml of $1.77 \cdot 10^{-2}$ *F* reagent and 5 ml of pH 4 buffer and diluting to 10 ml.

Fig. 4. Fluorescence spectra, MM 0.01 and S 0. (A) and (B) are excitation and emission spectra of tin(IV) (3.4 p.p.m.)–oxine complex in chloroform; (C) and (D) are similar spectra for tin(II) (3.4 p.p.m.) obtained by reduction of tin(IV) solution with sodium hydrosulphite.

tartrate reduce the intensity by 40–50%. Traces of aluminium (0.1 p.p.m.), zinc (1 p.p.m.), zirconium and hafnium (2 p.p.m.) increase the fluorescence of 0.1 p.p.m. of tin by 20–45%, whereas nickel (4 p.p.m.) reduces the fluorescence by 35%.

Nature of reaction

Both tin(II) and tin(IV) behave similarly with oxine-5-sulphonic acid. Their excitation and emission spectra are the same (Fig. 2) and the relative fluorescence intensities are essentially identical (47.5 and 48 for 0.1 p.p.m. tin) under the same experimental conditions; results are similar in the presence of 1000 times excess of reducing (hydrosulphite) or oxidizing (persulphate) agents. Figure 3 shows that the absorption spectra for both the tin(II) and tin(IV) complexes are practically identical with an absorption maximum at 362 nm; mole-ratio studies at this wavelength show that one mole of tin(II) or tin(IV) combines with two moles of reagent in complex formation. A possible explanation for the similar behaviour of tin(II) and tin(IV) may lie in the fact that both ions could be in a similar octahedral environment (for tin(II) the ns^2 electrons would occupy one coordination position); $[SnQ_2H_2O]^{2-}$ and $[SnQ_2(OH)_2]^{2-}$, where H_2Q represents oxine-5-sulphonic acid, might then be written for the tin(II) and tin(IV) complexes.

Figure 4 shows that oxine is similar to oxine-5-sulphonic acid in the fluorescence behaviour of its tin complexes; the reason for the large difference in fluorescent intensity of the oxine and oxine-5-sulphonic acid tin complexes is not clear. However, since polarity changes in the environment of the chelated metallic ion can result in marked alteration of emission intensity, such a difference between molecular (oxine) and ionic (oxine-5-sulphonic acid) complexes is not surprising.

This work was supported by grants from the National Research Council and Defence Research Board.

SUMMARY

Tin is selectively and simply determined in aqueous solution by measuring the fluorescence produced with oxine-5-sulphonic acid at a pH of 4–5.2; intensities are linear from 5 p.p.b. to 0.25 p.p.m. The fluorescence intensity attains a maximum after 10 min and is constant for hours. Few ions interfere and less than 1 p.p.b. can be determined in alcoholic solutions. Fluorescence spectra and intensities are independent of the valence state of the metal.

RÉSUMÉ

L'étain peut être dosé sélectivement et simplement en solution aqueuse en mesurant la fluorescence produite avec l'acide oxinesulfonique-5, à un pH de 4 à 5.2. Les intensités sont linéaires de 5 p.p.b. à 0.25 p.p.m. L'intensité de fluorescence atteint un maximum après 10 minutes: elle est constante pendant des heures. Peu d'ions gênent: il est possible de doser moins de 1 p.p.b. dans des solutions alcooliques. Les spectres de fluorescence et les intensités sont indépendants de la valence du métal.

ZUSAMMENFASSUNG

Zinn wird selektiv und einfach in wässriger Lösung durch Messung der Fluoreszenz bestimmt, welche durch Oxin-5-sulfonsäure beim pH 4–5.2 gebildet wird. Zwischen den Intensitäten besteht eine lineare Beziehung von 5 p.p.b. bis 0.25 p.p.m. Die Fluoreszenzintensität erreicht nach 10 Min ein Maximum und ist dann für Stunden konstant. Einige Ionen stören; weniger als 1 p.p.b. kann dann in alkoholischen Lösungen bestimmt werden. Die Fluoreszenzspektren und -intensitäten sind von der Wertigkeit des Metalles unabhängig.

REFERENCES

1 J. R. A. Anderson and J. L. Garnett, *Anal. Chim. Acta*, 8 (1953) 393.
2 J. R. A. Anderson and S. L. Lowy, *Anal. Chim. Acta*, 15 (1956) 246.
3 J. R. A. Anderson and J. L. Garnett, *Anal. Chim. Acta*, 17 (1957) 453.
4 J. R. A. Anderson and L. C. Lock, *Anal. Chim. Acta*, 17 (1957) 474.
5 J. R. A. Anderson and J. L. Garnett, *Anal. Chim. Acta*, 19 (1958) 257.
6 J. R. A. Anderson, J. L. Garnett and L. C. Lock, *Anal. Chim. Acta*, 22 (1960) 1.
7 C. E. White and C. F. Coyle, *Anal. Chem.*, 29 (1957) 1486.
8 E. P. Shkrobot and L. B. Ginzberg, *Zavodsk. Lab.*, 23 (1957) 527.
9 H. M. Stevens, *Anal. Chim. Acta*, 20 (1959) 389.
10 D. E. Ryan and B. K. Pal, *Anal. Chim. Acta*, 44 (1969) 385.
11 B. K. Pal and D. E. Ryan, *Anal. Chim. Acta*, 47 (1969) 35.
12 W. E. Ohnesorge and A. L. Burlingame, *Anal. Chem.*, 34 (1962) 1086.
13 W. E. Ohnesorge, *Anal. Chem.*, 35 (1963) 1137.
14 D. A. Carter and W. E. Ohnesorge, *Anal. Chem.*, 36 (1964) 327.
15 W. E. Ohnesorge, *J. Inorg. & Nucl. Chem.*, 29 (1967) 485.
16 E. A. Bozhevol'nov, *Oesterr. Chemiker-Ztg.*, 66 (3) (1965) 74.
17 G. V. Serebryakova, I. A. Krasavin, E. A. Bozhevol'nov and V. M. Dziomko, *Tr. Vses. Nauchn.-Issled. Inst. Khim. Reaktivov*, 26 (1964) 97.
18 A. I. Vogel, *A Textbook of Quantitative Inorganic Analysis*, Longmans, New York, 1951, p. 869.

Analytica Chimica Acta
Elsevier Publishing Company, Amsterdam
Printed in The Netherlands

ION EXCHANGE, EXTRACTION, SEPARATION AND RADIOCHEMICAL DETERMINATION OF NEPTUNIUM-237 IN PLUTONIUM-238

J. BUBERNAK, M. S. LEW AND G. M. MATLACK
University of California, Los Alamos Scientific Laboratory, Los Alamos, N. M. (U.S.A.)

(Received May 30th, 1969)

Enriched plutonium-238 is generally produced by neutron irradiation of neptunium-237, and a specification for the purified product is the neptunium content. While the radiochemical determination of neptunium-237 by α-counting is more sensitive than other methods of measurement[1], a highly effective separation from plutonium must first be made due to its intense α-activity. The separation of neptunium from uranium is also required, mainly to remove the α-emitting uranium-234 daughter of plutonium-238.

Two separation methods were studied. The first involved cation exchange with dilute acid as eluent, following work carried out by ZOLOTOV AND NISHANOV[2]. The second method employed solvent extraction from *ca.* 1 *M* acid with thenoyltrifluoroacetone (TTA) in xylene as described by MOORE[3]. The present study concerns modifications of each of these methods which have resulted in significant improvements of separation. Thus, cation exchange was best carried out in hydrobromic acid medium, while tin(II) chloride was found to be a superior reducing agent for use in the TTA extraction. Although neither cation exchange nor TTA extraction alone was adequate for producing a neptunium fraction free of plutonium-238, the sequential use of these two steps proved satisfactory.

EXPERIMENTAL

Apparatus

Ion-exchange columns, 0.5 cm i.d. and 20 cm in length.

Extraction equipment, consisting of a motor-driven rotating hollow glass tube with side hole at the organic–aqueous interface for mixing the phases in a 15 × 150-mm test tube.

Gamma counter, utilized a standard NaI(Tl) detector and was adjusted for the detection of γ-rays with energy above 30 keV.

Alpha counter, methane proportional type.

Alpha pulse-height Analyzer, 400-channel employing a silicon detector.

Reagents

The cation-exchange resin was Dowex 50-X4, 200–400 mesh size in purified form (Bio Rad Laboratories, Richmond, Calif., U.S.A.). It was used without further purification.

Hydrobromic acid of technical grade was redistilled at atmospheric pressure through a 200-mm long fractionating column, but the analytical grade acid obtained from Baker Chem. Co. (Philipsburg, N.J., U.S.A.) was used without further purification.

All other reagents used were of analytical grade.

Preparation of tin(II) chloride reducing solution

Tin(II) chloride dihydrate (25 g) was dissolved in 15 ml of concentrated hydrochloric acid, 0.2–0.5 g of iron(II) chloride dihydrate was added, and the solution was diluted to 50 ml with water.

Preparation of TTA extractant

A 0.5 *M* solution was made by dissolving 111 g of thenoyltrifluoroacetone in xylene and diluting to 1 l.

Preparation of neptunium tracer

A ready source of 2.3-d neptunium-239 tracer was constructed by absorbing 10–100 μg of americium-243 on a column, 0.8 cm in inside diameter and 8 cm long, filled with Dowex 50-X4, 200–400 mesh resin. When neptunium tracer was required, a few drops of 10% periodic acid solution were allowed to penetrate the top of the resin bed and remain for about an hour. Then the oxidized neptunium was eluted with 0.5 *M* hydrochloric acid. Upon collecting 2-ml fractions of eluate, the excess periodic acid was obtained first, followed by the desired neptunium. Milking of the column in this way could be repeated at approximately weekly intervals.

Neptunium-237 used in the present study was obtained from the metallurgy group of the Los Alamos Scientific Laboratory. The activity from this material contained 3% α-radiation from uranium-234. Corrections for this impurity were made in the calculations.

Procedure for separation and determination of neptunium

Aliquots of neptunium-239 tracer and of the plutonium sample were pipeted into a beaker and the mixture was evaporated to near dryness. Evaporation was repeated twice more after additions of 2 ml of concentrated hydrobromic acid (care being taken if the sample was in the nitrate form, because of its vigorous reaction with bromide). The final residue was treated with 10 drops of 9%(v/v) hydrobromic acid and 1 drop of liquid bromine, and the solution was allowed to stand for 10 min. It was then absorbed on the resin column. Upon eluting with 9%(v/v) hydrobromic acid, complete removal of neptunium was usually accomplished within the first six column volumes (*ca.* 12 ml) while that of uranium, when desired, required an additional twelve column volumes. The plutonium absorbed on the resin was recovered by eluting with 6 *M* hydrochloric acid.

The neptunium fraction was treated with 0.5 ml of tin(II) chloride reagent and allowed to stand for 10 min. TTA extractant (1 ml) was added. Extraction was carried out for 15 min and, after the phases had separated, an aliquot of the organic solution was evaporated on a counting plate and ignited. The amount of neptunium-237 in the sample was determined from its α-activity. Chemical recovery was calculated from the γ-activity of the original neptunium-239 tracer found in the neptunium fraction.

A minor correction was required in the chemical recovery calculations, because neptunium-237 emits γ-rays. This correction amounted to 0.143 γ per α under the conditions of these experiments. This factor should be re-determined for other counting arrangements by using neptunium-237 from which its daughter protactinium-233 has been separated by, *e.g.* cation exchange.

RESULTS AND DISCUSSION

Ion-exchange studies

Preliminary studies were made with plutonium-239 samples in place of the more radioactive plutonium-238. Since plutonium-239 samples contained very little neptunium activity some α-emitting neptunium-237 and/or γ-emitting neptunium-239 were added to follow the progress of its elution. Sufficient uranium-237 was present to act as a tracer for that element, while the behavior of plutonium was followed by means of α-activity measurements.

Evaporation of a sample containing plutonium and neptunium with hydrobromic acid produced the species plutonium(III) and neptunium(IV) as pointed out by NELSON AND MICHELSON[6]. Subsequent dilution and treatment with bromine caused partial oxidation of plutonium to plutonium(IV) and of neptunium to neptunium(V). Uranium remained in the uranium(VI) state. After the treated sample had been absorbed by the cation resin, elution with 9%(v/v) hydrobromic acid resulted in the removal of neptunium, followed by uranium, while plutonium remained essentially absorbed (Fig. 1). The combined neptunium fractions (*e.g.*, fractions 2–6) showed a decontamination factor for plutonium α-activity of about 10^8 consistently in a series of runs. The small amount of plutonium activity eluted was presumed to be due to plutonium(VI). In other similar ion-exchange elutions another plutonium activity peak preceded that of neptunium, probably caused by plutonium(V) and/or polymeric plutonium(IV). These suggestions as to plutonium species are based on their elution behavior compared with those of neptunium(V) and uranium(VI), following cation-exchange studies of DIAMOND *et al.*, for ionic species[4] and by OCKENDEN AND WELCH for plutonium polymer[5].

Mechanism of oxidation of neptunium(IV)

The present work indicates that neptunium(IV) is oxidized to the pentavalent state in the presence of plutonium but not in its absence. This confirms the study by NELSON AND MICHELSON[6] who found no oxidation of neptunium(IV) by bromine. Table I shows the effect of plutonium on the recovery of both neptunium-239 tracer and macro quantities of neptunium-237 from the cation resin column. Reduction by hydrobromic acid followed by treatment with bromine in the absence of plutonium yielded almost no weakly absorbable neptunium species in cation exchange, indicating that it remained tetravalent. However, when >0.5 mg of plutonium was present, essentially quantitative recovery of neptunium was found, indicating complete oxidation of neptunium(IV). Evidently the oxidation of neptunium(IV) must proceed indirectly by plutonium(IV). The curious fact is that this method is most suitable for the isolation of minute quantities of neptunium from plutonium, while it cannot be applied to substantially pure neptunium samples. Recoveries of neptunium were not changed in the presence of 1–200 mg of plutonium. As shown in Table I, recovery of uranium also was essentially quantitative.

In some of the cation-exchange experiments, the Pu(IV)/Pu(III) ratio was determined in the plutonium fraction removed from the resin column, by measuring the amount of plutonium(IV) which was extracted into TTA–xylene. This ratio varied from 0.05 to 0.20. Calculations show that if oxidation of neptunium(IV) proceeds by plutonium(IV) then a Pu(IV)/Pu(III) ratio of 0.01 is sufficient to ensure

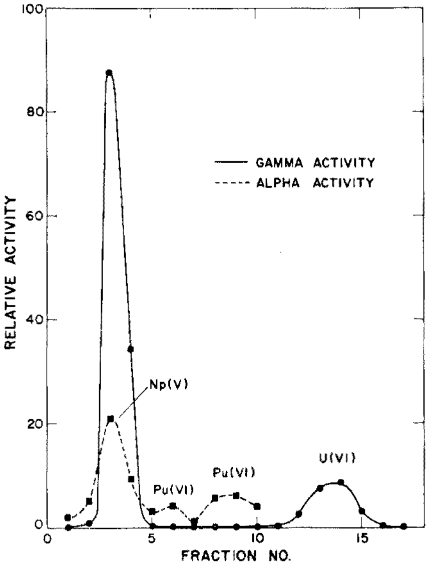

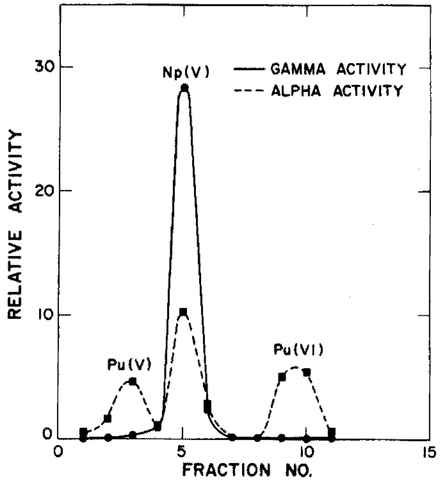

Fig. 1. Elution curve for ion exchange of ^{239}Pu with added ^{239}Np tracer. 9% (v/v) HBr as eluent. Each fraction represents approximately one column volume.

Fig. 2. Elution curve for ion exchange of ^{239}Pu with added ^{239}Np tracer. 0.5 *M* HNO_3 as eluent. Each fraction represents approximately one column volume.

TABLE I

NEPTUNIUM AND URANIUM RECOVERIES IN CATION EXCHANGE AFTER $HBr–Br_2$ TREATMENT

Pu added (mg)	*Np or U added*	*Recovery (%)*
0	^{239}Np tracer	2
0	13.8 mg ^{237}Np	1
0.2	13.8 mg ^{237}Np	59
0.4	13.8 mg ^{237} Np	94
1	13.8 mg ^{237} Np	100
4	^{239}Np + 13.8 mg ^{237}Np	100
8	^{239}Np + 13.8 mg ^{237}Np	100
40	^{239}Np	99
80	^{239}Np	100
120	^{239}Np	100
160	^{239}Np	99
200	^{239}Np	100
30	70.4 mg ^{234}U	99

complete oxidation. It is a relatively easy matter to oxidize neptunium completely while maintaining a low Pu(IV)/Pu(III) ratio, which in turn is a favorable situation for suppressing the formation of weakly absorbable plutonium(V) and (VI) in cation exchange. On this basis lies the success of this new technique.

Cation exchange with dilute nitric acid as eluent as described by ZOLOTOV AND NISHANOV[2] depends on the absorption of plutonium entirely as the plutonium(IV) species. An elution curve obtained by following their procedure is shown in Fig. 2. On combining those fractions which included all the neptunium activity (fractions 2–8), α-pulse analysis showed a decontamination factor of nearly 10^8 for plutonium. However, such behavior was not typical. Identical pretreatment of several samples in some cases showed this type of elution, while more often an undesirably large amount of plutonium appeared in the neptunium fraction. Evidently the formation of the desired plutonium(IV) to the complete exclusion of other species is difficult to accomplish.

Cation exchange of plutonium-238 samples

The hydrobromic acid elution technique yields elution curves for plutonium-238 samples which are similar to those for plutonium-239. However, one complication with plutonium-238 arises as a result of extensive radiolysis of its solutions by α-particles. It is important to evaporate with hydrobromic acid to very near dryness in order to destroy accumulated radiolysis products.

In Fig. 3, the elution curve (A) represents a case in which 10 mg of 80% (w/w) plutonium-238 in solution was evaporated with hydrobromic acid to *ca.* 0.5 ml, as was done with plutonium-239 samples. Under these conditions, tailing of neptunium into the uranium peak was observed. Because of this the yield of neptunium was as low as 95%. In addition, plutonium contamination was likely to be greater than desired. The next elution curve (B) represents a case in which evaporation of the sample was taken too far to dryness. This condition probably favors the formation of plutonium(V) species and/or plutonium(IV) polymer which results in considerable contamination of the neptunium fraction, and is therefore best avoided. At the same time, however, the neptunium activity is eluted sharply in just a few column volumes. The last curve (C) was obtained when evaporation with hydrobromic acid was made carefully to very near dryness. Neptunium elution was again quite sharp and was accompanied by minimal contamination. α-Decontamination factors for plutonium under these conditions often exceeded 10^8. When insufficient care was taken in the evaporations, the decontamination factors were only about 10^6. These contaminated neptunium fractions could still be salvaged, however, since subsequent extraction with TTA removed that amount of plutonium remaining.

After absorption of plutonium-238 samples on cation resin from dilute acid, the continual generation of radiolysis products and their eventual decomposition produces gas gubbles. This in turn causes disruption of the resin bed, which becomes serious for sample sizes in excess of about 12 mg of plutonium-238 with the columns used. Therefore the recommended sample size is one containing not more than 10 mg of plutonium-238.

Extraction with TTA

A TTA-extraction step is easily included for further purification to remove the

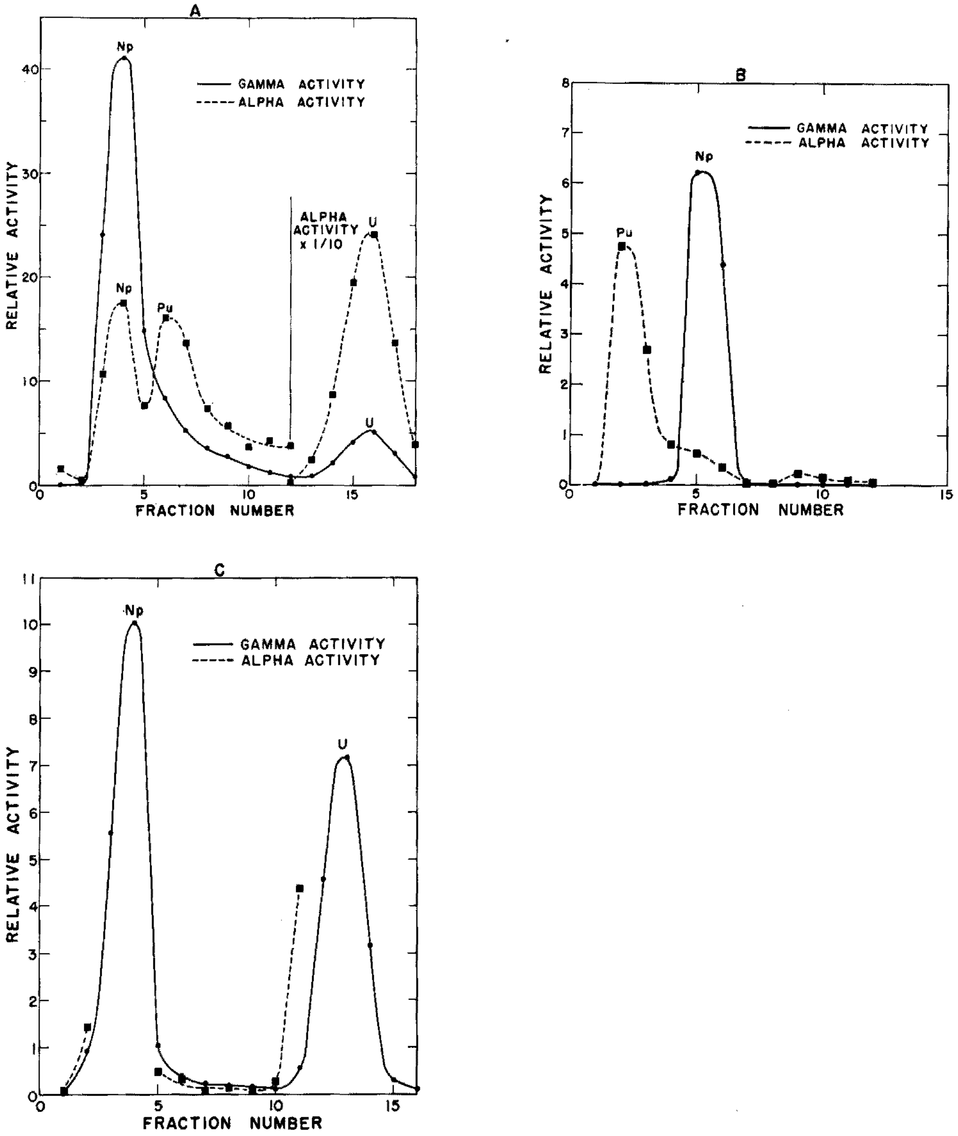

Fig. 3. Elution curves for ion exchange of ^{238}Pu with added ^{239}Np tracer. 9% (v/v) HBr as eluent. Effect of evaporations with HBr (A) not taken sufficiently to dryness, (B) taken to dryness, and (C) carefully made to near dryness. Each fraction represents approximately one column volume.

last amounts of plutonium and other foreign activities from the isolated neptunium. The preliminary step of ion exchange produces a neptunium fraction in 0.8 *M* hydrobromic acid. This is approximately the correct acidity for TTA-extraction. It is only necessary to add an appropriate reducing agent which will produce neptunium(IV) and plutonium(III), and then to extract the neptunium by the method of MOORE[3]. The various reducing agents which have been successfully employed by MOORE and others include iron(II), hydroxylamine, iodide, ascorbic acid, sulfamate and combinations of these. In the present study, tin(II) was found to be superior to these from the standpoint of providing decontamination from plutonium as well as allowing high recovery of neptunium from the cation-exchange eluate containing bromine.

Tin(II) reacts slowly with neptunium(V). However, in the presence of iron(II) as catalyst[7], reduction is complete in a few minutes. Preparation of the reducing agent in the manner described above provided the proper amount of iron(II), as well as a high concentration of chloride ion to prevent hydrolysis of tin. Surprisingly, this tin(II) reagent proved to be quite stable towards air oxidation, the reducing power decreasing by only 20% in six months.

Extraction of neptunium by TTA was quantitative when equal volumes of aqueous and organic phases were equilibrated. Thus, in six runs an average recovery of 99.7% of neptunium-239 tracer was found. In the overall procedure, however, it was desired to increase the aqueous/organic phase ratio to 10/1 in order to obtain a greater sensitivity. Under these conditions recoveries of neptunium in extraction averaged 96% in four runs. Decontamination factors for plutonium in the extraction showed an average of $3 \cdot 10^4$ in eight runs under the same conditions. The amount of tin extracted into TTA was very low and caused no interference in α-counting.

Recovery and reproducibility

Table II shows the results obtained when synthetic samples of 80%(w/w)

TABLE II

ANALYSIS OF 80% (w/w) PLUTONIUM-238 SAMPLES SPIKED WITH NEPTUNIUM-237

^{237}Np (p.p.m.)		*Error*
Added	*Found*	*(%)*
0	8[a]	—
52	54	+4
130	133	+2
519	504	−3
2596	2562	−1

[a] 'Blank' value, used in correcting subsequent values.

TABLE III

PRECISION AND CHEMICAL YIELDS FOUND IN NEPTUNIUM ANALYSIS

Run no.	*^{237}Np found (p.p.m.)*	*Chemical yield (%)*
1	856	88.5
2	905	94.8
3	870	96.0
4	869	86.5
5	879	96.3
6	867	93.1
7	888	94.5
8	870	92.4
	Average = 877	92.8
	Rel. std. dev. = 1.7%	

plutonium-238 containing known amounts of neptunium-237 were analyzed by the cation exchange–extraction procedure. The original stock solution of plutonium had previously been purified by cation exchange to reduce its neptunium content to less than 10 p.p.m. Agreement between the amounts of neptunium added and that found by analysis was satisfactory.

The reproducibility of analyses and chemical yields are shown in Table III. In 8 determinations made on a sample, an average of 877 p.p.m. neptunium was obtained, with a relative standard deviation of 2%. The average chemical yield in these determinations was 93%.

Application to typical samples

Table IV shows results of typical analyses for three different types of samples covering a wide range of neptunium contents. The first type represents bomb-reduced or electro-refined[8] plutonium-238 metal dissolved in hydrochloric acid. The abnormally high value for sample 10 was due to the fact that it was produced from the anolyte of the electro-refining cell where neptunium had concentrated. The second type of sample represents plutonium dioxide dissolved in nitric acid with the aid of some hydrofluoric acid. The fact that fluoride ion did not interfere in the analyses indicates the effectiveness of evaporation with hydrobromic acid towards volatilizing other acids. The third type of sample was a portion of sodium chloride–potassium chloride electrolyte from the electro-refining cell[8]. Since large amounts of sodium ion interfere with neptunium elution in ion exchange, a preliminary step was required involving precipitation of plutonium, neptunium and uranium as hydroxide. Sodium remained in solution and was removed with the supernate. The range for duplicate determinations for all analyses shown in Table III was less than 10%.

TABLE IV

NEPTUNIUM-237 CONTENTS FOUND AND PRECISION OBTAINED FOR TYPICAL 80% (w/w) PLUTONIUM-238 SAMPLES

Sample type	*Sample no.*	*Ave Np found (p.p.m.)*	*Range of duplicate determinations (%)*
I HCl	1	598	0.6
	2	827	4.6
	3	829	2.2
	4	865	6.0
	5	898	0.4
	6	1890	5.6
	7	2804	1.4
	8	3516	0.4
	9	4396	1.2
	10	20042	0.9
II HNO_3, with HF	11	795	2.0
	12	822	2.6
	13	1967	2.0
	14	1990	8.0
	15	3633	0
III NaCl	16	12.4	0.8
	17	27	1.0

Analysis of a sample in duplicate for neptunium content requires about 8 h; an additional 4 h is required for the further separation of uranium activity if this is desired. Based on an arbitrary lower limit of 10 counts/min α-activity, the sensitivity for detection of neptunium from a 10-mg sample is 2 p.p.m. Thus, 10 p.p.m. could be determined with reasonable precision.

Although the determination of uranium in samples of plutonium-238 was carried out simultaneously with that of neptunium, this subject is not critically evaluated in the present discussion. It suffices to mention that α-pulse analysis of the uranium fraction usually was possible in the presence of the small amount of plutonium contamination present. Separate activity peaks representing uranium-232 and uranium-234 were measured with little difficulty.

SUMMARY

Neptunium-237 in concentrations of 10 p.p.m. can be isolated from 10-mg quantities of plutonium-238, with sufficient purity to allow its determination by direct α-counting. After suitable treatment of the sample in hydrobromic acid medium, neptunium(V) is separated from the bulk of plutonium by cation exchange. The neptunium eluate is then treated with tin(II) chloride, and neptunium(IV) is extracted into TTA–xylene, leaving the last amount of plutonium in the aqueous phase. Uranium causes no problem and can be determined simultaneously in the same sample.

RÉSUMÉ

Le neptunium-237 en concentration de 10 p.p.m. peut être séparé d'avec 10 mg de plutonium-238: la pureté est suffisante et permet son dosage par comptage-α direct. Après traitement approprié de l'échantillon en milieu acide bromhydrique, le neptunium(V) est séparé d'avec le plutonium par échangeur de cations. L'éluat de neptunium est ensuite traité avec du chlorure d'étain(II); le neptunium(IV) formé est extrait dans le TTA-xylène, laissant les dernières traces de plutonium dans la phase aqueuse. L'uranium ne pose pas de problème et peut être dosé simultanément sur le même échantillon.

REFERENCES

1 G. A. Burney, E. K. Dukes and H. J. Groh, *Progr. Nucl. Energy, Ser. IX*, 6 (1966) 188.
2 Yu. A. Zolotov and D. Nishanov, *Radiokhimiya*, 4 (1962) 241.
3 F. L. Moore, *Anal. Chem.*, 29 (1957) 941.
4 R. M. Diamond, K. Street and G. T. Seaborg, *J. Am. Chem. Soc.*, 76 (1954) 1461.
5 D. W. Ockenden and G. A. Welch, *J. Chem. Soc.*, (1956) 3358; J. J. Katz and G. T. Seaborg (Editors), *The Chemistry of the Actinide Elements*, Methuen, 1957, p. 302.
6 F. Nelson and D. C. Michelson, *J. Chromatog.*, 25 (1966) 414.
7 J. C. Hindman, L. B. Magnusson and T. J. LaChapelle, *Natl. Nucl. Energy, Ser. IV*, 14B, Part II, McGraw-Hill, New York, 1949, p. 1032.
8 L. J. Mullins and J. A. Leary, *Trans. Am. Nucl. Soc.*, 11 (1968) 91.

Analytica Chimica Acta
Elsevier Publishing Company, Amsterdam
Printed in The Netherlands

CHLOROFORM EXTRACTION AND POLYMERIZATION OF TETRAPHENYLARSONIUM CHLORIDE*

J. S. FOK**, Z Z. HUGUS*** AND E. B. SANDELL
School of Chemistry, University of Minnesota, Minneapolis, Minn. 55455 (U.S.A.)

(Received August 19th, 1969)

Tetraphenylarsonium chloride is well known as a reagent forming slightly soluble ion-pair compounds with large anions, many of which can be extracted into chloroform. The extraction behaviour of tetraphenylarsonium chloride itself is incompletely known and its polymerization in chloroform has been overlooked. Conductance measurements show the salt to be extensively ionized in water, but have failed to give the dissociation constant[1]. The polymerization of tetraphenylarsonium chloride in chloroform has been investigated by two different methods and its partition constant (chloroform/water) and ionization constant in water have been determined.

EXPERIMENTAL

Reagents

Tetraphenylarsonium chloride hydrochloride (tetraphenylarsonium hydrogen dichloride, $(C_6H_5)_4AsCl \cdot HCl$, Light and Co., Colnbrook, England) was recrystallized 4 times by treating a saturated aqueous solution with thrice its volume of concentrated hydrochloric acid. The solution of the purified salt was neutralized with sodium carbonate, evaporated to dryness, and the residue was extracted with dry chloroform to separate sodium chloride. The chloroform was evaporated, the crystals were dissolved in a minimum volume of absolute ethanol, and tetraphenylarsonium chloride was precipitated by addition of ether and dried at 150° (m.p. 259.5–261°). Potentiometric titration with standard iodine solution[2] to form $(C_6H_5)_4AsI_3$ showed a purity of 99.9%, and potentiometric titration with silver nitrate a purity of 99.99%.

Pure chloroform was obtained by successively shaking a reagent-quality product (containing ethanol as preservative) with concentrated sulfuric acid, water, sodium hydroxide, and water, and distilling after drying with calcium chloride. The purified chloroform was stored under nitrogen, but was discarded after 2 days.

Apparatus

A Beckman Model DU spectrophotometer was used in quantitative spectral work, with 1-, 2-, and 5-cm fused silica cells, whose path lengths were checked with alkaline chromate solutions. Vapor pressures of chloroform solutions of tetraphenylarsonium chloride were measured with a recording osmometer[3].

---

* Based on the Ph D. thesis of J. S. FOK, University of Minnesota, 1963.
** Present address: E. I. du Pont de Nemours and Co., Wilmington, Del.
*** Present address: Department of Chemistry, North Carolina State University, Raleigh, N. C.

Pipets used with tetraphenylarsonium chloride solution were coated with a silicone (Desicote) film, since this solution tends to form droplets on untreated glass.

General procedures

Solubilities were determined by shaking solid tetraphenylarsonium chloride with chloroform and water in glass ampoules for 12 h or more. The concentration of the saturated solutions was obtained by evaporating to dryness and weighing the residue of $(C_6H_5)_4AsCl$ after vacuum drying at 150° or by titrating the aqueous solution potentiometrically with tri-iodide.

Extractions were carried out by shaking an aqueous solution of known tetraphenylarsonium chloride concentration with an equal volume of chloroform presaturated with water. The shaking time was usually 10 min, which was more than ample, because the same results were obtained by shaking for 2 min. After separation of the phases and filtration through glass wool, the analytical concentration of tetraphenylarsonium chloride was determined by measuring the absorbance of the chloroform and water solution at 264 nm (0.12 mm slit width) and referring to a standard curve ($\varepsilon_{264}=3400$ in water; $\varepsilon_{264}=3500$ in chloroform). Absorbance was proportional to concentration in both solvents up to $1.5 \cdot 10^{-4} M$ at least. The absorbance in water was not affected by sodium chloride or hydrochloric acid. Solutions were suitably diluted when necessary. As a rule, the concentration was determined in the phase containing the lesser amount of tetraphenylarsonium, and the concentration in the other was found by difference, but at low total concentrations it was determined in both phases. In some experiments, tetraphenylarsonium chloride was determined in the aqueous phase by potentiometric titration with tri-iodide.

RESULTS AND DISCUSSION

Solubilities

Table I summarizes determinations of the solubility of $(C_6H_5)_4AsCl \cdot 2H_2O$ in water and 1.00 *M* sodium chloride and of $(C_6H_5)_4AsCl$ and $(C_6H_5)_4AsCl \cdot HCl$ in chloroform. The averaged values compare as follows with earlier values:

	This work (25°)	*Earlier*
$(C_6H_5)_4AsCl \cdot 2H_2O$ in H_2O, *M*	0.990	0.776 (30°)[2]; 0.072 (25°)[4]
$(C_6H_5)_4AsCl \cdot 2H_2O$ in 1 *M* NaCl, *M*	0.284	0.240 (30°)[2]
$(C_6H_5)_4AsCl$ in $CHCl_3$, *M*	0.703	0.95 (25°)[4]

Partition and ionization constants of tetraphenylarsonium chloride from water–chloroform distribution

The extraction coefficient of tetraphenylarsonium chloride (RCl) for chloroform–water is the ratio of the analytical concentrations of all tetraphenylarsonium species in the two phases:

$$E_R = \frac{[RCl]_o + 2[(RCl)_2]_o + \ldots}{[R^+] + [RCl]}$$

where the subscript o refers to the chloroform phase; concentrations without subscripts refer to the aqueous phase. E_R is a function of the partition (P_{mon}) and ionization constants of the monomer and the polymerization constants of RCl in chloroform:

$$P_{mon} = \frac{[RCl]_o}{[RCl]} = fP^0_{mon}$$

where f is the activity coefficient of uncharged RCl in water; the activity coefficient of RCl in chloroform is taken as 1.

TABLE I

SOLUBILITY OF TETRAPHENYLARSONIUM CHLORIDE IN WATER AND CHLOROFORM AT 25.0±0.1°

Solid phase	*Shaking time (days)*	*Solvent*	*Solubility*	
			G anhydrous salt in 100 ml satd. soln.	*M*
$(C_6H_5)_4AsCl\cdot 2H_2O$	0.5	H_2O	41.34	0.988
$(C_6H_5)_4AsCl\cdot 2H_2O$	1	H_2O	41.52	0.992[a]
$(C_6H_5)_4AsCl\cdot 2H_2O$	3	H_2O	41.47	0.991
$(C_6H_5)_4AsCl\cdot 2H_2O$	0.5	1.00 *M* NaCl	0.1189	0.284[a]
$(C_6H_5)_4AsCl$	0.5	$CHCl_3$	29.38	0.702
$(C_6H_5)_4AsCl$	1	$CHCl_3$	29.34	0.701[a]
$(C_6H_5)_4AsCl$	3	$CHCl_3$	29.55	0.706[a]
$(C_6H_5)_4AsCl\cdot 2H_2O$[b]	1	$CHCl_3$	29.42	0.703
$(C_6H_5)_4AsCl\cdot HCl$	1	$CHCl_3$		0.0390[c]
$(C_6H_5)_4AsCl\cdot HCl$	3	$CHCl_3$		0.0392[c]

[a] By titration.

[b] Chloroform shaken with aqueous phase saturated with dihydrate (solid phase present).

[c] Stability of $(C_6H_5)_4AsCl\cdot HCl$ in chloroform is uncertain and these values represent total $(C_6H_5)_4AsCl$ from absorbance measurements.

$$K_{mon} = \frac{[R^+][Cl^-]}{[RCl]} = \frac{fK^0_{mon}}{f^+f^-}$$

where f^+ and f^- are the activity coefficients of R^+ and Cl^-.

The polymerization constants of RCl in chloroform are:

$$\beta_n = \frac{[(RCl)_n]_o}{[RCl]_o^n}$$

If the only tetraphenylarsonium species in water are R^+ and RCl (the polymerization of tetraphenylarsonium species in water is assumed to be negligible), then:

$$E_R = \frac{P^0_{mon}(1+2\beta_2[RCl]_o+3\beta_3[RCl]_o^2+\ldots)}{\dfrac{K^0_{mon}}{f^+f^-[Cl^-]}+\dfrac{1}{f}}$$

When the concentration of RCl in chloroform is sufficiently low that polymers can be neglected, $E_R = E_{mon}$ and

$$E_{mon} = \frac{P^0_{mon}}{\dfrac{K^0_{mon}}{f^+f^-[Cl^-]}+\dfrac{1}{f}}$$

or

$$\frac{1}{E_{\text{mon}}} = \frac{K^0_{\text{mon}}}{P^0_{\text{mon}}}\left(\frac{1}{f^+f^-[\text{Cl}^-]}\right) + \frac{1}{fP^0_{\text{mon}}}$$

Measurements of E_R at low chloride concentrations therefore allow determination of P^0_{mon} and K^0_{mon} from this linear function. The straight line in Fig. 1 is based on the 8 points lying farthest from the origin, for which $[\text{Cl}^-] \lesssim 0.02$ and $\Sigma[\text{R}]_0 \lesssim 2.2 \cdot 10^{-4}$. The values of f^+ and f^- were taken from KIELLAND[5], a radius of 8 Å being assumed for $(C_6H_5)_4As^+$. The value of f may differ appreciably from 1 even at $\mu = 0.1$, so that points for which μ ($\sim[\text{Cl}^-]$) is greater than 0.02 were not used (though plotted in Fig. 1) in finding the best straight line. The value of f was taken as unity for $[\text{Cl}^-] \lesssim 0.02$. The polymerization of RCl in chloroform at a concentration of $2 \cdot 10^{-4} M$ is not negligible ($\sim 5\%$), so that a correction was applied for the dimer present at this and similar concentrations, the value of β_2 found later being used. The omission of the four points nearest the origin in Fig. 1 reduces the precision of the determination of the intercept, but seems advisable because of the uncertainty in the value of f. From the intercept (0.305) of the least-squares line, P^0_{mon} is found to be 3.3; the slope gives 0.079 for K^0_{mon}. Because of the small value of the intercept and the rather long extrapolation, an error of 10–15% in P^0_{mon} would not be surprising.

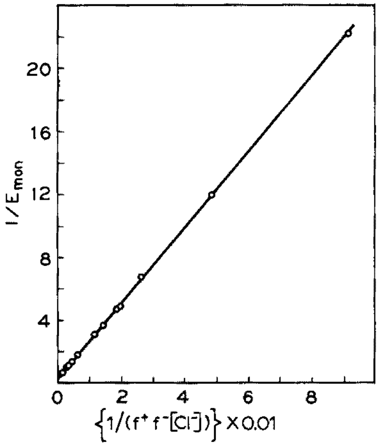

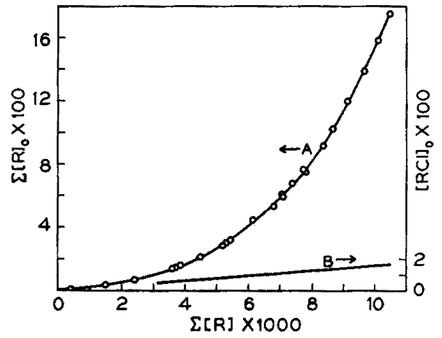

Fig. 1. Chloroform extractability of tetraphenylarsonium chloride (plotted as reciprocal of extraction coefficient) as a function of chloride ion activity in aqueous phase (25°). The straight line is based on the 8 points lying farthest from the origin.

Fig. 2. (A) Analytical concentration of tetraphenylarsonium chloride in chloroform phase as a function of its analytical concentration in 0.1000 M sodium chloride solution (25°). (B) Calculated concentration of monomeric tetraphenylarsonium chloride in chloroform phase.

Polymerization constants of tetraphenylarsonium chloride in chloroform from extraction data

When increasing amounts of RCl are added to a 0.1000 M sodium chloride solution and extraction is carried out with an equal volume of chloroform, $\Sigma[\text{R}]_0/\Sigma[\text{R}]$ increases with the total amount of RCl in the system as a consequence of extensive polymer formation in the chloroform (Fig. 2). If the concentration of monomer,

$[RCl]_o$, in the chloroform phase is known for each $\Sigma[R]_o/\Sigma[R]$, the polymerization constants can be computed.

E_{mon} for 0.1000 M sodium chloride solution can be obtained by extrapolating a plot of E_R *vs.* $\Sigma[R]_o$ or of E_R *vs.* $\Sigma[R]$ to zero concentration of RCl. These plots (not shown here) furnish a value of 1.51 for E_{mon}, with an error that could be as large as $\pm 3\%$.

The addition of RCl increases the Cl^- concentration (by about 3% for the largest amount of RCl added) and this increase must be taken into account. E_{mon} for sodium chloride solutions slightly stronger than 0.1000 M can be calculated from

$$E_{mon} = 1.51 \left\{\frac{K^0_{mon}}{f^+f^- \cdot 0.1000} + \frac{1}{f}\right\} \Big/ \left\{\frac{K^0_{mon}}{f^+f^-[Cl^-]} + \frac{1}{f}\right\}$$

$$= 1.51 \left\{\frac{0.079}{0.0615} + \frac{1}{1.1}\right\} \Big/ \left\{\frac{0.079}{0.615[Cl^-]} + \frac{1}{1.1}\right\}$$

The product f^+f^- was taken as 0.615 for 0.100 M and slightly stronger chloride solutions. The value of f was taken as 1.1 for $\mu \sim 0.1$ (calculated from $E_{mon} = 1.51$ in 0.1000 M sodium chloride). Multiplication of a particular $\Sigma[R]$ by its E_{mon} then gives the corresponding $[RCl]_o$.

Iterative least squares fits of these data to equations of the type

$$\Sigma[R]_o = \Sigma n\beta_n[RCl]_o^n$$

for various sets of n ($=2, 3, 4$) were carried out on the University of Minnesota's Control Data Corporation 1604 computer. As judged from the goodness of fit to the experimental data the choice of β_2 and β_4 was best, and the introduction of β_3 did not cause the fit to be significantly better. The standard errors in $\Sigma[R]_o$ and in $[RCl]_o$ were estimated to be 2%; however, χ^2 for the fit involving β_2 and β_4 was found to be 13.0, while the expectation value was 30, so that the error estimates were apparently somewhat conservative. The computed polymerization constants are $\beta_2 = 163 \pm 16$ and $\beta_4 = 4.5 \cdot 10^5 \pm 0.9 \cdot 10^5$.

It is concluded that the assumption that only the monomer, dimer, and tetramer of tetraphenylarsonium chloride exist in chloroform solutions serves to account very satisfactorily for the extraction data found.

Extraction of tetraphenylarsonium chloride at high chloride ion concentrations

If, in neutral chloride solutions, all activity coefficients remained at 1, the value of $[RCl]_o/\Sigma[R]$ would approach $[RCl]_o/[RCl] = P^0_{mon} = 3.3$ at high chloride ion concentrations. Actually, $[RCl]_o/\Sigma[R]$ increases rapidly above 0.1 M sodium chloride (Fig. 3). Tetraphenylarsonium chloride is strongly salted out by sodium chloride. Because f_{R^+} and f_{Cl^-} are not known at the higher sodium chloride concentrations, f_{RCl} cannot be found from E_{mon}, but since $P_{mon} > E_{mon}$, the minimum values of P_{mon} are 11.5 in 1 M sodium chloride, 43 in 2 M and 325 in 4 M. If the salting out coefficient is assumed to be given approximately by

$$k = \log f/\mu = \frac{\log \dfrac{P}{P^0}}{\mu} = \frac{\log \dfrac{P}{3.3}}{\mu}$$

it has values $\geq \sim 0.5$ (>0.54 in 1 *M* sodium chloride, >0.57 in 2 *M*, >0.50 in 4 *M*).

In hydrochloric acid solutions, E_{mon} declines at higher acid concentrations as a result of the formation of $RCl \cdot H^+$ and $RCl \cdot HCl$ in the aqueous phase (Fig. 3, in which E_R at $\Sigma[R]_o = 0.010$ is plotted).

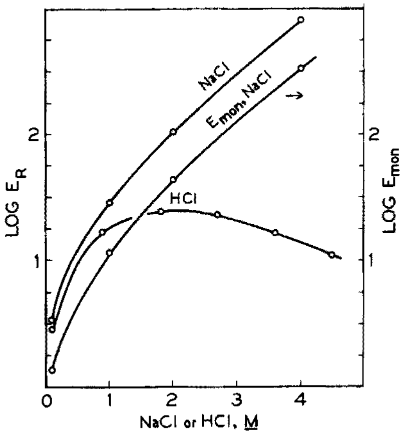

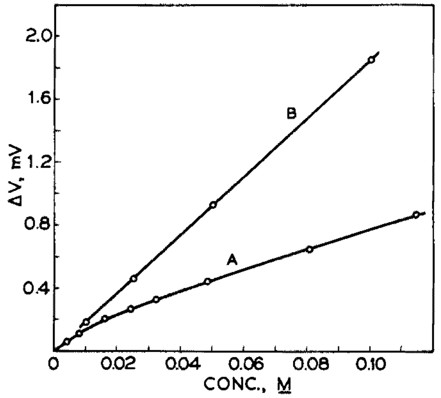

Fig. 3. Extraction coefficient ($CHCl_3/H_2O$) of tetraphenylarsonium chloride in all forms as a function of NaCl and HCl concentrations (initial $\Sigma[R]_o = 0.010$, equal phase volumes), and extraction coefficient of the monomer as a function of NaCl concentration.

Fig. 4. Comparative vapor pressure lowering produced by tetraphenylarsonium chloride (A) and naphthalene (B) in chloroform (25°). ΔV (mV) between osmometer thermistor beads in solvent and solution is plotted against analytical concentration of solute in chloroform ($\sum_n n[RCl]_n$).

Polymerization constants of tetraphenylarsonium chloride in chloroform from osmometric measurements

Vapor pressure measurements were made of chloroform solutions (dry) of tetraphenylarsonium chloride up to a stoichiometric concentration of approximately 0.1 *M*. Figure 4 shows the data.

The vapor pressure data also favor the interpretation that dimers and tetramers are formed in chloroform solution, and give $\beta_2 = 72 \pm 14$ and $\beta_4 = 4.0 \cdot 10^5 \pm 0.7 \cdot 10^5$ (25°). The value of β_2 from vapor pressure measurements is much lower than the value 163 derived from the extraction data. In the former series the chloroform solution is anhydrous; in the latter it is, of course, saturated with water.

SUMMARY

Measurements of the distribution of tetraphenylarsonium chloride between aqueous sodium chloride solutions and chloroform give an ionization constant, K^0, $=0.079$ and a partition constant ($CHCl_3/H_2O$), P^0, $=3.3$ for monomeric $(C_6H_5)_4AsCl$ at 25°. Distribution measurements at higher tetraphenylarsonium chloride concentrations show that polymerization occurs in chloroform. A system consisting of monomer, dimer and tetramer best represents the extraction data, which furnish the polymerization constants $\beta_2 = 163 \pm 16$, $\beta_4 = 4.5 \cdot 10^5 \pm 0.9 \cdot 10^5$. Vapor pressure measurements of dry chloroform solutions give the values $\beta_2 = 72 \pm 14$, $\beta_4 = 4.0 \cdot 10^5 \pm 0.7 \cdot 10^5$ (25°).

RÉSUMÉ

Des mesures de partage du chlorure de tétraphénylarsonium entre solutions aqueuses de chlorure de sodium–chloroforme ont donné une constante d'ionisation, $K^0,=0.079$ et un coefficient de partage ($CHCl_3/H_2O$), $P^0,=3.3$ pour $(C_6H_5)_4AsCl$ monomère à 25°. Des mesures de partage à des concentrations plus élevées de chlorure de tétraphénylarsonium ont montré qu'une polymérisation se produisait dans le chloroforme.

REFERENCES

1 F. F. Blicke and E. Monroe, *J. Am. Chem. Soc.*, 57 (1935) 720; A. I. Popov and R. E. Humphrey, 81 (1959) 2043.
2 H. H. Willard and G. M. Smith, *Ind. Eng. Chem., Anal. Ed.*, 11 (1939) 186.
3 R. Farm and S. Bruckenstein, *Anal. Chem.*, 40 (1968) 1651.
4 S. Tribalat, *Anal. Chim. Acta*, 3 (1949) 113.
5 J. Kielland, *J. Am. Chem. Soc.*, 59 (1937) 1675.

Analytica Chimica Acta
Elsevier Publishing Company, Amsterdam
Printed in The Netherlands

SELENAZONE: THE SELENIUM ANALOGUE OF DITHIZONE

R. S. RAMAKRISHNA* AND H. M. N. H. IRVING
Department of Inorganic and Structural Chemistry, The University of Leeds, Leeds 2 (England)
(Received August 14th, 1969)

Although dithizone (diphenylthiocarbazone, 3-mercapto-1,5-diphenylformazan; III$\rightleftharpoons$IV; $X = S$) is widely used in trace metal analysis, much remains to be learnt about the tautomeric forms of the reagent itself and the structures of the highly coloured metal complexes derived from it. Changes produced in the stability of metal complexes by replacing a donor sulphur atom by selenium have been a rewarding current interest in this laboratory[1] and this led us to attempt the synthesis of the selenium analogue of dithizone.

The familiar synthesis of dithizone by FISCHER's method[2] involves the condensation of carbon bisulphide and phenylhydrazine to give the phenylhydrazinium salt $[Ph{\cdot}NH{\cdot}NH_3]^+$ $[Ph{\cdot}NH{\cdot}NH{\cdot}CS{\cdot}S]^-$ which on cautious heating yields diphenylthiocarbazide (II; $X = S$), from which dithizone is obtained by oxidation with methanolic potash. This procedure failed for the selenium analogue, for carbon biselenide (prepared from dichloromethane and molten selenium[3]) failed to react with phenylhydrazine, even when the components were heated for some time under reflux in ethereal solution.

BAMBERGER's synthesis of dithizone[4] involves the preparation of the precursor, diphenylthiocarbazide (II; $X = S$) by the reduction of 3-nitro-1,5-diphenylformazan by an ammoniacal solution of ammonium hydrosulphide. This would appear[5] to proceed through the formation of 3-amino-1,5-diphenylformazan and a nuclear displacement of NH_2 by HS^-. This procedure proved suitable for the preparation of the selenium analogue 3-seleno-1,5-diphenylformazan (III$\rightleftharpoons$IV; $X = Se$), for which we propose the trivial name "selenazone". Dry hydrogen selenide was carried by a stream of dry nitrogen through a solution of 3-nitro-1,5-diphenylformazan (I) in ethanol saturated with dry ammonia at 0°. The 1,5-diphenylselenocarbazide (II; $X = Se$) which resulted was carefully oxidised under alkaline conditions, and subsequent acidification in the cold precipitated the desired selenazone.

A second successful synthesis was based on an observation by OGILVIE AND CORWIN[6], *viz.* that S-methyldithizone (VI; $X = S$) yielded diphenylthiocarbazide (II; $X = S$) on reduction with ammonia and hydrogen sulphide in ethanol at 0°. We have confirmed this reaction which we believe to involve a nucleophilic displacement of CH_3S^- by HS^-. By a similar nucleophilic displacement of CH_3S^- by HSe^-, it proved possible to prepare 1,5-diphenylselenocarbazide (II; $X = Se$) by the interaction of S-methyldithizone with ammonia and hydrogen selenide under similar conditions: selenazone resulted by oxidation of this product.

---

* Present address: Department of Chemistry, University of Ceylon, Colombo (Ceylon).

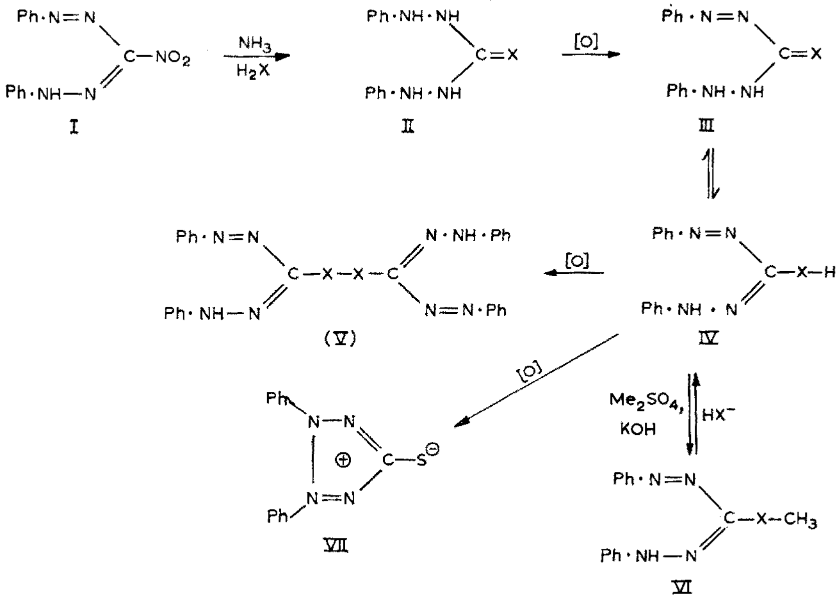

As obtained by either of the above routes, selenazone (3-seleno-1,5-diphenylformazan, III$\rightleftharpoons$IV; X = Se) forms a black microcrystalline powder of m.p. 116°. It is acidic and dissolves in dilute alkali to give red solutions doubtless derived by ionisation of the tautomeric selenol (IV; X = Se); on acidification the selenazone is precipitated unchanged. It is soluble in a variety of organic solvents to give green solutions which superficially resemble those of dithizone and which possess two absorption bands in the visible region. However, whereas the maxima for dithizone

TABLE I

OPTICAL CHARACTERISTICS OF SELENAZONE AND DITHIZONE

Solvent	$\lambda_{max}(1)$	λ_{min}	$\lambda_{max}(2)$	A_2/A_1
$CHCl_3$	482	550	622	0.655[b]
	(442)[a]	(504)	(605)	(2.59)
C_6H_6	482	560	635	0.432
	(450)	(514)	(620)	(1.80)
CCl_4	487	560	648	0.384
	(450)	(515)	(620)	(1.70)
C_6H_{14}	478	555	655	0.253
	(455)	(518)	(628)	(1.09)
Aq.NH_3			478[c]	
			(470)	
Pyridine[d]	392	450	512	
			(510)	

[a] Values for dithizone are given in parentheses.

[b] By assuming that selenazone forms a 1:2 complex with Hg^{2+} (as is known to be the case with dithizone) the molecular extinction coefficients determined by extractive titration[24] were

$$\varepsilon_{max}(1) = 31{,}670 \ (16{,}000)$$
$$\varepsilon_{max}(2) = 14{,}980 \ (41{,}490)$$

[c] Spectra of anions derived from IV.

[d] Spectrum changes with time and finally gives a single peak at 512 nm.

in chloroform occur at 442 and 605 nm, the peaks for selenazone in the same solvent are at 482 and 622 nm respectively (Fig. 1). This bathochromic shift of the entire spectrum consequent upon replacing sulphur by the heavier next lower member of Group VI recurs with all the solvents we have examined (Table I). There is, however, another striking difference; for, whereas with dithizone the peak at the longer wavelength (λ_2) is higher than that at the lower (λ_1), the position is reversed for selenazone.

However, the solvent-dependent peak-ratio (the ratio of the optical densities at the longer and shorter wavelength maxima, A_2/A_1) which is believed[5] to reflect the position of the thiol–thione equilibrium in dithizone (IV$\rightleftharpoons$III; X = S) decreases in the order $CHCl_3 > C_6H_6 > CCl_4 > C_6H_{14}$ for both reagents and indeed a plot of A_2/A_1 for dithizone against corresponding values for selenazone constitutes quite a good straight line (Fig. 2).

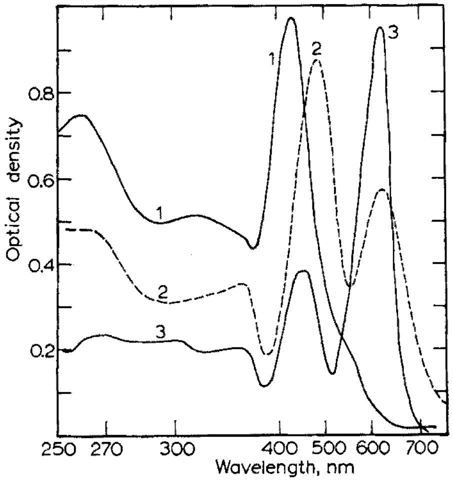

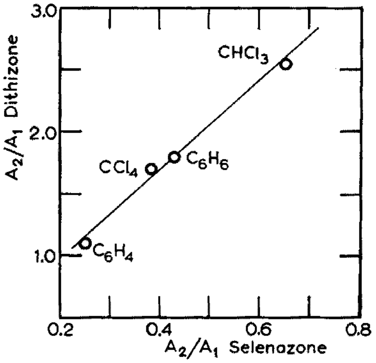

Fig. 1. The spectra in chloroform of (1) diselenide ($1.44 \cdot 10^{-2}$ g/l), (2) selenazone ($8.32 \cdot 10^{-3}$ g/l), and (3) dithizone ($5.85 \cdot 10^{-3}$ g/l).

Fig. 2. A plot of the absorbancy ratio A_2/A_1 for dithizone against the corresponding ratio for selenazone in a series of solvents.

The ready solubility of selenazone in organic solvents provides a good method for its purification. Crude selenazone is taken up in very dilute ammonia (1:100), filtered from insolubles and the aqueous solution extracted repeatedly with chloroform to remove non-acidic impurities. The separated aqueous phase is then acidified and the selenazone that separates is taken up in a fresh portion of pure chloroform. The cycle can be repeated until the spectrum of successive samples no longer changes. A sensitive test of purity is the constancy of the peak ratio which attains a constant value of 0.66.

Solutions of selenazone in organic solvents cannot be kept unchanged unless air is rigorously excluded. Figure 3 shows what happens with carbon tetrachloride solutions. The two characteristic peaks at 487 and 648 nm decrease progressively with time and a new peak of intermediate intensity appears at *ca.* 425 nm. The new oxidation product is formed in substantial quantities when a solution of selenazone in

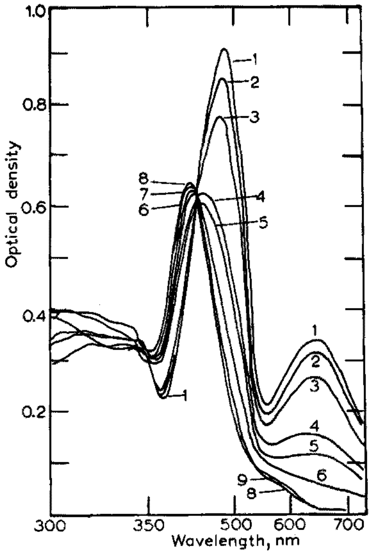

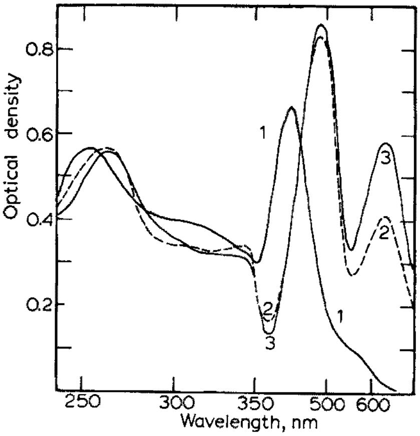

Fig. 3. Change with time in the spectrum of a solution of selenazone in carbon tetrachloride. After zero time (curve 1) and after 1, 3, 8, 48, 55, 120, 144 and 168 h (curves 2, 3, 4, 5, 6, 7, 8, and 9).

Fig. 4. Reduction of a solution of the diselenide in chloroform to selenazone by hypophosphorous acid. Curve (1) original spectrum. Curves (2) and (3) taken immediately and 10 min after adding hypophosphorous acid.

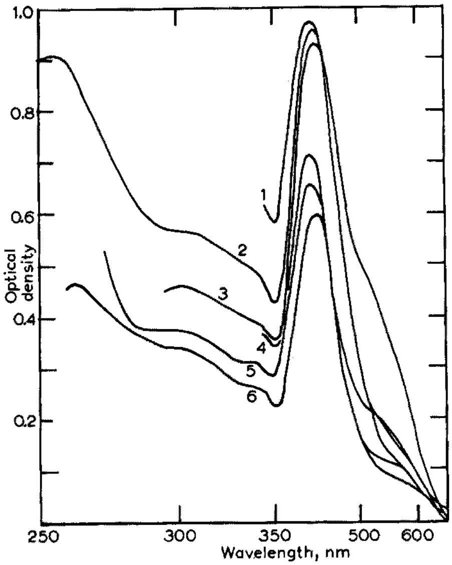

Fig. 5. Absorption spectra of the diselenide in various solvents. (1) $1.92 \cdot 10^{-2}$ g/l in pyridine; (2) $1.44 \cdot 10^{-2}$ g/l in chloroform; (3) $1.52 \cdot 10^{-2}$ g/l in benzene; (4) $1.24 \cdot 10^{-2}$ g/l in hexane; (5) $1.08 \cdot 10^{-2}$ g/l in acetone; (6) $1.08 \cdot 10^{-2}$ g/l in carbon tetrachloride.

chloroform is allowed to evaporate slowly in a fume-chamber. After the residue had been purified chromatographically the resultant microcrystalline brownish-black powder, m.p. 86–88°, analysed to $C_{13}H_{11}N_4Se$ but a determination of the molecular weight in chloroform by vapour pressure osmometry showed that this must be doubled (Found: M = 621.0. Calcd. for $C_{26}H_{22}N_8Se_2$, M = 604.0). The product is undoubtedly the diselenide (V; X = Se), for it could readily be reduced back to selenazone by heating with alkaline dextrose in aqueous ethanol, with sulphurous acid, or best of all with hypophosphorous acid. Figure 4 shows how this reduction, which is almost quantitative, can be followed spectrophotometrically.

Solutions of the diselenide in chloroform, benzene, carbon tetrachloride, *n*-hexane, acetone and pyridine give only a single band at *ca.* 425 nm in the visible region (Fig. 5): its position is substantially independent of the solvent used (Table II), thus confirming the absence of the tautomeric equilibrium (III$\rightleftharpoons$IV) characteristic of dithizone and its selenium analogue.

Although the solubility of selenazone in chloroform and carbon tetrachloride is comparable to that of dithizone itself, it is very sparingly soluble in acetic acid, dioxan, ether and alcohol, and solutions in these solvents undergo very rapid oxidation to the diselenide.

The ready oxidation of selenazone (III$\rightleftharpoons$IV; X = Se) to the diselenide (V; X = Se) is consistent with the known tendency[7,8] of compounds containing the groups $>$C–SeH and $>$C = Se to form diselenides. Thus CHIESI *et al.*[8] have recently reported the oxidation of selenourea to the α,α′-diselenobisformamidinium cation

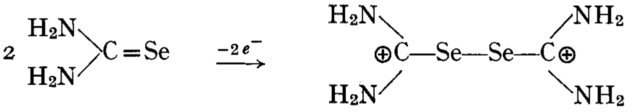

and have confirmed the structure of the diselenide by X-ray structure analysis.

Under different conditions dithizone can be oxidised to a variety of products that include a sydnone (anhydro-5-mercapto-2,3-diphenyltetrazolium hydroxide, VII)[5,6,9], 1,5-diphenylformazan-3-sulphonic acid[10], the purple oxidation product [5,11] whose structure as 2-phenylazo-5,6-benzo-1,3,4(4H)thiadiazine has recently been confirmed by an X-ray structure determination[12], and a very labile disulphide (as V; X = S) which readily undergoes self-oxidation and reduction to give dithizone (III$\rightleftharpoons$IV; X = S) and the sydnone (VII) in equal amounts[5,9]. In contrast, the oxidation of selenazone under comparable sets of conditions invariably yielded the diselenide (V; X = Se) which showed no tendency to disproportionate like its sulphur analogue. BARNARD AND WOODBRIDGE[13] have noted that the replacement of sulphur by selenium in many types of compounds, particularly in disulphides, markedly increases their resistance to further oxidation.

In contrast to selenazone, the diselenide is not acidic and nothing can be extracted by alkali from its solutions in organic solvents. This circumstance greatly facilitates the preparation of pure selenazone from a partly oxidised crude product. The presence of an –SeH group in the tautomeric form (IV; X = Se) is confirmed by the action of dimethylsulphate on its solution in alkali which yields Se-methylselenazone (VI; X = Se) as a brownish-black crystalline solid, m.p. 136–8°. The absorption

TABLE II

ABSORPTION SPECTRA OF DISELENIDE

(Molecular extinction coefficients in parentheses given as $10^3\varepsilon$)

Chloroform	*Benzene*	*Acetone*	*Carbon tetrachloride*	*Pyridine*[a]	*Hexane*
λ_{max} 425 nm (40.14) (Shoulder at 570 nm) λ_{min} 355 nm (17.95) λ_{max} 259 nm (38.30)	λ_{max} 425 nm (36.96) (Shoulder at 570 nm) λ_{min} 355 nm (14.11)	λ_{max} 422 nm (36.91) (Shoulder at 560 nm) λ_{min} 355 nm (19.29)	λ_{max} 422 nm (33.56) (Shoulder at 570 nm) λ_{min} 350 nm (12.58)	λ_{max} 425 nm (30.67) (Shoulder at 550 nm) λ_{min} 352 nm (18.40)	λ_{max} 415 nm (38.83) (Shoulder at 570 nm) λ_{min} 340 nm (15.37)

[a] Spectrum changes with time and finally gives a single peak at 510 nm.

TABLE III

THE EFFECT OF pH ON THE EXTRACTION OF METAL–SELENAZONE COMPLEXES INTO CHLOROFORM[a]

pH of aq. buffer	Ag^+	Mn^{2+}	Fe^{2+}	Co^{2+}	Ni^{2+}	Cu^{2+}	Zn^{2+}	Cd^{2+}	Hg^{2+}	Pb^{2+}	Tl^+	Bi^{3+}
1.00	y (y)	— (—)	— (—)	— (—)	— (—)	g–br (p)	— (—)	— (—)	o–y (o–y)	— (—)	— (—)	o–r (—)
3.60	g–y (—)	— (—)	— (—)	— (—)	— (—)	g–br (p)	— (—)	— (—)	o–y (o–y)	— (—)	— (—)	b–g (—)
4.85	g–y (g–y)	— (—)	— (—)	— (—)	— (—)	v–r (br)	m (m)	o–r (v–r)	o–y (o–y)	o–r (p)	— (—)	o–r (—)
6.80	y (v–r)	br–r (—)	— (—)	— (—)	— (—)	v–r (br)	p (p)	o–br (v–r)	o–y (v–r)	— (—)	— (—)	— (p)
8.60	y (v–r)	— (Slight b–p)	— (—)	br–g (b–p)	— (—)	v–r (br)	m (m)	o–r (v–r)	o–y (v–r)	— (—)	g–y (—)	— (p)
9.85	g–y (v–r)	— (Slight b–p)	— (—)	v–r (v–r)	—[b] (Slight b–p)	v–r (br)	m (m)	o–r (v–r)	o–y (v–r)	b–g (b–p)	o–pk (p)	b–g (p)

[a] Results for dithizone in parentheses. b = blue; br = brown; g = green; m = magenta; o = orange; p = purple; pk = pink; r = red; v = violet; y = yellow.

[b] Above pH 10 Ni^{2+} gave a violet solution with dithizone but only a greyish-yellow with selenazone.

spectra of its solutions in organic solvents are very similar to those of its sulphur analogue (Fig. 6).

When, however, S-methyldithizone is dissolved in pyridine, the peak at the longer wavelength is the less intense, whereas the reverse is true for Se-methylselenazone (Fig. 7). Moreover, whereas the spectra of S-methyldithizone and Se-methylselenazone in pyridine remain unchanged for several hours, solutions of selenazone and of the diselenide show marked changes with time. Selenazone (0.0164 g/l pyridine) gave an initial spectrum with two absorption bands at λ_{max} 392 and 512 nm respectively. On standing, the intensities of both absorption bands decreased at first: then the band at 392 nm continued to decrease again until finally a single peak at 512 nm remained. On the contrary a solution of the diselenide (0.0192 g/l pyridine) initially showed a single absorption peak at 425 nm which was gradually replaced by one at 510 nm (Figs. 8 and 9).

Such changes do not occur with solutions of dithizone in pyridine, which are characterised by a single absorption peak at 510 nm normally attributed to the anion of IV (X = S)[14]. When 1 ml of pure pyridine (a factitious excess) was added to a solution of the diselenide in benzene (0.0212 g/l), the spectrum with a peak at *ca.* 425 nm remained unchanged even after 24 h. No clear explanation is apparent for the changes observed in the spectra of the selenium compounds in pyridine.

Formation of metal complexes

Like its sulphur-containing analogue, selenazone forms strongly coloured complexes with a range of metals. These can be extracted into organic solvents to an extent depending on the pH of the aqueous phase. Qualitative comparisons with the behaviour of dithizone are illustrated by Table III. Although this is by no means exhaustive, it immediately suggests a number of analytical possibilities which will be described fully in later papers.

A point of special interest is the observation that the diselenide (V; X = Se) is also capable of forming extractable metal complexes. However, it is appreciably more selective than selenazone (or dithizone), and of the metals so far studied this behaviour is restricted to Hg^{2+}, Ag^{+}, Ni^{2+} and Pd^{2+}. Details of a selective procedure for the determination of mercury(II) will be communicated later.

The stoicheiometry of the complexes, as determined by extractive titration, appears to be nearly 1:1 and it thus resembles superficially the known reactions of many disulphides[15].

For example, cleavage of the type

$$R\text{–}S\text{–}S\text{–}R + HgCl_2 \rightarrow R\text{–}S\text{–}HgCl + R\text{–}S\text{–}Cl$$

is well established, though the stoicheiometry of the resulting mercury complex depends on the particular disulphide taken[15]. Thus LATVIJAS[16] reports that di-8-quinolyl disulphide is cleaved by a number of metal ions and he has utilised the specificity of this reaction in analytical procedures for the detection of palladium(II) and platinum(II). Reactions of diselenides have been interpreted as of the radical type[7]. We have failed to find any evidence for such radicals derived from the cleavage of the diselenide (V; X = Se), for no e.s.r. signals were detectable when its solution in carbon tetrachloride was irradiated with ultraviolet light in the resonance cavity of an electron spin spectrometer. Since no signals could be detected even with frozen solutions,

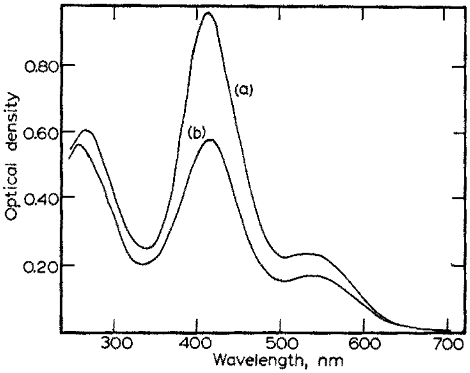

Fig. 6. Spectra in chloroform of curve (a) S-methyldithizone ($6.562 \cdot 10^{-5}$ mole l^{-1}) and curve (b) Se-methylselenazone ($6.519 \cdot 10^{-5}$ mole l^{-1}).

	$\lambda_{max}(1)$	$\lambda_{max}(2)$	λ_{min}	$\lambda_{max}(3)$
S-Methyldithizone	267(9.25)	414(14.67)	504(3.45)	532(3.54)
Se-Methylselenazone	259(8.55)	415(8.75)	502(2.30)	540(2.53)

(Molecular extinction coefficient are given in parentheses as $10^3\varepsilon$)

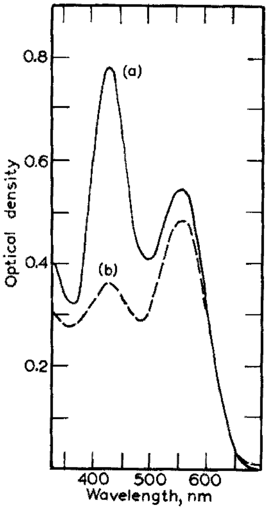

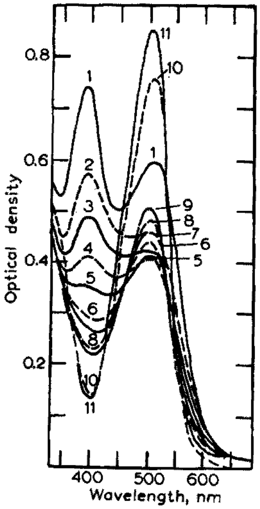

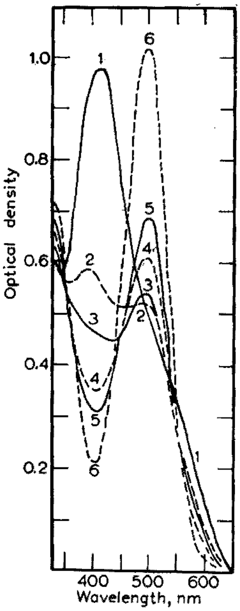

Fig. 7. Spectra in pyridine of curve (a) S-methyldithizone ($6.815 \cdot 10^{-5}$ mole l^{-1}) and curve (b) Se-methylselenazone ($6.814 \cdot 10^{-5}$ mole l^{-1}).

	$\lambda_{max}(1)$	λ_{min}	$\lambda_{max}(2)$
S-Methyldithizone	428(11.42)	495(6.02)	555(8.00)
Se-Methylselenazone	425(5.28)	482(4.26)	558(7.07)

(Molecular extinction coefficients are given in parentheses as $10^3\varepsilon$)

Fig. 8. Variation with time of the absorption spectrum of the selenazone in pyridine ($1.64 \cdot 10^{-2}$ g/l). Curve 1 initial spectrum. Curves 2–11 after 0.75, 1.75, 3.75, 4.75, 6, 7, 8, 9, 30 and 48 h respectively.

Fig. 9. Variation with time of the absorption spectrum of the diselenide in pyridine ($1.92 \cdot 10^{-2}$ g/l). Curve 1, initial spectrum. Curves 2–6 after 3, 5, 7, 8 and 30 h respectively.

it must be concluded that if any species in an excited state are formed, they must have an extremely short half-life. Yellow prismatic crystals have been obtained (admixed with red amorphous material) by concentrating *in vacuo* the organic phase obtained by equilibrating an aqueous solution of mercury(II) ions at pH 3.5 with a solution of the diselenide in chloroform. Their structure is under investigation by X-ray crystallography.

Infrared spectra

The infrared spectra of selenazone, diselenide and Se-methylselenazone (VI; X = Se) were obtained in KBr discs and compared with those obtained for dithizone, diphenylcarbazone (III, X = O), 3-nitro-1,5-diphenylformazan (I) and S-methyldithizone (VI, X = S). Such comparisons of the spectra of thio-compounds with those of the related seleno compounds[17] have been useful in "isolating" and identifying infrared absorptions, which include a contribution from a $>C=S$ and $>C=Se$ stretching vibration in nitrogen-containing thio- and seleno-compounds. Although earlier assignments[18,19] for the $>C=S$ stretching frequency have ranged as high as 1400–1200 cm^{-1}, recent studies[20,21] report contributions to the $>C=S$ stretching vibration near 700 cm^{-1}. The present studies indicate that an absorption around 715 cm^{-1} in dithizone could be identified with a contribution from $>C=S$ stretching frequency, and in selenazone this band is shifted to a lower frequency of 705 cm^{-1} which could be identified with the $>C=Se$ stretching. The replacement of sulphur by selenium in thioamides and thiosemicarbazones[16,22] is known to produce such shifts to lower frequencies. The only reported assignment of the $>C=S$ stretching vibration in dithizone compounds, has been the assignment by MATH, FERNANDO AND FREISER[23] of a strong band at 1210 cm^{-1} to indicate the presence of a thiocarbazone group $>C=S$ in their nickel dithizonate. However, this is believed to be a faulty assignment, for the present studies show the presence of a strong band in the region 1200–1220 cm^{-1} in nitroformazan (I) as well as in diphenylcarbazone (III, X = O), two compounds in which the $>C=S$ group does not exist. It now seems somewhat substantiated that the $>C=S$ stretching vibration in nitrogen-containing compounds will normally be found around 700 cm^{-1}.

JENSEN AND NIELSEN[17] report that the infrared spectra of the corresponding thio- and seleno-compounds are similar and that the replacement of sulphur by selenium could be used as a 'diagnostic probe', because the spectra of the S and Se compounds are often superimposable down to 800–900 cm^{-1} and the only changes are essentially the bands due to $>C=S$ vibration. They also observed that substitution of sulphur with oxygen, on the other hand, changed the infrared spectrum so completely that it was not possible to obtain much useful information from a comparison of the sulphur compound with the oxygen compound. In the present studies, similar observations were found with the O, S, and Se compounds (III, X = O, S and Se respectively) investigated. The C–N vibration in these compounds is identified by a strong but a somewhat broad and split band near 1480–1490 cm^{-1} in dithizone, selenazone and diphenylcarbazone (III, X = S, Se and O respectively), whereas in S-methyldithizone (VI, X = S), Se-methylselenazone (VI, X = Se), diselenide (V, X = Se), and the nitroformazan (I), this band is shifted to higher frequencies: 1545 cm^{-1} in nitroformazan (I) and 1520 cm^{-1} in the diselenide (V, X = Se), S-methyldithizone and Se-methylselenazone. This shift is attributed to increased double bond

TABLE IV

INFRARED SPECTRA OF O, S AND ANALOGOUS Se COMPOUNDS

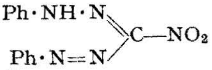 $\begin{matrix}Ph\cdot NH\cdot N\\ Ph\cdot N{=}N\end{matrix}\!>\!C{-}NO_2$ I	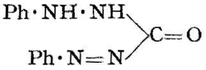 $\begin{matrix}Ph\cdot NH\cdot NH\\ Ph\cdot N{=}N\end{matrix}\!>\!C{=}O$ III; X=O	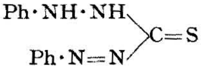 $\begin{matrix}Ph\cdot NH\cdot NH\\ Ph\cdot N{=}N\end{matrix}\!>\!C{=}S$ III; X=S	 $\begin{matrix}Ph\cdot NH\cdot NH\\ Ph\cdot N{=}N\end{matrix}\!>\!C{=}Se$ III; X=Se
		442 (w)	442 (w)
461 (m)	450 (m)		
		496 (s)	490 (s)
	510 (s)		502 (vw)
		520 (w)	
560 (vw)		541 (vw)	541 (vw)
590 (w)	570 (w)	575 (m)	
	605 (vw)	605 (w)	605 (w)
	630 (w)		
682 (s)		680 (s)	680 (s)
	692 (s)		
		715 (s)	705 (s)
755 (s)	750 (s)	750 (s)	750 (s)
770 (w)		775 (vw)	775 (vw)
780 (w)			
			800 (w)
845 (w)	865(vw)	830 (vw)	830 (vw)
860 (m)	880 (w)	890 (m)	890 (m)
900 (vw)	905 (vw)	902 (vw)	902 (vw)
1000 (w)			
	1022 (w)		
1070 (w)	1075 (w)	1070 (m)	1070 (m)
1110 (vw)	1120 (s)		
1160 (vw)		1135 (s)	1150 (s)
1170 (vw)	1150 (m)		
	1180 (m)	1170 (s)	1175 (s)
1220 (m)	1200 (m)	1215 (s)	1215 (s)
1280 (s)	1250 (m)	1250 (sh)	
	1290 (m)		
1335 (sh)	1310 (sh)	1315 (m)	1315 (m)
1350 (s)			
		1380 (m)	1380 (m)
	1435 (s)	1435 (s)	1440 (s)
1455 (m)	1450 (sh)	1455 (m)	1455 (m)
	1490 (s)	1470 (s)	1490 (s)
1545 (s)			
1590 (w)		1588 (m)	1585 (m)
—	1605 (s)	—	—
	1660 (s)		
	1710 (s)	—	—

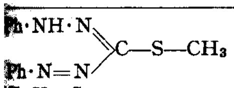 VI; X=S	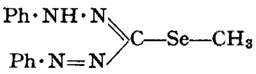 VI; X=Se	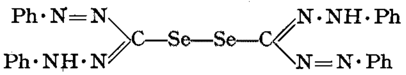 V; X=Se
		400 (bw)
482 (s)	480 (m)	470 (wsh)
508 (m)	510 (m)	
528 (m)	530 (m)	
590 (w)	585 (vw)	598 (w)
618 (vw)	605 (vw)	
	670 (w)	
675 (m)		688 (s)
685 (s)triplet	680 (m)triplet	
695 (s)	692 (m)	
755 (s)	755 (s)	750 (s)
775 (s)	772 (m)	770 (msh)
795 (vw)		
	800 (w)	805 (s)
840 (m)	845 (vw)	
870 (m)	870 (vw)	890 (vwsh)
895 (m)	890 (w)	
920 (vw)	920 (vw)	920 (vw)
975 (vw)		
1022 (w)	1022 (wsh)	1020 (ssh)
1075 (m)	1070 (w)	
	1095 (m)	1090 (s)
1108 (s)		
1148 (m)	1145 (w)	1150 (m)
1160 (w)	1170 (vw)	
1170 (w)		1182 (w)
1185 (vw)	1185 (vw)	
1220 (w)	1215 (vw)	1260 (s)
1265 (s)	1260 (s)	
1310 (m)	1310 (w)	1305 (vw)
1322 (w)		1390 (s)
1385 (s)		
1435 (m)	1430 (w)	1420 (vw)
1455 (w)	1455 (w)	1455 (w)
1505 (m)	1500 (m)	
1525 (s)	1520 (m)	1520 (s)
		1595 (s)
1600 (s)	1600 (m)	
—	—	—
—	—	—

character of the C–N bond on alkylation of the S or Se atom (in dithizone and selenazone respectively) and the presence of the C=N band in the diselenide (V, X = Se) and nitroformazan (I). Table IV gives the characteristic infrared absorption bands in the region 1800 cm^{-1}–250 cm^{-1} for the series of compounds investigated.

EXPERIMENTAL

Reagents

Unless otherwise stated all solvents and reagents were of AnalaR grade. Glassware and buffer solutions were freed from metallic impurities and oxidants by methods previously reported[10]. Absorptiometric measurements were carried out in matched 1-cm silica cells with a Unicam SP500 spectrophotometer and spectra were also recorded with the Unicam SP700 recording spectrophotometer.

Preparation of aluminium selenide (Al_2Se_3)

Aluminium powder (30 g), freed from oil by washing with acetone and ether, was thoroughly mixed in a mortar with finely divided AnarlaR selenium powder (50 g). About 5 g of this mixture was placed in a 200-ml heavy walled clay crucible furnished with a well fitting cover. A small piece of magnesium ribbon was ignited, dropped into the crucible and the cover immediately replaced. After a few seconds the cover was again removed and about 3 g of the powdered mixture of aluminium and selenium was added to the glowing mass and the cover was immediately replaced again. Further 3-g portions of the mixture were then added, waiting a few seconds between each addition, and the procedure was repeated until all the mixture had been added.

When cold the reaction product was removed from the crucible and stored in a tightly stoppered container until it was required.

Preparation of "selenazone" (3-seleno-1,5-diphenylformazan, III$\rightleftharpoons$IV; X = Se)

Hydrogen selenide, liberated by dropping water onto aluminium selenide (20 g) was transferred by a stream of dry nitrogen gas into a solution of 3-nitro-1,5-diphenylformazan (7 g) in ethanol (250 ml) which had been saturated with dry ammonia gas at 0°. Moisture and oxygen were carefully excluded by passing the hydrogen selenide through tubes containing calcium chloride and phosphorus pentoxide and by maintaining a steady stream of dry nitrogen throughout the entire preparation. After 15 min the solution was filtered and the solid product washed with water and dried *in vacuo*. The crude product obtained (3.2 g; m.p. 120–122°) was added to a solution of potassium hydroxide (2 g) in methanol (50 ml) which had previously been brought to its boiling point. After having been refluxed for 5 min the solution was poured with constant stirring into 1 *N* sulphuric acid (500 ml) cooled at 0°. Selenazone which separated as a black powder was collected, washed free from acid with water and dried *in vacuo*. Yield 2.1 g.

For purification a sample was dissolved in pure chloroform and, after filtration to remove any insoluble matter, the solution was shaken in a separatory funnel with 1:100 aqueous ammonia prepared from isopiestically pure ammonia[24]. The aqueous extract was washed with several successive portions of chloroform which were rejected. Pure chloroform was then added and the selenazone was back-extracted into the organic phase by acidifying the aqueous phase with isopiestic hydrochloric acid[24].

After removal of the solvent *in vacuo*, selenazone was obtained as an odourless microcrystalline black powder, m.p. 116°. (Found: C 51.4; H 4.3; N 18.6%. $C_{13}H_{12}N_4Se$ requires C 51.5; H 4.0; N 18.5%.)

Reduction of S-methyldithizone by ammonium hydrosulphide

S-Methyldithizone (3-methylmercapto-1,5-diphenylformazan; VI, X = S; 0.3 g) was added to ethanol (20 ml) contained in a Pyrex test-tube immersed in an ice-bath. Dry ammonia gas was passed into the mixture for 30 min, during which time most of the S-methyldithizone had dissolved to give a brownish-red solution. Dry hydrogen sulphide was then passed in for about 20 min during which time the colour became a deep brown. The mixture was removed from the ice bath and allowed to stand at room temperature for 4–5 h, during which the colour changed to greenish yellow and a small amount of a white solid separated. Concentration of the filtrate gave a further quantity of the same material which readily turned blue-violet and melted with decomposition at 132–134°, behaviour characteristic of 1,5-diphenylthiocarbazide (II; X = S). Identity was established by comparison of its infrared spectrum with that of an authentic sample and by oxidation with methanolic potash whereupon acidification yielded dithizone (0.15 g; m.p. 162–164°) as a black microcrystalline powder after purification from chloroform (Found: C 60.7; H 4.6%. Calcd. for $C_{13}H_{12}N_4S$: C 60.9; H 4.7%). Its spectrum in chloroform (λ_{max} 440, 606 nm, λ_{min} 505 nm) was identical with that of an authentic specimen.

Reduction of S-methyldithizone by ammonia and hydrogen selenide: preparation of selenazone

A solution of S-methyldithizone (0.5 g) in ethanol (20 ml) saturated at 0° with dry ammonia was prepared as described above.

Dry hydrogen selenide was then introduced in a stream of dry nitrogen for 40 min and the mixture was then removed from the ice-bath and allowed to stand for 4–5 h at room temperature. On filtration a small amount of a white solid was obtained which gradually turned violet in the air. Concentration of the filtrate gave a further quantity of this material (80 mg; m.p. 122°) which proved to be 1,5-diphenylselenocarbazide (II; X = Se). On oxidation with methanolic potash and subsequent acidification, it yielded a dark brown solid (45 mg) which after purification chromatographically on alumina followed by reprecipitation of its solution in chloroform by the cautious addition of ethanol was identified as the diselenide (*q.v.*) (V; X = Se). The m.p. was 86–88° and the spectrum in chloroform showed $\lambda_{max} = 258, 422$ nm and $\lambda_{min} = 352$ with a slight shoulder at *ca.* 550 nm. Reduction with an alkaline solution of dextrose gave selenazone, m.p. 115–116°, identified by its characteristic spectrum and ultimate analysis.

Oxidation of selenazone to the diselenide (V; X = Se)

A solution of crude selenazone (1 g) in chloroform (150 ml) was filtered to remove any insoluble material and the solvent was allowed to evaporate in an open dish at room temperature with free access to the air. A sticky brown residue was left which yielded a black solid (0.6 g) on addition of alcohol. It was taken up in chloroform (20 ml) and transferred to a column of neutral alumina ('Camag'; 100–240 mesh).

Elution with benzene gave a pale yellow band, a dark brown band which contained most of the desired product, and a very slow moving greenish-purple band. The main fraction was collected and after the solvent had been removed *in vacuo*, the residue was rechromatographed to yield finally the diselenide (V; X = Se) as a brownish-black microcrystalline powder (m.p. 86–88°: yield 0.4 g). (Found: C 51.8; H 4.0; N 18.0 %. Calcd. for $C_{26}H_{22}N_8Se_2$: C 51.7; H 3.6; N 18.5%.) The molecular weight was determined by vapour pressure osmometry on a solution of 0.0175 g of diselenide in 3.0567 g of chloroform. (Found: M = 621.0. $C_{26}H_{22}N_8Se_2$ requires M = 604.0.)

Reduction of the diselenide (V; X = Se) to selenazone by an alkaline solution of dextrose

A solution of the diselenide (0.2 g), dextrose (0.75 g), sodium hydroxide (0.15 g), water (20 ml) and ethanol (20 ml) was heated under reflux (15 min) during which the colour changed from light yellow to dark red. The solution was filtered and poured onto ice (50 g). On acidification with dilute sulphuric acid, a black precipitate was thrown down which was collected, washed with water and dried *in vacuo*. This product (50 mg) was identified as selenazone (III$\rightleftharpoons$IV; X = Se) by its m.p. 114–116° and by its spectrum in chloroform (λ_{max}=482, 622 nm and λ_{min}=550 nm) (Found: C 51.2; H 4.4%; $C_{13}H_{12}N_4Se$ requires C 51.5; N 4.0%).

Reduction of the diselenide with hypophosphorous acid

The spectrum of a solution of the diselenide in chloroform ($1.55 \cdot 10^{-5}$ *M*) was measured in a 1-cm stoppered silica cell at λ_{max} 259 and 425 nm. Hypophosphorous acid (1 ml of 50% solution) was added to each of two 10-ml portions of the above solution. The organic phase of the first (1) was withdrawn immediately and its spectra recorded at once. The organic phase of the second (2) was withdrawn and measured after 10 min. Both spectra showed the presence of bands due to selenazone (λ_{max} = 482, 622 nm). The following measurements were obtained.

	Absorbancy at (nm)			
	259	*425*	*482*	*622*
Before treatment with H_3PO_2	0.570	0.665	0.310	0.022
After treatment with H_3PO_2	(1)0.515	0.355	0.840	0.400
	(2)0.485	0.350	0.880	0.586

By taking ε_{max} = 31,670 at 482 nm, obtained by extractive titration[25], the concentration of selenazone in solutions (1) and (2) was calculated as $2.65 \cdot 10^{-5}$ and $2.78 \cdot 10^{-5}$ *M*, corresponding respectively to 85 and 90% reduction.

Changes in the spectra of a purified solution of selenazone in carbon tetrachloride due to aerial oxidation

A solution of selenazone in carbon tetrachloride was purified by repeated extraction with 1:100 isopiestic ammonia and back-extraction into pure carbon tetrachloride by acidification of this alkaline solution. After appropriate dilution the spectrum was recorded after varying intervals of time in 1-cm stoppered silica cells with a SP700 Unicam spectrophotometer. No attempt was made to deaerate the solvents used. The results are shown in Fig. 3.

Preparation of S-methylselenazone

A solution of selenazone (170 mg) in chloroform (25 ml) was shaken with 2 *M* sodium hydroxide (10 ml) and water (50 ml). The organic layer was rejected and the aqueous phase was washed with successive small portions of chloroform until the organic layer was colourless. The separated aqueous phase was then shaken mechanically with dimethylsulphate (0.2 ml) in an atmosphere of nitrogen. The initially orange yellow colour became paler and a black solid separated. Excess dimethylsulphate was destroyed by warming with 2 *M* sodium hydroxide (5 ml) at 100° (10 min), and after cooling the crude product was taken up in successive quantities of chloroform. The combined extracts were washed with 0.01 *M* sodium hydroxide and then with water and dried over anhydrous sodium sulphate. Removal of the solvent gave a black solid (95 mg) which was dissolved in chloroform (5 ml) and transferred to a column of alumina. Elution with benzene gave a deep brown band containing most of the product, followed by a faint yellow and a small brownish-pink band. Removal of the solvent gave a product which on recrystallisation from ethanol formed brownish-black crystals with a metallic bronze-like lustre (40 mg; m.p. 136–138°). (Found: C 52.5; H 4.75; N 17.7%; $C_{14}H_{14}N_4Se$ requires C 53.0; H 4.4, N 17.2%.)

One of us (R.S.R.) wishes to thank the Department of Inorganic and Structural Chemistry for a Research Fellowship.

SUMMARY

The selenium analogue of dithizone has been synthesised by treating 3-nitro-1,5-diphenylformazan or 3-methylmercapto-1,5-diphenylformazan with ammonia and hydrogen selenide in oxygen-free ethanol. The new reagent "selenazone" exists as tautomeric forms analogous to the thiol and thione forms of dithizone and is readily oxidised to a diselenide, $C_{26}H_{22}N_8Se_2$, from which the parent selenazone is recoverable by reduction with alkaline dextrose, sulphurous acid or hypophosphorous acid. The spectra of selenazone and the diselenide in a variety of organic solvents are reported and compared with similar data for dithizone itself.

Selenazone forms a range of brilliantly coloured metallic complexes which are soluble in organic solvents. It thus permits of the solvent extraction of the ions Ag^+, Mn^{2+}, Fe^{2+}, Co^{2+}, Ni^{2+}, Cu^{2+}, Zn^{2+}, Cd^{2+}, Hg^{2+}, Pb^{2+}, Tl^+ and Bi^{3+} from aqueous solution, the percentage extraction being governed by the pH. The diselenide also forms extractable coloured complexes; it is more selective than selenazone or dithizone, for the behaviour appears to be limited to Ag^+, Hg^{2+}, Ni^{2+} and Pd^{2+}.

RÉSUMÉ

On a réussi à synthétiser la "sélénazone", analogue à la dithizone, en traitant le nitro-3-diphényl-1,5-formazan ou le méthyl-3-mercapto-diphényl-1,5-formazan avec l'ammoniaque et le séléniure d'hydrogène dans l'éthanol exempt d'oxygène. Le nouveau réactif "sélénazone" existe sous des formes tautomères analogues aux formes thiol et thione de la dithizone; il est facilement oxydé en un diséléniure $C_{26}H_{22}N_8Se_2$ et et retransformé en sélénazone par réduction à l'aide de dextrose alcalin, acide sulfureux ou acide hypophosphoreux. La sélénazone forme des complexes métalliques très colorés, solubles dans des solvants organiques avec Ag^+, Mn^{2+}, $Fe_2{}^+$, Co^{2+}, Ni^{2+}, Cu^{2+}, Zn^{2+}, Cd^{2+}, Hg^{2+}, Pb^{2+}, Tl^+ et Bi^{3+}. Le disélénure forme également des complexes colorés; il est plus sélectif, réagissant seulement avec Ag^+, Hg^{2+}, Ni^{2+} et Pd^{2+}.

ZUSAMMENFASSUNG

Das selenanaloge Dithizon wurde durch Behandlung von 3-Nitro-1,5-diphenylformazan oder 3-Methylmercapto-1,5-diphenylformazan mit Ammoniak und Selenwasserstoff in sauerstofffreiem Äthanol synthetisiert. Das neue Reagenz "Selenazon" existiert in tautomeren Formen analog den Thiol- und Thion-Formen des Dithizons. Es ist leicht oxidierbar zum Diselenid $C_{26}H_{22}N_8Se_2$, aus welchem das Selenazon wieder durch Reduktion mit alkalischer Dextrose, schwefliger Säure oder hypophosphoriger Säure zurückgewonnen werden kann. Die Spektren von Selenazon und dem Diselenid in einer Anzahl organischer Lösungsmittel werden angegeben und mit ähnlichen Daten für Dithizon verglichen. Selenazon bildet eine Reihe starkgefärbter Metallkomplexe, welche in organischen Lösungsmitteln löslich sind. Dadurch ist eine Flüssigextraktion folgender Ionen aus wässriger Lösung möglich: Ag^+, Mn^{2+}, Fe^{2+}, Co^{2+}, Ni^{2+}, Cu^{2+}, Zn^{2+}, Cd^{2+}, Hg^{2+}, Pb^{2+}, Tl^+ und Bi^{3+}. Das Mass der Extraktion wird durch den pH-Wert bestimmt. Das Diselenid bildet ebenfalls extrahierbare gefärbte Komplexe. Es ist selektiver als Selenazon oder Dithizon und extrahiert Ag^+, Hg^{2+}, Ni^{2+} und Pd^{2+}.

REFERENCES

1 L. D. Pettit, C. Sherrington and R. J. Whewell, *J. Chem. Soc.*, 1968(A) 2204.
2 E. Fischer, *Ann.*, 118 (1878) 190.
3 D. J. G. Ives, R. W. Pittman and W. Wardlaw, *J. Chem. Soc.*, (1947) 1080.
4 E. Bamberger, R. Padova and E. Ormerod, *Ann.*, 446 (1925) 260.
5 H. M. N. H. Irving, unpublished results.
6 J. W. Ogilvie and A. H. Corwin, *J. Am. Chem. Soc.*, 83 (1961) 5023.
7 T. W. Campbell, H. G. Walker and G. M. Coppinger, *Chem. Rev.*, 50 (1952) 279.
8 A. Chiesi, G. Grossoni, M. Nardellio and M. E. Vidoni, *Chem. Commun.*, D8 (1969) 404.
9 S. S. Sahota, *Ph.D. Thesis*, Leeds, 1964.
10 H. M. N. H. Irving, D. C. Rupainwar and S. S. Sahota, *Anal. Chim. Acta*, 45 (1969) 249.
11 U. S. Mahnot, *Ph.D. Thesis*, Leeds, 1966.
12 W. S. McDonald, H. M. N. H. Irving, G. Raper and D. C. Rupainwar, *Chem. Commun.*, (1969) 392.
13 D. Barnard and D. T. Woodbridge, *J. Chem. Soc.*, 2922 (1961).
14 G. I. Iwantscheff, *Das Dithizon und Seine Anwendung in der Mikro- und Spurenanalyse*, Verlag Chemie, Weinheim, 1958.
15 L. F. Lindoy, *Coordination Chem. Rev.*, 4 (1969) 41.
16 P. S. R. Latvijas, *Zinatnu Akademijas Vestis Khim. Ser.*, 1 (1962) 29.
17 K. A. Jensen and P. F. Nielsen, *Acta Chem. Scand.*, 20 (1966) 597.
18 J. E. J. Stewart, *J. Chem. Phys.*, 26 (1957) 248.
19 C. N. R. Rao and R. Venkataraghavan, *Spectrochim. Acta*, 18 (1962) 541.
20 H. M. N. H. Irving and K. Swaminathan, *J. Inorg. & Nucl. Chem.*, 26 (1964) 1291.
21 A. Yamaguchi, R. B. Penland, S. Mizushima, T. J. Lane, C. Curran and J. V. Quagliano, *J. Am. Chem. Soc.*, 80 (1958) 527.
22 D. M. Wiles and T. Suprunchuk, *Can. J. Chem.*, 45 (1967) 2258.
23 K. S. Math, Q. Fernando and H. Freiser, *Anal. Chem.*, 36 (1964) 1762.
24 H. M. N. H. Irving and J. J. Cox, *Analyst*, 83 (1958) 526.
25 H. M. N. H. Irving and R. S. Ramakrishna, *Analyst*, 85 (1960) 860.

Analytica Chimica Acta
Elsevier Publishing Company, Amsterdam
Printed in The Netherlands

THE EXTRACTION OF SILVER(I) FROM HYDROCHLORIC ACID BY SOLUTIONS OF TRI-*n*-HEXYLAMMONIUM AND TETRA-*n*-HEXYLAMMONIUM CHLORIDE IN ORGANIC SOLVENTS

H. M. N. H. IRVING AND A. D. DAMODARAN
Department of Inorganic and Structural Chemistry, The University of Leeds, Leeds, 2 (England)

(Received August 8th, 1969)

In previous papers[1,2] the extraction of copper(II) and copper(I) by a solution of quaternary *n*-hexylammonium chloride in ethylenedichloride has been reported. The effect of increase in the concentration of chloride ions in the aqueous phase in increasing the percentage of copper(II) extracted, but decreasing the percentage of copper(I) extracted, was correlated with the respective class (a) and class (b) character of these ions[3]. The silver(I) ion, Ag^+, also belongs to class (b), for it forms strong complexes with halide ions which increase in stability in the order $F^- \ll Cl^- < Br^- < I^-$ [3,4]. Its extraction from hydrochloric acid by organic solutions of certain quaternary ammonium iodides ($R_4N^+I^-$; R = Pr,Bu,Hexyl) has been briefly reported in a preliminary survey covering all the elements[5] but the nature of the extracted species was not determined and it seems not improbable (*cf.* Ref. 2, p. 84) that an anionic complex involving iodide rather than chloride ions may have partitioned under the conditions used.

By using tracer silver(I) (^{110m}Ag; $t_{1/2} = 274$ days) it was possible to determine the distribution of silver between an aqueous phase containing known concentrations of halide ion $[Cl]_{tot}$ and solutions of tetra-*n*-hexylammonium chloride $[NR_4Cl]_{tot}$ in 1,2-dichloroethane.

If the equation governing the extraction is written as

$$(NR_4Cl)_{org} + Ag^+ + Cl^- \rightleftharpoons (NR_4{}^+AgCl_2{}^-)_{org}$$

(where the subscript org is used to distinguish materials in the organic phase), we can define an extraction constant by:

$$\bar{K}_2 = [NR_4{}^+AgCl_2{}^-]_{org}/[NR_4{}^+Cl^-]_{org}[Ag^+][Cl^- \qquad (1)$$

If however species such as $AgCl_3{}^{2-}$ and $AgCl_4{}^{3-}$ are involved, we have in addition

$$\bar{K}_3 = [(NR_4{}^+)_2AgCl_3{}^{2-}]_{org}/[NR_4{}^+Cl^-]^2{}_{org}[Ag^+][Cl^-]^2 \qquad (2)$$

and

$$\bar{K}_4 = [(NR_4{}^+)_3AgCl_4{}^{3-}]_{org}/[NR_4{}^+Cl^-]^3{}_{org}[Ag^+][Cl^-]^3 \qquad (3)$$

It follows that the radiometrically determined distribution ratio

$$D = \frac{\text{Total concentration of silver in the organic phase}}{\text{Total concentration of silver in the aqueous phase}}$$

$$= \frac{[NR_4{}^+AgCl_2{}^-] + [(NR_4)_2{}^+AgCl_3{}^{2-}] + \ldots}{[Ag^+] + [AgCl] + [AgCl_2{}^-] + [AgCl_3{}^{2-}] + \ldots}$$

$$= \frac{[NR_4{}^+Cl^-]_{org}[Cl^-]\{\bar{K}_2 + \bar{K}_3[NR_4{}^+Cl^-]_{org}[Cl^-]\} + \ldots}{1 + \beta_1[Cl^-] + \beta_2[Cl^-]^2 + \ldots} \quad (4)$$

where the overall stability constant $\beta_j = [AgCl_j]/[Ag][Cl]^j$. It follows that a plot of log D against log $[NR_4{}^+Cl^-]_{org}$ at constant $[Cl]^-$ will be linear and of unit slope provided that all $\bar{K}_j (j \geq 3)$ are negligible, *i.e.* if the anion $AgCl_2{}^-$ is the only extractable species.

Figure 1 shows the experimental data for extraction from 0.65 M hydrochloric acid. Although the measured slope is slightly greater than unity (*ca.* 1.1) there is no obvious curvature to suggest the co-extraction of more highly charged anionic complexes.

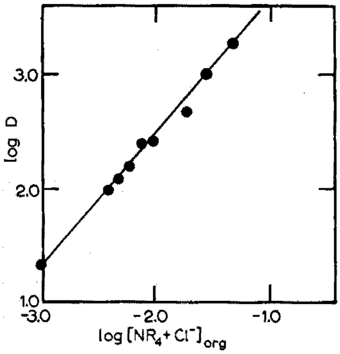

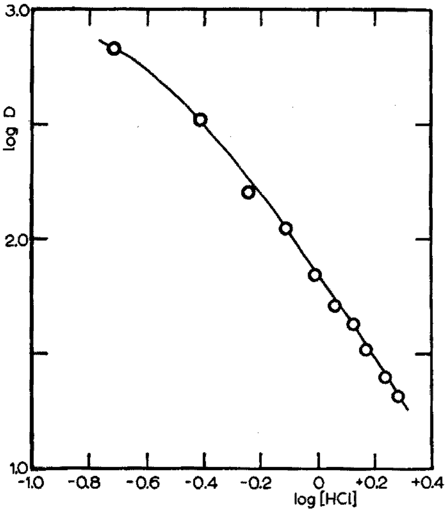

Fig 1. The effect of varying the concentration of a solution of quaternary hexylammonium chloride in ethylenedichloride on the extraction of silver(I) from 0.65 M hydrochloric acid.

Fig. 2. The extraction of silver(I) from hydrochloric acid by a $4 \cdot 10^{-3}$ M solution of tetra-*n*-hexylammonium chloride in ethylenedichloride.

The results of measurements in which the concentration of quaternary ammonium salt was held constant at $[NR_4]_{tot} = 4 \cdot 10^{-3}$ M whilst that of the chloride ion was varied are shown in Fig. 2. Differentiation of log D with respect to log $[Cl^-]$ in eqn. (4) (remembering that $\bar{K}_3 = 0$ and $[NR_4{}^+Cl^-]_{org}$ is constant) yields

$$\partial \log D / \partial \log [Cl^-] = 1 - \bar{n}$$

where the formation constant

$$\bar{n} = \Sigma j \beta_j [Cl^-]^j / \beta_j [Cl^-]^j. \quad (5)$$

with the stability constants $K_1 = 10^{2.85}$, $K_2 = 10^{1.87}$, $K_3 = 10^{0.32}$ and $K_4 = 10^{0.86}$, which are valid for 25° and 0.2 M sodium perchlorate[4], we see that the maximum value of log D, which should occur when $\bar{n}=1$, would occur with $(\mathrm{Cl}^-)\sim 0.004\ M$ and Fig. 2 only shows the descending portion of the graph. The measured slope decreases from -1.7 to -1.86 corresponding to $\bar{n}=2.7$ to 2.9. These values for the degree of formation of anionic complexes $\mathrm{AgCl}_n{}^{1-n}$ in the aqueous phase are consistent with those calculated from the above stability constants ($\bar{n}=2.4$ to 3.4) for the range of $[\mathrm{Cl}^-]$ used. (Since tracer silver was employed at a maximum concentration of $10^{-5}\ M$, it is legitimate to set $[\mathrm{Cl}^-]=[\mathrm{Cl}^-]_{\mathrm{tot.}}$) The higher value ($\bar{n}=3.4$) may well be overestimated, for many authors[4] report a negative value for log K_4: the effect of this would be to reduce calculated values of $\bar{n}$ for high (Cl^-).

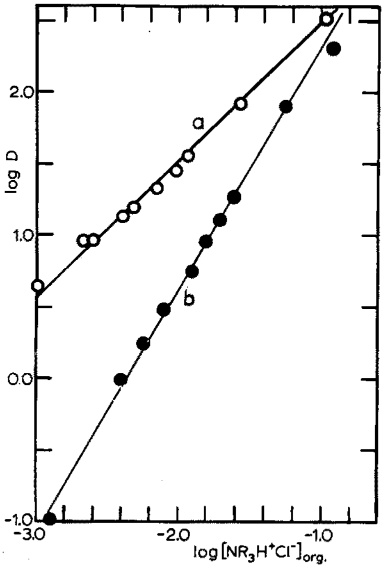

Fig. 3. The extraction of silver(I) from 0.65 M hydrochloric acid by solutions of tri-n-hexylammonium chloride in nitrobenzene (curve (a), open circles) and m-xylene (curve (b), blackened circles).

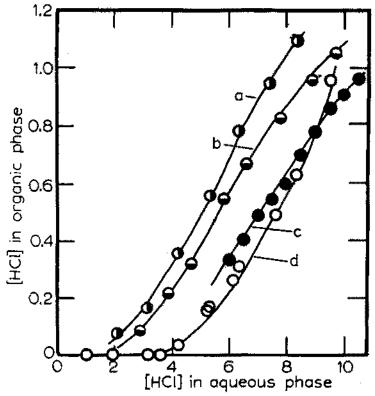

Fig. 4. The extraction of hydrogen chloride by liquid anion exchangers from hydrochloric acid of varying concentrations. (a) 1 M tetrahexylammonium chloride in ethylenedichloride; (b) 0.095 M tetrahexylammonium chloride in ethylenedichloride. Data from ref. 2; (c) 0.2 M trihexylammonium chloride in toluene. Data from ref. 6; (d) 1 M trihexylammonium chloride in m-xylene. All data have been referred to 1 M solutions of extractants by dividing the molarity of hydrochloric acid extracted by that of the extractant.

If the quaternary ammonium chloride used as an extractant is replaced by the hydrochloride of a tertiary amine, *viz.* tri-n-hexylamine, there is a substantial change in pattern. Figure 3, curve a, shows that when nitrobenzene is the solvent, the slope of the plot of log D against log $[\mathrm{R_3NH^+Cl^-}]_{\mathrm{org}}$ at constant $[\mathrm{HCl}]_{\mathrm{tot}}=0.65\ M$ is *ca.* 0.9, which implies the extraction of the anion $\mathrm{AgCl_2}^-$. However, when the nitrobenzene is replaced by the less polar solvent m-xylene (Fig. 3, curve b), the steeper slope (~ 1.8) indicates an increasing tendency towards the co-extraction of a bi-negative anion, $AgCl_3^{2-}$, whose existence in an aqueous phase has been demonstrated by studies with an anion-exchange resin[4]. Whether the extraction involves the ion-triplet $(NR_3H^+)_2(AgCl_3^{2-})$ or the quadruplet $(NR_3H^+)(Cl^-)(NR_3H^+)(AgCl_2^-)$ cannot of course be decided without further evidence.

GOOD *et al.*[6] have shown that solutions of tricaprylmethylammonium chloride in toluene can extract hydrogen chloride from aqueous hydrochloric acid and have identified the extracted species as containing the species HCl_2^- although this could not account for all the material partitioned from high concentrations of hydrochloric acid. Since a different liquid exchanger and different organic solvents were used in the present work, their potentialities as extractants for hydrochloric acid were examined with the results shown in Fig. 4. For comparison, the data for different concentrations of extractants have been normalised by assuming that the concentration of extracted hydrogen chloride will be proportional to the concentration of extractant: this hypothesis was not tested experimentally and the original results are reported in the experimental section. The quaternary ammonium salt is clearly the more effective extractant. However, the amount of hydrochloric acid extracted even with the highest concentration of extractant and aqueous phase encountered in the work with silver(I) will clearly be too insignificant to influence the results or their interpretation.

Figure 2 shows that silver(I) can be extracted very efficiently from dilute hydrochloric acid (99.8% even from 0.2 *M*) but that some 95% is extracted even from 2 *M* acid. This contrasts with the behaviour of copper(II) where the percentage extracted does not reach 90% until the chloride concentration exceeds 4 *M* and is very low from dilute hydrochloric acid. Conditions for separation are thus easily achieved and the main difficulty is that of stripping silver from the organic phase. The most effective agent would appear to be perchlorate ions.

EXPERIMENTAL

Chemicals

Tri-*n*-hexylamine (Eastman Organic Chemicals) made up to 0.1 *M* in the chosen organic solvent was equilibrated three times with an equal volume of *ca.* 1 *M* hydrochloric acid. The organic layer was carefully washed once with distilled water to remove any adhering acid.

Quaternary-*n*-hexylammonium chloride was prepared from the commercially available iodide (Eastman Kodak) by dissolving it (5 g) in 100 ml of acetone–water (70% v/v) and passing the solution slowly (100 ml/h) through a column (12″ × 1″) of anion-exchange resin (IRA-400; 100 g) which had been washed repeatedly with 2 *M* hydrochloric acid and finally with the aqueous acetone. The effluent was warmed on a water bath in a brisk current of air and when all the acetone had evaporated the residual viscous quaternary ammonium chloride was taken up in 100 ml of ethylenedichloride or other chosen organic diluent. The concentration of this solution was obtained as described previously[7].

^{110m}Ag ($t_{1/2} = 272$ days; 0.1 g), obtained by neutron irradiation of pure silver foil at A.E.R.E. (Harwell), was taken up in dilute nitric acid (5 ml) and fumed to dryness, and the residue was taken up in 0.001 *M* sulphuric acid. The concentration of tracer used was always *ca.* 10^{-5} *M*.

Methods

Equilibrations were carried out by shaking equal volumes (5 ml) of aqueous phase and the liquid exchanger dissolved in the chosen solvent in a stoppered centrifuge tube overnight at 22 ± 2°. After centrifugation 2 ml of each phase were removed and the activity measured with a well-type scintillation counter.

The following results were obtained for the extraction of silver(I) ($8 \cdot 10^{-5}$ *M*) by a $4 \cdot 10^{-3}$ *M* solution of tetrahexylammonium chloride in ethylenedichloride.

$[\mathrm{HCl}]_{\mathrm{tot}}$	0.194	0.387	0.581	0.774	0.968
$\log D$	2.84	2.52	2.22	2.06	1.86
$[\mathrm{HCl}]_{\mathrm{tot}}$	1.162	1.355	1.549	1.742	1.936
$\log D$	1.72	1.64	1.52	1.40	1.32

The results obtained for the extraction of silver(I) from 0.65 *M* hydrochloric acid by solutions of tetrahexylammonium chloride in ethylenedichloride and by solutions of tri-*n*-hexylammonium chloride in nitrobenzene or *m*-xylene, are shown in Table I.

TABLE I

EXTRACTION OF SILVER(I) FROM 0.65 *M* HYDROCHLORIC ACID

With tetrahexylammonium chloride in ethylenedichloride					
$\log [\mathrm{NR_4^+Cl^-}]_{\mathrm{org}}$	−3.00	−2.70	−2.40	−2.30	−2.22
$\log D$	1.35	1.61	1.98	2.08	2.18
$\log [\mathrm{NR_4^+Cl^-}]_{\mathrm{org}}$	−2.10	−2.00	−1.70	−1.52	−1.30
$\log D$	2.40	2.42	2.68	3.00	3.28
With tri-n-hexylammonium chloride in nitrobenzene					
$\log [\mathrm{NR_3H^+Cl^-}]_{\mathrm{org}}$	−2.98	−2.67	−2.61	−2.38	−2.31
$\log D$	0.65	0.95	0.95	1.14	1.20
$\log [\mathrm{NR_3H^+Cl^-}]_{\mathrm{org}}$	−2.14	−2.07	−1.91	−1.56	−0.98
$\log D$	1.31	1.45	1.56	1.92	2.52
With tri-n-hexylammonium chloride in m-xylene					
$\log [\mathrm{NR_3H^+Cl^-}]_{\mathrm{org}}$	−2.91	−2.40	−2.22	−2.10	−1.91
$\log D$	−1.00	−0.07	0.22	0.44	0.75
$\log [\mathrm{NR_3H^+Cl^-}]_{\mathrm{org}}$	−1.80	−1.70	−1.61	−1.22	−0.91
$\log D$	0.96	1.12	1.28	1.91	2.32

TABLE II

EXTRACTION OF HYDROGEN CHLORIDE WITH $\mathrm{NR_4^+Cl^-}$ OR $\mathrm{NR_3H^+Cl^-}$

With 1 M tetra-n-hexylammonium chloride in ethylenedichloride										
[HCl]	aqueous	2.10	3.15	4.20	5.26	6.31	7.36	8.41	9.46	10.51
[HCl]	organic	0.08	0.17	0.36	0.56	0.78	0.95	1.10	1.31	1.77
With 1 M tri-n-hexylammonium chloride in m-xylene										
[HCl]	aqueous	3.10	3.60	4.20	5.20	5.30				
[HCl]	organic	0	0	0.04	0.16	0.17				
[HCl]	aqueous	6.10	6.30	7.60	8.30	9.50				
[HCl]	organic	0.26	0.31	0.49	0.63	0.96				

To study the extraction of hydrogen chloride in the absence of silver, equal volumes of hydrochloric acid of known concentration and a 1 *M* solution of $\mathrm{NR_4^+Cl^-}$ (or $\mathrm{NR_3H^+Cl^-}$) in the appropriate organic solvent were equilibrated as before.

Hydrochloric acid was stripped from an aliquot portion of the centrifuged organic phase and titrated with standard alkali. The results shown in Table II were obtained.

SUMMARY

Silver(I) is very readily extracted from hydrochloric acid by solutions of tetrahexylammonium chloride (NR_4Cl) in 1,2-dichloroethane as the ion-pair $NR_4{}^+AgCl_2{}^-$. Solutions of tri-*n*-hexylammonium chloride in nitrobenzene extract silver(I) as $NR_3H^+AgCl_3{}^{2-}$ but with solutions in *m*-xylene the species $(NR_3H^+)_2AgCl_3{}^{2-}$ (or the quadrupole $(NR_3H^+)(AgCl_2{}^-)(NR_3H^+)(Cl^-)$) is favoured. In each case the distribution ratio decreases with increase in chloride ion concentration. Hydrochloric acid itself is extracted more effectively by the quaternary liquid exchanger.

RÉSUMÉ

L'argent(I) est très facilement extrait en milieu acide chlorhydrique par des solutions de chlorure de tétrahexylammonium (NR_4Cl) dans le dichloro-1,2-éthane comme $NR_4{}^+AgCl_2{}^-$. Avec les solutions de chlorure de tri-*n*-hexylammonium dans le nitrobenzène, on extrait $NR_3H^+AgCl_2{}^-$; mais en milieu *m*-xylène on a $(NR_3H^+)_2AgCl_3{}^{2-}$ (ou $(NR_3H^+)(AgCl_2{}^-)(NR_3H^+)(Cl^-)$). Dans chaque cas le coefficient de partage diminue avec l'augmentation de la concentration en chlorure. L'acide chlorhydrique lui-même est extrait plus efficacement avec l'échangeur quaternaire liquide.

REFERENCES

1 H. M. N. H. Irving and A. H. Nabilsi, *Anal. Chim. Acta*, 41 (1968) 505.
2 H. M. N. H. Irving and A. H. Nabilsi, *Anal. Chim. Acta*, 41 (1968) 79.
3 S. Ahrland, D. J. Chatt and N. R. Davies, *Quart. Rev.*, 12 (1958) 265.
4 *Stability Constants*, Chem. Soc. Special Publ. No. 17, 1964.
5 W. J. Maek, G. L. Booman, M. E. Kussy and J. E. Rein, *Anal. Chem.*, 33 (1961) 1775.
6 M. L. Good, S. E. Bryan, F. F. Holland and G. J. Maus, *J. Inorg. & Nucl. Chem.*, 25 (1963) 1167.
7 H. M. N. H. Irving and A. D. Damodaran, *Analyst*, 90 (1965) 180.

Analytica Chimica Acta
Elsevier Publishing Company, Amsterdam
Printed in The Netherlands

SELECTIVITY IN FOAM SEPARATION BY CONTROL OF CHARGE ON THE EXTRACTING SOLUTE: METAL–CHLORO COMPLEXES

BARRY L. KARGER AND MICHAEL W. MILLER
Department of Chemistry, Northeastern University, Boston, Mass. 02115 (U.S.A.)

(Received June 9th, 1969)

Foam separation of surface-inactive species has interested workers for a number of years. In this procedure, ionic species are made surface-active by attachment to a surfactant of opposite charge. This ion-association complex is then able to adsorb at the gas–liquid interface of gas bubbles rising through bulk liquid. The enriched surfaces are subsequently removed from the bulk by a foam column and appropriately collected.

Foam separation is a subdivision of the more general technique of adsorptive bubble separation[1]. Very recently, two reviews have been written on this subject[2,3]. RUBIN AND GADEN[4] list a number of species that have been successfully foam-separated, including surface-inactive ions. In general, metallic ions have been most often selected as the surface-inactive ions for study, especially with the aim of clean-up of nuclear wastes. A particularly noteworthy achievement in this regard was the work of SCHONFELD AND KIBBEY[5] in the removal of ^{90}Sr by controlled reflux in a counter-current, continuous foam fractionation column. Organic ions have also been examined[6]. GRIEVES[7], for example, has studied the removal of phenolate ion from polluted streams by foam separation.

If removal of surface-inactive ions from bulk aqueous media involves the formation of an ion-association complex with surfactant, then it should be possible to cause selective removal of species by control of the charge on the ion. In the ion-exchange field, KRAUS AND NELSON[8] have used this approach for the separation of metal ions by means of anionic metal chloro complexes. Essentially, anion-exchange resins are used, and the distribution coefficient for a given metal is a function of hydrochloric acid concentration. For example, a maximum in the distribution coefficient occurs at 0.3 *M* hydrochloric acid for mercury(II) and 8–9 *M* hydrochloric acid for iron(III). These differences are largely the result of different formation constants for the chloro complexes.

In a previous note[9], the foam separation of anionic chloro complexes of metals was briefly discussed. Indeed, the results are quite relatable to those of KRAUS AND NELSON. In this paper, studies on the foam separation of mercury(II), iron(III), and cobalt(II), along with a model for an understanding of the behavior of these anionic chloro complexes, are described in detail.

THEORY

Distribution factors in foam separation

A foam can be conceptualized as containing two liquid regions—one at the gas–liquid interface and the other at the interstices or Plateau borders between gas bubbles. In general, a rising foam without internal reflux will find surface-active material enriched at the interface and the bulk liquid composition in the Plateau borders. Thus, separation only occurs at the interfaces in this simple mode.

One can measure separation in terms of the enrichment ratio, E = concentration in foam/concentration in bulk, and this ratio will indicate the overall carry-over of surface-active material. However, it is clear that E will be a function of the wetness of the foam, with smaller values as the Plateau borders contribute a more significant percentage of the total liquid in the foam. Thus, we desire a separation measure which is independent of foam characteristics. This measure is Γ/C, the distribution factor, where Γ is the surface excess of solute (moles of solute per unit area at the defined interface in excess of the number of moles of corresponding unit area in the bulk solution) and C is the bulk equilibrium concentration of solute. The distribution factor takes account of the varying wetness of the foam in different experiments, as well as other varying parameters, such as foam bubble diameter. Γ/C can be conveniently measured in a recycling steady state foam separation apparatus as described below.

An expression for the distribution factor can be derived for the foam separation column used in this work[10]. The following assumptions are made:

1. the column operates at steady state;
2. the foam is composed of uniform polyhedral bubbles;
3. there is no bubble coalescence;
4. the interstitial liquid has the same concentration as the bulk liquid; and
5. adsorption at the surface is instantaneous.

From these assumptions, the foam liquid can be subdivided into two parts, the interstitial liquid and material from the gas–liquid interface. Let C_f represent the collapsed foam liquid concentration of surface-active species; C_b, the bulk liquid concentration of surface-active species; L, the collapsed foam liquid flow rate; G, the gas flow rate; and S, the interfacial area per unit volume (specific surface area) of foam. The material balance equation for the collapsed foam can then be written as

$$C_f L = C_b L + G S \Gamma \tag{1}$$

Equation (1) can be rearranged and solved for Γ

$$\Gamma = \frac{L}{GS}(C_f - C_b) \tag{2}$$

and dividing by C_b we obtain

$$\frac{\Gamma}{C_b} = \frac{L}{GS}\left(\frac{C_f}{C_b} - 1\right) \tag{3}$$

The term C_f/C_b is just the enrichment ratio, E. Also for a well drained foam, the bubbles can be assumed to be approximately regular dodecahedra for which S is equal to $6.59/d$[11], where d is a measure of the foam bubble diameter. Substitution of the above into eqn. (3) results in the final equation

$$\frac{\Gamma}{C} = (E-1)\frac{Ld}{6.59G} \tag{4}$$

Every parameter on the right-hand side of this equation is experimentally determinable. In the experimental section the measurement of Γ/C for metal chloro complexes will be discussed.

It should be pointed out that errors in the measurement of foam bubble diameter do not permit a true measure of Γ/C to be obtained. Nevertheless, these errors should be fairly constant, if the bubbles are measured in the same way each time. The major emphasis of this work has been an examination of changes in Γ/C with changes in conditions of the initial solution. The results of these changes should be valid, even though Γ/C may not be the true value. It is estimated that Γ/C may be about 15% different from the true value.

Model for separation of anionic metal chloro complexes

For simplicity, the gas–liquid interface in foam separations can be considered as a mobile two dimensional ion-exchange medium[12]. In this case the anionic metal chloro complex can exchange with chloride at the interface. The positive charge centers result from the cationic surfactant adsorbed at the gas–liquid interface.

The reaction for the formation of the complex in the bulk solution can be written as

$$M_b^{r+} + Z\mathrm{Cl}_b^- \rightleftarrows (\mathrm{MCl}_Z)_b^{r-Z}$$

where $Z > r$. The formation constant for this complex is just

$$K_F = \frac{[(\mathrm{MCl}_Z)^{r-Z}]_b}{[\mathrm{M}^{r+}]_b[\mathrm{Cl}^-]_b^Z} \tag{5}$$

This reaction assumes that only one complex of importance forms and that only this complex interacts with surfactant.

The general exchange reaction at the interfacial surface in this model is then

$$(\mathrm{MCl}_Z)_b^{r-Z} + (r-Z)\mathrm{Cl}_s^- \rightleftarrows (\mathrm{MCl}_Z)_s^{r-Z} + (r-Z)\mathrm{Cl}_b^-$$

where subscripts "b" and "s" represent bulk and surface media, respectively. Also, the absolute value of $r-Z$ must be used as the coefficient in front of Cl^-, since the charge on the metal complex is negative. The exchange constant is thus

$$K_s = \frac{[(\mathrm{MCl}_Z)^{r-Z}]_s[\mathrm{Cl}^-]_b^{|r-Z|}}{[(\mathrm{MCl}_Z)^{r-Z}]_b[\mathrm{Cl}^-]_s^{|r-Z|}} \tag{6}$$

Now the surface concentration of a given species is equal to the surface excess, Γ, divided by the thickness of the defined interfacial layer, δ. Equation (6) thus can be transformed to

$$K_s = \frac{\left[\dfrac{\Gamma(\mathrm{MCl}_Z)^{r-Z}}{\delta}\right][\mathrm{Cl}^-]_b^{|r-Z|}}{[(\mathrm{MCl}_Z)^{r-Z}]_b\left[\dfrac{\Gamma\mathrm{Cl}^-}{\delta}\right]^{|r-Z|}} \tag{7}$$

In the case that $|r-Z|$ is equal to one, δ cancels in eqn. (7); otherwise, it can be put in K_s to give a new constant $K_s' = K_s/\delta^{|r-Z|-1}$. At this point, let us assume for simplicity that $r-Z=-1$; eqn. (7) then becomes

$$K_s = \frac{\Gamma(\mathrm{MCl}_Z)^{-1}[\mathrm{Cl}^-]_b}{[(\mathrm{MCl}_Z)^{-1}]_b\Gamma\mathrm{Cl}^-} \tag{8}$$

We must now relate Γ/C, the experimentally determined distribution factor, to K_s and the formation constant of the complex, K_F. The concentration, C, in the experimentally measured distribution factor is the total bulk metal ion concentration. Thus

$$\frac{\Gamma}{C}=\frac{\Gamma(\mathrm{MCl}_Z)^{-1}}{[(\mathrm{MCl}_Z)^{-1}]_b+[\mathrm{M}^{r+}]_b} \tag{9}$$

In eqn. (9) it is assumed that no uncomplexed metal ion will be found at the interface. Substitution from eqn. (8) for $\Gamma(\mathrm{MCl}_Z)^{-1}$ into eqn. (9) results in

$$\frac{\Gamma}{C}=\frac{K_s[(\mathrm{MCl}_Z)^{-1}]_b\Gamma\mathrm{Cl}^-}{[\mathrm{Cl}^-]_b\{[(\mathrm{MCl}_Z)^{-1}]_b+[\mathrm{M}^{r+}]_b\}} \tag{10}$$

Now substitution from eqn. (5) for $[\mathrm{M}^{r+}]_b$ into eqn. (10) gives

$$\frac{\Gamma}{C}=\frac{K_s\Gamma\mathrm{Cl}^-}{[\mathrm{Cl}^-]_b\left\{1+\dfrac{1}{K_F[\mathrm{Cl}^-]_b{}^Z}\right\}} \tag{11}$$

Rearrangement of eqn. (11) leads to the expression

$$\frac{\Gamma}{C}=K_s\left(\frac{\Gamma\mathrm{Cl}^-}{[\mathrm{Cl}^-]_b}\right)\left\{\frac{K_F[\mathrm{Cl}^-]_b{}^Z}{1+K_F[\mathrm{Cl}^-]_b{}^Z}\right\} \tag{12}$$

There are two parts to the right-hand side of eqn. (12), the term in brackets and $K_s\left(\frac{\Gamma\mathrm{Cl}^-}{[\mathrm{Cl}^-]_b}\right)$, each playing a role in determining Γ/C. The term in brackets is the fraction of metal ion in the form of the chloro complex in the bulk solution, F, so that eqn. (12) can alternatively be written as

$$\frac{\Gamma}{C}=K_s\left(\frac{\Gamma\mathrm{Cl}^-}{[\mathrm{Cl}^-]_b}\right)F \tag{13}$$

In this form, eqn. (13) is similar to that developed for ion-exchange studies[13]. The term, $K_s\left(\frac{\Gamma\mathrm{Cl}^-}{[\mathrm{Cl}^-]_b}\right)$, is the value of the distribution factor of the metal, when only the chloro complex exists in solution, *i.e.* $F=1$. As such it may be termed the distribution factor for the chloro complex.

Let us first examine the affect of F on Γ/C. When $K_F[\mathrm{Cl}^-]_b{}^Z \gg 1$ or F is close to one, we achieve the distribution factor equivalent to the chloro complex. As $K_F[\mathrm{Cl}^-]_b{}^Z$ becomes smaller, either because of a smaller K_F value or less chloride ion in solution, F will decrease, and as seen in eqn. (13), Γ/C will also decrease. Eventually, if $[\mathrm{Cl}^-]_b$ or K_F is very small, $\Gamma/C \to 0$. Thus we see that Γ/C can be readily controlled by the concentration of chloride ion in solution or the ability of the metal species to form an anionic chloro complex. In the RESULTS AND DISCUSSION section of this paper, maxima in Γ/C as a function of hydrochloric acid concentration for iron(III) and mercury(II) will be seen (Figs. 4 and 6); these are largely caused by the changing value of F. It will also be seen that control of the charge on the ion in solution can be a very effective means of selective removal of trace species from aqueous media by foam separation.

The distribution factor of the chloro complex, $K_s \frac{\Gamma\text{Cl}^-}{[\text{Cl}^-]_b}$ can be rewritten, if, as suggested by RUBIN[10], a Langmuir adsorption isotherm is assumed:

$$K_s \frac{\Gamma\text{Cl}^-}{[\text{Cl}^-]_b} = \frac{K_1K_2}{1+K_2[(\text{MCl}_Z)^{-1}]_b} \tag{14}$$

where K_1 and K_2 are two constants resulting from the Langmuir model. Equation (14) may be substituted into eqn. (13) to give

$$\frac{\Gamma}{C} = \frac{K_1K_2}{1+K_2[(\text{MCl}_Z)_b{}^{-1}]} F \tag{15}$$

Now, let us assume F is equal to unity (or at least constant), then when $K_2[(\text{MCl}_Z)_b{}^{-1}] \ll 1$, Γ/C will be a constant. As the concentration of the anionic metal chloro complex increases, a point will be reached at which $K_2[(\text{MCl}_Z)_b{}^{-1}]$ can no longer be neglected. Γ/C will then start to decrease with increase in the concentration of the complex. This trend has been observed in this work, when Γ/C has been measured as a function of initial metal concentration, while maintaining the hydrochloric acid concentration constant (Fig. 5). Equation (15) can thus be a valuable tool in the understanding of the foam separation of anionic chloro complexes by means of cationic surfactants.

Equation (15) has been used in the qualitative sense in this work. It is possible to use it quantitatively, if K_1 and K_2 are determined[10]. However, this determination requires an accurate measurement of the surface excess of the foaming agent, as well as the anionic chloro complexes, and carefully designed equipment is necessary. Also, the influence of micelles and the high ionic strength on F would have to be known. It was decided that the difficulty in developing the quantitative basis of eqn. (15) did not warrant the additional effort. The experimental procedures described below are designed to demonstrate the trends in the distribution factors as certain parameters are varied, in order to indicate the importance of charge control on the ionic species in aqueous solution in foam separation.

EXPERIMENTAL

Gas flow apparatus

Figure 1 is a diagram of the gas handling apparatus. Water pumped dry nitrogen gas was saturated with water vapor by passing it through two 250-ml gas washing bottles; this was done to prevent evaporation of liquid from the bulk solution. A Moore flow controller maintained the gas flow rate within 60 ± 1 ml/min. Needle valves placed before and after the flow controller were used to adjust the flow rate. A rotameter was used as a convenient reference in establishing the gas flow rate. A soap-bubble flow meter was used to measure the actual gas flow rate before reaching the spinnerette, while the actual gas pressure was measured by an open tube mercury manometer. Appropriate corrections for the pressure differential in the bulk liquid column were made on the measured flow rate.

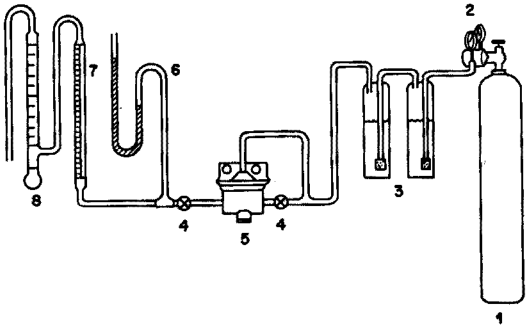

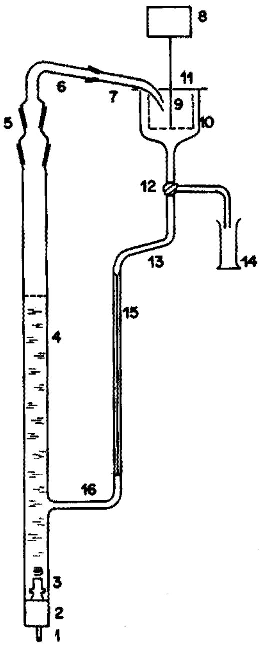

Fig. 1. Gas flow apparatus. (1) N_2 gas, Med. Tech., purified; (2) regulator, 2-stage, Hooke, 17228-1; (3) gas saturators, 250 ml, Corning, 3950; (4) needle valves, Nupro, B-4M; (5) flow controller, Moore 63BUL; (6) mercury manometer; (7) rotameter, Roger Gilmont Instrument, Inc.; (8) soap bubble flow meter.

Fig. 2. Foam recycling apparatus for measurement of distribution factors. (1) 8-mm gas line connection; (2) rubber stoppers; (3) Pt/Au spinnerette, J. Bishop & Co., 30 holes, 89-μ diameter; (4) foam column 84 cm × 34 mm; (5) standard tapered joint reducing adapter (40/50-24/40); (6) right angle bend (24/40 standard taper joints); (7) tube adapter, 105°, Corning 8840; (8) synchronous, cone drive stirrer, Lapine 383-31; (9) polyethylene basket, 8.5 cm × 9.0 cm; (10) glass collector funnel, 20 cm × 14 cm, 130°, 8-mm stem; (11) polyethylene sheet cover; (12) three-way stopcock, 8 mm; (13) tygon tubing; (14) graduated cylinder, 10 ml, 0.1 ml division; (15) capillary tubing, 2 mm; (16) side arm, 8 mm.

Apparatus and procedures

A foam recycling apparatus for determining distribution factors at steady state is diagrammed in Fig. 2. It is similar to the previous design of RUBIN[10]. Nitrogen gas, saturated with water vapor, was passed through a Pt/Au spinnerette (30 holes, 89-μ diameter) which was attached to the system by rubber stoppers. After the gas flow had begun, 500 ml of solution was poured into the column forming a liquid pool 52 cm high and a foam column 32 cm high. The gas flow was adjusted to the proper flow rate. Foam travelled up the column and then to the foam breaker section by means of a 20-mm diameter right angle tube and tapered adapter of exit diameter 10 mm.

The foam breaker section consisted of a spinning polyethylene basket with a polyethylene covered shaft. The polyethylene basket was formed by cutting off the top of a 9.0-cm diameter bottle and randomly perforating the remaining 8.5-mm high section with a hot nail. Polyethylene was used to prevent corrosion when high concentrations of hydrochloric acid were used. A synchronous motor rotated the basket in a 14-cm diameter glass funnel. The funnel was attached to a three-way stopcock by tygon tubing. The stopcock allowed either the return of collapsed foam to the liquid pool through the 2-mm diameter capillary (designed to decrease liquid hold up), or directed collapsed foam into a 10-ml graduated cylinder collection vessel. The top of the glass funnel was covered with a polyethylene sheet during the run to reduce evaporation. The starting time of a run was taken as the time when collapsed foam entered the three-way stopcock.

The sparger in the apparatus shown in Fig. 2 requires mention. When a coarse porous glass frit was used in the column, a very wet foam was produced with a range of equivalent bubble diameters (see later) of 1.22 to 2.44 mm. The reproducibility for Γ/C measurements with this set-up was poor, being only 20%. The wet foam resulted in low enrichment ratio values such that errors in E were magnified in eqn. (4) from the $(E-1)$ term. Also with the spread in bubble diameters, the reproducibility of bubble diameter measurement from run to run was not completely satisfactory.

In agreement with BRUNNER AND LEMLICH[14], it was found that conversion to a spinnerette resulted in a marked improvement in reproducibility. The bubble diameter then varied from 1.6 to 1.8 mm and the foam was considerably drier, resulting in larger E values. RUBIN[10] also recommended the use of a spinnerette.

TABLE I

REPRODUCIBILITY OF MEASUREMENTS

(Conditions: 1 M HCl; $1\cdot10^{-3}$ M HDT; $2\cdot10^{-7}$ M $HgCl_2$; 60-min recycle; gas flow rate 60 ml/min)

Run no.	*d (cm)*	*L (ml/min)*	*E*	*$\Gamma/C\cdot10^4$ (cm)*[a]
1	0.17	0.22	51	47
2	0.17	0.18	60	44
3	0.17	0.16	70	47
4	0.18	0.20	53	46

[a] Average $46 \pm 2\cdot10^{-4}$ cm, average deviation 5%.

Table I presents some typical data on the foam separation distribution coefficient of the anionic chloro complex of mercury to illustrate the kind of reproducibility possible. It can be seen that the average deviation is only about 5%.

Foam bubble diameter

It was necessary to determine the average diameter of the foam bubbles in order to compute the distribution factor. A photographic technique was used to determine this bubble diameter. Pictures of the foam were taken at the top of the foam column rather than at the bottom in order to allow for possible coalescence of foam bubbles in their travel up the column. A Polaroid camera (Model 110B) with a #1 close-up lens and a measuring magnifier (Edmund Scientific Co., magnifying power 12 ×) attached directly to the camera was used. The column was illuminated with a photoflood lamp (Westinghouse, RFL-no. 2) at a distance of 20 cm from the column and normal to the camera. Polaroid 146L transparency film was used. A transparency of the magnified scale was made as a reference. The image of the scale was then projected on graph paper and the 3 × 5 lantern slide projector distance adjusted to obtain suitable magnification. In each experiment over 150 bubbles were measured.

A completely dry foam has foam bubble shapes of pentagonal dodecahedra[15]. In our particular case, photographs revealed distorted pentagonal dodecahedra on the sides of the glass column. It was thus impossible to obtain the true foam bubble diameter. Consequently an approximate procedure was followed to be outlined below. It must be recognized again that the true distribution coefficients are not determined in this manner; however, since the major objective was to examine changes in Γ/C, the approximately constant error introduced in the bubble diameter measurements should not affect the final conclusions. It is estimated that the bubble diameter measured differs by no more than 15% from the true diameter.

The length, l, of the sides of the polyhedral bubbles were determined from the photograph. This length was then converted to the diameter of a sphere of equivalent surface area, $d = 2.44\ l$. The average specific surface area (interfacial area per unit volume), $\bar{S}$, is then[16]

$$\bar{S} = \frac{6.59}{\bar{d}} = 6.59 \frac{\sum\limits_{i} n_i d_i^2}{\sum\limits_{i} n_i d_i^3}$$

where n_i equals the number of bubbles of equivalent diameter d_i. Note that the average bubble diameter, $\bar{d}$, is determined as an area to volume ratio.

Chemicals

The cationic surfactant, hexadecyltrimethylammonium bromide (HDT; Matheson, Coleman, and Bell, technical grade) was recrystallized from water–acetone three times and dried in a vacuum desiccator. Iron(III) chloride, mercury(II) chloride and cobalt(II) chloride (Fisher, reagent grade) were used without further purification. ^{203}Hg, ^{59}Fe, and ^{60}Co tracers, carrier-free, were obtained (Baird Atomic, Inc.) as the chlorides with an activity of 1 μC. In order to obtain sufficient counts above background, about 2 ml of tracer in 500 ml of solution were needed. Because ^{203}Hg and ^{59}Fe have short half-lives, 46.5 and 46 days respectively, fresh samples were needed to obtain the necessary activity for counting.

Analytical procedures

Radioactive tracer analysis was used to determine the relative concentration of cobalt(II), iron(III) and mercury(II) ions in the solutions. The following radiation analysis equipment (Nuclear Chicago, Inc.) was used: a shielded scintillation well detector equipped with a 2″ NaI (Tl) crystal (model 965), a radiation analyzer (model 1810), and a decade scaler (model 181B). A scaler voltage of 2500 V, analyzer voltage of 832 V, and an analyzer window of 5 V was used. The analyzer base voltages were: ^{60}Co, gain 2, 1.12 MeV; ^{203}Hg, gain 4, 0.258 MeV; ^{59}Fe, gain 2, 1.03 MeV. With these settings ^{203}Hg could be determined in the presence of each other.

RESULTS AND DISCUSSION

As noted in the introduction, the present work involves an examination of the foam separation behavior of anionic chloro complexes of iron(III), mercury(II), and cobalt(II). The distribution factors of these species were determined as a function of several conditions (*e.g.* concentration of metal ion, concentration of hydrochloric acid) in order to obtain information that would be useful in the optimization of the separation.

Anionic chloro complex of iron(III)

In order to measure the distribution factor of iron(III) in high concentrations of hydrochloric acid, it was first necessary to determine the time required for steady state in the recycle apparatus of Fig. 2. From the results of KRAUS AND NELSON[8] it is clear that the anionic complex, $FeCl_4^-$, is extensively formed in 8 M hydrochloric acid media, hence this concentration was taken as the starting point. A cationic surfactant, hexadecyltrimethylammonium bromide (HDT), was used for removal of the anionic complex.

TABLE II

EFFECT OF RECYCLING TIME ON THE DISTRIBUTION FACTOR

(Conditions: 8 M HCl; $1 \cdot 10^{-3}$ M HDT; $2 \cdot 10^{-6}$ M $FeCl_3$; gas flow rate 60 ml/min)

Recycle time (min)	*d (cm)*	*L (ml/min)*	*E*	*$\Gamma/C \cdot 10^4$ (cm)*
0	0.19	0.27	20	24
15	0.18	0.21	68	64
30	0.18	0.23	64	66
60	0.17	0.27	50	59
90	0.16	0.27	52	56

Table II presents the results of the effect of recycle time on Γ/C. In all cases the gas flow rate was 60 ml/min and the HDT concentration was $1 \cdot 10^{-3}$ M. It can be noted that the variation of Γ/C with recycle time becomes small after 15 min (6.6%), and that this variation is close to the experimental error. An average value of Γ/C of $61 \pm 4 \cdot 10^{-4}$ cm for runs between 15 and 90 min was obtained. The small decrease in Γ with time beyond 30 min may be due either to adsorption of the surface-active salt on the walls of the glass column, or, more likely, the slow evaporation of hydrogen chloride from the system. In this latter case, as will be shown later, a drop in hydrochloric acid concentration below 8 M will decrease Γ/C through the formation of less $FeCl_4^-$. A recycle time of 60 min was chosen for all studies, and steady state conditions were assumed. The loss of hydrogen chloride during this period was deemed negligible and its effect on the results was neglected.

Since the concentration of surfactant is important in terms of forming the ion–surfactant complex and foam column stability, the variation of Γ/C with HDT concentration for $1 \cdot 10^{-6}$ M iron(III) chloride and 8 M hydrochloric acid was next studied. The results of this study (Fig. 3) show a very sharp increase in Γ/C between $1 \cdot 10^{-3}$ M and $2 \cdot 10^{-4}$ M HDT. At HDT concentrations greater than $1 \cdot 10^{-3}$ M, Γ/C decreases slowly. These trends agree in part with those found by RUBIN[10] and BANFIELD *et al.*[12] in the removal of cationic metal ions with anionic surfactants. Undoubtedly, for a large excess of surfactant, relative to the anionic complex, the free surfactant effectively competes with the surface-active $HDT^+–FeCl_4^-$ complex for adsorption sites on the gas bubble surface. As the surfactant concentration is decreased, this competition diminishes and as a consequence more of the complex can be removed. The drop in Γ/C at $1 \cdot 10^{-4}$ M HDT may result from extensive bubble coalescence and loss in foam stability.

It was decided to select $1 \cdot 10^{-3}$ M HDT as the surfactant concentration for the majority of foam separation studies in order to avoid large variation in Γ/C

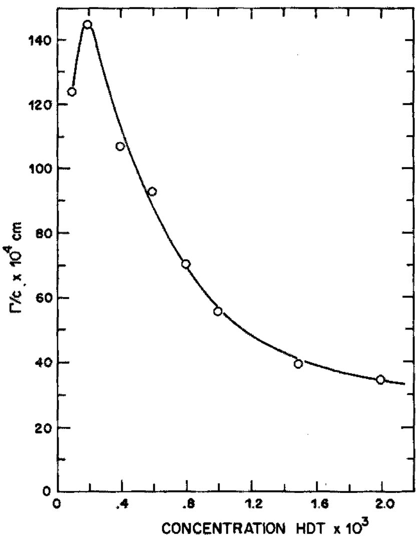

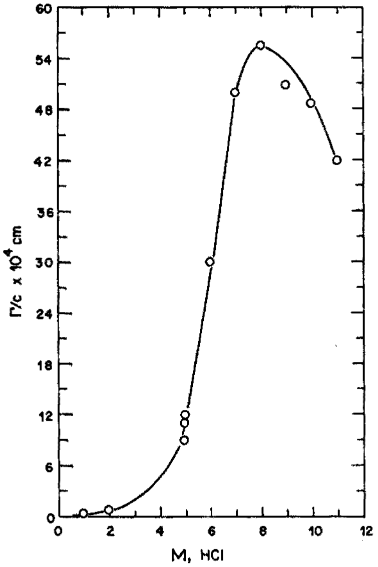

Fig. 3. Distribution factor of iron(III) chloro complex as a function of HDT concentration. Conditions: $1 \cdot 10^{-6}$ *M* $FeCl_3$; 8 *M* HCl; recycle time, 60 min; gas flow rate, 60 ml/min.

Fig. 4. Distribution factor of iron(III) chloro complex as a function of hydrochloric acid concentration. Conditions: $2 \cdot 10^{-6}$ *M* $FeCl_3$; $1 \cdot 10^{-3}$ *M* HDT; recycle time, 60 min; gas flow rate, 60 ml/min.

with small variation in HDT concentration. Secondly, there was considerably less concern with maintaining a stable foam column during the 60-min recycle period for $1 \cdot 10^{-3}$ *M* HDT compared to $2 \cdot 10^{-4}$ *M* HDT.

Owing to the high ionic strength of 8 *M* hydrochloric acid, the HDT concentration was above the critical micelle concentration (CMC) in all the experiments of Fig. 3. Previous studies[17] have shown that the CMC of a pure aqueous solution of HDT was $2 \cdot 10^{-3}$ *M* and that of a solution containing 2 *M* hydrochloric acid and 10^{-4} *M* iron(III) chloride was $1 \cdot 10^{-4}$ *M*. The higher the ionic strength, the lower the CMC. There are basically contradictory conclusions[18,19] concerning the harm of micelles in the removal of ionic species by foam separation.

In order to decrease the tendency of HDT to form micelles under conditions of high ionic strength, a mixed solvent system of alcohol–water was investigated. The HDT was dissolved in enough absolute ethanol to make the final iron(III) chloride solutions used in the experiments 5% and 10% by volume ethanol. The results of this study are shown in Table III and it is noted that Γ/C decreases with increasing percentage of alcohol. Evidently, the decrease is caused by a competition for surface adsorption sites between ethanol and the surface-active $HDT^+ : FeCl_4^-$ complex (as well as free HDT). This method was consequently abandoned. It may be noted in passing that it is unfortunate that mixed solvents seem to be detrimental to foam separation, as such solvents would extend the solubility range of species that might be used in aqueous media.

After the above preliminary factors had been examined the distribution factor was next measured as a function of molarity of hydrochloric acid in order to obtain the

TABLE III

EFFECT OF ETHANOL CONCENTRATION ON THE DISTRIBUTION FACTOR OF IRON(III) CHLORO COMPLEXES

(Conditions: $1\cdot10^{-3}$ *M* HDT; 8 *M* HCl; $FeCl_3$ $2\cdot10^{-6}$ *M*; gas flow rate 60 ml/min; recycle time 60 min)

Percentage ethanol	*d (cm)*	*L (ml/min)*	*E*	*Γ/C (cm)*
0	1.7	0.26	51	$56\cdot10^{-4}$
5	2.0	0.21	38	$38\cdot10^{-4}$
10	1.9	0.18	28	$23\cdot10^{-4}$

optimum acid concentration. Figure 4 is a plot of Γ/C *vs.* acid concentration for an initial solution of iron(III) chloride ($2\cdot10^{-6}$ *M*) and HDT (10^{-3} *M*) and a recycle time of 60 min. It can be noted that a maximum occurs at 8 *M* hydrochloric acid, and the large value of Γ/C at this point is indicative of a strong ion pair complex between HDT and $FeCl_4^-$. The important point is made that the foam separation behavior of iron(III) can be markedly controlled by the acid molarity. The results in Fig. 4 strongly resemble those of KRAUS AND NELSON who studied the ion-exchange distribution coefficients of metal chloro complexes as a function of hydrochloric acid concentration.

Calculations based on the formation constants for the iron chloro complexes indicate that the fraction of $FeCl_4^-$ at 8 *M* hydrochloric acid is 0.8 and continues to increase with increasing hydrochloric acid concentration; however, Γ/C begins to decrease at hydrochloric acid concentrations greater than 8 *M*. A possible explanation of the decrease in Γ/C at high acid concentrations may be the adsorption of hydrogen chloride by the HDT to form the hydrogen dichloride ion, HCl_2^-, at the gas–liquid interface. LINDENBAUM AND BOYD[20] reported the presence of the HCl_2^- ion in their studies of the liquid anion exchanger, tri-*n*-octylamine hydrochloride. BRINKMAN *et al.*[21] have also found indication of extraction of HCl_2^- ion by quaternary amines from aqueous solution at high concentrations of hydrochloric acid.

The variation of Γ/C with initial concentration of iron(III) chloride at 8 *M* hydrochloric acid and 1.0^{-3} *M* HDT was then examined. Figure 5 presents the results of this study in terms of Γ/C *vs.* steady state bulk iron(III) concentration. The Γ/C approaches a constant value at concentrations of less than $4\cdot10^{-6}$ *M* iron(III) and decreases very rapidly at higher concentrations. RUBIN[10] obtained similar results in his studies of the foam fractionation of uranyl ion and strontium(II) with Aresket 300. The distribution factors for these ions remained fairly constant below an ion concentration of *ca.* $1\cdot10^{-6}$ *M*.

The distribution isotherm in Fig. 5 indicates linear behavior at low concentrations. Above $4\cdot10^{-6}$ *M*, Γ is constant, but C continues to increase with initial concentration of iron(III). Thus it appears that Γ/C is fairly constant until the surface is saturated, at which point it must decrease. The study was not extended below a concentration of $2\cdot10^{-7}$ *M* iron(III) chloride because of possible iron impurity in the reagent-grade hydrochloric acid (Fisher). Obtaining the Γ/C value of iron(III) chloride below $2\cdot10^{-7}$ *M* was not deemed important enough to undertake the preparation of the ultrapure acid.

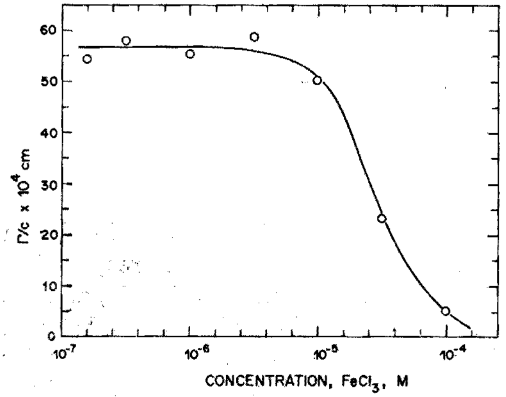

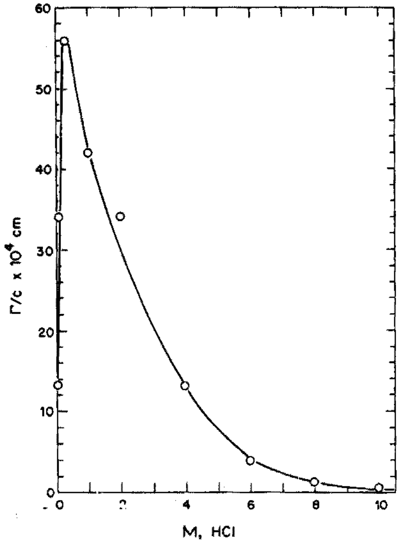

Fig. 5. Distribution factor of iron(III) chloro complex as a function of bulk steady state concentration of iron(III). Conditions: $1 \cdot 10^{-3}$ *M* HDT; 8 *M* HCl; recycle time, 60 min; gas flow rate, 60 ml/min.

Fig. 6. Distribution factor of mercury(II) chloro complex as a function of hydrochloric acid concentration. Conditions: $2 \cdot 10^{-7}$ *M* $HgCl_2$; $1 \cdot 10^{-3}$ *M* HDT; recycle time, 60 min; gas flow rate, 60 ml/min.

Anionic chloro complexes of mercury(II) and cobalt(II)

From these studies with iron(III), it can be seen that the amount of iron(III) removed in the foam layer is a strong function of the acid molarity. It was next of interest to examine other metal ions that might exhibit a different functionality of Γ/C with molarity of hydrochloric acid. Accordingly, KRAUS AND NELSON's data[8] were examined to find a metal chloro complex with a large distribution coefficient at a hydrochloric acid molarity different from that of the iron chloro complex. The mercury chloro complex case was selected since a high distribution coefficient was found at low acid concentration.

Figure 6 shows a plot of Γ/C *vs.* hydrochloric acid molarity for foam removal of the mercury chloro complexes. A recycle time of 60 min was used with the steady state apparatus, and the initial concentrations were $1 \cdot 10^{-3}$ *M* HDT and $2 \cdot 10^{-7}$ *M* $HgCl_2$. It is seen that Γ/C rises very rapidly from 0.01 *M* hydrochloric acid to a maximum at about 0.3 *M*, followed by an almost exponential decrease in the distribution factor. This behavior, as expected, closely follows that obtained by KRAUS AND NELSON[8].

The decrease in adsorption for the mercury complex at high acid concentrations may be explained on the basis of the formation of a new complex. BUTLER[22] has pointed out that below roughly 0.5 *M* hydrochloric acid, $HgCl_3^-$ is the predominant complex species present, whereas above 0.5 *M*, $HgCl_4^{2-}$ becomes the major chloro complex. Further, KRAUS AND MOORE[23] have shown in ion exchange that singly charged anionic species are more strongly adsorbed to a resin than doubly charged anions. If then adsorption at the gas–liquid interface is similar to adsorption on the ion-exchange resin, $HgCl_4^{2-}$ could compete with $HgCl_3^-$ for surface exchange sites, thus reducing the total Γ/C. Activity effects could also cause a decrease in Γ/C as the hydrochloric acid concentration is increased. A plot of Γ/C *vs.* activity of hydrochloric acid (from literature values[24]) up to 5 M hydrochloric acid revealed, however, no major change in the distribution factor plot.

The decrease in Γ/C at acid concentrations below 0.3 M may be due to the formation of an insoluble adduct of the mercury chloro complexes and HDT. During preliminary runs, the concentration of $HgCl_2$ had to be reduced from $2 \cdot 10^{-5}$ M to $2 \cdot 10^{-7}$ M at low concentrations (< 1 M) of hydrochloric acid because of precipitate formation. According to BUTLER[22], the fraction of $HgCl_2$ complex present below 0.2 M hydrochloric acid increases very rapidly, decreasing the amount of negative chloro complexes available to complex with the surfactant.

The variation of the distribution factor of the mercury chloro complexes with the initial bulk concentration of mercury(II) chloride was studied in solutions that were 1 M in hydrochloric acid and $1 \cdot 10^{-3}$ M in HDT. Concentrations of mercury(II) chloride were taken between $2 \cdot 10^{-7}$ M and $2 \cdot 10^{-5}$ M. The value of Γ/C was fairly constant from $2 \cdot 10^{-7}$ M to $5 \cdot 10^{-6}$ M $HgCl_2$ and began to decrease at concentrations greater than $5 \cdot 10^{-6}$ M. As with iron, the adsorption isotherm was linear until saturation was reached, at which point Γ/C decreases. An attempt to obtain Γ/C at $1 \cdot 10^{-4}$ M mercury(II) chloride was unsuccessful because a precipitate of $Hg(OH)_2$ formed. Calculations based on the equilibrium constants of hydroxy complexes predict the formation of a $Hg(OH)_2$ precipitate in a solution containing 1 M H_3O^+ ion and $1 \cdot 10^{-4}$ M mercury(II) ion.

These distribution factor studies indicate that it is possible to remove mercury(II) efficiently from solutions containing low molarities of hydrochloric acid The removal should be very effective at mercury(II) concentrations less than $1 \cdot 10^{-6}$ M. Since the Γ/C maximum occurs at a hydrochloric acid concentration different from that of the iron chloro complex, one should be able to remove selectively mercury(II) from a solution containing iron(III).

The data from KRAUS AND NELSON[8] showed that cobalt can be separated as the chloro complexes by ion exchange. Cobalt forms a series of chloro complexes; two are negatively charged, $CoCl_3^-$ and $CoCl_4^{2-}$ [25]. Since ^{60}Co was readily available for isotope dilution analysis, foam separation of cobalt chloro complexes with HDT was studied.

The variation of Γ/C for the cobalt chloro complexes with concentration of hydrochloric acid was examined. A recycle time of 60 min was used to ensure that the system was at steady state. In all experiments, $2 \cdot 10^{-7}$ M $CoCl_2$ and $1 \cdot 10^{-3}$ M HDT were used. These conditions were chosen to be the same as the best conditions determined for the iron and mercury studies. Compared to the results for iron(III) and mercury(II) chloro complexes, the values of Γ/C for cobalt(II) chloro complexes are lower by factors as large as 100 (*e.g.* $2 \cdot 10^{-5}$ cm). Further, low enrichment ratios were obtained, (*e.g.* 1.1–1.3) so that the error in Γ/C from $E-1$ was large. The reproducibility of Γ/C was thus poor, and no indication of a maximum in the distribution factor was possible. The ion-exchange results[8] also showed considerably smaller distribution coefficients for cobalt(II) compared to the maxima for iron(III) and mercury(II). However, a definite maximum at 9 M hydrochloric acid was obtained for cobalt. Evidently the foam separation experiment is not as sensitive as the ion-exchange method in observing small changes in complexation of the metal chloro species. Nevertheless, the foam separation results with cobalt(II) show that it should be possible to separate cobalt from iron and mercury.

Selective enrichment by foam separation

Since it was found that the maximum Γ/C value for the mercury chloro complexes occurred at a different acidity from the Γ/C value for iron(III) and further that the Γ/C values of the cobalt(II) chloro complexes were very low, the selective enrichment of one chloro complex from a mixture of metal chloro complexes by foam separation was investigated. The distribution factors were first measured for mixtures of mercury and iron chloro complexes to determine interferences.

The ratio of mercury(II) chloride concentration to iron(III) chloride concentration was varied from 1:1 to 1:500 and the distribution factors for mercury and iron chloro complexes were determined at the following hydrochloric acid concentrations: 1 *M*, 5 *M*, and 8 *M*. From the individual experiments of iron and mercury previously discussed, it was found that at 1 *M* acid, the Γ/C for a mercury chloro complex was approximately 200 times that of an iron chloro complex. At 5 *M*, the distribution factors were approximately equal, and at 8 *M* the Γ/C for the iron chloro complex was approximately forty-four times that of the mercury chloro complex. Table IV presents the results of this study, and it is seen that the distribution factors did not change significantly in mixtures of iron and mercury chloro complexes. In establishing the concentration ratios of mercury and iron, the concentration of mercury(II) chloride was kept at or below $2\cdot10^{-7}$ *M* and the concentration of iron(III) chloride below $1\cdot10^{-5}$ *M* whenever possible, in order to maintain the system below the region where the gas–liquid interface becomes saturated with the given metal. The effect of saturation can be seen in Table IV for the distribution factor of iron at 8 *M* acidity. Two experiments are presented where the ratio of $HgCl_2$ to $FeCl_3$ is 1:500; the concentrations of iron(III) in these experiments are $1\cdot10^{-4}$ *M* and $2.5\cdot10^{-5}$ *M*, respectively. These concentrations are in the region where the gas–liquid interface is saturated. The distribution factor of the iron chloro complexes in these samples is reduced, in agreement with Fig. 5. From the results in Table IV it can be predicted that in a mixture of iron and mercury, mercury can be concentrated selectively in *M* hydrochloric acid, iron at 8 *M*, and little separation is possible at 5 *M*.

TABLE IV

DISTRIBUTION FACTORS IN MIXTURES OF $HgCl_2$ AND $FeCl_3$

Concentration (M)	*Ratio Hg/Fe*	*$\Gamma/C\cdot10^4$ cm*					
Hg Fe		*1 M HCl*		*5 M HCl*		*8 M HCl*	
		Hg	*Fe*	*Hg*	*Fe*	*Hg*	*Fe*
$2\cdot10^{-7}/2\cdot10^{-7}$	1:1	40	0.19	9.6	9.1	1.5	55
$2\cdot10^{-7}/2\cdot10^{-6}$	1:10	41	0.17	11	11	1.5	46
$1\cdot10^{-7}/1\cdot10^{-5}$	1:100	48	0.45	8.4	9.2	1.6	49
$2\cdot10^{-7}/1\cdot10^{-4}$	1:500	47	0.23	—	—	1.4	9.8
$5\cdot10^{-8}/2.5\cdot10^{-5}$	1:500	45	0.33	—	—	0.78	33
$0/2\cdot10^{-6}$	0:1	—	—	—	11	—	55
$2\cdot10^{-7}/0$	1:0	42	—	6.5	—	—	—

KARGER *et al.*[26] have shown that total reflux is an efficient and convenient method for concentrating solutes at trace levels by foam separation. In this method the foam is thermally broken at the top of the column during the total reflux period and surface-active material in the interstices between the gas bubbles becomes concentrated at the top of the foam column. After total reflux, the hot zone is cooled, and the foam is allowed to travel out of the column to be appropriately collected as a collapsed liquid.

Total reflux experiments were thus performed to concentrate on a selective basis mercury(II) and iron(III) chloro complexes. The Friedrich's condenser total reflux apparatus previously described[26] was used with a 20-cm liquid pool and 45-cm foam column. To establish the most suitable conditions for total reflux of mixtures, a study of percent recovery, $\%R$ [(moles in foam/moles in original)$\cdot 10^2$], *vs.* reflux time for the mercury(II) chloro complexes was made. For this work, the 30-hole Pt/Au spinnerette with an initial gas flow rate of 30 ml/min was adopted for generation of the foam column. After the total reflux period, the gas flow rate was increased to 60 ml/min for collection of the collapsed foam, with the spinning perforated polyethylene basket.

Table V presents the data of the above study; it is seen that the enrichment ratio, E, is large without any reflux and increases rapidly with time. The percentage recovery increases from 52% to 79% in a 60-min total reflux period for a 4-ml sample of collapsed foam. In addition, the volume reduction is 37-fold and the decontamina-

TABLE V

TOTAL REFLUX OF $HgCl_2$ SOLUTIONS

(Conditions: 1 M HCl; $1\cdot 10^{-7}$ M $HgCl_2$; $1\cdot 10^{-3}$ M HDT)

Time (min)	*D*	*E*	*Volume reduction*	*Volume collected (ml)*	*% Recovery*
0	4.8	94	38	4.0	52
10	10	190	37	4.1	53
60	24	710	37	4.1	79

TABLE VI

TOTAL REFLUX: MIXTURES OF $HgCl_2$ AND $FeCl_3$

(A) Conditions: 10-min reflux; $HgCl_2$ $1\cdot 10^{-7}$ M; $FeCl_3$ $1\cdot 10^{-5}$ M; HDT $1\cdot 10^{-3}$ M

M HCl	*D-Hg*	*E-Hg*	*% R Hg*	*D-Fe*	*E-Fe*	*% R Fe*	*ml*	*Volume reduction*
1	5.3	94	40	1	1	2.3	3.4	44
5	1.5	12	19	1.9	11	25	3.5	43
8	1.1	2.6	6.4	4.3	78	46	3.8	40

(B) Conditions: 60-min reflux; $1\cdot 10^{-3}$ M HDT

M HCl	*Conc. $HgCl_2$*	*Conc. $FeCl_3$*	*D-Hg*	*E-Hg*	*% R Hg*	*D-Fe*	*E-Fe*	*% R Fe*	*ml*	*Volume reduction*
1	$1\cdot 10^{-7}$ M	$1\cdot 10^{-5}$ M	21	710	78	1.7	2.3	3.1	3.5	43
8	$1\cdot 10^{-7}$ M	$1\cdot 10^{-7}$ M	1	1	2.3	17	630	84	3.5	43
8	$1\cdot 10^{-5}$ M	$1\cdot 10^{-7}$ M	1.1	4.0	8.5	17	540	76	3.6	42

tion factor, *D* (conc. original/conc. bulk residue) increases to a factor of 24. Thus Table V illustrates further the value of total reflux in recovery and connection of surface-active material by foam separation.

The total reflux of the mixtures of mercury and iron chloro complexes was then performed at several hydrochloric acid molarities with 10-min and 60-min reflux times. Part A of Table VI presents the results of the 10-min reflux period in which there is initially a 100-fold excess of iron. The results correspond to the predictions of the distribution factor experiments: the mercury was recovered selectively at 1 *M* hydrochloric acid, roughly equal recovery was obtained at 5 *M* hydrochloric acid, and the iron was recovered selectively from 8 *M* acid. Further, iron did not appear to interfere with mercury at 1 *M* acidities, since the %*R* values were similar to those obtained in Table V for a 10-min total reflux period for mercury(II) alone.

Table VIB presents the results of the 60-min total reflux period on the mixture of iron and mercury chloro complexes. As expected, significantly better recoveries are obtained compared with the 10-min reflux period for the species which is predominantly removed. For example, at 8 *M* hydrochloric acid, the recovery of iron(III) goes from 46% at 10-min reflux to roughly 80% at 60-min reflux. It is further worth noting that for the minor constituent removed, there seems to be little difference in the 10- and 60-min reflux periods. As a result, a better selective enrichment occurs for the longer reflux period. Thus in 1 *M* hydrochloric acid, the enrichment ratio (Hg/Fe) is 94 for 10-min reflux, and this ratio rises to 310 for 60-min reflux. Moreover, in this latter example, mercury, which is initially 100-fold less concentrated (10^{-7} *M*), is enriched 310 times compared to iron. This result strongly indicates the power of foam separation for selective enrichment of trace components via control of charge on the given species.

In Table VIB, two results are presented for 8 *M* acid, one in which the concentration ratio of the two metals is 1:1 and the other 100:1. When the ratio is 100:1, the recovery of iron reduces from 84% to 76%, while the recovery of mercury increases from 2.3% to 8.5%. Thus in this case there appears a slight interference of mercury on the removal of iron. This interference is not altogether surprising since anionic mercury chloro complex exists in 8 *M* hydrochloric acid. In this case, as in others, the selective concentration might be improved by refoaming the foamate or by using a stripping column[27].

A study of the selective enrichment of the mercury chloro complexes, in a mixture of mercury and cobalt complexes, was also made. An examination of Γ/C for mercury(II) in a mixture of 1:1 mercury(II) and cobalt(II) chlorides ($2 \cdot 10^{-7}$ *M*) showed that cobalt does not influence the distribution factor of mercury. A 60-min total reflux experiment was then performed on the above mixture at 0.3 *M* hydrochloric acid and 10^{-3} *M* HDT, in the Friedrich's condenser apparatus. For 3.5 ml of collapsed foam sample, the mercury enrichment was 8.4 with 69% recovery, and the *E* value for cobalt was only 1.7 with 4% recovery. The results indicate that mercury chloro complexes can be selectively recovered from a solution containing cobalt ions.

CONCLUSION

Total reflux foam separation can be a useful tool for concentration of trace components (*ca.* 10^{-7} M) on a selective basis via charge control of the various species. The data of KRAUS AND NELSON[8] can be used for selection of the proper acid concentration to remove one or more metal species as their chloro complexes. Quite obviously, other charged complexes can be envisioned both anionic and cationic, and again, ion-exchange distribution data can be examined to find proper conditions. New systems, on which sparse ion-exchange data are available, can be directly studied by foam separation. For an understanding of the chemical factors involved in the removal (compared to foam characteristics), the distribution factors should be determined, as described in this paper.

The work was supported by Grant WP 01129-01 from the Federal Water Pollution Control Administration, U.S. Dept. of Interior. A portion of this work was presented at the 154th National ACS Meeting held in Chicago, Ill., September, 1967.

SUMMARY

The application of selective concentration by foam separation of trace species via control of charge on these species has been investigated. The removal of anionic chloro complexes of iron(III), mercury(II), and cobalt(II) has been examined. Distribution factors, Γ/C, as a function of hydrochloric acid concentration have been measured with the cationic surfactant, hexadecyltrimethylammonium bromide; the trends have been found to be similar to those obtained in ion-exchange measurements, with an anionic exchanger. In the case of iron(III), Γ/C has also been measured as a function of surfactant concentration, initial $FeCl_3$ concentration, and % ethanol in water. Total reflux foam separation measurements were performed for selective removal. It was found that 10^{-7} M $FeCl_3$ could be selectively removed in the presence of a 100-fold excess of $HgCl_2$. Further, $HgCl_2$ could be selectively concentrated at 1 M hydrochloric acid and 10^{-7} M in the presence of $CoCl_2$. A model based on a mobile ion-exchanger surface is presented to explain qualitatively the trends observed.

RÉSUMÉ

On examine les possibilités d'applications de concentration sélective par séparation de mousse, et en particulier l'élimination des chlorocomplexes anioniques du fer(III), du mercure(II) et du cobalt(II). Les coefficients de partage ont été mesurés à l'aide de bromure d'hexadécyltriméthylammonium (surfactant cationique). On peut ainsi séparer $FeCl_3$ 10^{-7} M sélectivement, en présence de 100 fois la quantité de $HgCl_2$. $HgCl_2$ peut ensuite être concentré sélectivement en présence de $CoCl_2$. Un exemple basé sur un système surface–échangeur d'ions-mobile est présenté.

ZUSAMMENFASSUNG

Es wurde die selektive Konzentration von Spuren durch Schaumtrennung unter Berücksichtigung der Ladung dieser Spezies untersucht. Die Abtrennung anionischer Chlorokomplexe von Eisen(III), Quecksilber(II) und Koball(II) wurde geprüft. Die Abhängigkeit des Verteilungskoeffizienten von der Salzsäurenkonzentration wurde unter Verwendung des kationischen Hexadecyltrimethylammoniumbromids gemessen. Die Abhängigkeiten sind ähnlich denen, die bei Messungen mit Anionenaustauschern erhalten wurden. Für Eisen(III) wurde der Verteilungskoeffizient ebenso als Funktion der Konzentration des grenzflächenaktiven Stoffes, der anfänglichen $FeCl_3$-Konzentration und dem Gehalt an Äthanol gemessen. Es wurde gefunden, dass 10^{-7} *M* $FeCl_3$ in Gegenwart eines hundertfachen Überschusses von $HgCl_2$ selektiv abgetrennt werden kann. 10^{-7} *M* $HgCl_2$ kann aus salzsaurer Lösung in Gegenwart von $CoCl_2$ selektiv konzentriert werden. Ein Modell, das auf einer mobilen Ionenaustauscheroberfläche beruht, wird zur qualitativen Deutung der beobachteten Ergebnisse angegeben.

REFERENCES

1 B. L. Karger, R. B. Grieves, R. Lemlich, A. J. Rubin and F. Sebba, *Sepn. Sci.*, 2 (1967) 401.
2 B. L. Karger and D. G. DeVivo, *Sepn. Sci.*, 3 (1968) 392.
3 R. Lemlich, *Ind. Eng. Chem.*, 60 (1968) 16.
4 E. Rubin and E. L. Gaden, Jr., in H. M. Schoen, *New Chemical Engineering Techniques*, chap. 5, Wiley–Interscience, New York, 1962.
5 E. Schonfeld and A. H. Kibbey, *Nucl. Appl.*, 3 (1967) 353.
6 B. L. Karger and L. B. Rogers, *Anal. Chem.*, 33 (1961) 1165.
7 R. B. Grieves, *Brit. Chem. Eng.*, 13 (1968) 77.
8 K. A. Kraus and F. Nelson, *Proc. Intern. Conf. Peaceful Uses At. Energy, Geneva*, 7 (1955) 113.
9 B. L. Karger, R. P. Poncha and M. W. Miller, *Anal. Letters*, 1 (1968) 437.
10 E. Rubin, *Ph.D. Dissertation*, Columbia University, 1963.
11 S. Fanto and R. Lemlich, *A.I.Ch.E.–International Chem. Eng. Symposium*, No. 9 (1965) 75.
12 D. L. Banfield, H. I. Newson and P. J. Adler, *A.I.Ch.E. Symp. Ser.*, 1 (1965) 1.
13 O. Samuelson, *Ion Exchange Separations in Analytical Chemistry*, Wiley, Interscience, New York, 1963.
14 C. A. Brunner and R. Lemlich, *Ind. Eng. Chem., Fundamentals*, 2 (1963) 297.
15 J. J. Bikerman, *Ind. Eng. Chem.*, 57 (1965) 56.
16 R. A. Leonard and R. Lemlich, *A.I.Ch.E.J.*, 11 (1965) 18.
17 R. P. Poncha, *Ph.D. Dissertation*, Northeastern University, 1967.
18 F. Sebba, *Ion Flotation*, Elsevier, Amsterdam, 1962.
19 A. J. Rubin and J. D. Johnson, *Anal. Chem.*, 39 (1967) 298.
20 S. Lindenbaum and G. E. Boyd, *ORNL No. 3220*, 1962.
21 U. A. Th. Brinkman, G. De Vries and E. Van Dalen, *J. Chromatog.*, 31 (1967) 182.
22 J. N. Butler, *Ionic Equilibrium*, Addison–Wesley, Reading, Mass., 1964, p. 296.
23 K. A. Kraus and G. E. Moore, *J. Am. Chem. Soc.*, 74 (1953) 843.
24 R. A. Robinson and R. H. Stokes, *Electrolyte Solutions*, Butterworths, London, 1955, p. 476.
25 *Stability Constants*, Part I, The Chemical Society (London), Special Publication, No. 17, 1964.
26 B. L. Karger, R. P. Poncha and M. W. Miller, *Anal. Chem.*, 38 (1966) 764.
27 C. Jacobelli-Turi, S. Terenzi and M. Palmera, *Ind. Eng. Chem., Process Design Develop.*, 6 (1967) 162.

Analytica Chimica Acta
Elsevier Publishing Company, Amsterdam
Printed in The Netherlands

THE SOLUTION CHEMISTRY OF ETHYLMETHYLGLYOXIME

PART II. THE NICKEL COMPLEX

BIRGITTA EGNEUS
Department of Analytical Chemistry, University of Gothenburg, 402 20 Göteborg 5 (Sweden)

(Received August 15th, 1969)

Dioximes are often used as specific analytical reagents for nickel. Much of the earlier work on this group of reagents has been summarized by BABKO[1], BANKS[2], DYRSSEN[3,4], and BURGER[5]. Many investigations have been carried out, especially with dimethylglyoxime (DMG), in order to explain the selectivity of the reagents, and it was thought that similar studies with ethylmethylglyoxime (EMG) might further elucidate the analytical properties of the dioximes and make it possible to predict whether or not higher alkyldioximes ought to have advantages over DMG as specific reagents for nickel. An investigation of the proton complex of EMG was reported in Part I[6], and is now followed by Part II which deals with the nickel complex.

Two different solid modifications of $Ni(EMG)_2$ have been reported[7], one orthorhombic[8] and one monoclinic[9]. This has not previously been taken into consideration in solubility experiments[10,11]. An attempt was therefore made to measure not only the solubility of each form, but also the X-ray powder diffraction and u.v.–vis.–i.r. spectra. In addition the complex formation and extraction constants as well as the u.v.–vis. spectra in chloroform have been measured.

One property of the nickel dioximes has been the subject of much discussion, namely the strength of the nickel–nickel bond in the solid state. In this Department, the view is held that the length of the nickel–nickel distance in $Ni(DMG)_2$ is governed by the close-packing of the ligands and that the long nickel–nickel bond must be weak. If so, the most stable structure of $Ni(EMG)_2$ ought also to be determined by the close-packing of the somewhat larger ligands and not by the nickel–nickel distance.

EXPERIMENTAL

Chemicals

The ethylmethylglyoxime was prepared by the method of BELCHER *et al.*[12] and recrystallized three times from a water–alcohol mixture. The yellow or tangerine form of nickel ethylmethyldioxime was precipitated by adding a stoichiometric amount of nickel sulfate to a heated solution containing a 2:1 molar ratio of EMG and sodium carbonate[11]. The sodium perchlorate was prepared by a method used at KTH, Stockholm[13]. The chloroform was washed three times with water before use, in order to remove alcohol and saturate the solvent with water. All chemicals were of analytical grade. The ionic strength of the aqueous phase was kept constant at 0.1 *M*.

Instrumental techniques

The pH measurements were performed with a Radiometer pHM 4 equipped with Radiometer's glass electrode G 202B and saturated calomel electrode K 401. The pH-meter was standardized against 0.01 M perchloric acid + 0.09 M sodium perchlorate (pH = 2.000).

The quantitative analyses for nickel were performed either on a Perkin-Elmer Model 303 atomic absorption spectrophotometer, with an air–acetylene gas mixture, or on a Perkin-Elmer Hitachi 139 spectrophotometer, in 1-cm quartz cells.

The u.v.–vis. spectra of $Ni(EMG)_2$ in solution were recorded on a Perkin-Elmer Hitachi 139, and the spectra of the solid forms of $Ni(EMG)_2$ were recorded on a Shimadzu MPS-50L spectrophotometer, quartz cells and quartz plates being used respectively. The i.r. spectra of the solid forms of $Ni(EMG)_2$, ground with potassium bromide and pressed to pellets, were recorded on a Beckman IR9 spectrophotometer.

The X-ray powder diagrams were obtained with a Guinier camera, under Cu Kα-radiation, $\lambda = 1.54051$ Å. The lattice constants were refined and the lattice spacings calculated with the computer program POWDER[14], written for the IBM 360/50 computer.

Solubility experiments

The solubility of nickel ethylmethylglyoxime was determined by filtering solutions with decreasing amounts of glyoximate anion through a column containing the yellow-coloured complex. The solutions had an initial concentration of EMG of 0.005 M and the hydrogen ion concentration of the solutions was measured before and after they were filtered through the column. The saturated filtrates were analyzed for nickel by atomic absorption. The calibration curve was constructed without EMG, and the absorbances were corrected for the increase in absorbance caused by EMG before evaluation from the calibration graph.

Distribution experiments

Equal volumes (10 or 15 ml) of chloroform and an aqueous solution containing nickel sulfate, EMG in excess, sodium acetate, perchloric acid and sodium perchlorate were shaken for 2–3 h in centrifuge tubes. After separation of the two phases, the pH was measured in the aqueous phase. The organic phase was analyzed spectrophotometrically for nickel at 378 nm without any further treatment. Ethanol-free chloroform saturated with water was used as a reference. A calibration curve was constructed by extracting known amounts of nickel at pH 5.8–6.9 with EMG, the pH range being checked by repeated shaking of the aqueous phase with 2–3 portions of chloroform. The nickel content in the aqueous phase was either set equal to the difference between the added amount and the concentration of the organic phase, or determined spectrophotometrically at 445 nm by ROLLET's method[15], with bromine as oxidant and sodium hydroxide to provide the alkaline medium. ROLLET's method was used for low concentrations, $2 \cdot 10^{-6}$–$1.5 \cdot 10^{-5}$ M.

CALCULATIONS AND RESULTS

Determination of the solubility and stability constants

During the solubility experiments it was noticed that the yellow-coloured precipitate gradually turned red when the pH was lowered, the change starting at about pH 4.5. The yellow form was completely transformed into the red form after standing for some days in the column with an 0.005 M acetate buffer solution of pH 4.3. The solubility experiment was then repeated with the red compound after checking the phase transformation by X-ray powder diffraction.

The symbols used in the following pages are defined in Table I.

TABLE I

H_2A = the acid form of EMG or a dioxime in general
h = $[H^+]$
K_{a1} = $h[HA^-][H_2A]^{-1}$
K_{s1} = $[Ni(HA)_2]$ (solution saturated with $Ni(HA)_2$), intrinsic solubility
K_{s0} = $[Ni^{2+}][HA^-]^2$(solution saturated with $Ni(HA)_2$), solubility product
S = total molar solubility of $Ni(HA)_2$
$\beta_1 = K_1$ = $[NiHA^+][Ni^{2+}]^{-1}[HA^-]^{-1}$
$\beta_2 = K_1K_2$ = $[Ni(HA)_2][Ni^{2+}]^{-1}[HA^-]^{-2}$
K_2 = $[Ni(HA)_2][NiHA^+]^{-1}[HA^-]^{-1}$
p = $\sqrt{K_1/K_2}$
K_{D1} = $[H_2A]_{org}/[H_2A]_{aq}$
K_{D2} = $[Ni(HA)_2]_{org}/[Ni(HA)_2]_{aq}$
D = net distribution ratio of nickel (org/aq)
$[H_2A]_0$ = initial total concn. of H_2A in the aqueous phase
$[Ni^{2+}]_0$ = initial concn. of nickel in the aqueous phase
K = $h^2[Ni(HA)_2]_{org}[Ni^{2+}]^{-1}[H_2A]^{-2} = K_{D2}\beta_2K_{a1}^2$
I = molar ionic strength
ε = molar absorptivity

The total solubility of $Ni(EMG)_2$ is given by

$$S = [Ni(HA)_2] + [NiHA^+] + [Ni^{2+}] \tag{1}$$

or in saturated solution, where K_{s1} is the intrinsic solubility of $Ni(EMG)_2$,

$$S = K_{s1}(1 + \beta_1\beta_2^{-1}[HA^-]^{-1} + \beta_2^{-1}[HA^-]^{-2}) \tag{2}$$

For each filtered solution, $[H_2A]$ was calculated from the following equation:

$$[H_2A] = [H_2A]_0 + [NiHA^+] + 2[Ni^{2+}] - [HA^-] - [A^{2-}] \tag{3}$$

In the actual experiments the formation of $NiHA^+$, HA^- and A^{2-} could be neglected, and, by eliminating $[Ni^{2+}]$, the concentration of free H_2A can be calculated from

$$[H_2A] = [H_2A]_0 + 2(S - K_{s1}) \tag{4}$$

$[HA^-]$ can then be calculated from $[H_2A]$, pK_{a1} and pH.

The experimental data were plotted as $\log S$ against $-\log [HA^-]$ (see Fig. 1). The asymptotes to the solubility curves are

$$\log S = \log K_{s1} \text{ when } [HA^-] \to \infty \tag{5}$$

$$\log S = \log K_{s1} - 2 \log \beta_2 - 2 \log [HA^-] \text{ when } [HA^-] \to 0 \tag{6}$$

and, from the intersection of the asymptotes, $\log K_{s1}$ and $\log \beta_2$ can be calculated.

The experimental curve can be fitted[16,17] to the normalized curve $Y = \log (1 + pv + v^2)$, $X = \log v$. The best fit is for $p = 0$, which shows that the assumption that $NiHA^+$ could be neglected in eqn. (3) is valid. The data give $\log K_{s1} = -4.92$

and log $\beta_2 = 17.84$ for the yellow form, and log $K_{s1} = -5.56$ and log $\beta_2 = 17.74$ for the red form of Ni(EMG)$_2$. The two values of β_2 should theoretically be the same, and the difference of 0.10 reflects the experimental accuracy.

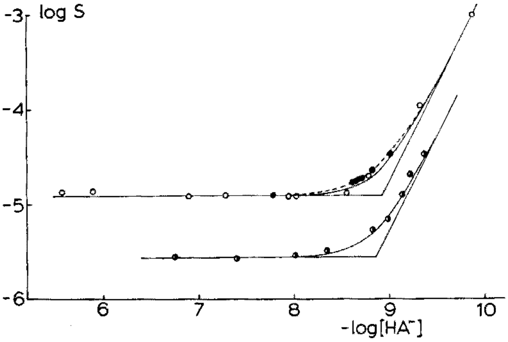

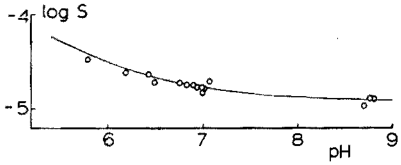

Fig. 1. The solubility of the red and the yellow forms of Ni(EMG)$_2$ in aqueous solution as a function of [HA$^-$]. The full-line curves are the normalized curve $Y = \log(1 + pv + v^2)$, $X = \log v$ for $p = 0$, and the dashed curve is for $p = 0.32$. (○) Yellow form when EMG added; (●) yellow form when no EMG added; (◑) red form when EMG added.

Fig. 2. The solubility of the yellow form of Ni(EMG)$_2$ as a function of pH. No EMG has been added. The full-line curve was calculated from eqn. (2) with log $K_{s1} = -4.92$ and log $\beta_2 = 17.84$. The circles represent experimental data.

TABLE II

THE STABILITY CONSTANTS (β_2), INTRINSIC SOLUBILITIES (K_{s1}) AND SOLUBILITY PRODUCTS (K_{s0}) FOR Ni(DMG)$_2$ AND Ni(EMG)$_2$

($K_{s1}/K_{s0} = \beta_2$)

	log β_2	pK_{s1}	pK_{s0}	*I*	*Ref.*
Ni(DMG)$_2$	17.36	6.02	23.37	0.05	18
	17.98	5.68	23.66	0	19
	17.24	5.82[a]	23.06	0.1	20
Ni(EMG)$_2$	17.57[b]	5.70	23.27	0.1	10
	—	5.56	—	—	11
Ni(EMG)$_2$ (yellow form)	17.84	4.92	22.76	0.1	This work
Ni(EMG)$_2$ (red form)	17.74	5.56	23.30	0.1	This work

[a] Estimated value from the solubility in wet chloroform.
[b] Estimated from measurements in a 75% dioxane–25% water mixture.

A summary of the values of log β_2, log K_{s1} and log K_{s0} for Ni(DMG)$_2$ and the two forms of Ni(EMG)$_2$ is given in Table II. Although the solubility products of Ni(DMG)$_2$ and red Ni(EMG)$_2$ are not significantly different, the intrinsic solubility of red Ni(EMG)$_2$ is definitely higher than that of Ni(DMG)$_2$. The solubility product and intrinsic solubility of the yellow form of Ni(EMG)$_2$ are higher than for the red form. Thus the red form is the thermodynamically more stable one. This will be discussed below.

Whether yellow or red Ni(EMG)$_2$ is formed depends to a great extent on how the precipitation is carried out. Rapid precipitation gives the yellow form, but if the components are mixed very slowly, the red form predominates in the solid phase. Anex and Krist[7] obtained small crystals of the red form by growing them from saturated chloroform solutions. Similarly, the yellow form is slowly transformed into the red by shaking the yellow precipitate with chloroform for 24 h.

Since the yellow form is roughly ten times as soluble as $Ni(DMG)_2$, there is no advantage in using EMG for gravimetric determinations of nickel, in spite of the higher solubility[6] of EMG compared with DMG, a fact that would reduce the volume of reagent needed and diminish the loss due to dissolved $Ni(HA)_2$.

In another solubility experiment with the yellow form, solutions with increasing concentrations of hydrogen ions but without EMG (*i.e.* $[H_2A]_0 = 0$) were passed through the column. This should favour the contribution of $NiHA^+$ to the solubility in eqn. (1).

TABLE III

STABILITY CONSTANTS $\log K_1$ AND $\log K_1K_2 = \beta_2$ FOR $Ni(DMG)_2$ AND $Ni(EMG)_2$ IN DIOXANE–WATER MIXTURES

	% Dioxane	*Ionic medium*	*log K_1*	*log K_1K_2*	*p[a]*	*Ref.*
$Ni(DMG)_2$	75	0.1 M $NaClO_4$	10.96	23.10	0.26	10
	50	—	10.62	21.70	0.58	4,21
	50	—	10.80	22.35	0.42	22
	50	0.3 M $NaClO_4$	11.50	22.50	1.80	23
	0[b]	0.1 M $NaClO_4$	7.91	17.00	0.26	10
	0	0.1 M $NaClO_4$	—	17.24	≤ 0.25	20
$Ni(EMG)_2$	75	0.1 M $NaClO_4$	10.41	23.97	0.027	10
	50	—	11.50	22.50	1.80	22
	0[b]	0.1 M $NaClO_4$	7.27	17.69	0.027	10
	0	0.1 M $NaClO_4$	8.42	17.84	0.32	[c]

[a] $p = \sqrt{K_1K_2^{-1}}$ independent of % dioxane and ionic strength.
[b] Extrapolated from a 75% dioxane–25% water mixture.
[c] This work.

From the values of S, K_{s1}, β_2 and pH, values of $[HA^-]$ and β_1 were calculated by successive approximation. In Fig. 2 the experimental data, log S and pH, are compared with a curve calculated with $\log \beta_1 = 8.42$, *i.e.* $\log K_2 = 17.84 - 8.42 = 9.42$. The agreement is satisfactory. In Fig. 1 the data are plotted as log S and $-\log [HA^-]$, and again the agreement is good for the normalized curve with $p = \sqrt{K_1/K_2} = \sqrt{0.1} = 0.32$, which is not too far from the value of $p \leq 0.25$ reported earlier[20].

The values of $\log \beta_1$ and $\log \beta_2$ obtained in this work can be compared with earlier determinations in dioxane–water mixtures, if these are extrapolated to 0 % dioxane. From Table III it is seen that β_2 for $Ni(EMG)_2$ is about four to five times larger than for $Ni(DMG)_2$. The Table also reveals the uncertainty in the values of $\log K_1$ and p, but it is probably safe to state that $K_1 < K_2$, *i.e.* $p < 1$. The formation of two strong hydrogen bonds in $Ni(EMG)_2$ could easily account for this, and for most analytical purposes the formation of $NiHA^+$ can be neglected.

If K_1 is not too low, *i.e.* $p > 0.1$, it might be possible to observe changes in the absorption spectra of saturated solutions of $Ni(EMG)_2$ in 96 % ethanol upon the addition of nickel chloride, caused by the formation of $NiHA^+$,

$$NiCl_2 + Ni(HA)_2 \rightleftharpoons 2\ NiHACl.$$

Determination of distribution equilibrium constants

The distribution equilibria are given by

$$\mathrm{Ni(HA)_2\ (aq) \rightleftharpoons Ni(HA)_2\ (CHCl_3)}$$

$$\mathrm{Ni^{2+} + 2\ H_2A \rightleftharpoons Ni(HA)_2\ (CHCl_3) + 2\ H^+}$$

with equilibrium constants K_{D2} and K, respectively.

The net distribution ratio is given by

$$D = \frac{[\mathrm{Ni(HA)_2}]_{\mathrm{org}}}{[\mathrm{Ni^{2+}}]+[\mathrm{NiHA^+}]+[\mathrm{Ni(HA)_2}]} \tag{7}$$

or

$$D = \frac{K_{D2}\beta_2[\mathrm{HA^-}]^2}{1+\beta_1[\mathrm{HA^-}]+\beta_2[\mathrm{HA^-}]^2} \tag{8}$$

where $[\mathrm{HA^-}]$ is calculated from

$$[\mathrm{HA^-}] = [\mathrm{H_2A}]K_{a1}/h \tag{9}$$

By neglecting $[\mathrm{NiHA^+}]$, *i.e.* $\beta_1[\mathrm{HA^-}]$, $[\mathrm{H_2A}]$ can be calculated from the initial concentration of $\mathrm{H_2A}$

$$[\mathrm{H_2A}] = ([\mathrm{H_2A}]_0 - 2[\mathrm{Ni^{2+}}]_0 D/(D+1))/(1+K_{D1}) \tag{10}$$

The asymptotes to the distribution curve log D as a function of log $[\mathrm{HA^-}]$ or log $[\mathrm{H_2A}]/h$ are

$$\log D = \log K_{D2} \text{ when } [\mathrm{HA^-}] \rightarrow \infty \tag{11}$$

$$\log D = \log K_{D2} + \log \beta_2 - 2\ \mathrm{p}K_{a1} + 2 \log [\mathrm{H_2A}][\mathrm{H^+}]^{-1} \text{ when } [\mathrm{HA^-}] \rightarrow 0 \tag{12}$$

The experimental values are plotted as log D against log $[\mathrm{H_2A}]/h$ in Fig. 3.

The distribution curve shows no dependence on $[\mathrm{H_2A}]_0$, and the points fall on a straight line with a slope of two according to eqn. (12). From the value of log $[\mathrm{H_2A}][\mathrm{H^+}]^{-1} = -0.26$ at log $D = 0$, the value of log $K = \log K_{D2} + \log \beta_2 - 2\ \mathrm{p}K_{a1}$ is calculated as log $K = 0.52$. By inserting log $\beta_2 = 17.79$ (mean value from Table II) and $\mathrm{p}K_{a1} = 10.51$ from Part I[6], a value of log $K_{D2} = 3.75$ is obtained. This value is too high to be determined accurately from distribution measurements at high $[\mathrm{H_2A}]/h$, where a bend in the distribution curve should occur theoretically.

The substitution of a methyl group by an ethyl group in the ligand would change the distribution constant by a factor of 4, or 0.6 log units[24]. The value of log K_{D2} for $\mathrm{Ni(DMG)_2}$ is[20] log $K_{D2} = 2.51$ and the theoretical value of log K_{D2} for $\mathrm{Ni(EMG)_2}$ should thus be 3.71, which is very close to the experimental value of 3.75.

The ratio between the solubilities of $\mathrm{Ni(EMG)_2}$ (probably red $\mathrm{Ni(EMG)_2}$) in chloroform and water given by CATON AND BANKS[11] is $10^{3.90}$, which is somewhat higher than the experimental value of $K_{D2} = 10^{3.75}$. In the case of $\mathrm{Ni(DMG)_2}$, however, the value of K_{D2} calculated from the solubilities in chloroform and water was also slightly higher than that obtained experimentally[18,20,25]. In Fig. 4 the percentage extraction of $\mathrm{Ni(EMG)_2}$ and $\mathrm{Ni(DMG)_2}$ is plotted *vs.* the pH for the same concentration of $\mathrm{H_2A}$. It is seen that maximum extraction is attained for EMG at a pH value about one unit lower than for DMG.

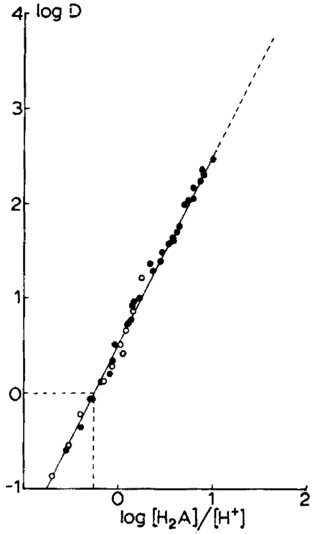

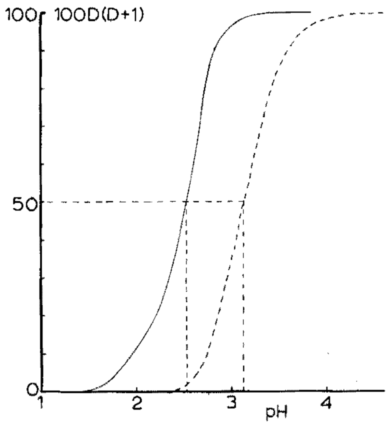

Fig. 3. The distribution of $Ni(EMG)_2$ between $CHCl_3$ and 0.1 M $(H,Na)ClO_4$. The experimental data log D is plotted against log $[H_2A]/[H^+]$. The straight line is drawn with the slope two, and has the equation $\log D = \log K_{D2} + \log \beta_2 - 2pK_{a1} + 2 \log [H_2A] + 2pH$. For $\log D = 0$, $\log [H_2A]/[H^+] = -0.26$ and thus $\log K = 0.52$. (○) 2.503 mM EMG, (●) 3.508 mM EMG.

Fig. 4. The percentage extraction of $Ni(DMG)_2$ (dashed curve) and $Ni(EMG)_2$ (full-line curve) as a function of pH when $[H_2A]_{tot} = 3.33$ mM.

The distribution constants obtained experimentally for EMG and $Ni(EMG)_2$ agree well with those predicted from the values of K_{D1} and K_{D2} of DMG. This suggests that the extraction of nickel with higher alkyldioximes can be estimated from the distribution constants for DMG and EMG. The acid dissociation constant K_{a1} and the stability constant β_2 can be assumed to be almost invariable when the sizes of the alkyl groups in the dioxime $R(CNOH)_2R'$ are increased. For each additional CH_2 group, K_{D1} will rise four times and K_{D2} sixteen times[24].

The overall extraction equilibrium is

$$Ni^{2+} + 2\ H_2A \rightleftharpoons Ni(HA)_2(org) + 2\ H^+$$

If the reagent is added in excess compared with the metal concentration and $pH \leq 9$, then

$$[H_2A] = [H_2A]_0 - [H_2A]_{org} \qquad (10a)$$

or

$$[H_2A]_0 = (1 + K_{D1})[H_2A] \qquad (10b)$$

If K_{D1} and K_{D2} for $Ni(DMG)_2$ are denoted by $K_{D1}{}^0$ and $K_{D2}{}^0$, respectively, and n is the number of CH_2 groups in the two alkyl groups—2, *i.e.* $n = 0$ for DMG and $n = 1$ for EMG, $[H_2A]_0$ can be expressed as

$$[H_2A]_0 = [H_2A](1 + K_{D1}{}^0 4^n) \qquad (13)$$

where $K_{D1}{}^0 = 1/12$ according to CHRISTOPHERSON AND SANDELL[18].

Similarly, $K_{D2} = K_{D2}{}^0 4^{2n}$ (14)

where $K_{D2}{}^0 = 10^{2.51}$ according to DYRSSEN, KRAŠOVEC AND SILLÉN[20]. When the number

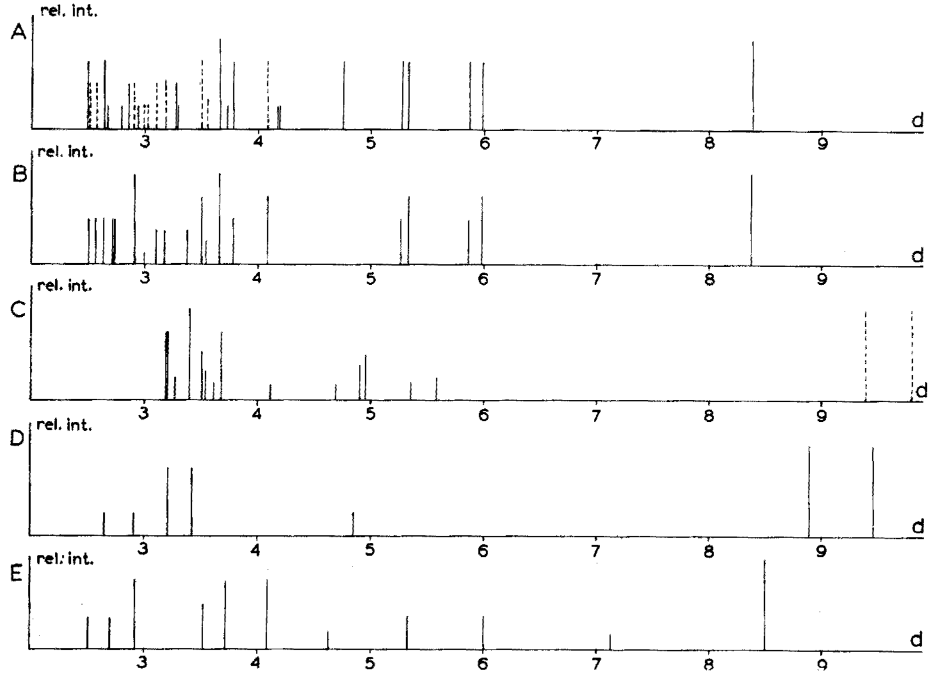

Fig. 5. Values of d reported or calculated from the literature and values of d from powder diagrams of red (α-form) and yellow (β-form) Ni(EMG)$_2$. (A) Lines generated from values given by FRASSON AND PANATTONI[9] (α-Ni(EMG)$_2$); (B) lines given by the red Ni(EMG)$_2$-powder; (C) lines generated from lattice constants given by SHARPE AND WAKEFIELD[8] (β-Ni(EMG)$_2$); (D) lines given by the yellow Ni(EMG)$_2$-powder; (E) lines according to Cox *et al.*[26] (α-Ni(EMG)$_2$).

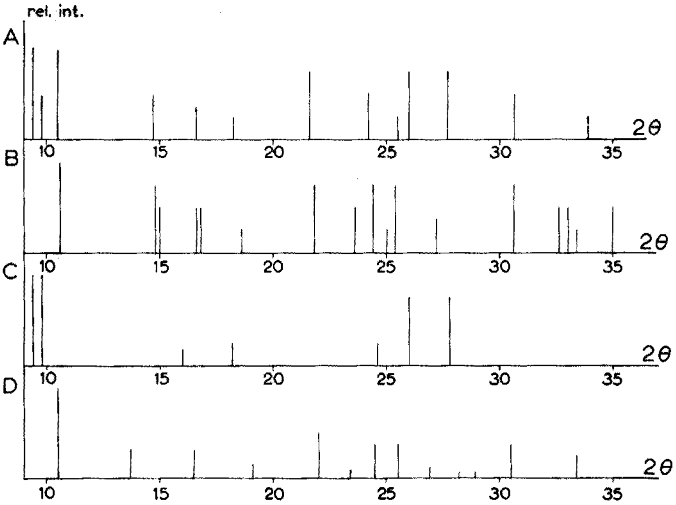

Fig. 6. X-ray powder diagrams of yellow and red Ni(EMG)$_2$ and of Cu(EMG)$_2$. (A) Ni(EMG)$_2$, according to ref. 27; (B) red Ni(EMG)$_2$, this work; (C) yellow Ni(EMG)$_2$, this work; (D) Cu(EMG)$_2$, according to ref. 27.

of CH_2 groups is increased and $n \geq 4$, the dioxime will be found mainly in the organic phase, and the equilibrium

$$Ni^{2+} + 2\ H_2A(org) \rightleftharpoons Ni(HA)_2(org) + 2\ H^+$$

can be characterized as an ion exchange between the aqueous and organic phases. The equilibrium constant is

$$K' = K_{D2}\beta_2 K_{a1}{}^2/K_{D1}{}^2 \qquad (15)$$

or, if eqns. (13) and (14) are used,

$$K' = 4^{2n}K_{D2}{}^0\beta_2 K_{a1}{}^2/(4^n K_{D1}{}^0)^2$$

or

$$K' = K_{D2}{}^0\beta_2 K_{a1}{}^2/(K_{D1}{}^0)^2$$

If K_{a1} and β_2 are unchanged when the sizes of the alkyl groups are increased, K' is independent of the choice of dioxime when $n \geq 4$, because the increase in K_{D2} is counteracted by the increase in K_{D1}.

X-Ray measurements

In connection with the solubility experiments, the structural difference between the two solid forms of $Ni(EMG)_2$ was studied by means of X-ray powder diffraction. Previously, two different crystal structures of $Ni(EMG)_2$ had been noted and labelled[7] α-$Ni(EMG)_2$ and β-$Ni(EMG)_2$. The lattice constants for α-$Ni(EMG)_2$ determined by FRASSON AND PANATTONI[9] were used to calculate[14] $\sin^2\theta$, θ, and the lattice spacings d_{hkl}. The intensities are plotted in Fig. 5 against d_{hkl}, the dashed lines representing values that were not reported by FRASSON AND PANATTONI[9], who only published lines from the *hol* and *okl* planes. The same procedure was carried out for β-$Ni(EMG)_2$ with the constants given by SHARPE AND WAKEFIELD[8].

In Fig. 5 these values are compared with those obtained from the X-ray powder diagrams of yellow and red $Ni(EMG)_2$. In addition, the values of d_{hkl} given by COX *et al.*[26] have been included. It is seen that the red form must be identical with α-$Ni(EMG)_2$ (Fig. 5A) as both show practically the same reflections. The yellow form shows, however, a somewhat worse agreement with β-$Ni(EMG)_2$ (Fig. 5C), which is probably due to the paucity of lines registered.

FRASSON *et al.*[27] have determined the powder spectra of $Ni(EMG)_2$ and $Cu(EMG)_2$. Though the powders are isomorphous, there is a slight discrepancy in the reflection pattern as shown in Fig. 6A and 6D, in which the intensities have been plotted against 2θ. If, however, these powder spectra are compared with those of yellow and red $Ni(EMG)_2$ (Fig. 6B and 6C) obtained in this work, the conclusion is that the $Ni(EMG)_2$ (Fig. 6A) used by FRASSON *et al.*[27] consisted of a mixture of the yellow and red forms. It can also be seen that the red form is isomorphous with $Cu(EMG)_2$ (Fig. 6D). The difference between the red $Ni(EMG)_2$ and $Cu(EMG)_2$ patterns is probably due to a distorted octahedral configuration of ligands about copper.

The cell constants for red $Ni(EMG)_2$ were obtained from the X-ray powder data in the following way. Firstly all $\sin^2\theta_{calc}$ values corresponding to the cell constants given by FRASSON AND PANATTONI[9] were generated by means of the program POWDER[14], those values violating the systematic absences of the space group, *i.e.* *hol* with *l* odd and *oko* with *k* odd, being eliminated. The remaining lines

TABLE IV

COMPARISON OF OBSERVED AND CALCULATED REFLECTIONS FOR RED $Ni(EMG)_2$

($a = 4.740$, $b = 11.713$, $c = 11.971$ Å, $\beta = 91.736°$)

hkl	$\sin^2\theta$ *obs.* $\cdot 10^6$	$\sin^2\theta$ *calc.* $\cdot 10^6$	Δ $\sin^2\theta$ $\cdot 10^6$	d_{hkl} *obs.*	d_{hkl} *calc.*	*Rel. intensities*
011	8464	8468	−4	8.372	8.370	vs
002	16528	16575	−47	5.991	5.983	s
020	17192	17297	−105	5.874	5.857	m
012	20794	20899	−105	5.341	5.328	m
021	21336	21441	−105	5.273	5.260	m
111	35570	35537	33	4.084	4.086	s
013	41548	41618	−70	3.779	3.776	m
102	44353	44278	75	3.657	3.660	s
−121	47139	47243	−104	3.548	3.544	w
121	48562	48511	51	3.495	3.497	s
032	55458	55495	−37	3.271	3.270	m
−122	58963	59040	−77	3.172	3.170	m
122	61416	61576	−160	3.108	3.104	m
004	66244	66301	−57	2.993	2.991	vw
113	69855	69956	−101	2.914	2.912	vs
−123	79099	79125	−26	2.739	2.738	m
−132	80702	80663	39	2.711	2.712	m
042	85810	85767	43	2.629	2.630	m
−104	90122	90200	−78	2.568	2.565	s
−114	94455	94525	−70	2.506	2.505	m

not published by FRASSON AND PANATTONI[9] (shown as dashed lines in Fig. 5) were then indexed, and a least squares refinement of the cell dimensions based on a total of 20 indexed reflections was performed with the program POWDER[14]. The result of the refinement is given in Table IV, and the cell constants obtained agree favourably with those reported by FRASSON AND PANATTONI[9] (latter values within parentheses):

$a = 4.740 \pm 0.005$ (4.75 ± 0.01)Å
$b = 11.713 \pm 0.009$ (11.75 ± 0.03)Å
$c = 11.971 \pm 0.009$ (11.97 ± 0.03)Å
$\beta = 91.74° \pm 0.05°$ $(92.00° \pm 0.11°)$

The distance between two planar $Ni(EMG)_2$ molecules in the red form[9] is thus 3.32 Å and the distance between the nickel atoms is 4.74 Å.

The yellow modification of $Ni(EMG)_2$ showed, unfortunately, very few measurable reflections. In order to ascertain that it was the same compound as that reported by SHARPE AND WAKEFIELD[8], the lattice constants were calculated in the same way as they did, supposing the compound to be isomorphous[28] with $Ni(DMG)_2$. Calculated $\sin^2\theta$ values corresponding to systematically absent reflections were eliminated, the values of *hkl* for $Ni(DMG)_2$ reported by GODYCKI AND RUNDLE[28] being used. A least squares refinement[14] of the cell dimensions based on eight indexed reflections yielded the following values:

$a = 19.65 \pm 0.38$ (19.6 ± 0.1)Å
$b = 10.68 \pm 0.12$ (10.7 ± 0.1)Å
$c = 6.87 \pm 0.05$ (6.8 ± 0.1)Å

TABLE V

COMPARISON OF OBSERVED AND CALCULATED REFLECTIONS FOR YELLOW $Ni(EMG)_2$

($a = 19.65$, $b = 10.68$, $c = 6.87$ Å)

hkl	$\sin^2\theta$ *obs.* $\cdot 10^6$	$\sin^2\theta$ *calc.* $\cdot 10^6$	$\Delta\sin^2\theta$ $\cdot 10^6$	d_{obs}	d_{calc}	*Rel. intensities*
200	6625	6145	480	9.46	9.82	vs
110	7504	6740	764	8.89	9.38	vs
310	19310	19031	279	5.57	5.58	vw
400	25151	24582	569	4.86	4.91	w
002	50790	50304	486	3.42	3.43	s
112	57618	57044	574	3.21	3.22	s
312	70072	69335	737	2.91	2.93	w
431	84556	83991	565	2.65	2.66	w

A comparison with the values within parentheses reported by SHARPE AND WAKEFIELD[8] shows good agreement. Unfortunately, SHARPE AND WAKEFIELD did not give a list of indexed reflections, and the lines given in Fig. 5 correspond to the indexed d_{hkl} given by GODYCKI AND RUNDLE[28]. In Table V the calculated $\sin^2\theta$ and d_{hkl} based on the refined cell constants of the yellow $Ni(EMG)_2$ are compared with the observed values.

The distance between two planar $Ni(EMG)_2$ molecules in the yellow form is 3.44 ± 0.03 Å, which is also the distance between the nickel atoms, since they are stacked directly over one another. Thus the yellow form is more symmetrical than the red form, but the distance between the planar $Ni(EMG)_2$ molecules is greater by about 0.1 Å. The transformation of the yellow form to the more stable red form therefore results in a closer packing of the planar $Ni(EMG)_2$ molecules.

Spectral measurements

The spectra of yellow and red $Ni(EMG)_2$ dissolved in chloroform were recorded in the range 245–550 nm. As expected, the two spectra proved to be identical (Fig. 7), and to have the same appearance as that given by CATON AND BANKS[11] with peaks at 262–264, 327–329 and 375–378 nm, and shoulders at *ca.* 425 and 500 nm. As seen in Table VI the wavelengths of the absorption maxima and molar absorptivities in chloroform are almost unaltered when going from $Ni(DMG)_2$ to $Ni(EMG)_2$. The wavelength of the absorption at about 260 nm, caused by the π–π^* transition in the ligand, is practically the same in $Ni(HA)_2$ and HA^-. However, the molar absorptivity per HA^- is 10,500 in $Ni(EMG)_2$, but 14,600 in EMG^-. This difference in intensity can be used in the calculation of the oscillator strength as shown by ROOS[33]. The absorbance at 260 nm cannot be used analytically and one has to rely upon weaker bands at the wavelengths 329 and 378 nm, where the absorptivity of HA^- is negligible.

The u.v.–vis. and i.r. spectra of the red and yellow solid forms of $Ni(EMG)_2$ were also recorded, as well as those of solid $Ni(DMG)_2$. The u.v.–vis. spectra are shown in Fig. 8. The two modifications of $Ni(EMG)_2$ exhibit spectra very different from each other and from the chloroform solution spectra. Both forms show, however, an intense absorption band at 280 nm, which corresponds to the ligand band at 262 nm in chloroform solution. The red form shows no well-defined maxima at all

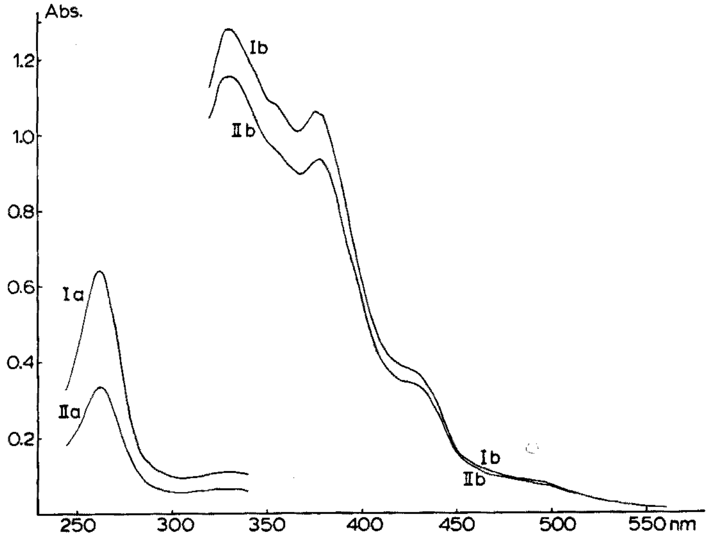

Fig. 7. The u.v.–vis. spectra of red and yellow $Ni(EMG)_2$ dissolved in $CHCl_3$, in the range 245–550 nm. (Ia) Yellow $Ni(EMG)_2$, 0.1 mg/10 ml $CHCl_3$; (Ib) yellow $Ni(EMG)_2$, 1.15 mg/10 ml $CHCl_3$; (IIa) red $Ni(EMG)_2$, 0.05 mg/10 ml $CHCl_3$; (IIb) red $Ni(EMG)_2$, 1.0 mg/10 ml $CHCl_3$.

TABLE VI

U.V.–VIS. SPECTRA OF $Ni(DMG)_2$ AND $Ni(EMG)_2$ IN $CHCl_3$

Compound	*Max. (nm)*	$\varepsilon \cdot 10^{-3}$ *l cm mol*$^{-1}$	*Ref.*
$Ni(DMG)_2$	262	24.5	29
	327	4.58	
	374	3.43	
	261	23.3	30
	326	4.28	
	375	3.67	
	325 (328)	2.0	31
	370 (372)	1.44	
	262	29.6	32
$Ni(EMG)_2$	262	21.0	This work
	329	4.42	
	378	3.62	
DMG anion A^{2-}	265[a]	17.8	32
EMG anion HA^-	258	14.6	6

[a] The molar absorptivity spectra of EMG^- and EMG^{2-} are quite similar to each other[6]. This should be true for DMG^- and DMG^{2-} as well.

between 350 and 550 nm. Owing to the low crystal symmetry of red $Ni(EMG)_2$, the recorded spectrum may show both reflectance and absorption by the powder and this could explain the featureless curve. A comparison can be made with polarized single crystal absorption and reflection spectra of red $Ni(EMG)_2$, reported by Anex and Krist[7], which also lack distinct maxima. The yellow modification of $Ni(EMG)_2$ shows an intense absorption band in the green range at about 500 nm, whereas the

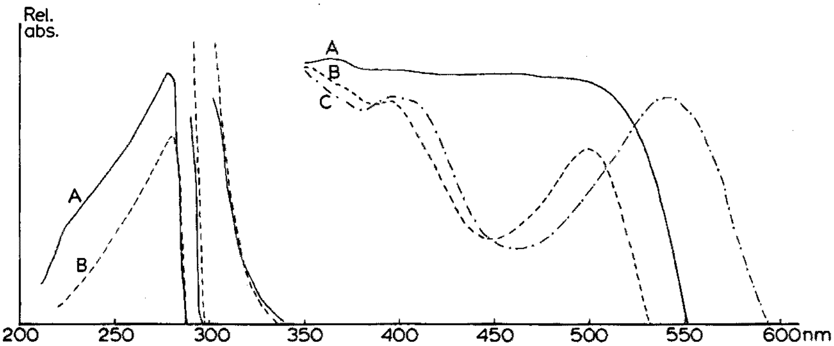

Fig. 8. The u.v.–vis. spectra of solid red and yellow Ni(EMG)$_2$ and of Ni(DMG)$_2$ in the ranges 210–290, 290–300, 300–340 and 350–600 nm. (A) Red Ni(EMG)$_2$, (B) yellow Ni(EMG)$_2$, (C) Ni(DMG)$_2$.

corresponding band for Ni(DMG)$_2$, which is red and not yellow, is at about 540 nm. These maxima are not observed in the solution spectra (*cf.* Fig. 7), and it has been proposed[28,34–36] that the stacking of the metal ions in the solid phase is responsible for the band. The difference between Ni(EMG)$_2$ and Ni(DMG)$_2$ is probably due to the longer distance between the molecular planes in Ni(EMG)$_2$ (see above).

TABLE VII

I.R. SPECTRA (cm^{-1}) OF Ni(EMG)$_2$ AND Ni(DMG)$_2$ IN KBr PELLETS

	y·*Ni(EMG)*$_2$	*r*·*Ni(EMG)*$_2$	*Ni(EMG)*$_2$ *(ref. 37)*	*Ni(DMG)*$_2$
ν OH	2390	2390	2388	Not visible[a]
δ OH	1790	1782	1784	1790
C=N	1570	1568		1572
NO	1542	1537		1540
NO	1120	1117		1105

[a] CATON AND BANKS[37] report 2322 cm^{-1} for this band.

The i.r. spectra of red and yellow Ni(EMG)$_2$ have the same appearance and the position of the absorption bands differs very little. In Table VII the frequencies of the absorption maxima for some vibrations are compared with corresponding values for Ni(DMG)$_2$. The differences are very small except for the OH stretching frequencies, where, according to CATON AND BANKS[37], the short hydrogen bonds in Ni(EMG)$_2$ cause the OH absorption to be shifted to a higher frequency than do the somewhat longer hydrogen bonds in Ni(DMG)$_2$.

The same phenomenon of a nickel complex with two different structures has been reported for α-benzildioxime[38]. The precipitate comes down as a red compound, but changes colour to yellow-orange on standing or heating. Diffuse reflectance spectrophotometry indicates that the crystals have different structures, but there is no difference in the absorption spectra of the chloroform solutions. For this complex, however, the yellow form seems to be more stable.

DISCUSSION

When a methyl group in dimethylglyoxime is replaced by an ethyl group the following equilibria are only slightly shifted:

$$H_2A \rightleftharpoons H^+ + HA^-$$
$$HA^- \rightleftharpoons H^+ + A^{2-}$$
$$Ni^{2+} + 2HA^- \rightleftharpoons Ni(HA)_2$$

and the solution spectra of H_2A, HA^-, A^{2-}, and $Ni(HA)_2$ are not appreciably altered.

The solubilities and distribution constants (chloroform/aq) of H_2A and $Ni(HA)_2$ are, however, considerably changed, as may be seen from Table VIII where the properties of $Ni(DMG)_2$ and the two forms of $Ni(EMG)_2$ are summarized (for H_2A see part I[6]). This means that the increase in the size of the alkyl groups affects both the forces in the solid state as well as the forces between the water molecules. The energy needed to squeeze in a hydrophobic CH_2 group in water is $0.62 \cdot 2.303$ $RT = 0.846$ kcal/mol at 25°. This explains the increase of log K_{D2} by 1.24 and of log K_{D1} by 0.63 (see Table I in Part I[6]). This hydrophobic effect must also be taken into account when considering the values of the solubilities *in water*. Qualitatively, the forces between the nickel dichelate rings should diminish with the distance between the planar $Ni(HA)_2$ molecules, and it might be possible to express $\Delta G = -2.303\ RT \log K_{s1}$ as follows

TABLE VIII

PROPERTIES OF $Ni(DMG)_2$, α-$Ni(EMG)_2$ AND β-$Ni(EMG)_2$

	$Ni(DMG)_2$	*α-$Ni(EMG)_2$*	*β-$Ni(EMG)_2$*
Crystal system	Orthorhombic	Monoclinic	Orthorhombic
Colour of solid	Red	Red	Yellow
Cell constants	$a = 16.68$ Å $b = 10.44$ Å $c = 6.49$ Å $Z = 4$	$a = 4.740 \pm 0.005$ Å $b = 11.713 \pm 0.009$ Å $c = 11.971 \pm 0.009$ Å $\beta = 91.74 \pm 0.05°$ $Z = 2$	$a = 19.65 \pm 0.38$ Å $b = 10.68 \pm 0.12$ Å $c = 6.87 \pm 0.05$ Å $Z = 4$
Nickel–nickel distance (Å)	3.233	4.74 ± 0.005	3.44 ± 0.03
Distance between two planar molecules of $Ni(HA)_2$ (Å)	3.233	3.32	3.44
Rotation of alternate molecules (°)	90	—	90
Solubility in 0.1 M $NaClO_4$	$\log K_{s1} = -5.82$	$\log K_{s1} = -5.56$	$\log K_{s1} = -4.92$
$\Delta G = -2.303\ RT \log K_{s1}$	$\Delta G = 7.95$ kcal/mol	$\Delta G = 7.59$ kcal/mol	$\Delta G = 6.71$ kcal/mol
Stability constant $\log \beta_2$	17.24	17.79	17.79
Distribution constant $\log K_{D2}$ ($CHCl_3$–aq)	2.51	3.75	3.75

$$\Delta G = 2(x+y)0.846 + Bd^{-z} + C \qquad (16)$$

where $x+y$ is the number of CH_2 groups in the dialkyl glyoxime and d is the distance between the planar rings. C is an almost constant term which contains the bonding energies due to van der Waals forces between the $Ni(HA)_2$ molecules in the solid phase and the weak hydration of $Ni(HA)_2$ in the aqueous phase. From the plot of $\Delta G-2(x+y)0.846$ against d in Fig. 9, it seems as if the forces between the planar molecules can account for the greater solubility of the nickel complexes of ethylmethylglyoxime as compared with $Ni(DMG)_2$, in spite of the larger value of $x+y$.

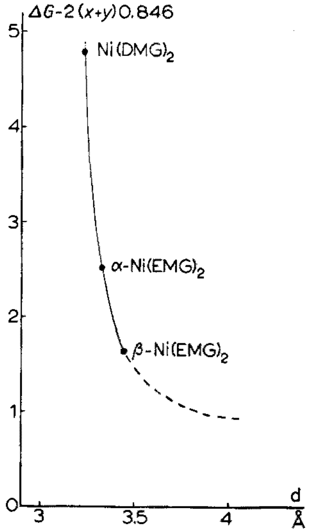

Fig. 9. $\Delta G - 2(x+y)0.846$ (eqn. 16) as a function of the distance d between adjacent planar molecules. (●) Experimental data ($\Delta G = -2.3\ RT \log K_{s1}$).

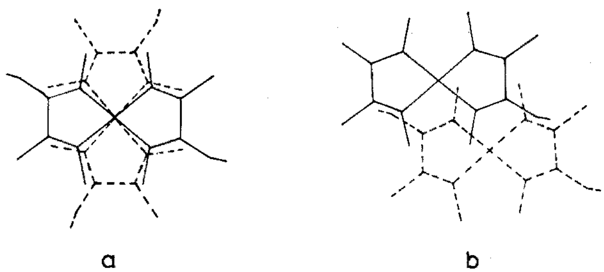

Fig. 10. The arrangements of two adjacent molecules in (a) yellow β-$Ni(EMG)_2$ (the same packing as in $Ni(DMG)_2$[28]), (b) red α-$Ni(EMG)_2$ according to FRASSON AND PANATTONI[9].

It might be possible to obtain the minimum value of d from an X-ray determination of the structure of nickel glyoxime ($x+y=0$). Above 4 Å the forces between the planar molecules can probably be neglected. Thus $C \sim 0.9$ kcal/mol. From Fig. 9 one may estimate ΔG for $Ni(DEG)_2$ to be $2 \times 4 \times 0.846 + 1.2 \approx 8.0$ kcal/mol and for $Ni(DPG)_2$ to be $2 \times 5 \times 0.846 + 1.0 \approx 9.5$ kcal/mol. Thus the values of K_{s1} reported by BANKS AND ANDERSON[10] seem to be too high.

In the discussion above the different packing systems for α- and β-$Ni(EMG)_2$ have not been taken into consideration. In Fig. 10 the different arrangements of two adjacent molecules in the red and yellow crystals of $Ni(EMG)_2$ are shown. It is seen that the close-packing in $Ni(DMG)_2$ and the yellow β-$Ni(EMG)_2$ is obtained by rotating alternate planar $Ni(HA)_2$ molecules through 90°, the nickel atoms thus lying directly over one another. In the red α-$Ni(EMG)_2$, close-packing is obtained by displacing the planar molecules by mere gliding without rotation. This gives a Ni–O distance of 3.44 Å, and a distorted configuration. The Ni–Ni distance of 4.74 Å excludes the possibility of any Ni–Ni bond.

It seems as if the distance between the planar $Ni(HA)_2$ molecules is determined by the size of the alkyl groups, but it would be advisable to determine the structure for the nickel complexes of glyoxime, methylglyoxime, diethylglyoxime and dipropylglyoxime before drawing any definite conclusions.

Figure 10 might explain why $Ni(EMG)_2$ is first precipitated in the symmetrical yellow β-form although the red form is thermodynamically the more stable. Transformation of the yellow form to the red one by rotation of molecules in alternate layers is not likely to take place. This explains why the yellow form is kinetically rather stable. Practically, the transformation is accomplished by shaking the yellow crystals with chloroform, in which the solubility is rather high (*ca.* 0.05 *M*), or by filtering an aqueous solution of pH 4.5 through a column packed with yellow β-Ni(EMG)$_2$. At this pH, $Ni(EMG)_2$ is slightly dissolved by dissociation ($Ni(HA)_2+2H^+ \rightleftharpoons Ni^{2+}+2H_2A$). Both processes involve dissociation and recrystallization at thermodynamic equilibrium. Mere thermal heating of the yellow form will not give the red one.

The green absorption band in $Ni(DMG)_2$ has been the subject of several investigations[7,30,34–36,39], including molecular orbital calculations. The opinions concerning the origin of the band differ, but the occurrence of a nickel–nickel bond is denied in later investigations[7,30,39]; nor is any stabilizing effect[35,36] due to the stacking of nickel atoms indicated by the results of this work. The nature of the forces between the planar molecules must be clarified by further work. Figure 9 would imply that they decrease very rapidly with increasing distance, *d*, between the planar $Ni(HA)_2$ molecules.

The author would like to thank the head of the department, Professor DAVID DYRSSEN, for extensive discussion of the results, and Mrs. SUSAN JAGNER, fil. lic., M.A. for help with the computer treatment of the X-ray powder diffraction data and for revising the English text. She also wishes to thank Dr. HANS EGNEUS at the Department of Plant Physiology for recording the solid state spectra with the Shimadzu MPS-50L spectrophotometer.

SUMMARY

The following properties of the two modifications of nickel ethylmethylglyoxime have been examined: X-ray powder diffraction patterns, u.v.–vis.–i.r. solid state spectra, solubility products and intrinsic solubilities. In addition, the complex formation and chloroform distribution constants have been measured as well as the u.v.–vis. chloroform solution spectra. Differentiating properties are summarized and compared with those of nickel dimethylglyoxime. The influence of the crystal structures on the intrinsic solubilities is discussed and the distribution constants and solubilities of other nickel dialkylglyoximes are predicted.

RÉSUMÉ

On examine les caractéristiques suivantes des deux modifications de l'éthylglyoxime de nickel: pouvoir de diffraction aux rayons X, spectres u.v., vis., i.r., produits de solubilité et solubilités. On a mesuré également la formation du complexe et les constantes de distribution dans le chloroforme. Un tableau de comparaison avec le complexe nickel–diméthylglyoxime est donné. On examine également d'autres nickel–dialcoylglyoximes.

ZUSAMMENFASSUNG

Es wurden die folgenden Eigenschaften der 2 Modifikationen von Nickeläthylglyoxim untersucht: Röntgenbeugung an Pulvern, u.v.-, vis.- und i.r.-Spektren im festen Zustand, Löslichkeitsprodukte und Eigenlöslichkeiten. Zusätzlich wurde die Komplexbildung und die Verteilung in Chloroform untersucht, ebenso wie die u.v.- und vis.-Spektren in Chloroform. Die unterschiedlichen Eigenschaften wurden zusammengestellt und mit denen von Nickeldimethylglyoxim verglichen. Der Einfluss der Kristalstrukturen auf die Eigenlöslichkeiten werden diskutiert und Verteilungskonstanten und Löslichkeiten anderer Nickeldialkylglyoxime werden vorhergesagt.

REFERENCES

1 A. K. Babko, *Nauk. Zap., Kiivs'k Derzh. Univ.*, (1956) 241; *C.A.*, 56 (1962) 9473e.
2 C. V. Banks, *16th Annual Summer Symposium on Analytical Chemistry, Tucson, U.S.A., June 19–21, 1963.*
3 D. Dyrssen, *Svensk Kem. Tidskr.*, 75 (1963) 618.
4 D. Dyrssen, *Trans. Roy. Inst. Technol. Stockholm*, 220 (1964).
5 K. Burger, in H. A. Flaschka and A. J. Barnárd, Jr., *Chelates in Analytical Chemistry*, Vol. II, Marcel Dekker, New York, 1969, p. 179–212.
6 B. Egneus, *Anal. Chim. Acta*, 43 (1968) 53.
7 B. G. Anex and F. K. Krist, *J. Am. Chem. Soc.*, 89 (1967) 6114.
8 A. G. Sharpe and D. B. Wakefield, *J. Chem. Soc.*, (1957) 281.
9 E. Frasson and C. Panattoni, *Acta Cryst.*, 13 (1960) 893.
10 C. V. Banks and S. Anderson, *Inorg. Chem.*, 2 (1963) 112.
11 J. E. Caton, Jr. and C. V. Banks, *Talanta*, 13 (1966) 967.
12 R. Belcher, W. Hoyle and T. S. West, *J. Chem. Soc.*, (1958) 2475.
13 *Some Laboratory Methods*, Department of Inorganic Chemistry, Royal Institute of Technology, Stockholm, manuscript, 1959.
14 O. Lindqvist and F. Wengelin, *Arkiv Kemi*, 28 (1967) 179.
15 E. B. Sandell, *Colorimetric Determinations of Traces of Metals*, 3rd Edn., Interscience, New York, 1958, p. 668.
16 D. Dyrssen and L. G. Sillén, *Acta Chem. Scand.*, 7 (1953) 663.
17 L. G. Sillén, *Acta Chem. Scand.*, 10 (1956) 186.
18 H. Christopherson and E. B. Sandell, *Anal. Chim. Acta*, 10 (1954) 1.
19 C. V. Banks and D. W. Barnum, *J. Am. Chem. Soc.*, 80 (1958) 3579.
20 D. Dyrssen, F. Krašovec and L. G. Sillén, *Acta Chem. Scand.*, 13 (1959) 50.
21 R. G. Charles and H. Freiser, *Anal. Chim. Acta*, 11 (1954) 101.
22 V. M. Bochkova and V. M. Peshkova, *Zh. Neorgan. Khim.*, 3 (1958) 1131.
23 K. Burger and I. Ruff, *Talanta*, 10 (1963) 329.
24 D. Dyrssen, S. Ekberg and D. H. Liem, *Acta Chem. Scand.*, 18 (1964) 135.
25 D. Dyrssen and M. Hennichs, *Acta Chem. Scand.*, 15 (1961) 47.
26 E. G. Cox, E. Sharrat, W. Wardlaw and K. C. Webster, *J. Chem. Soc.*, (1936) 129.
27 E. Frasson, C. Panattoni and R. Zannetti, *Ric. Sci.*, 29 (1959) 783.
28 L. E. Godycki and R. E. Rundle, *Acta Cryst.*, 6 (1953) 487.
29 C. V. Banks and D. W. Barnum, *J. Am. Chem. Soc.*, 80 (1958) 4767.
30 G. Basu, G. M. Cook and R. L. Belford, *Inorg. Chem.*, 3 (1964) 1361.
31 G. Maki, *J. Chem. Phys.*, 29 (1958) 1129.
32 K. Burger, I. Ruff and F. Ruff, *J. Inorg. & Nucl. Chem.*, 27 (1965) 179.
33 B. Roos, *Acta Chem. Scand.*, 19 (1965) 1715.
34 S. Yamada and R. Tsuchida, *Bull. Chem. Soc. Japan*, 27 (1954) 156.
35 R. E. Rundle, *J. Phys. Chem.*, 61 (1957) 45.
36 C. V. Banks and S. Andersson, *J. Am. Chem. Soc.*, 84 (1962) 1486.
37 J. E. Caton, Jr. and C. V. Banks, *Inorg. Chem.*, 6 (1967) 1670.
38 R. J. Magee, J. C. Rowe and L. Gordon, *Talanta*, 12 (1965) 303.
39 L. L. Ingraham, *Acta Chem. Scand.*, 20 (1966) 283.

Analytica Chimica Acta
Elsevier Publishing Company, Amsterdam
Printed in The Netherlands

THE RELATIVE ACIDITIES OF PHENOLS AND BENZOIC ACIDS IN DIMETHYLSULFOXIDE

RAUL MORALES
E. I. du Pont de Nemours & Company, Inc., Industrial and Biochemicals Department, Wilmington, Del. 19898 (U.S.A.)

(Received August 21st, 1969)

Dimethylsulfoxide has become a very important solvent as evidenced by the many experimental studies conducted with it[1,2]. Properties which make it desirable as a medium are its high dielectric constant (46.7), basicity, ability to solvate large anions, and stability. It was of interest therefore, to evaluate the behavior in dimethylsulfoxide (DMSO) of such Bronsted acids as benzoic acids and phenols. The latter in particular are important as a class of compounds and for this reason their acid behavior has been studied in such solvents as pyridine[3], dimethylformamide[4,5], methanol[5], benzene[6,7], and acetonitrile[8]. The acidities of a few phenols in DMSO have been measured by KOLTHOFF AND REDDY[9], CLARE *et al.*[5], and STEINER AND GILBERT[10]. These authors have made significant contributions in their attempts to elucidate the complicated phenomena that take place in nonaqueous solvents such as DMSO. The present work was undertaken to provide a comprehensive potentiometric study on the acid behavior of phenols and some benzoic acids in dimethylsulfoxide.

EXPERIMENTAL

Apparatus

Metrohm E-436 Potentiograph, Metrohm electrodes: glass (EA-109) and Ag/-AgCl reference (EA-425) filled with methanol saturated with potassium chloride. The titration vessels used were those supplied with the instrument.

Chemicals

DMSO (Wilmington Packaging Co.) was dried over molecular sieves, Linde 4A. The phenols and benzoic acids (Eastman Kodak or Aldrich Chemical Co.) were used as received except for phenol which was distilled under vacuum at 45 mm pressure. Tetrabutylammonium hydroxide (TBAH; Southwestern Analytical Chemicals), 1 N in methanol, was diluted with reagent-grade isopropanol to a final concentration of 0.1 N and standardized against primary standard benzoic acid.

Stock solutions (0.01 N) of the acids in DMSO displayed no color changes after standing for three weeks.

Procedure

Exactly 10 ml of the stock solutions were pipetted into the titration vessel and diluted to 60 ml with DMSO. A constant stirring speed was maintained during all titrations as well as a constant rate of titrant delivery (1 ml/min). Before the titration, the system was allowed to equilibrate until no drift in potential was observed; this normally took 15–20 min. At least three runs were made on each compound. The titration blank for DMSO was found to be negligible.

The TBAH was standardized daily against benzoic acid both to detect changes in the half-neutralization potential of benzoic acid and to evaluate the quantitativeness of the titrations. Identical results were obtained with or without a nitrogen blanket.

RESULTS AND DISCUSSION

Titration curves

Typical titration curves for phenols and benzoic acids are depicted in Fig. 1. All titrations, except for 3,4- and 3,5-dichlorophenol, were found to be stoichiometric; 97–100% recoveries were obtained, corresponding to the estimated purity range for the samples used. The numbers on the curves correspond to those acids designated in Table I. Most of the titration curves exhibited steep slopes regardless of whether or not the acids were stronger or weaker than benzoic, the reference

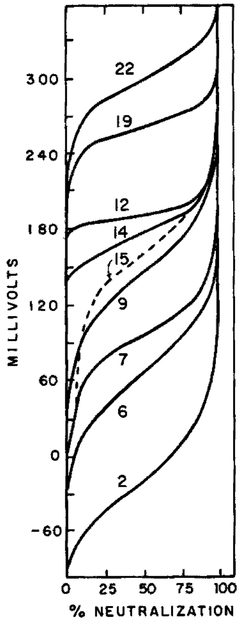

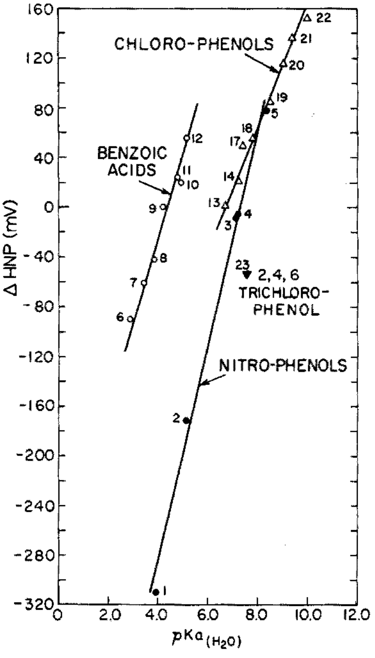

Fig. 1. Titration curves of phenols and benzoic acids in DMSO. The numbers on the curves indicate compounds listed in Table I.

Fig. 2. Acidities of substituted phenols and benzoic acids in DMSO and water. The numbers refer to compounds listed in Table I.

TABLE I

ACIDITIES OF PHENOLS AND BENZOIC ACIDS IN VARIOUS SOLVENTS

No.	*Compound*	*DMSO* Δ *HNP*[a] *(mV)*	*Pyridine*[3,12] Δ*HNP (mV)*	pK_a[13] *(Lit.)*	pK_a *(Calc. DMSO)*	ΔpK_a
1	2,4-Dinitrophenol	−310	−359	3.96	3.80	−0.16
2	2,5-Dinitrophenol	−172	—	5.16	5.36	0.20
3	*p*-Nitrophenol	−9	−50	7.14	7.20	0.06
4	*o*-Nitrophenol	−7	−25	7.23	7.20	0.08
5	*m*-Nitrophenol	78	139	8.35	8.10	−0.25
6	*o*-Chlorobenzoic	−90	−65	2.89	2.92	0.03
7	*p*-Nitrobenzoic	−61	−110	3.40	3.34	−0.06
8	*m*-Chlorobenzoic	−42	−49	3.81	3.71	−0.10
9	Benzoic	0	0	4.20 (4.16)	—	—
0	*p*-Aminobenzoic	20	105	4.92	4.73	−0.19
1	*m*-Aminobenzoic	24	38	4.79	4.80	0.01
2	3,5-Diaminobenzoic	56	—	5.30	5.32	0.02
3	2,6-Dichlorophenol	1	—	(6.72)	6.68	−0.04
4	2,5-Dichlorophenol	21	—	(7.22)	7.09	−0.13
5	3,5-Dichlorophenol	20	—	—	—	—
6	3,4-Dichlorophenol	38	—	—	—	—
7	2,3-Dichlorophenol	50	—	(7.43)	7.69	0.26
8	2,4-Dichlorophenol	55	78	7.85 (7.76)	7.79	−0.06
9	2-Chlorophenol	85	190	8.48	8.42	−0.06
0	3-Chlorophenol	115	220	9.02 (8.87)	9.04	0.02
1	4-Chlorophenol	136	248	9.38	9.48	0.12
2	Phenol	152	340	9.95	9.81	−0.14
3	2,4,6-Trichlorophenol	−54	−49	7.59	—	—

Half-neutralization potential compared to that of benzoic acid.

standard. The shapes of the curves are a result of such factors as intrinsic acidity, hydrogen bonding between solute molecules, and steric effects. FRITZ AND YAMAMURA[11], STREULI AND MIRON[12], and others have emphasized primarily solute association as the reason for the shapes of such potentiometric curves. This would indicate that the steepness of the curves would increase in cases where solvents of low dielectric constants were used. That this is not so is seen by the rather flat titration curves of phenol in benzene, gasoline, toluene, and dioxane, reported by HARLOW AND BRUSS[7]. It is of interest to note, however, that steep curves do result with phenols, benzoic and other organic acids in those instances where the solvent has hydrogen-bonding capabilities, *e.g.* dimethylformamide, pyridine, acetone, water, DMSO, etc. Solute–solvent association, therefore, should be expected to contribute to the shapes of titration curves.

Of the acids titrated, 3,4- and 3,5-dichorophenol displayed what could be interpreted as "abnormal" curves in the sense that they exhibited more than one explicit inflection point. The two dichlorophenols showed an inflection point corresponding to *ca.* 10% of the total neutralization. The total neutralization, however, corresponded to ≥97% of the equivalent weights taken. Thin-layer chromatography of the dichlorophenols produced three ultraviolet (254 nm) absorbing spots. Apparently the nature of these extraneous compounds is such that they yield an essentially stoichiometric value for the weight of dichlorophenol taken. Thus, because of the presence of unknown contaminants, there is a certain error in the differential half-neutralization potential (Δ HNP) values reported in Table I.

The effects of homoconjugation *i.e.*, acid–anion association, were not obvious in dimethylsulfoxide for the acids studied. Some of the potentiometric curves, *e.g.* 7, 9, and 22 exhibited early "breaks" almost horizontal to the mV axis. VAN DER HEIJDE[14] explained many of the anomalies of titration curves for phenols as being due to homoconjugation. These anomalies usually took place at about the half-neutralization potentials or simple fractions thereof. Early inflections such as those depicted in Fig. 1, however, are not due to solvent "blanks" and are as yet unexplained. It is possible that these early inflections are also due to homoconjugation.

Comparison of acidities in different media

Table I lists the acids studied and their relative acidities in dimethylsulfoxide, pyridine, and water. A variation in the half-neutralization potential (HNP) was found from day to day for the acids and consequently the differential half-neutralization potential was adopted as the criterion for acidity in DMSO. The HNP for benzoic acid was taken as the reference, and the Δ HNP for the other acids were obtained by subtracting algebraically their HNP value from that of benzoic. The Δ HNP was reproducible within ±12 mV. The Δ HNP values in pyridine media are taken from the work of STREULI AND MIRON[12] and the pK_a (H_2O) from HUBER[13]. The pK_a in parentheses were calculated in this laboratory by determining the pH at 50% neutralization for 1.5 mmoles of the acids in distilled water. The aqueous titrations were conducted in duplicate and were reproducible to within 0.1 pH unit.

Inspection of Table I shows that the organic acids follow the same order of acidity in all three solvents. Exceptions are the reversed acidity order of *p*-nitrobenzoic and *o*-chlorobenzoic in pyridine, compared to that in water and DMSO. The Δ HNP range in pyridine is 1.5 times that in DMSO and this indicates the latter to be a better levelling solvent for these compounds. It is recognized that different electrode systems were used in both investigations and that these comparisons may not be as meaningful as one would wish. It is felt, nevertheless, that a certain validity exists (Fig. 3) and that pyridine, in general, is a better differentiating solvent for the compounds studied.

Acidities in water and dimethylsulfoxide

Figure 2 shows plots of pK_a (water) *vs.* Δ HNP (DMSO) values for most of the compounds 1 through 22. As in Table I, the data in Fig. 2 shows that the organic acids follow the same order of acidity in DMSO as in water and that this is irrespective of positions of substitution, *i.e.*, the ortho-substituent effect is not apparent. That the nature of the substituent is important in the case of phenols is dramatized by the differing slopes of the nitro and chloro derivatives. 2,4,6-Trichlorophenol behaves as a stronger acid in DMSO than in water but does not fall in with the rest of the chlorinated phenols. The increased acidity of the trichlorophenol in DMSO, compared with, *e.g.* 2,3-dichlorophenol, can be attributed to the better solvation of the larger polarizable anion. This solvation reinforces the "absolute" strength of the trichloro species.

The relationship between pK_a and Δ HNP (DMSO) values is given by the expressions:

(*a*) benzoic acids $pK_a = 4.40 + 0.0165\ \Delta$ HNP
(*b*) chlorophenols $pK_a = 6.66 + 0.0207\ \Delta$ HNP
(*c*) nitrophenols $pK_a = 7.30 + 0.0113\ \Delta$ HNP

The intercepts and slopes for the above equations were determined with the aid of a Wang Model 300 Calculator. These values were used to plot the lines in Fig. 2. The deviations obtained between the literature pK_a values and those calculated from the equations is given in the Table and is no greater than 0.26 in any case.

The equations for nitrophenols and benzoic acids have similar slopes differing primarily in the intercept constant. The difference of 2.73 pK_a units is a measure of the increased acidity of nitrophenols over the carboxylic acids. The fact that the lines all differ in their slopes emphasizes the thesis, "that acid–base equilibria in water may behave very differently on transfer to other solvents so that chemistry in non-aqueous solvents cannot logically be correlated with pK_a in water"[5]. The data in Fig. 2 strongly indicate that relationships *do* exist (even though they are empirical at this time).

Acidities in dimethylsulfoxide and pyridine

Figure 3 is a plot of the differential half-neutralization potentials of benzoic acids and phenols in dimethylsulfoxide and pyridine. There is a scatter of points around the line, as is to be expected, but that there is a direct relationship for these compounds in the two solvents is indicated by the close approximation of the data to a straight line. Such plots should be of value in ascertaining the advantage of one solvent over another for the titrimetric resolution of acids or bases in a mixture. For a plot that involves equivalent units of the abscissa and ordinate, a line having a slope of 1 indicates that both solvents have similar differentiating properties. A line intersecting either of the axes points to the solvent of that axis as the better levelling

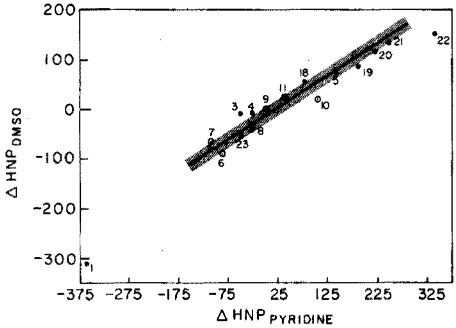

Fig. 3. Differential half-neutralization potentials for phenols and benzoic acids in DMSO and pyridine. (●) phenols, (⊙) benzoic acids.

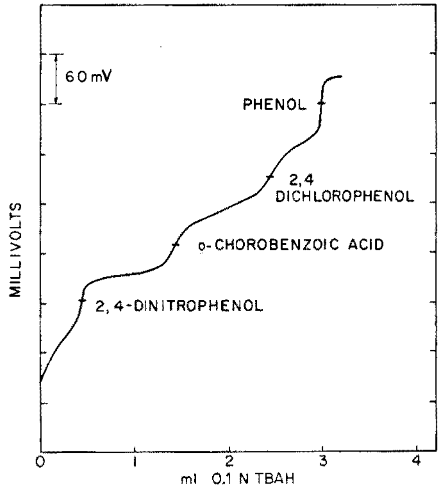

Fig. 4. The resolution of phenols and *o*-chlorobenzoic acid in DMSO.

solvent. Figure 3 indicates pyridine to be the better resolving solvent. This concept can be extrapolated to include a three-dimensional diagram for a third solvent.

Differentiating titrations in dimethylsulfoxide

The resolution of a mixture of 2,4-dinitrophenol, *o*-chlorobenzoic acid, 2,4-dichlorophenol, and phenol in DMSO media is depicted in Fig. 4. The end-point for each individual acid is quite distinct. In the case of 2,4-dinitrophenol, a 5% deviation from that added was found. The others produced results corresponding to 98% of the theoretical recoveries. In general, it was found that acids differing by at least 140 mV were resolvable; however, this does not seem to be the only criterion. For example, the stepwise titration of 2,4- and 2,5-dinitrophenols is almost indistinguishable; yet the resolution of phenol and 2,4-dichlorophenol is quite marked. Solute–solute association may explain these anomalies.

The author thanks J. J. KIRKLAND for his helpful suggestions in the preparation of this manuscript.

SUMMARY

An attempt is made to correlate the relative acidities of phenols and benzoic acids in dimethylsulfoxide and water. Mathematical expressions relating the acidity of the acids in the two solvents are presented and the data show that phenols display a greater increase in their relative acidity in dimethylsulfoxide than do benzoic acids. Differentiating titrations are presented and such titrations are feasible where the acids differ by 140 mV in their half-neutralization potentials. Comparative data are presented for the pyridine solvent system.

RÉSUMÉ

Une étude est faite sur les acidités relatives des phénols et des acides benzoïques dans le diméthylsulfoxyde et l'eau. Des expressions mathématiques de l'acidité des acides dans les deux solvants sont données; les valeurs obtenues montrent que les phénols présentent une plus grande augmentation de leur acidité relative dans le diméthylsulfoxyde que les acides benzoïques. Des titrages différentiels sont possibles lorsque le potentiel de demi-neutralisation varie de 140 mV. Des valeurs comparatives sont également données pour le système pyridine comme solvant.

REFERENCES

1 A. J. PARKER, *Quart. Rev.*, 16 (1962) 163.
2 D. MARTIN, A. WEISE AND H. J. NICLUS, *Angew. Chem., Intern. Ed. Engl.*, 6 (1967) 318.
3 C. A. STREULI, *Anal. Chem.*, 32 (1960) 407.
4 J. JUILLARD, *J. Chim. Phys.*, 63 (1963) 1190.
5 B.W. CLARE, D. COOK, E.C.F. KO, Y.C. MAC AND A. J. PARKER, *J. Am. Chem. Soc.*, 88 (1966) 1911.
6 J. STEIGMAN AND P. LORENZ, *J. Am. Chem. Soc.*, 88 (1966) 2083.
7 G. A. HARLOW AND D. B. BRUSS, *Anal. Chem.*, 30 (1958) 1833, 1836.
8 I. M. KOLTHOFF, M. K. CHANTOONI, JR. AND S. BHOWMIK, *J. Am. Chem. Soc.*, 88 (1966) 5430.
9 I. M. KOLTHOFF AND T. B. REDDY, *Inorg. Chem.*, 1 (1962) 189.
10 E. C. STEINER AND J. M. GILBERT, *J. Am. Chem. Soc.*, 85 (1963) 3054.
11 J. S. FRITZ AND S. S. YAMAMURA, *Anal. Chem.*, 29 (1957) 1079.
12 C. A. STREULI AND R. R. MIRON, *Anal. Chem.*, 30 (1958) 1978.
13 W. HUBER, *Titrations in Nonaqueous Solvents*, Academic Press, New York, 1967, pp. 217, 218.
14 H. G. VAN DER HEIJDE, *Anal. Chim. Acta*, 16 (1957) 392.

Analytica Chimica Acta
Elsevier Publishing Company, Amsterdam
Printed in The Netherlands

LOW-TEMPERATURE PRECIPITATION TITRATION OF PERCHLORATE AND TETRAFLUOROBORATE WITH TETRAPHENYLARSONIUM CHLORIDE AND ION-SELECTIVE ELECTRODES

MICHAEL J. SMITH AND STANLEY E. MANAHAN
Department of Chemistry, University of Missouri, Columbia, Mo. 65201 (U.S.A.)

(Received July 12th, 1969)

Tetraphenylarsonium chloride has long been used as a reagent for the gravimetric determination of tetrafluoroborate ion and perchlorate ion[1]. The precipitates obtained are finely divided and difficult to handle. Furthermore, accurate analyses are limited to relatively large samples. Other non-gravimetric methods have been developed for perchlorate with tetraphenylarsonium chloride or similar reagents. These methods include an amperometric titration of perchlorate with tetraphenylstibonium sulfate[2] and a conductometric determination with tetraphenylarsonium chloride as a titrant[3].

With the recent development of a perchlorate ion-selective electrode (Orion Research, Inc.), the potentiometric titration of perchlorate with tetraphenylarsonium chloride titrant has been described[4]. The method is simple, rapid and relatively free from interferences. Samples containing as little as *ca.* 1.5 millimoles of perchlorate may be analyzed by the method.

Tetrafluoroborate ion also forms a precipitate with tetraphenylarsonium ion. The recently marketed electrode selective for tetrafluoroborate ion (Orion Research, Inc., Model 92-05) has made feasible the potentiometric titration of tetrafluoroborate with tetraphenylarsonium chloride. However, because of the comparatively high solubility of the tetraphenylarsonium tetrafluoroborate precipitate, usable titration curves cannot be obtained below *ca.* $2 \cdot 10^{-2}$ *M* tetrafluoroborate (1.0 millimole in a 50-ml sample). Furthermore, the concentration limit in the conventional perchlorate titration is *ca.* $5 \cdot 10^{-3}$ *M* (0.25 millimole in a 50-ml sample). In the present paper, it is shown that these limits can be extended by a factor of *ca.* 5 by employing a titration at low temperature (2°). The potentiometric determination of as little as 0.25 millimole of tetrafluoroborate and 0.05 millimole of perchlorate (in a 50-ml sample) is thereby possible. Although samples below 50 ml in volume have not been used, it would be possible to construct a titration cell for the low-temperature titration of as little as 5 ml of sample, thus extending the limits of potentiometric tetrafluoroborate and perchlorate determinations to 0.025 and 0.005 millimole, respectively.

EXPERIMENTAL

Reagents

Stock tetraphenylarsonium chloride solutions were prepared from hydrated tetraphenylarsonium chloride (Aldrich Chemical Company). The stock solutions were filtered through a medium-porosity, sintered-glass filter to remove insoluble matter. One drop of Triton X-100 surfactant (Rohm and Haas) was added to each 500 ml of stock solution to prevent incomplete draining of the buret because of drops clinging to the buret surface.

Standard perchlorate solutions were prepared by neutralizing to pH 6.5–7.5 with sodium hydroxide known amounts of previously standardized perchloric acid (Baker and Adamson, reagent grade). This method was found to be the best way of preparing accurately a perchlorate solution of known concentration. Tetrafluoroborate solutions were prepared from solid sodium tetrafluoroborate (Alfa Inorganics, Inc.) and filtered. The concentrations of the tetrafluoroborate solutions were found to decrease by up to 1% over a 24-h period. Presumably the hydrolysis of the tetrafluoroborate ion is responsible.

Saturated solutions of tetraphenylarsonium perchlorate and tetraphenylarsonium tetrafluoroborate were prepared by stirring the salt in suspension at constant temperature for at least 12 h.

Apparatus

Potential measurements were taken with a Corning Model 12 Expanded Scale pH meter. The electrode used to measure perchlorate ion concentration was an Orion Model 92-81 liquid ion exchange electrode and the tetrafluoroborate electrode was the Orion Model 92-05. The reference electrode used was a calomel electrode of special design[5] with 4 M sodium chloride filling solution and an internal agar bridge having a very low leakage rate.

The solutions were maintained at constant temperature in a jacketed cell through which fluid was circulated from a constant temperature circulator (Forma Scientific Model 2095-2). A temperature of 2° rather than 0° was chosen for the titrations to prevent freezing of the more dilute solutions.

Procedure

A 50-ml aliquot of the solution to be titrated was pipetted into the jacketed titration cell. In the case of the low-temperature titration, the measuring and reference electrodes were immersed in the solution and allowed to cool for 20 min. The titrant, *ca.* 10-fold higher in concentration than the solution being titrated, was added from a 10-ml microburet. Near the equivalence point, 1 min was allowed for equilibration after each addition of titrant. Equilibration was somewhat slower at 2° than at room temperature. The equivalence point was taken as the inflection point of the titration curve.

The solubilities of tetraphenylarsonium perchlorate and tetraphenylarsonium tetrafluoroborate were measured at 2.0° and 25.0° by measuring the potential of the appropriate saturated solution and comparing it to a series of standard solutions of the anion. From the concentration of perchlorate or tetrafluoroborate thus determined in the saturated solution, the solubility product was readily calculated.

RESULTS AND DISCUSSION

Figure 1 shows a series of titration curves for the titration of 50 ml of perchlorate ranging in concentration from $1 \cdot 10^{-3}$ M to $5 \cdot 10^{-2}$ M taken at 25° and 2°. In each case the concentration of titrant was 10-fold higher than the concentration of solution being titrated. It is apparent that for a given concentration the break in the titration curve obtained at low temperature is appreciably sharper than the break obtained at room temperature. Furthermore it may be seen that usable titration curves are obtainable at lower concentrations at 2° than at 25°. It is apparent that for the case of perchlorate at room temperature the titration curve of the $5\cdot10^{-3}$ *M* solution is close to the lower limit of analysis, whereas at 2° the titration curve of the $1\cdot10^{-3}$ *M* solution may still be used.

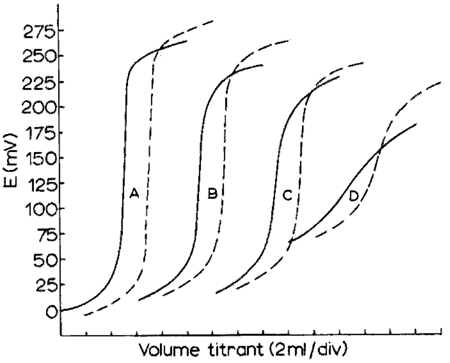

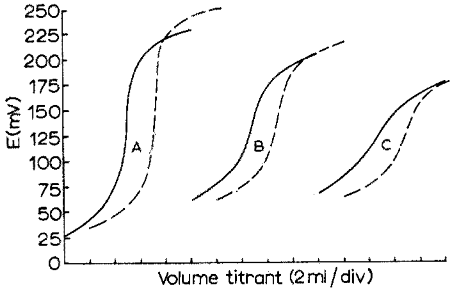

Fig. 1. Titration of 50-ml aliquots of perchlorate with standard tetraphenylarsonium chloride of 10-fold higher concentration at 25° (solid line) and 2° (dashed line). The origin of the volume axis is offset for each titration curve. The initial perchlorate concentrations are (A) $5.00\cdot10^{-2}$ *M*; (B) $1.000\cdot10^{-2}$ *M*; (C) $5.00\cdot10^{-3}$ *M*; (D) $1.000\cdot10^{-3}$ *M*.

Fig. 2. Titration of 50-ml aliquots of tetrafluoroborate with standard tetraphenylarsonium chloride of 10-fold higher concentration at 25° (solid line) and 2° (dashed line). The origin of the volume axis is offset for each titration curve. The initial tetrafluoroborate concentrations are (A) $5.00\cdot10^{-2}$ *M*; (B) $1.000\cdot10^{-2}$ *M*; (C) $5.00\cdot10^{-3}$ *M*.

TABLE I

RECOVERY OF SODIUM PERCHLORATE AND SODIUM TETRAFLUOROBORATE IN 50.00-ml SAMPLES AT VARIOUS CONCENTRATIONS

	Salt added (mmol)	*Salt recovered (mmol)*		*Error (%)*	
		25°	*2°*	*25°*	*2°*
$NaClO_4$	2.500	2.499	2.500	0.0	0.0
	0.5000	0.4990	0.5000	−0.2	0.0
	0.2500	0.2485	0.2495	−0.6	−0.2
	0.0500	—	0.0505	—	1.0
$NaBF_4$	2.500	2.508	2.513	0.3	0.5
	0.5000	0.4980	0.5000	−0.4	0.0
	0.2500	—	0.2500	—	0.0

Figure 2 shows the titration curves for various concentrations of tetrafluoroborate ion at 2° and 25°. Again the advantage of the lower temperature is obvious. It may be seen that at 2° the titration curve for the $5\cdot10^{-3}$ *M* solution is still sufficiently sharp to enable the determination of the equivalence point.

In Table I recovery data are given for the titration of 50.00-ml samples of perchlorate and tetrafluoroborate with standard tetraphenylarsonium chloride of 10-fold higher concentration. It may be seen that as little as 0.05 mmol of perchlorate at the 100-p.p.m. level may be determined to within 1% relative accuracy by titration at 2°. By using a miniaturized apparatus and a much smaller volume of solution as little as 0.005 mmols of perchlorate could be titrated. Although the low-temperature titration is somewhat inconvenient, it is well worth using for perchlorate and tetrafluoroborate concentrations near the lower limit of analysis.

The solubility product values determined for tetraphenylarsonium perchlorate were $5.9 \pm 0.5 \cdot 10^{-9}$ at 25° and $1.1 \pm 0.2 \cdot 10^{-9}$ at 2°. For tetraphenylarsonium tetrafluoroborate the corresponding values obtained were $2.1 \pm 0.1 \cdot 10^{-7}$ at 25° and $1.2 \pm 0.2 \cdot 10^{-7}$ at 2°. At 25° the literature values of the solubility products determined spectrophotometrically are $1.2 \cdot 10^{-8}$ for the perchlorate[3] and $2.2 \cdot 10^{-7}$ for the tetrafluoroborate[6]. Although the differences in solubility product at different temperatures do not appear to be large, theoretical plots of the titration curves reveal that the curve expected at the lower temperature is indeed appreciably sharper.

An interesting observation is that the potential reached by both electrodes in the presence of excess of tetraphenylarsonium ion is considerably more positive than that obtained in the complete absence of both perchlorate (or tetrafluoroborate) and tetraphenylarsonium ion. It is likely that in the latter case perchlorate (or tetrafluoroborate) is exchanged from the resin to provide a low concentration of the ion in solution, whereas in the presence of excess of tetraphenylarsonium ion, the equilibrium concentration of perchlorate or tetrafluoroborate in solution is much lower and it is continually being removed from the resin by the excess tetraphenylarsonium ion which is present beyond the equivalence point thus yielding a higher electrode potential.

This research was supported through the United States Department of the Interior Office of Water Resources Research Matching Grant B-023-MO.

SUMMARY

Perchlorate and tetrafluoroborate have been determined at low concentrations by precipitation titration with tetraphenylarsonium chloride, the appropriate anion-selective electrodes being used to follow the course of the titration potentiometrically. A low temperature, 2°, was employed to sharpen the titration curves, thus resulting in greater accuracy and lower limits of analysis. As little as 0.05 mmol of perchlorate and 0.25 mmol of tetrafluoroborate have been determined to within 1% relative accuracy. These limits could easily be extended by a factor of 10 by using a miniaturized titration apparatus.

RÉSUMÉ

Les perchlorates et les tétrafluoborates peuvent être dosés, en faible concentration, par titrage de précipitation à l'aide de chlorure de tétraphénylarsonium; on utilise des électrodes anioniques sélectives appropriées pour suivre le cours du titrage potentiométriquement. On travaille à basse température, 2°, pour rendre plus nettes les courbes de titrage, ce qui permet d'obtenir une plus grande exactitude et d'abaisser les limites de l'analyse. On a dosé ainsi 0.05 mmol de perchlorate et 0.25 mmol de tétrafluoborate avec une exactitude relative de 1%. Ces limites peuvent facilement être étendues par un facteur de 10 en utilisant un appareil de titrage miniature.

ZUSAMMENFASSUNG

Perchlorat und Tetrafluoroborat wurden bei niedrigen Konzentrationen durch Fällungstitration mit Tetraphenylarsoniumchlorid bestimmt unter Verwendung von geeigneten anionenselektiven Elektroden zur potentiometrischen Verfolgung der Titration. Es wurde eine Temperatur von 2° verwendet, um die Titrationskurven zu verbessern, und eine grössere Genauigkeit und niedrigere Nachweisgrenzen zu erzielen. 0.05 mmol Perchlorat und 0.25 mmol Tetrafluorborat wurden mit einer relativen Genauigkeit von 1% bestimmt. Diese Grenzen können leicht um den Faktor 10 durch Verwendung einer Mikroapparatur erweitert werden.

REFERENCES

1 G. M. Smith and H. Willard, *Ind. Eng. Chem., Anal. Ed.*, 11 (1939) 186.
2 M. D. Morris, *Anal. Chem.*, 37 (1965) 977.
3 R. J. Baczuk and W. T. Bolleter, *Anal. Chem.*, 39 (1967) 93.
4 R. J. Baczuk and R. J. DuBois, *Anal Chem.*, 40 (1968) 685.
5 M. J. Smith and S. E. Manahan, to be published.
6 H. E. Affsprung and V. S. Archer, *Anal. Chem.*, 36 (1964) 2512.

Analytica Chimica Acta
Elsevier Publishing Company, Amsterdam
Printed in The Netherlands

AN INDIRECT POTENTIOMETRIC DETERMINATION OF CHLORIDE IN CLEANING SOLUTIONS FOR POWER PLANT BOILERS

JACK G. FROST
Chemical Research and Development Department, Halliburton Company, Duncan, Okla. 73533 (U.S.A.)

(Received July 8th, 1969)

In certain areas of industrial chemical operations, such as in the chemical cleaning of power plant boilers constructed of chloride-sensitive Austinitic stainless steels, there is a need for fast and reliable methods for determining low chloride concentrations in aqueous solutions. A further requirement is that such determinations should be accomplished with relatively inexpensive and portable equipment. There are several basically different approaches to consider for trace chloride analyses, including colorimetry, potentiometry, turbidimetry, and coulometry, each of which has merits and limitations. A standard method for analyzing low-level chloride solutions is found in *U.O.P. Laboratory Test Methods for Petroleum and its Products*[1]. Chloride ion is determined by a colorimetric method which depends on the formation of a highly colored iron(III) thiocyanate complex. The success of the method depends on obtaining consistently low and precise spectrophotometric blanks, and on making spectrophotometric measurements on all samples and blanks at a fixed time after sample preparation.

Turbidimetry, as a method for trace chloride analysis, has been examined in these laboratories[2]. In this method, silver ion is added to the chloride solution containing a surface-active agent to keep the silver chloride precipitate in a uniform suspension. Again, the method appears reliable if care is taken to make spectrophotometric measurements on all samples after a fixed time lapse.

A coulometric analysis might be applicable here. One such method described by LAITINEN AND LIN[3] involves anodic deposition of silver chloride on a silver working electrode followed by cathodic stripping of the deposited silver chloride. One major drawback to this and similar methods is the complexity and high cost of the analytical equipment involved.

Another method for chloride analysis is direct potentiometry. With the recent development of specific-ion electrodes which can be used with any pH meter as a measuring device, potentiometry as an analytical method no longer presents the problems it once did. Reliable potentiometric methods for many ions are now available to any laboratory of modest means. Further, since an individual measurement is no more involved than that of a pH measurement, electrochemical expertise on the part of the analyst is no longer a prerequisite for reliable analyses. However, in analyzing directly for chloride ion by way of the chloride-specific electrode there are some limitations, including one whose importance for the present applications overshadows all others. The chloride electrode is not designed to analyze chloride solutions below about $5 \cdot 10^{-4}$ *M* (*ca.* 18 mg/l), since in weaker solutions than this the solubility of the silver chloride membrane comes into play.

The method to which this report is specifically devoted is an indirect chloride analysis by potentiometric sensing of an excess of added silver ion in equilibrium with a freshly formed silver chloride precipitate. Reference curves are drawn from data taken with an expanded scale pH meter and a silver ion sensing electrode. These reference curves can subsequently be used with data taken with any pH meter and a silver-sensing electrode for chloride analyses with an accuracy of better than ±1 mg/l. The aqueous media in which the analyses were conducted are representative of solutions commonly used in the chemical cleaning of power plant boilers.

THEORY

If a solution with an initial chloride activity, c, is treated with silver ion whose activity in this solution before precipitation would be A, precipitation of silver chloride in excess of its solubility will occur, and an equilibrium is set up which fixes the equilibrium activity of silver at a level which can be expressed as a function of the original chloride activity. Conversely, the original chloride activity can be expressed as an explicit function of the equilibrium silver activity as is developed below.

The equilibrium chloride activity is related to the original activity and the activity, p, lost owing to precipitation:

$$a_{\mathrm{Cl}} = c - p \tag{1}$$

also,

$$a_{\mathrm{Ag}} = A - p \tag{2}$$

Eliminating the term p between these two equations we have:

$$c = a_{\mathrm{Cl}} - a_{\mathrm{Ag}} + A \tag{3}$$

The equilibrium chloride activity, a_{Cl}, can be eliminated from this equation through the solubility product constant, K_0.

Thus, $$c = K_0/a_{\mathrm{Ag}} + A - a_{\mathrm{Ag}} \tag{4}$$

The equilibrium activity of silver in the sample is related to the electrode potential through the Nernst equation:

$$E(\mathrm{S}) = E^0 + (RT/nF) \ln a_{\mathrm{Ag}}(\mathrm{S}) \tag{5}$$

In eqn. (5) the value of the term E^0 can at best be only estimated, hence it should be eliminated in the final form of the equation to be used. This is accomplished by making potential measurements on a reference solution of known concentration:

$$E(\mathrm{R}) = E^0 + (RT/nF) \ln a_{\mathrm{Ag}}(\mathrm{R}), \tag{5a}$$

and combining eqns. (5) and (5a) to eliminate E^0 as is shown in eqns. (6)–(8).

$$\Delta E = E(\mathrm{R}) - E(\mathrm{S}) = (RT/nF) \ln a_{\mathrm{Ag}}(\mathrm{R}) - (RT/nF) \ln a_{\mathrm{Ag}}(\mathrm{S}) \tag{6}$$

$$\ln a_{\mathrm{Ag}}(\mathrm{S}) = \frac{-\Delta E + (RT/nF) \ln a_{\mathrm{Ag}}(\mathrm{R})}{RT/nF} \tag{7}$$

$$a_{\mathrm{Ag}}(\mathrm{S}) = \exp \left[\frac{-\Delta E + (RT/nF) \ln a_{\mathrm{Ag}}(\mathrm{R})}{RT/nF}\right] \tag{8}$$

By substituting this expression for $a_{Ag}(S)$ into eqn. (4), an equation is obtained from which values of c can be calculated explicitly from constants and experimentally measured parameters.

$$c = K_0/\exp\left[\frac{-\Delta E + (RT/nF)\ \ln a_{Ag}(R)}{RT/nF}\right] + \\ - \exp\left[\frac{-\Delta E + (RT/nF)\ \ln a_{Ag}(R)}{RT/nF}\right] + A \qquad (9)$$

To obtain reference curves by the present treatment, a computer program was used to calculate best fits to the several sets of c *vs.* ΔE data by a multiple linear regression analysis on each set of data. Without transforms the program used would fit the linear curve:

$$y = C_0 + C_1 x_1 + C_2\, x_2 \qquad (10)$$

where x_1 and x_2 are independent variables, y is the dependent variable, and C_0, C_1, and C_2 are empirical constants. However, to fit a function of the form of eqn. (9), the following transforms were specified:

$$x_1 = 1/\exp\left[\frac{-\Delta E + (RT/nF)\ \ln a_{Ag}(R)}{RT/nF}\right] \qquad (11a)$$

$$x_2 = \exp\left[\frac{-\Delta E + (RT/nF)\ \ln a_{Ag}(R)}{RT/nF}\right] \qquad (11b)$$

The value of RT/nF in the above equations is theoretically 0.0257 V, but it is well known that experimental determinations of this quantity rarely coincide with its theoretical value. For this reason the value of RT/nF for each of the five different media was determined experimentally by making a linear plot of E_{Ag} *vs.* ln (c_{Ag}) in silver solutions containing no chloride. Regarding the silver activity of the reference solution, the assumption was made that $a_{Ag}\,(R) \cong c_{Ag}\,(R)$.

EXPERIMENTAL

Apparatus

Data for the reference curves were obtained with an Orion Model 801 digital readout pH meter. For doing simulated chloride analyses based on these reference curves, data were obtained with a Beckman Zeromatic pH meter. In all cases the electrode system consisted of an Orion silver sulfide membrane electrode and an Orion double-junction electrode (outer filling solution of 10% chloride-free potassium nitrate).

Preparation of reference curve plots

Samples were prepared from stock solutions made from reagent-grade chemicals where possible. The water had been distilled and passed through a mixed bed ion-exchange column for chloride removal. Five different aqueous media were considered for this report: (*1*) 3% citric acid, (*2*) 2% glycolic + 1% formic acids (G-F acid), (*3*) 0.35% trisodium phosphate + 0.15% disodium phosphate, (*4*) 0.1% "pen-6" (a detergent formulated from a non-ionic and an amphoteric surfactant), and (5) "Rodine 31A" (an acid corrosion inhibitor formulated by Amchem Products, Inc.). For each of these five different media twenty-one 100-ml samples were prepared to contain 0, 1, 2, 3, ..., 19 and 20 ml/l chloride. Each sample was treated with enough chloride-free concentrated nitric acid, where necessary, to lower the pH to around 2.0 (± 0.5). Then, exactly 1.0 ml of a silver reagent (0.02821 M) was added with constant stirring. Next, the electrodes were immersed into the treated sample and a potential reading was recorded after a 60-sec equilibration time. The electrodes were then wiped clean and immersed into a silver reference solution ($1.0 \cdot 10^{-3}$ M). After 60 sec, this potential was also recorded. These values were subtracted, E(reference) $-$ E(sample), and this difference was plotted against chloride concentration.

In the preparation of the 0.1% Rodine 31A series, it was apparent that some component of this inhibitor was complexing silver, since no visible precipitate occurred on silver addition. Infrared analysis indicated the presence of a sulfur-containing organic material. The interference was eliminated by treating each sample with 1 g of chloride-free activated charcoal and filtering.

Determination of RT/nF values

A series was prepared in each of the above media to contain silver in the concentration range $5 \cdot 10^{-6}$ M to $5 \cdot 10^{-4}$ M, and potential measurements were made. From slopes of the semilog plots of these series, values of RT/nF to be used in the transforms in eqns. (11a) and (11b) were determined.

Procedure for simulated chloride determinations

The procedure for sample treatment was identical to that described above for preparation of reference curve plots. When a value for $E(\mathrm{R}) - E(\mathrm{S})$ was determined on a Beckman Zeromatic pH meter, it was compared to the appropriate reference curve, and the unknown chloride concentration was found by interpolation.

DISCUSSION

In an analysis situation such as the one described, the primary concern is to insure that the concentration of an undesirable impurity in a solution is below a specified level. Should the concentration of this impurity exceed that level, then either the offending solution component must be excluded or the prepared solution may have to be rejected. For this reason, it is desirable to have an analysis method which has its greatest sensitivity for the impurity in the concentration range at or near this specified and critical level. As is well known (also see Fig. 1a), the slope of a potentiometric titration curve is greatest at the stoichiometric point. It follows that an analysis by interpolation from a potentiometric titration curve used as a reference standard curve in this type of application can have specific merit over a Nernstian plot, since the greater slope implies a greater sensitivity in this concentration range of interest. Figure 1a shows a typical reference curve plotted from actual data for chloride solutions ranging from 0 to 20 mg/l, to which had been added $2.821 \cdot 10^{-5}$ moles of silver ion (equivalent to 10 mg/l chloride in 100 ml of solution). Figure 1b is a calculated Nernstian plot on linear coordinates (for the purpose of comparison) for the same concentration range. In only the low chloride concentration range is the rate of change of

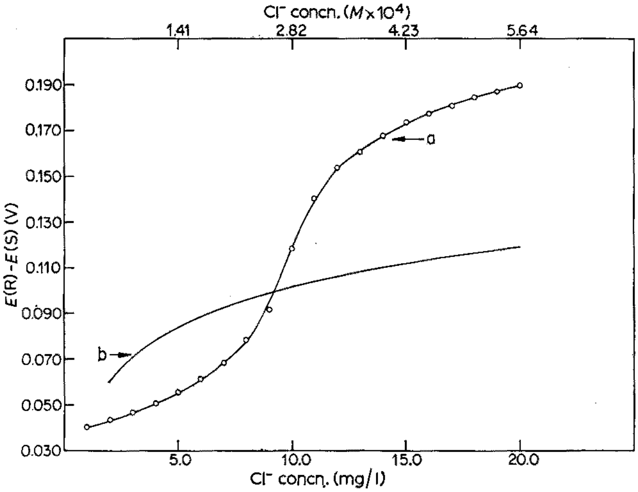

Fig. 1. Plots of potential *vs.* chloride concentration. (a) Reference curve for 2% glycolic + 1% formic acid medium. (b) Calculated curve from Nernst equation.

potential response per incremental chloride change greater in the Nernstian plot. Elsewhere this slope is measurably greater in curve 1a, especially at [Cl] = 10 mg/l.

Plotting the reference curves

As an illustration a single data series for plotting chloride reference curves is presented in Table I, and the curve from this data is plotted in Fig. 1a. The first two

TABLE I

POTENTIAL *VS.* CONCENTRATION DATA FOR REFERENCE CURVE PLOT: 2% GLYCOLIC + 1% FORMIC ACID MEDIUM

($RT/nF = 0.0250$; $C_0 = 2.764 \cdot 10^{-4}$; $C_1 = 1.457 \cdot 10^{-10}$; $C_2 = -1.247$)

E(R)−E(S) (mV)	*Chloride concn. (·10⁻⁴ M)*	
	Actual	*Calculated*
37.3	0.000	−0.030
40.6	0.282	0.317
43.2	0.564	0.560
46.7	0.846	0.850
50.5	1.128	1.123
55.4	1.410	1.419
61.1	1.692	1.700
78.6	2.257	2.261
91.6	2.539	2.502
118.5	2.821	2.822
139.9	3.103	3.110
153.3	3.385	3.408
160.7	3.667	3.645
167.7	3.948	3.941
173.9	4.231	4.280
177.3	4.513	4.504
180.9	4.795	4.777
184.1	5.077	5.054
187.8	5.359	5.421
189.4	5.641	5.598

columns of Table I show the experimental data for this series. From this data with an experimentally determined value of RT/nF, a computer was programmed to calculate the best values of the constants C_0, C_1, and C_2 of eqn. (10). Once the best values of these constants had been determined, the computer was then programmed to determine the calculated chloride values in Column 3 of Table I. These values plotted against the respective $E(\mathrm{R})-E(\mathrm{S})$ values formed the basis for the solid line of Fig. 1a.

Reproducibility of the reference curves

In accordance with eqns. (9)–(11) the shape of a curve such as Fig. 1a is governed by the values of the constants C_0, C_1 and C_2 which represent experimental estimates of the concentration of the silver reagent, the solubility product constant of silver chloride, and unity, respectively. Before these curves were used as reference curves for subsequent chloride analyses, it was of interest to see how reproducible these constants—hence, the shapes of the curves—were from one data series to the next.

TABLE II

MULTIPLE DETERMINATIONS OF THE CONSTANTS OF EQN. (10)

Solution medium	C_0	C_1	C_2
2% Glycolic + 1%	$2.76 \cdot 10^{-4}$	$1.46 \cdot 10^{-10}$	−1.25
formic acids	2.76	1.35	−1.27
	2.74	1.46	−1.25
(Average)	2.76	1.42	−1.26
3% Citric acid	$2.83 \cdot 10^{-4}$	$1.29 \cdot 10^{-10}$	−1.40
	2.85	1.20	−1.34
(Average)	2.84	1.24	−1.37
0.1% "Pen-6"	$2.83 \cdot 10^{-4}$	$1.36 \cdot 10^{-10}$	−1.27
	2.81	1.26	−1.23
(Average)	2.82	1.31	−1.25
0.35% TSP +	$2.86 \cdot 10^{-4}$	$2.05 \cdot 10^{-10}$	−1.53
0.15% DSP	2.81	1.90	−1.47
	2.81	2.09	−1.49
(Average)	2.82	2.01	−1.50
0.1% "Rodine 31A"	$2.79 \cdot 10^{-4}$	$2.42 \cdot 10^{-10}$	−1.31
	2.86	2.30	−1.48
(Average)	2.83	2.36	−1.39

TABLE III

EFFECT OF VARIATIONS IN C_0, C_1 AND C_2

Potential (mV)	*Calculated chloride* ($\cdot 10^{-4}$ *M*)	*Effect of* $\Delta C_0 = \pm 0.05$ ($\cdot 10^{-4}$ *M*)	*Effect of* $\Delta C_1 = \pm 0.1 \cdot 10^{-10}$ ($\cdot 10^{-4}$ *M*)	*Effect of* $\Delta C_2 = \pm 0.1$ ($\cdot 10^{-4}$ *M*)
43.2	0.560	± 0.056	± 0.003	± 0.183
55.4	1.419	± 0.054	± 0.003	± 0.113
118.5	2.822	± 0.056	± 0.014	± 0.011
167.7	3.941	± 0.054	± 0.087	0
187.8	5.421	± 0.054	± 0.195	0

Table II shows duplicate and triplicate determinations of C_0, C_1 and C_2 all calculated by the procedure described above from different data sets. Although the precision of these constants appears to be reasonably good, a better way of demonstrating the effect of fluctuations of C_0, C_1 and C_2 on interpolated results is by calculation through eqn. (10). This has been done for selected points of the data set in Table I and is presented in Table III. For the purpose of these calculations the "calculated chloride" values of Table I were assumed to be correct. The effect on these calculated chloride concentrations of a reasonable variation of each constant individually was considered, holding the other two constants to their original value. From the results of these calculations in Table III, it can be concluded that variations in the determined values of C_0, C_1 and C_2 of magnitudes indicated in Table II can be tolerated.

Simulated chloride determinations

After reference curves had been established as described above, their accuracy for use with data taken on a less elaborate pH meter such as the Beckman Zeromatic

TABLE IV

DETERMINATION OF CHLORIDE IN DIFFERENT MEDIA

E(R)−E(S) *(V)*	*Cl added* $(\cdot 10^{-4}\ M)$	*Cl found* $(\cdot 10^{-4}\ M)$	*Error* $(\cdot 10^{-4}\ M)$	*% Error*
2% Glycolic + 1% formic acids				
0.054	1.41	1.32	−0.09	− 6.4
0.076	1.97	2.18	+0.21	+10.7
0.110	2.82	2.72	−0.10	− 3.6
0.144	3.39	3.17	−0.22	− 6.5
0.172	4.23	4.13	−0.10	− 2.4
3% Citric acid				
0.054	1.41	1.39	−0.02	− 1.4
0.076	1.97	2.28	+0.31	+15.7
0.110	2.82	2.81	−0.01	− 0.4
0.144	3.39	3.29	−0.10	− 2.9
0.166	4.23	4.04	−0.19	− 4.5
0.1% "Pen-6"				
0.054	1.41	1.48	+0.07	+ 5.0
0.070	1.97	2.14	+0.17	+ 8.6
0.110	2.82	2.81	−0.01	− 0.4
0.144	3.39	3.28	−0.11	− 3.2
0.166	4.23	4.02	−0.21	− 5.0
0.35% Trisodium phosphate + 0.15% disodium phosphate				
0.056	1.41	1.26	−0.15	−10.6
0.070	1.97	1.96	−0.01	− 0.5
0.110	2.82	2.81	−0.01	− 0.4
0.140	3.39	3.33	−0.06	− 1.8
0.160	4.23	4.05	−0.18	− 4.3
0.1% "Rodine 31 A"				
0.054	1.41	1.29	−0.12	− 8.5
0.070	1.97	2.05	+0.08	+ 4.1
0.104	2.82	2.78	−0.04	− 1.4
0.132	3.39	3.26	−0.13	− 3.8
0.154	4.23	4.01	−0.22	− 5.2

was examined. Table IV shows the results of these chloride determinations in each of the five aqueous media under consideration. Although there is no ready explanation for the obvious negative bias in the data and results reported in this Table, the results are (with one exception) within the tolerance limit of ±1 mg/l ($0.28 \cdot 10^{-4}$ M). Further, at a concentration of 10 mg/l ($2.82 \cdot 10^{-4}$ M), which is considered in the present work as a critical chloride concentration above which a sample would be rejected, the errors are considerably less than ±0.5 mg/l.

SUMMARY

The potentiometric determination of chloride in cleaning solutions for power plant boilers is described. The procedure is based on a potentiometric sensing of excess added silver reagent. Curves prepared from data taken on an expanded scale pH meter can subsequently be used as reference curves for data taken on less precise pH meters.

RÉSUMÉ

On décrit une méthode de dosage des chlorures dans les solutions de rinçage de chaudières. Elle consiste à doser par potentiométrie l'excès d'argent ajouté. Les courbes obtenues à l'aide d'un pH-mètre avec expansion d'échelle peuvent servir de courbes de référence pour des valeurs obtenues avec un pH-mètre moins précis.

ZUSAMMENFASSUNG

Die potentiometrische Bestimmung von Chlorid in Reinigungslösungen für Kraftwerkskessel wird beschrieben. Das Verfahren beruht auf der potentiometrischen Anzeige eines Überschusses an zugegebenem Silberreagenz.

REFERENCES

1 D. P. THORNTON, *U.O.P. Laboratory Test Methods for Petroleum and its Products*, 4th Edn., Universal Oil Products, Des Plains, Ill., 1959, p. 425.
2 R. SLATE, unpublished studies at Halliburton Laboratories.
3 H. A. LAITINEN AND Z. F. LIN, *Anal. Chem.*, 35 (1963) 1405.

Analytica Chimica Acta
Elsevier Publishing Company, Amsterdam
Printed in The Netherlands

INVESTIGATION OF SOME CONTINUOUS VOLTAMMETRIC SENSORS FOR THE DETERMINATION OF CALCIUM IN THE PRESENCE OF MAGNESIUM

M. D. BOOTH, B. FLEET, SOE WIN* AND T. S. WEST
Department of Chemistry, Imperial College, London, S.W.7 (England)

(Received June 13th, 1969)

Continuous automated methods for the determination of calcium and magnesium have been surprisingly rare despite the large demand for such analytical methods. Colorimetric (absorptiometric) sensing is employed in almost all cases; for example, in a recommended automatic method for calcium[1], the absorbance of a coloured calcium complex is measured, and any interference by magnesium is compensated by additions of magnesium to the standard. Most magnesium methods are based on the development of a coloured complex between magnesium hydroxide and a lake-forming reagent[2]. Electrochemical sensors are ideally suited for monitoring complexation reactions. The mercury pM indicator electrode[3] has been employed by BLAEDEL AND STROHL[4,5] for continuous EDTA titration of metal ion.

NOVAK[6] has given an extensive review of continuous polarographic and galvanic analysers and more recently ŠTRÁFELDA AND DOLEŽAL[7] have described a fully automated polarographic analyser for concentrated sulphite solutions.

The anodic polarographic behaviour of complexones has been shown to have analytical utility[8,9] and some preliminary results on a continuous polarographic analyser have recently been reported[10]. The present paper describes a comparative evaluation of several types of continuous voltammetric sensor. In addition to the D.M.E., the hanging mercury drop electrode (H.M.D.E.), the tubular platinum electrode, the mercury-coated tubular platinum electrode and a pyrolytic graphite electrode (P.G.E.) have been examined.

EXPERIMENTAL

Apparatus

A Heyrovský Polarograph type LP 55A (Czechoslovakia) was used. A 4.2 kΩ resistor was placed across the galvanometer terminals and the potential drop was displayed on a Servoscribe recorder.

An AutoAnalyzer peristaltic pump (Technicon AutoAnalyzer Proportioning Pump) was used to pump liquid and gas streams. Standard AutoAnalyzer manifold units were used for the construction of the flow-systems.

A cam-operated tap assembly was used to control the various reagent/solution lines. The cam-shaft was driven via a gear-train by the motor of the peristaltic pump; the cams operated push-rods which were placed vertically above the solution lines. An automatic sampling device (AutoAnalyzer Sampler II) was coupled to the

---

* Present address: Department of Chemistry, Arts and Science University, Rangoon (Burma).

assembly as follows. The micro-switch which controlled the sampling rate was disconnected and the input leads were taken to a micro-switch which was operated by a cam on the drive shaft of the tap assembly. This was activated after each complete cycle to change samples.

The flow-through cell for the D.M.E. or the H.M.D.E. was constructed from 1-in sheet perspex (Fig. 1). The connections to the solution lines were made by drilling the holes oversize and fitting 1-cm sleeves of polyethylene tubing to attach the glass connecting pieces.

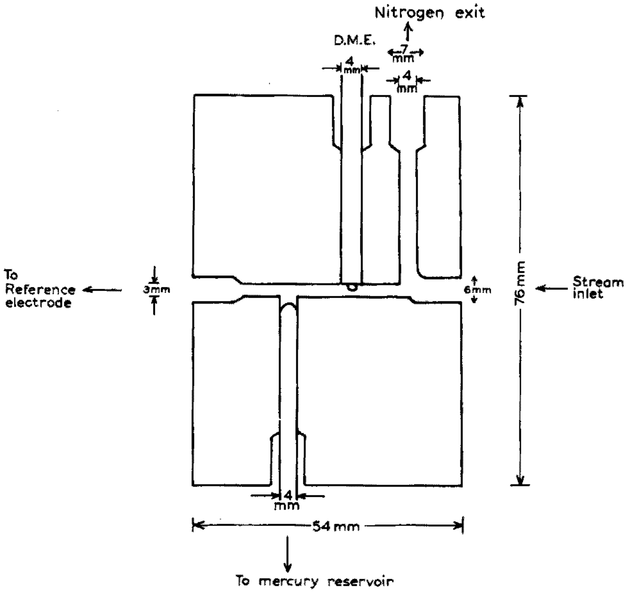

Fig. 1. Flow-through polarographic cell.

A low resistance calomel reference electrode was situated immediately downstream of the cell. This consisted of a mercury pool (4 cm^2) covered with 1 N potassium chloride and connected to a porous glass sinter via a 1 N potassium chloride liquid junction. The glass sinter was formed by carefully fusing a 5-mm layer of coarse ground glass into the stem of a T-piece. One arm of the T-piece was connected to the cell outlet with the stem in a vertical position, the other arm forming the solution outlet. The porosity of the sinter allowed a slow seepage of the junction electrolyte into the solution stream.

More recently a modified version of the flow cell has been developed in which the reference electrode is incorporated in the cell block. Electrical contact with the solution is made through a porous "Vycor" tube[11]. Although this makes a more compact cell, "Vycor" tubing is very fragile and certain precautions are necessary when it is used. It is particularly important to note that although the tubing is stable indefinitely in electrolyte solution, once having been immersed it should not be allowed to dry out as this causes it to fracture.

Electrode assemblies

Hanging mercury drop electrode. The H.M.D.E. used was a model E 410 (Metrohm Ltd., Switzerland).

Tubular platinum electrode. A platinum cylinder 1.5 cm long was carefully cut from seamless platinum tubing (1.0 mm i.d.) and the ends smoothed to avoid causing turbulence in the flow stream. The tubular electrode was directly connected to the solution line from the pump with the reference electrode connected immediately downstream.

Mercury-coated tubular platinum electrode. The assembly used was similar to that employed by OESTERLING AND OLSON[12]. It was designed to provide for independent pumping of the solution and mercury streams and also for both forward and backward pumping of the mercury stream which are necessary in the mercury-plating process[11]. The tubular electrode was mounted in an upright position and was connected at both ends to plastic nipple connectors via tight-fitting polythene sleeves. The upper nipple connector fits in a rubber stopper at the lower end of a 15-mm i.d. glass tube provided with a side arm which goes to waste. The glass tube formed the reference electrode compartment into which a saturated potassium chloride salt-bridge was inserted. The lower nipple connector from the electrode was connected by means of a tight-fitting polythene sleeve to an H-shaped glass tube, one arm of which was filled with mercury connected via polythene tubing to an external levelling reservoir. The other arm was connected to the solution line from the peristaltic pump and was fitted with a pinch-clip. The electrode used was a piece of platinum cylinder of 1 mm i.d. and 10 mm length cut from seamless platinum tubing.

Of the many methods described for plating a platinum surface with mercury, the wetting method described by ENKE *et al.*[13] was used. For a successful application of the method a clean surface free from any surface oxides is necessary. The electrode was therefore first degreased in alcoholic caustic potash, then cleaned in hot nitric acid, and finally rinsed with distilled water. It was then fitted in the cell assembly and a solution of 1 *M* perchloric acid was pumped through the cell whilst the electrode was cathodised to the point of vigorous hydrogen evolution for 15 min by applying a potential of -3 V *vs.* the S.C.E. (or a large tubular platinum electrode). Pumping of the solution was then stopped, the pinch-clip closed, and very pure mercury introduced to make contact with the entire inner surface of the tubular electrode by raising the mercury reservoir, whilst the negative potential was still maintained. The mercury level was raised and lowered several times to remove hydrogen bubbles from the electrode surface and then allowed to stand in contact with the electrode for a period of 15–30 min. The mercury level was then returned to the junction level.

The efficiency of the coating was tested by running a current–potential curve for a solution of deaerated 0.1 *M* sodium sulphite at a flow-rate of 0.32 ml/min. The plating was considered adequate if the residual current was only about 1 μA at a potential of -1.0 V *vs.* S.C.E. and if the anodic and cathodic discharge potentials were in the region of $+0.2$ V and -2.0 V *vs.* S.C.E. respectively. If necessary the plating process was repeated.

All solutions were thoroughly deaerated before measurement with oxygen-free nitrogen. The purification train consisted of a 2% solution of anthraquinone-2-sulphonic acid (disodium salt) in 2 *N* sodium hydroxide containing granulated zinc.

Pyrolytic graphite electrode. The pyrolytic graphite electrode was prepared by fitting pyrolytic graphite (length 1 cm, diam. 0.2 cm) to a glass tube holder by means of a silicone rubber adhesive (Midland Silicones Ltd.). The electrode surface was plane perpendicular to the hexagonal axis. The tip of the graphite rod was then filed off and smoothed so as to expose a circular disc about 1 mm in diameter. The sides of the graphite rod were carefully sealed from contact with the solution by means of the silicone adhesive. Electrical contact with the graphite was made by means of a copper wire and a low melting conducting alloy.

Reagents

Approximately 0.01 *M* stock solutions of the EDTA and EGTA (ethyleneglycol-bis(β-aminoethyl ether)-N,N,N',N'-tetraacetic acid) were prepared as their sodium salts.

An ammonia buffer pH 9.3 (3 *M* ammonia/1 *M* ammonium nitrate) was employed.

Method

The development of the procedure was based on a manual polarographic method described previously[6]. Both EDTA and EGTA give anodic waves at the D.M.E. corresponding to mercury complex formation at pH 9–10. The sum of calcium and magnesium is determined from the decrease in the height of the anodic wave of EDTA. Calcium is then determined separately from the decrease in the height of the anodic wave of EGTA by virtue of the fact that the calcium–EGTA complex is far more stable (log $K_{CaY} = 11.0$) than the corresponding magnesium complex (log $K_{MgY} = 5.2$). The weak complexing ability of the magnesium, however, does distort the anodic wave of EGTA and it is necessary to add an auxiliary masking agent, pentasodium tripolyphosphate, to overcome this.

The flow plan for the adaptation of these methods for continuous analysis is shown in Fig. 2. The flow-through polarographic cell (Fig. 1) is used and the anodic current from mercury complex formation of the free complexone is monitored. The solutions are added sequentially via the cam-operated tap assembly. Initially a solution of EDTA is presented to the D.M.E. by opening taps T_1 and T_4 and closing

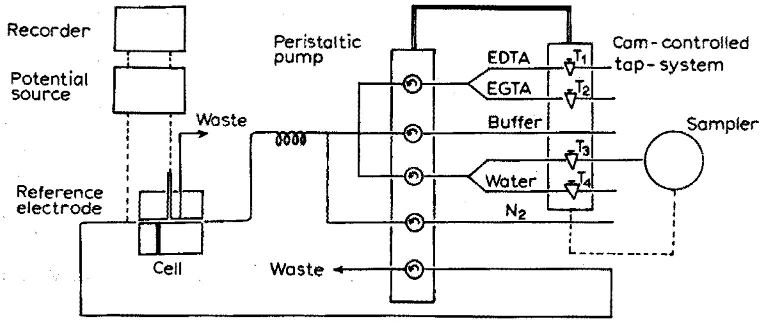

Fig. 2. Flow plan of the continuous polarographic analyser for the simultaneous determination of calcium and magnesium. Pumping rate: complexone solutions and buffer (0.3 *M* NH_3/0.1 *M* NH_4NO_3 buffer with $1.25 \cdot 10^{-3}$ *M* sodium tripolyphosphate), 0.32 ml/min, nitrogen, 1.2 ml/min, waste, 0.42 ml/min. Double lines and dotted lines represent mechanical and electrical connections respectively.

T_2 and T_3. The buffer/masking agent and the nitrogen segmenting gas are introduced continuously. In the second phase the sample is introduced to the EDTA stream by opening T_3 and closing T_4. The decrease in anodic current indicates the total calcium and magnesium content. In the third phase EGTA is introduced (T_2, T_4 open, T_1, T_3 closed) and finally the sample is again added to the stream by opening T_3 and closing T_4. The recorder response for the complete cycle is shown in Fig. 3. During the present study the various factors involved in optimisation of the response time were examined. By altering the flow-cell design so that the exit for the segmenting gas was placed *ca.* 1 cm from the D.M.E., the transition time was reduced to less than 1 min. By allowing a measuring interval of 2 min per phase a complete analysis could be carried out in 8 min. When a series of samples is analysed, the total time required is much less as the EDTA and EGTA standards need only be measured at the beginning and the end of the cycle.

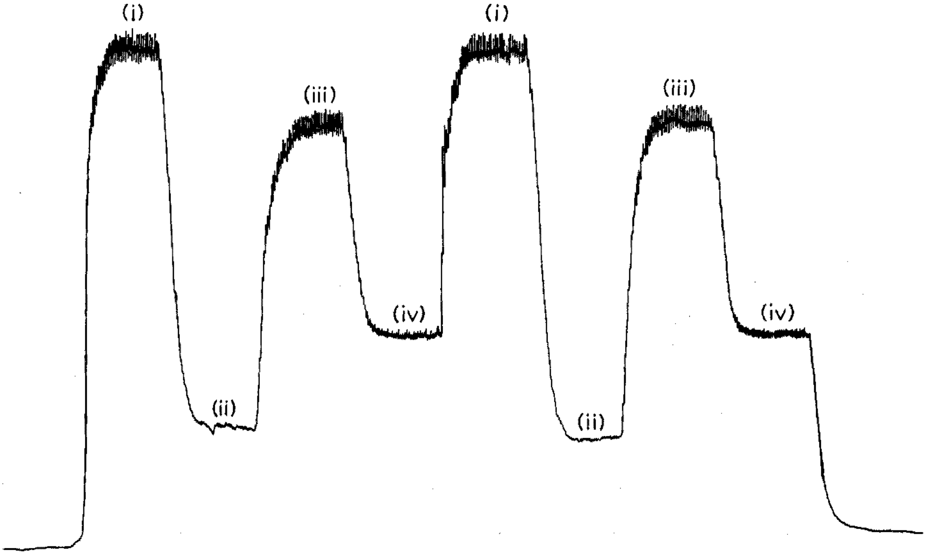

Fig. 3. Recorder response for a complete cycle of the continuous polarographic analyser. (i) 0.5 m*M* EDTA, (ii) (i) + sample (0.25 m*M* Ca + 0.15 m*M* Mg), (iii) 0.5 m*M* EGTA, (iv) (iii) + sample. 1.25 m*M* Sodium tripolyphosphate present as masking agent, 0.3 *M* NH_3/0.1 *M* NH_4NO_3 buffer. Sens. = 3 μA f.s.d.

RESULTS AND DISCUSSION

The results obtained on a series of synthetic samples are shown in Table I.

The reproducibility of the system was studied by carrying out measurements on a series of identical samples containing $3 \cdot 10^{-4}$ *M* magnesium and/or $1.1 \cdot 10^{-3}$ *M* calcium over a period of several hours; the long-term stability of the system was good, the precision on an individual measurement being $\pm 3\%$. The accuracy of the method was slightly superior to the conventional polarographic procedure[9] owing to the fact that measurements were made at a fixed potential. As the result depends on the accuracy with which the decrease in anodic wave height can be measured then

TABLE I

RESULTS OBTAINED FOR A SERIES OF SYNTHETIC SAMPLES OF CALCIUM AND MAGNESIUM WITH THE CONTINUOUS POLAROGRAPHIC ANALYSER

Sample no.	*(Ca + Mg)*					*Ca*				
	Present (mM)	*Found (mM)*				*Present (mM)*	*Found (mM)*			
		1	*2*	*3*	*4*		*1*	*2*	*3*	*4*
1	0.70	—	0.73	0.69	—	0.60	—	0.60	0.60	—
2	0.80	0.76	0.82	0.82	—	0.60	0.60	0.59	0.60	—
3	0.90	0.88	0.94	0.94	—	0.60	0.62	0.61	0.60	—
4	1.00	1.01	1.03	1.06	—	0.60	0.63	0.61	0.59	—
5	1.10	1.09	1.12	1.14	—	0.60	0.57	0.62	0.58	—
6	1.30	1.32	1.26	1.26	—	0.60	0.56	0.63	0.60	—
7	1.40	1.40	1.40	1.44	1.40	0.80	0.78	0.78	0.81	0.76
8	1.40	—	1.40	1.44	1.40	0.85	—	0.86	0.85	0.86
9	1.40	1.40	1.40	1.41	1.40	0.90	0.88	0.88	0.90	0.88
10	1.40	1.40	1.40	1.41	1.40	1.00	1.00	0.99	1.00	0.98

clearly accuracy is improved when a large fraction of the complexone has reacted.

A possible source of error in continuous analysis is the change in anodic current due to changes in solution flow rate. There has been no specific treatment of the case of laminar flow to the D.M.E. but the analogous case of convective diffusion to a liquid electrode was studied by KOLTHOFF AND OKINAKA[14] who derived an equation for the current at a rotated D.M.E.

$$i = 230nCD^{1/2}[m^{2/3}t^{1/6} + 103D^{1/2}(mt)^{1/3} + 7.45u_0^{1/2}(mt)^{1/2}] \qquad (1)$$

where u_0 denotes the speed of the solution at the electrode surface in cm sec^{-1}. The first two terms in this equation are independent of solution speed and constitute less than 10% of the total current, hence for large values of u_0 eqn. (1) simplifies to

$$i = 1714nCD^{1/2}u_0^{1/2}(mt)^{1/2} \qquad (2)$$

In both original and simplified forms the limiting current is proportional to concentration. Although in the case of the rotated D.M.E. it was assumed that the speed of the solution is uniform over the whole electrode surface, this situation does not apply to the D.M.E. in a flowing stream where only one half of the electrode surface faces the solution flow. However, it was found that the current at the D.M.E. is a linear function of C and of $u_0^{1/2}$ indicating that the theory of a rotated D.M.E. can be applied to flowing stream systems. A significant dependence of limiting current on h was observed in accordance with eqn. (1). This was to be expected as the relatively low flow-rates did not permit the first two terms in the equation to be neglected. In the system employed the flow-rate through the cell is controlled from a single outlet tube, the remainder of the solution flowing to waste. As the precision quoted for the delivery rate of this tube is better than 1% then in accordance with eqn. (1), the maximum error obtained would be approximately 0.2%. The flow system developed for the D.M.E. was used in examinations of several other types of electrode.

Hanging mercury drop electrode

A hanging mercury drop electrode (H.M.D.E.), whilst preserving most of the merits of the D.M.E., offers possibilities from both the theoretical and practical points of view. From the latter point of view, elimination of capillary noise and decrease in the charging current when compared to the D.M.E. are important advantages. The utility of the H.M.D.E. in stripping voltammetry is well known but its application to continuous sensing has so far not been reported.

EDTA and EGTA at 10^{-3} *M* concentrations in 0.3 *M* ammonia–0.1 *M* ammonium nitrate buffer give normal well-defined S-shaped voltammetric curves with a limiting current plateau. At a flow-rate of 0.42 ml/min, the voltammogram was completely noise-free. The reproducibility of the limiting current and of the half-wave potential with $5 \cdot 10^{-4}$ *M* solutions of EDTA or EGTA in a pH 9.5 buffer were measured with a solution flow-rate of 0.42 ml/min and an electrode with a drop diameter of 0.66 mm. Variations of 0.01–0.03 μA for the current and 0.003–0.004 V for the half-wave potentials were obtained from five different voltammetric curves. The results were obtained with a single mercury drop, without renewal between the individual measurements. This independence of the history of the drop is due to the solubility of the electrolysis products, which are continuously removed by the flowing stream.

The rate of increase of the limiting current (i_{lim}) with increasing surface area (A) of the mercury drop was found to be much higher than that of the residual current (i_r) resulting in a net increase in sensitivity. The ratio i_{lim}/i_r for a $1 \cdot 10^{-3}$ *M* solution of EGTA increased from 20 to 50 as the drop surface area changed from 0.5 to 3 mm^2. The half-wave potential remained unaffected, the shape of the wave was not altered and no increase of noise in the recordings was observed within the range studied. A plot of i_{lim} *vs.* $A^{3/4}$ gave a straight line passing through the origin in accordance with LEVICH's equation[15] for the current at a liquid drop where mass transfer is by convective diffusion.

A linear dependence of i_{lim} on C was found over the concentration range 10^{-4} to 10^{-3} *M*. With the H.M.D.E., it was possible to tolerate a greater amount of pentasodium tripolyphosphate without distortion of the wave shape, hence the determination of calcium in the presence of a 30-fold amount of magnesium could be carried out.

Tubular platinum electrode

A detailed study of the anodic voltammetric behaviour of various complexones at the rotated platinum electrode has been made by VYDRA AND STULIK[16], who showed that the electrode process in all cases involves oxidative decarboxylation; the waves occur at very positive potentials and are often masked by oxidation of the solvent.

The voltammograms of EDTA and EGTA showed high sensitivity but both waves were markedly time-dependent in 0.2 *M* perchloric acid, hence the reproducibility was poor. This time-dependence of the wave has been attributed to the cumulative adsorption on the electrode surface of the various electrode reaction products[16].

Mercury-coated tubular platinum electrode

The main problem associated with the use of this electrode was found to be the large residual currents which resulted from the reduction of slight traces of oxygen at the mercury surface. Even after very thorough deaeration with "deoxygenated" nitrogen, a residual current as high as 8 μA was obtained for a solution of 0.1 M perchloric acid flowing at 0.32 ml/min.

Anodic voltammograms were obtained for both EDTA and EGTA, the waves being reasonably well-defined but slightly elongated presumably due to some influence of the large cathodic residual current. Standard deviations of 0.001 V in the apparent half-wave potentials and of 0.08 μA in the limiting currents were found for a solution of 10^{-4} M EDTA in 0.3 M ammonia–0.1 M ammonium nitrate at a flow-rate of 0.32 ml/min. Sensitivities of 56.5 μA/mM were obtained for EDTA. A linear dependence of limiting current on concentration was found over the concentration range $2 \cdot 10^{-5}$–$1 \cdot 10^{-3}$ M. The limiting currents in these experiments were measured from the zero current axis as it was impossible to measure a residual-current base-line.

The calibration curve for the determination of calcium in the presence of magnesium gave a different slope from the corresponding graph in the absence of magnesium. Insufficient tripolyphosphate masking agent may have been present, but further additions completely distorted the wave.

Pyrolytic graphite electrode

The voltammograms of EGTA and EDTA at this electrode in a stationary solution were even more poorly defined than those obtained at the tubular platinum electrode. All measurements were carried out on a single anodic scan at a freshly cleaned electrode surface[17]. Variation of the buffer composition did not improve the situation and on increasing the pH the residual currents were increased. It was concluded that the P.G.E. was of no value as a continuous sensor for the measurement of EDTA or EGTA.

CONCLUSIONS

Of the several electrodes studied, the D.M.E. and H.M.D.E. are clearly the most suitable. The D.M.E. is more convenient than the H.M.D.E. for use in a flowing stream, but in this particular system the voltammogram at the H.M.D.E. was less distorted by the presence of the masking agent than was the corresponding polarogram at the D.M.E. Thus a larger excess of magnesium could be tolerated. The mercury-coated tubular platinum electrode with large surface area naturally offers high sensitivity together with an ideal geometric configuration, but these advantages are invalidated by the large residual currents.

Non-mercury electrodes are not suited to the continuous sensing of EDTA and EGTA, as the oxidation waves are far too poorly defined. The present system was chosen to show the utility of the continuous voltammetric measurement of EDTA and EGTA for the determination of metal ions in a flowing stream. By the introduction of suitable masking agent systems, a wide range of metal ions could be determined.

One of us would like to thank the Government of the Union of Burma for financial support (S.W.) and one of us the Science Research Council for the award of a studentship (M.D.B.). We would also like to thank Imperial Chemical Industries

(Agricultural Division) for the loan of a proportioning pump and Technicon Corporation for the loan of an automatic sampler.

SUMMARY

Several types of voltammetric sensor have been studied for the continuous sensing of complexones in a flowing stream. The determination of the calcium and magnesium has been based on the automation of two manual polarographic procedures. In the first the sum of calcium and magnesium is determined from the decrease in the height of the anodic wave of EDTA. The calcium concentration is then determined in a similar manner with ethyleneglycol-bis(β-aminoethyl ether)-N,N,N′,N′-tetraacetic acid (EGTA).

RÉSUMÉ

Divers types de senseurs voltammétriques ont été examinés pour application en continu à des complexones. Le dosage du calcium et du magnésium est basé sur l'automation de deux procédés polarographiques manuels. On dose calcium + magnésium en mesurant la diminution de hauteur de la vague anodique de l'EDTA. Le calcium est ensuite dosé de la même manière à l'aide de l'EGTA (acide éthylèneglycol bis(β-aminoéthyléther)-N,N,N′,N′-tétraacétique).

ZUSAMMENFASSUNG

Verschiedene Typen voltametrischer Sensoren wurden in Hinblick auf die kontinuierliche Anzeige von Komplexonen im fliessenden System untersucht. Die Bestimmung von Calcium und Magnesium beruhte auf einem automatischen polarographischen Verfahren. Zunächst wird die Summe von Calcium und Magnesium aus der Verringerung der Höhe der anodischen Stufe von AeDTE bestimmt. Dann erfolgt die Bestimmung der Calciumkonzentration auf ähnliche Weise mit Äthylenglykol-bis(β-aminoäthyläther)-N,N,N′,N′-tetraessigsäure.

REFERENCES

1 G. Kessler and M. Wolfman, *Clin. Chem.*, 10 (1964) 686.
2 F. J. Welcher, *Organic Analytical Reagents*, Vol. IV, Van Nostrand, New York, 1948, p. 393; E. B. Sandell, *Colorimetric Methods for Metals*, 3rd Edn., Interscience, New York, 1963.
3 C. N. Reilley and R. W. Schmid, *Anal. Chem.*, 29 (1957) 264.
4 W. J. Blaedel and J. H. Strohl, *Anal. Chem.*, 33 (1961) 1631.
5 W. J. Blaedel and J. H. Strohl, *Anal. Chem.*, 36 (1964) 445.
6 J. V. A. Novak, in *Progress in Polarography*, Vol. 2, Interscience, New York, 1962, p. 569.
7 F. Štráfelda and J. Doležal, *Collection Czech. Chem. Commun.*, 32 (1967) 2707.
8 D. Monnier and A. Rouèche, *Anal. Chim. Acta*, 35 (1966) 231.
9 B. Fleet, Soe Win and T. S. West, *Analyst*, 94 (1969) 269.
10 B. Fleet, Soe Win and T. S. West, *Proc. Intern. Symp. Automation in Analysis*, Technicon, 1967.
11 Corning Glass Works, Corning, New York.
12 T. O. Oesterling and C. L. Olson, *Anal. Chem.*, 39 (1967) 1543.
13 C. G. Enke, L. Ramaley and R. L. Brubaker, *Anal. Chem.*, 35 (1963) 1088.
14 I. M. Kolthoff and Y. Okinaka, *J. Am. Chem. Soc.*, 79 (1957) 3326.
15 B. Levich, *Discussions Faraday Soc.*, 1 (1947) 37.
16 F. Vydra and K. Stulik, *J. Electroanal. Chem.*, 16 (1968) 375.
17 J. F. Alder, B. Fleet and P. O. Kane, *J. Electroanal. Chem.*, in press.

Analytica Chimica Acta
Elsevier Publishing Company, Amsterdam
Printed in The Netherlands

SPECTROPOLARIMETRIC TITRIMETRY

KARL H. PEARSON* AND STANLEY KIRSCHNER
Department of Chemistry, Wayne State University, Detroit, Mich. 48202 (U.S.A.) and The University of São Paulo (Brazil)

(Received August 8th, 1969)

In the present paper, titrations of the weak acids, trifluoroacetic, trichloroacetic, dichloroacetic, and *l*-mandelic acids, with sodium hydroxide, and titrations of the weak bases, piperidine, triethylamine, and *d*-tartrate, with perchloric acid are described. A change in optical rotation (of added asymmetric indicators, where appropriate) as detected by a spectropolarimeter at a suitable wavelength is used as an end-point indicator.

Spectropolarimetric titrations of an optically inactive ligand, ethylenediaminetetraacetate, with zinc(II) nitrate (using *l*-histidine as an asymmetric indicator), of an optically active ligand, *l*-propylenediamine, with nickel(II) perchlorate as well as of the ligand to metal ratio in a complex ion are also described.

Because of the inherent limitations in making optical rotation determinations with a visual polarimeter, this type of instrument is not very suitable for spectropolarimetric titrimetry, although this instrument is quite useful for the comparison of optical rotations of samples with that of the standards. MATTOCK[1], FREEGARDE[2] and JUVET[3,4] have used the visual polarimeter in continuous variation studies of metal complexes with asymmetric ligands for determining ligand–metal ratios in solution.

Recent developments in the construction of photoelectric spectropolarimeters[5] and in the availability of commercial spectropolarimeters[6–8] have resulted in a renewal of interest in spectropolarimetric titrimetry[9]. These instrumental developments render unnecessary the use of visual polarimeters and of the human eye for matching polarimeter fields (with their attendant disadvantages), and such electronic polarimeters and spectropolarimeters can easily be utilized as detectors in titrimetry with optically active substances.

An attachment for a monochromator which is simple, relatively inexpensive and rapid, and which gives results of high precision, has been described in a previous paper[5]. A modification of the instrument described above was used for part of this research. Quartz prisms were substituted for the calcite prisms; therefore modifications of the polarimeter section of the instrument were necessary to cut out the extraordinary ray which is obtained along with the ordinary ray when the quartz prisms are used for the polarizer and analyzer. The quartz prisms allow greater transmission in the ultraviolet than the calcite prisms. With this instrument the optical rotation is a func-

---

* Present address: Department of Chemistry, Texas A and M University, College Station, Texas 77843, U.S.A.

tion of the measured difference in optical absorbance of the solution between the two positions of the analyzer prism, which leads to simple, rapid determinations. For the spectropolarimetric determination of metal ions, both optically active and inactive ligands, and the ratio of ligands to metal in the complex ions, a Perkin-Elmer Model 141 Photoelectric Polarimeter which was modified to take a Bausch and Lomb high-intensity monochromator was used for these titrations. All the titrations were run at room temperature.

SPECTROPOLARIMETRIC TITRIMETRY OF OPTICALLY INACTIVE WEAK ACIDS AND BASES

Indicator selection

For the spectropolarimetric titration of optically inactive weak acids and bases, it is necessary to use an optically active indicator which is itself a significantly weaker acid or base than the inactive acid or base being titrated. It was found experimentally that the dissociation constant of the optically active indicator must be at least two orders of magnitude smaller than that of the optically inactive substance being titrated, in order to obtain reasonably accurate and precise results. The second criterion is that the asymmetric indicator must show a marked change in optical rotation at the end-point of the titration. Therefore, it is useful to determine the optical rotatory dispersion of the asymmetric indicator in both its acidic and basic forms to aid in the selection of the wavelength giving the most appropriate rotation change and transmittance for the titration under study. This points out the distinct advantage of spectropolarimetric titrimetry over titrimetry using a visual polarimeter at one or two wavelengths. With the spectropolarimeter, after the optical rotatory dispersion of the asymmetric indicator has been determined, the wavelength at which the greatest change in rotation occurs with suitable transmittance can easily be selected and used. For the optically inactive weak acids titrated, *l*-mandelic acid proved to be suitable as an asymmetric indicator, and for the optically inactive weak bases, sodium *d*-tartrate was found to be a suitable asymmetric indicator.

Titrimetric procedure for the optically inactive weak acids

A relatively large volume (*ca.* 50 ml) of a relatively dilute solution of an optically inactive weak acid (*ca.* 0.1 *N*) of known or unknown concentration, containing an added optically active indicator whose optical rotation changes markedly on going from an acidic to a basic solution (*e.g.*, *l*-mandelic acid) is titrated with a relatively concentrated solution of base (*ca.* 5 *N*) of unknown or known concentration, respectively, using a Koch microburet which is readable to 0.001 ml. The optical rotation is determined after addition of small increments of titrant both before and after the end-point for these systems. Like conductometric titrations, spectropolarimetric titrations require only a few points before and after the end-point in order to determine the end-point itself by graphical procedures (Fig. 1). With the instrument described above, either the observed optical rotation ($\alpha_{\text{obs.}}$) or ΔA (the absorbance difference observed on the spectropolarimeter when the analyzer prism is placed in each of its two possible positions) can be plotted against volume of titrant; this absorbance difference (ΔA) is directly proportional (for small angles of rotation) to the observed optical rotation.

The volume relationships between the substance being titrated and the titrant are chosen so as to minimize the dilution effects. As with conductometric titrations, conditions near the end-point of the titration are usually relatively unfavorable for the detection of the end-point, so that the points selected for the graphical end-point determinations should not be very near the end-point itself (Fig. 1).

Another factor which affects the titration points in the vicinity of the end-point is the acid dissociation constant(s) of the optically active indicator. It should be emphasized that the acid dissociation constant(s) of the asymmetric indicator must be at least two orders of magnitude smaller than that of the weak acid being titrated. Figure 1 shows the curve for trichloroacetic acid and Table I shows the calculated and observed values for the titrations of three optically inactive weak acids in aqueous solution, with standard (5.341 *N*) sodium hydroxide as the titrant.

Titrimetric procedure for the optically inactive weak bases

The optically inactive weak bases are titrated in a manner analogous to that described above for the optically inactive weak acids. Thus, a relatively dilute (*ca.* 0.1 *N*) solution of the optically inactive base of known or unknown concentration, containing an added optically active indicator (*e.g.*, sodium *d*-tartrate) whose optical rotation changes markedly upon going from a basic to an acidic solution, is titrated with a

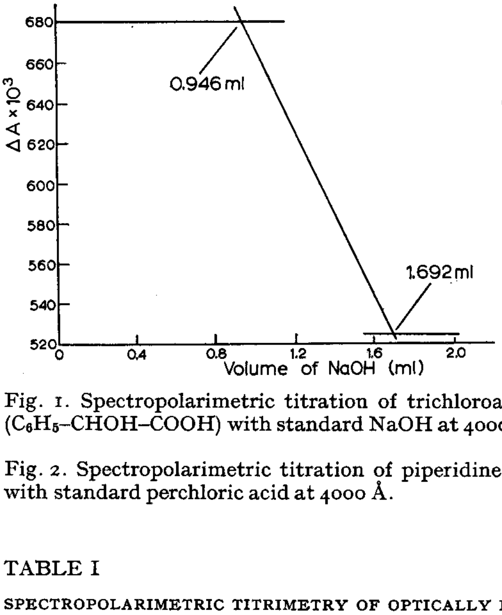

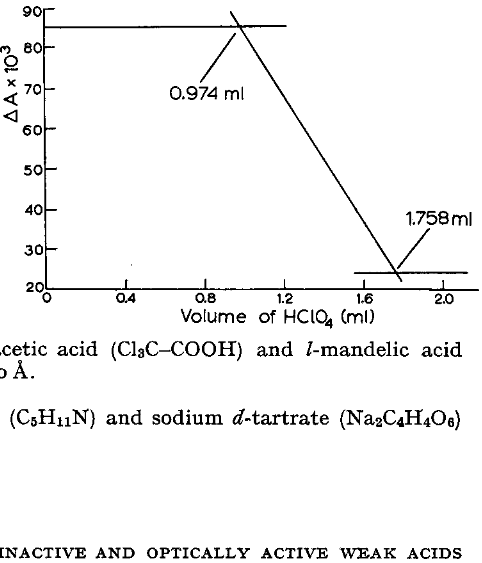

Fig. 1. Spectropolarimetric titration of trichloroacetic acid ($Cl_3C{-}COOH$) and *l*-mandelic acid ($C_6H_5{-}CHOH{-}COOH$) with standard NaOH at 4000 Å.

Fig. 2. Spectropolarimetric titration of piperidine ($C_5H_{11}N$) and sodium *d*-tartrate ($Na_2C_4H_4O_6$) with standard perchloric acid at 4000 Å.

TABLE I

SPECTROPOLARIMETRIC TITRIMETRY OF OPTICALLY INACTIVE AND OPTICALLY ACTIVE WEAK ACIDS

(Wavelength: 4000 Å. $F_3C{-}COOH$: 0.1000 *N*. $Cl_3C{-}COOH$: 0.1009 *N*. $Cl_2HC{-}COOH$: 0.1059 *N*. NaOH: 5.341 *N*. Indicator: *l*-mandelic acid. Volume of acids: 50.00 ml. Solvent: water)

Acid	*Vol. of NaOH calcd. (ml)*	*Vol. found (ml)*	*Vol. of NaOH calcd. to neutralize acid + indicator (ml)*	*Vol. found (ml)*
Trifluoroacetic acid	0.936	0.930	—	—
Trichloroacetic acid	0.945	0.946	1.692	1.692
Dichloroacetic acid	0.991	0.987	1.738	1.730

relatively concentrated solution of strong acid (*ca.* 5 *N*) of unknown or known concentration, respectively. Figure 2 shows the spectropolarimetric titration curve for piperidine with standard perchloric acid, and Table II shows the calculated and observed values for the titrations of two optically inactive weak bases in aqueous solution with standard perchloric acid (5.008 *N*) as the titrant.

TABLE II

SPECTROPOLARIMETRIC TITRIMETRY OF OPTICALLY INACTIVE AND OPTICALLY ACTIVE WEAK BASES

(Wavelength: 4000 Å. Piperidine: 0.09776 *N*. Triethylamine: 0.08754 *N*. $HClO_4$: 5.008 *N*. Indicator: sodium *d*-tartrate. Volume of bases: 50.00 ml. Solvent: water)

Base	*Vol. of $HClO_4$ calcd. (ml)*	*Vol. found (ml)*	*Vol. of $HClO_4$ calcd. to neutralize base + indicator (ml)*	*Vol. found (ml)*
Piperidine	0.976	0.974	1.756	1.758
Triethylamine	0.874	0.871	—	—

SPECTROPOLARIMETRIC TITRIMETRY OF OPTICALLY ACTIVE WEAK ACIDS AND BASES

Indicators

Since only asymmetric weak acids and bases which change rotation significantly with a change in pH were used, the optically active materials being titrated act as self-indicators.

Titrimetric procedure for the optically active weak acids

As in the previous spectropolarimetric titrations, a relatively large volume of relatively dilute optically active weak acids is titrated with a relatively small volume of relatively concentrated sodium hydroxide solution, and the end-point is determined by graphical procedures as described above. The second part of the curve in Fig. 1 shows an example of the titration of an optically active weak acid. The volume of titrant corresponding to the quantity of the optically active weak acid (*l*-mandelic acid) present is calculable from the difference in volumes between the first and second breaks in the spectropolarimetric titration curve. Table III gives the data for the calculated and observed values for systems in which *l*-mandelic acid is titrated with standard sodium hydroxide (5.341 *N*) in aqueous solution.

Titrimetric procedure for optically active weak bases

The principles for this titration are exactly the same as those for the optically active weak acids. The optically active weak base (*d*-tartrate ion) is titrated with standard perchloric acid. The volume of the titrant, corresponding to the quantity of optically active weak base present, is the difference in volumes between the two breaks or end-points as shown in Fig. 2. Table II gives the data for the calculated and observed values in which the *d*-tartrate ion is titrated with standard perchloric acid (5.008 *N*).

Results

Tables I and II and Figs. 1 and 2 give the results of the titrations of optically inactive weak acids and bases, and optically active weak acids and bases. Since the determination of an observed optical rotation at a single wavelength takes between 3 and 5 sec with the spectropolarimeter employed, the entire titration can be performed in less than 30 min. It was found that the best results are obtained when the selected wavelength is near the Cotton region[10], the region of both anomalous rotatory dispersion and of an optically active absorption band (where the specific rotation tends to be at a maximum) but not very near the center of the absorption maximum, since the strong absorption of light causes serious problems in the crossed prism (total extinction) type of spectropolarimeter employed in this work. The results obtained by spectropolarimetric titrimetry deviated an average of less than 0.3% from the results obtained from other standard wet chemical methods.

SPECTROPOLARIMETRIC TITRIMETRY OF METAL IONS AND OPTICALLY INACTIVE LIGANDS

Indicator selection

For the spectropolarimetric titration of metal ions and optically inactive ligands, the metal ion must rapidly form a complex with the optically active indicator which has an optical rotation that is markedly different from that of the asymmetric compound alone at the wavelength chosen. A second criterion is that the metal ion must rapidly form a complex with the optically inactive ligand which is significantly stronger (more stable) than the metal–indicator complex. If the metal ion–inactive ligand complex is not significantly more stable than the metal ion–asymmetric indicator complex, the end-point is indistinct and the titration can lead to erroneous results. Therefore, as in the acid–base titrations, the optical rotation of the system should remain fairly constant until the end-point; thereafter, the larger the change in rotation of the system, the more accurate is the determination of either the metal ion or the optically inactive ligand.

Because of the above, excellent use of the optical rotatory dispersion curves of the asymmetric indicator and the metal ion–asymmetric indicator complex can be made for the selection of the wavelength and transmittance giving the greatest observable rotational change per unit volume of titrant. This again points out the distinct advantage of spectropolarimetric titrimetry over visual polarimetry at one or two wavelengths. For this research, *l*-histidine proved to be an excellent asymmetric indicator.

Titration procedure for metal ions and optically inactive ligands

As in the previous cases involving the spectropolarimetric titrations of acids and bases, a relatively large volume (*ca.* 40 ml) of a relatively dilute optically inactive coordinating agent (in this case, ethylenediaminetetraacetate containing 10 ml of ammonia–ammonium chloride buffer and the asymmetric indicator) of known or unknown concentration may be titrated with a relatively concentrated solution of a metal ion, in this case zinc(II) cation, of unknown or known concentration, respectively, from a Koch microburet which is readable to 0.001 ml. Measurements of the optical rotation of the system at a few points before as well as after the end-point permit a relatively rapid determination of the end-point by graphical methods. The titrations resemble conductometric titrations in that the equilibrium conditions are unfavorable near the end-point; thus the titration points should not be determined too near the end-point. The ammonia buffer is needed to keep the pH of the system nearly constant throughout the whole titration, since the *l*-histidine forms different species in solution depending upon the pH of the solution. Therefore, since the different acid–base species of *l*-histidine have different optical rotations at the wavelength chosen, the pH-dependence of the system is very critical, and highly concentrated buffer solutions with a large buffer capacity are essential for this type of spectropolarimetric titrimetry. Since, in the over-all equilibrium reaction between zinc(II) ion and the disodium dihydrogen ethylenediaminetetraacetate, two equivalents of hydrogen ion are released during complex formation, the need for a buffer with a large buffer capacity is evident. The volume relationships between the optically inactive ligand being titrated and the metal ion titrant are again selected so as to minimize the dilution effects.

Stability constants

The log K value (stability constant) for the zinc–EDTA complex is *ca.* 16.5, whereas $\log K_1 = 6.63$ and $\log K_2 = 5.63$ gives $\log K_{12} = 12.26$ for the over-all stability constant for the zinc–*l*-histidine complex[11]. Thus, the difference in order of magnitude between the stability constants of these complexes allows the spectropolarimetric titration to be carried out, since essentially all of the ethylenediaminetetraacetate is complexed before the *l*-histidine starts to form complexes with the zinc ion.

Results

Table III and Fig. 3 give the results of the spectropolarimetric titrations of the optically inactive ligand, ethylenediaminetetraacetate, with zinc(II) ion. From the data given, it can be seen that the determination of the concentration of the optically inactive ligand or the metal ion, depending upon which one is the known or the unknown solution, can be rapidly and accurately determined by spectropolarimetric titrimetry. The results obtained by spectropolarimetric titrimetry deviated on the average of less than 0.15% from the results obtained by other standard volumetric methods.

TABLE III

SPECTROPOLARIMETRIC TITRATIONS OF DISODIUM DIHYDROGEN ETHYLENEDIAMINETETRAACETATE WITH STANDARD ZINC(II) NITRATE

(Wavelength: 3500 Å. $Zn(NO_3)_2$: 1.492 *M*. Na_2H_2 EDTA·$2H_2O$. Set 1: 0.5555 g. Set 2: 0.3332 g. Indicator: *l*-histidine. Buffer: NH_4Cl–NH_4OH solution. Solvent: water)

Set number	*Volume of $Zn(NO_3)_2$ calculated (ml)*	*Volume of $Zn(NO_3)_2$ found (ml)*
1	1.000	0.999
2	0.600	0.598

SPECTROPOLARIMETRIC TITRIMETRY OF METAL IONS, OPTICALLY ACTIVE LIGANDS AND LIGAND-TO-METAL ION RATIOS

Indicator

For the spectropolarimetric titration of ligand to metal ion ratios, the metal ion must rapidly form stable complexes with the optically active ligand which have optical rotations that are markedly different from that of the asymmetric ligand at the wavelength chosen. If the metal ion–asymmetric ligand complexes do not have markedly different optical rotations from the asymmetric ligand at the given wavelength, the end-point is indistinct and the titration can lead to erroneous results. Therefore, the larger the differences in optical rotation between the complexes formed and between the complexes and the optically active ligand, the more accurate are the determinations of the metal ion–ligand ratios, the metal ions, and the optically active ligand. It should be noted that the optically active complexes formed are self-indicators. Because of the above, excellent use of the optically rotatory dispersion and absorption curves of the asymmetric ligand and different ratios of ligand to metal ions can be made in the selection of the wavelength giving the greatest observable rotational differences. Again the distinctive advantage of spectropolarimetric titrimetry over visual polarimetric titrimetry can readily be seen (Fig. 4).

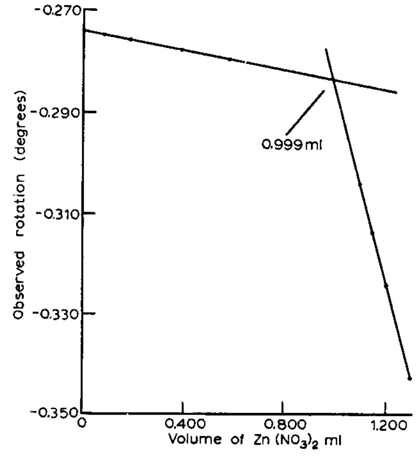

Fig. 3. Spectropolarimetric titration of disodium dihydrogen ethylenediaminetetraacetate with standard zinc(II) nitrate.

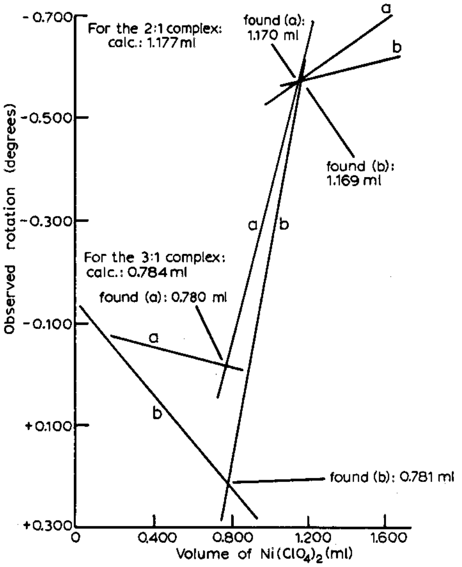

Fig. 4. Spectropolarimetric titration of *l*-propylenediamine with nickel(II) perchlorate at 546 nm (a) and 436 nm (b).

Titration procedure for ligand-to-metal ion ratios

A relatively large volume (*ca.* 40 ml) of a relatively dilute optically active coordinating ligand (in this case, *l*-propylenediamine)[12] of known concentration may be titrated with a relatively concentrated solution of a metal ion, in this case, 1.457 *M* nickel(II), of known concentration from a Koch microburet which is readable to 0.001 ml. Measurements of the optical rotation of the system at a few points before and after the end-points for the formation of the different complexes permit a rapid determination by graphical methods of the ligand–metal ion ratios of the complexes formed. The volume relationships between the optically active ligand being titrated and the metal ion titrant are carefully selected to minimize any dilution errors.

Titration procedure for metal ions and optically active ligands

A relatively large volume (*ca.* 40 ml) of a relatively dilute asymmetric coordinating ligand of known or unknown concentration may be titrated with a relatively concentrated solution of a metal ion of unknown or known concentration, respectively, as in the above procedure. If the ligand-to-metal ion ratios of the stable complexes formed are known, the concentration of either the asymmetric ligand or metal ion can easily be calculated from the titration data.

Results

Table IV and Fig. 4 give the results of the spectropolarimetric titrations. From the data given, it is obvious that the determination of metal ion–asymmetric ligand ratios, as well as the concentrations of the optically active ligand or metal ion (depending upon which is the known or unknown solution) can be rapidly and accurately determined for certain systems by spectropolarimetric titrimetry. The slightly larger deviations observed for these titrations compared to the titrations involving ethylenediaminetetraacetate, are probably due to the greater inherent cumulative errors in the standardization of *l*-propylenediamine compared to the standardization of ethylenediaminetetraacetate, since in both sets of titrations at different wavelengths, the relative error is practically the same. The results obtained by spectropolarimetric titrimetry deviated on the average of about 0.4% from the results calculated from other volumetric methods for the ligand–metal ion ratios of 3:1.

TABLE IV

SPECTROPOLARIMETRIC TITRATIONS OF *l*-PROPYLENEDIAMINE WITH STANDARD NICKEL(II) PERCHLORATE

(*l*-Propylenediamine: 0.2286 *M*. Vol. of *l*-propylenediamine: 15.00 ml. $Ni(ClO_4)_2$: 1.457 *M*. Solvent: 20 ml water)

Wavelength (nm)	*Vol. of $Ni(ClO_4)_2$ calcd. for 3:1 ligand: metal ratio (ml)*	*Vol. of $Ni(ClO_4)_2$ found (ml)*	*Vol. of $Ni(ClO_4)_2$ calcd. for 2:1 ligand: metal ratio (ml)*	*Vol. of $Ni(ClO_4)_2$ found (ml)*
546	0.784	0.780	1.177	1.170
436	0.784	0.781	1.177	1.169

CONCLUSIONS

The application of spectropolarimetry to titrimetric procedures provides a simple, accurate, and rapid means for the determination of unknown components in certain systems. In particular, this method has been successfully applied to the titrimetric determination of strong acids and bases as well as weak acids and bases utilizing an asymmetric indicator and a spectropolarimeter as the end-point detector. This method is also applicable to two-component titrimetry, as long as the second component (*e.g.*, the asymmetric indicator) is significantly weaker (at least one-hundred fold weaker) than the acid or base substance being titrated. Besides the above criterion, the optical rotation of the asymmetric indicator has to change markedly with the pH change of its environment at the wavelength selected for the spectropolarimetric titration.

The application of spectropolarimetric titration procedures to systems forming inorganic coordination compounds provides a very simple, rapid, and accurate method for the determination of the unknown constituents in certain systems. In particular, this method can be successfully applied to the titrimetric determination of optically inactive ligands and metal ions if the complex is formed rapidly and is significantly more stable than the complex formed between the metal ion and the optically active indicator. If the optically active indicator–metal ion complex is significantly weaker (compare the log K values of the complexes) than the optically inactive ligand–metal ion complex, and the indicator–metal ion complex has a significantly different optical rotation from the asymmetric indicator alone at the selected wavelength, very accurate determinations on the system can be made by graphical procedures. It should be emphasized that another criterion for this type of titrimetry is that the pH must remain essentially constant throughout the titration in order to obtain extremely accurate results. If a buffer with high capacity is not added to the solution, the asymmetric indicator may form different species in the system, causing changes in optical rotation which are not directly related to the complex formation, thereby giving erroneous results.

The application of spectropolarimetric titration procedures to many systems, such as the *l*-propylenediamine–nickel(II) system, provides a very simple, rapid and accurate method for the determination of the concentrations of optically active ligands, metal ions, and metal ion–ligand ratio of the stable complexes formed. To systems for which this method is applicable (*i.e.*, those containing suitable optical activity), the determination of the ligand–metal ion ratios is extremely fast compared to the other standard methods used for these determinations.

The authors wish to express their sincere appreciation to the National Science Foundation for a fellowship grant (NSF-GP8450) which contributed significantly to the progress of this investigation.

SUMMARY

Because of the recent development of high-precision photoelectric spectropolarimeters, it is possible to purchase or construct instruments which will permit the rapid determination of optical rotation at various wavelengths. The method of spectropolarimetric titrimetry previously described for strong acids and bases is extended to include optically inactive weak acids and bases as well as optically active weak acids and bases. In the former cases an asymmetric substance which acts as an indicator is added to the material being titrated, whereas in the latter cases, the optically active acids or bases serve as self-indicators. Extensions of this spectropolarimetric titrimetric technique to the determination of metal ions, both optically active and optically inactive ligands, and the ratio of ligands to metal in a complex ion in solution are described.

RÉSUMÉ

Grâce au récent développement des spectropolarimètres photoélectriques de haute précision, il est possible de se procurer des instruments permettant la détermination rapide de rotation optique à diverses longueurs d'onde. La méthode de titrimétrie spectropolarimétrique précédemment décrite pour les acides et bases forts est étendue aux bases et acides faibles optiquement actifs de même qu'aux non-optiquement actifs. Dans ces derniers cas une substance asymétrique agissant comme indicateur est ajoutée au matériel à titrer. On décrit des possibilités de titrimétrie spectropolarimétrique pour le dosage d'ions métalliques, de ligands et pour la détermination de proportions ligands–métal dans un complexe en solution.

ZUSAMMENFASSUNG

Aufgrund der jüngsten Entwicklung sehr genauer photoelektrischer Spektralpolarimeter ist es möglich, solche Instrumente zu kaufen, oder zu konstruieren, die eine schnelle Bestimmung der optischen Rotation bei verschiedenen Wellenlängen erlauben. Die Methode der spektralpolarimetrischen Massanalyse, die früher für starke Säuren und Basen beschrieben wurde, wird auf optisch inaktive weiche Säuren und Basen ebenso wie auf solche, die optisch aktive sind ausgedehnt. Wie in früheren Fällen wird eine asymetrische Substanz als Indikator dem zu titrierenden Material zugegeben. Dagegen dienen im letzeren Falle die optisch aktiven Säuren oder Basen als Eigenindikatoren. Die Ausdehnung dieser spektralpolarimetrischen, massanalytischen Technik auf die Bestimmung von Metallionen sowohl mit optisch aktiven als auch optisch inaktiven Liganden und die Bestimmung der Ligandenzahl in Lösung wird beschrieben.

REFERENCES

1 G. J. Mattock, *J. Chem. Soc.*, (1954) 989.
2 M. Freegarde, *Chem. & Ind. (London)*, (1957) 984.
3 R. S. Juvet and R. L. Pescok, *J. Am. Chem. Soc.*, 78 (1956) 3967.
4 R. S. Juvet, *J. Am. Chem. Soc.*, 81 (1959) 1796.
5 M. J. Albinak, D. C. Bhatnagar, S. Kirschner and A. Sonnessa, in S. Kirschner, *Advances in the Chemistry of the Coordination Compounds*, Macmillan, New York, 1961, pp. 154 ff.
6 C. Djerassi, *Optical Rotatory Dispersion*, McGraw-Hill, New York, 1960.
7 P. Crabbe, *Optical Rotatory Dispersion and Circular Dichroism in Organic Chemistry*, Holden-Day, San Francisco, 1965.
8 S. Kirschner, *Coord. Chem. Rev.*, 2 (1967) 461.
9 S. Kirschner and D. C. Bhatnagar, *Anal. Chem.*, 35 (1963) 1069.
10 W. Heller and D. D. Fitts, Polarimetry, in A. Weissberger, *Physical Methods of Organic Chemistry*, 3rd Edn., Vol. 1, Part 3, Ch. 33, Interscience, New York, 1960.
11 Chemical Society, London, *Stability Constants of Metal-Ion Complexes*, 2nd Edn., 1964.
12 F. P. Dwyer, F. L. Garvan and A. Shulman, *J. Am. Chem. Soc.*, 81 (1959) 290.

Analytica Chimica Acta
Elsevier Publishing Company, Amsterdam
Printed in The Netherlands

SPECTROPHOTOMETRIC DETERMINATION OF TRACE AMOUNTS OF TITANIUM(IV), ZIRCONIUM(IV) AND THORIUM(IV) WITH MOLYBDOPHOSPHORIC ACID SOLUTION

KATSUO MURATA, YU YOKOYAMA AND SHIGERO IKEDA
Department of Chemistry, Faculty of Science, Osaka University, Toyonaka, Osaka (Japan)

(Received July 24th, 1969)

The yellow color of molybdophosphoric acid solution is enhanced by titanium(IV), zirconium(IV), and thorium(IV) ions. By using this experimental fact, VEITSMAN determined titanium(IV)[1] and zirconium(IV)[2] in the form of a phosphomolybdenotitanium(IV) and of a phosphomolybdenozirconium(IV) complex, respectively. To explain the enhancement of the intensity caused by titanium(IV)[3] and zirconium(IV)[4], BABKO AND SHKARAVSKII proposed the formation of a molybdotitanophosphate and molybdozirconophosphate complex having the composition Ti(IV) or Zr(IV):P:Mo=1:1:12 in the solution; they named these complexes the ternary heteropoly complexes. Recently, BABKO[5] has reviewed ternary complexes including ternary heteropoly complexes. However, the behavior of heteropoly complexes remains unclarified in many aspects.

As a part of extensive investigations of heteropoly complexes, the present authors have examined the determination of trace amounts of titanium(IV), zirconium(IV), and thorium(IV), by the formation of ternary heteropoly complexes, and have studied the reactions in detail. The proposed methods, which are based on the formation of ternary heteropoly complex followed by the elimination of binary heteropoly complex by extraction, are simpler and more convenient than VEITSMAN's methods.

EXPERIMENTAL

Reagents and apparatus

Molybdophosphoric acid solution. A $5 \cdot 10^{-3}$ *M* molybdophosphoric acid solution of pH 1 was prepared by dissolving 7.260 g of sodium molybdate and 0.3403 g of potassium dihydrogen phosphate of analytical-reagent grade, in dilute perchloric acid solution and diluting to 500 ml.

Stock solutions of titanium(IV), zirconium(IV) and thorium(IV). These were prepared from titanium metal, zirconium oxychloride, and thorium nitrate, respectively, and stored as 2 *M* perchloric acid solutions to avoid hydrolysis. Each solution of titanium(IV), zirconium(IV) or thorium(IV) was standardized gravimetrically, by ignition of the precipitate of titanium cupferronate, zirconium cupferronate or thorium oxalate, respectively.

n-Butyl acetate (analytical reagent grade) was used without purification.

Absorbance and absorbance spectra were measured with a Shimazu QV-50 spectrophotometer and a Hitachi EPS-2 automatic recording spectrophotometer. The pH values of solutions were measured with a Horiba F-5 pH meter.

Procedure

A 5-ml aliquot of $4 \cdot 10^{-4}$ *M* molybdophosphoric acid solution of pH 1 containing trace metal ion was pipetted into a stoppered centrifuge tube and an equal volume of *n*-butyl acetate was added. The vessel was shaken for 5 min at room temperature with an electric shaker, and centrifuged to separate the phases. The absorbance of the aqueous phase was measured at 350 nm against a reagent blank solution treated in the same way.

RESULTS AND DISCUSSION

Formation of ternary heteropoly complexes

The formation of binary and ternary heteropoly complexes is affected by the acidity of solutions as shown in Fig. 1. Ternary heteropoly complexes form over wider pH regions and show higher optical density than the binary heteropoly complex, molybdophosphoric acid. In order to form the ternary heteropoly complex, there are three cases in the order of reagent addition because it is composed of three main components: molybdate, phosphate, and metal ion. It was found that the time required for complete formation was different according to the order of addition. For instance, when phosphate solution was finally added to mixed solutions of metal ion and molybdate, the longest time (50 min) was needed; when molybdate solution was added last, 30 min were required; and when the metal ion solution was added last, 20 min were necessary at room temperature. The fairly long time required for complete formation suggests that in these cases the complex formation is more complicated

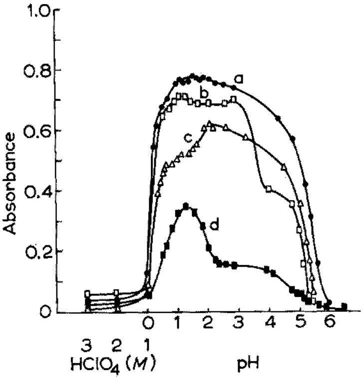

Fig. 1. Influence of acidity on the formation of heteropoly complexes. (a) Molybdotitanophosphate, (b) molybdozirconophosphate, (c) molybdothorophosphate, (d) molybdophosphoric acid. [P] = [Me] = $1 \cdot 10^{-3}$ *M*; [Mo] = $1.2 \cdot 10^{-2}$ *M*; λ = 420 nm; l = 1 cm.

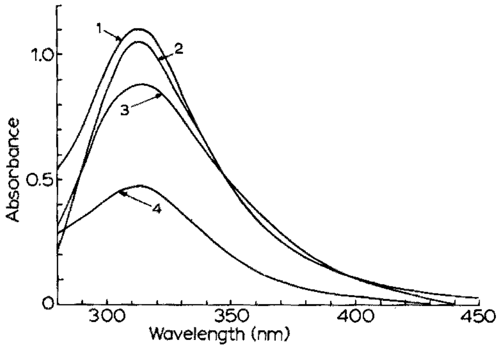

Fig. 2. Near-ultraviolet absorption spectra of heteropoly complexes. (1) Molybdotitanophosphate, (2) molybdozirconophosphate, (3) molybdothorophosphate, (4) molybdophosphoric acid. [P] = [Me] = $6 \cdot 10^{-4}$ *M*; [Mo] = $8 \cdot 10^{-3}$ *M*; pH = 1; l = 0.1 cm.

than a simple bimolecular reaction. The necessity of the much longer time when phosphate is added last, can probably be attributed to an extensive change in structure; phosphate destroys the structure of the previously formed metal molybdates to produce yellow ternary heteropoly complexes. The formation constants of ternary heteropoly complexes are considered to be greater than those of metal molybdates, because it was observed that precipitates of titanium, zirconium, and thorium molybdate gradually change into yellow ternary heteropoly complexes in the presence of phosphate in appropriate acidic solutions. In the practical procedure for the determination, the metal ion to be determined was always added last because this gave the minimal time for completion of the reaction, *i.e.* a previously prepared molybdophosphoric acid solution was added to the solution containing metal ion.

Near-ultraviolet spectra of the ternary and binary heteropoly complexes are shown in Fig. 2. They are very similar except for intensity. Therefore, ternary heteropoly complexes appear not to possess different structures, affecting the spectra of near-ultraviolet region, from that of binary heteropoly acid. Considering these spectra and the above-mentioned formation aspects, it seems probable that the structures of ternary heteropoly complexes are quite similar to that of binary heteropoly complex, molybdophosphoric acid.

Composition of ternary heteropoly complexes

The ratio of phosphorus to metal was determined to be 1:1 by the continuous variation method as shown in Fig. 3. The total concentration was held constant to $1.4 \cdot 10^{-2}$ *M*, and the pH of solutions was 1. Similarly, the ratio of phosphorus to molybdenum, or metal to molybdenum was determined to be 1:12 as shown in Fig. 4. Consequently, the three kinds of ternary heteropoly complexes all have the composition of Me:P:Mo = 1:1:12 in aqueous solutions of pH 1. With regard to the titanium and zirconium complexes, the results obtained were the same as those reported by BABKO AND SHKARAVSKII[3,4].

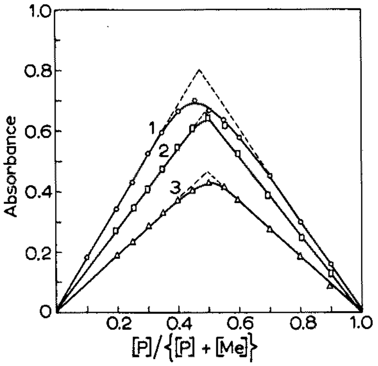

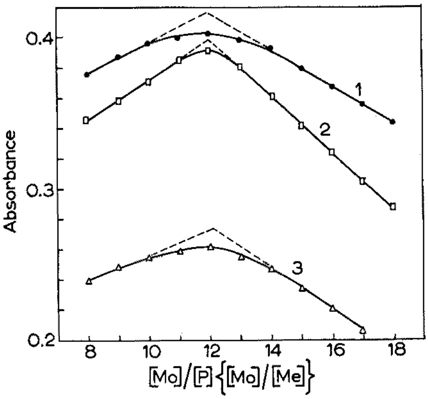

Fig. 3. Determination of P:Me ratio by continuous variation method. (1) Molybdotitanophosphate, (2) molybdozirconophosphate, (3) molybdothorophosphate complex. ([P] + [Me]) = $2 \cdot 10^{-3}$ *M* const.; [Mo] = $1.2 \cdot 10^{-2}$ *M*; pH = 1; λ = 420 nm.

Fig. 4. Determination of Mo:P (or Mo:Me) by continuous variation method. (1) Molybdotitanophosphate, (2) molybdozirconophosphate, (3) molybdothorophosphate. ([Me] + [P] + [Mo]) = $8 \cdot 10^{-3}$ *M* const. ; [P] = [Me]; pH = 1; λ = 420 nm.

Separation of binary and ternary heteropoly complex

When the proposed method is applied to samples containing trace amounts of the pertinent metal, the coexistence of a large excess of the binary heteropoly complex interferes with spectrophotometric measurements of the ternary complexes. *n*-Butyl acetate is known to be a selective solvent for molybdophosphoric acid[6], and was therefore used to separate the binary from the ternary heteropoly complex. Molybdophosphoric acid was selectively extracted with *n*-butyl acetate from molybdophosphoric acid solutions containing zurconium (1–10 p.p.m.) as shown in Fig. 5. In the organic phase, the absorbance at 350 nm decrease as the concentration of zirconium(IV) increases, while in the aqueous phase, the absorbance at 330 nm increases in proportion to the zirconium concentration. This indicates that molybdophosphoric acid is extracted into the organic phase, while the zirconium(IV) ternary heteropoly complex produced remains in the aqueous phase; as the concentration of zirconium(IV) increases, that of unreacted molybdophosphoric acid decreases.

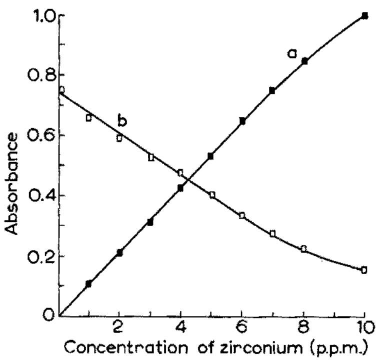

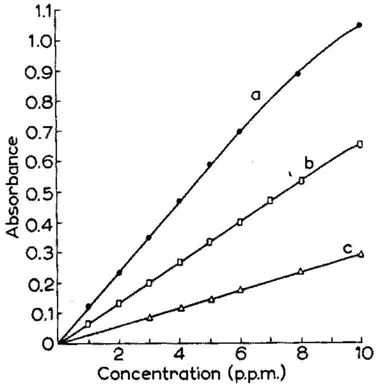

Fig. 5. Difference in absorbance of the aqueous and organic phases of molybdozirconophosphate solution after extraction with *n*-butyl acetate. (a) Aqueous phase, (b) organic phase. $[P] = 2 \cdot 10^{-4}$ *M*; $[Mo] = 2.4 \cdot 10^{-3}$ *M*; pH = 1; $\lambda = 330$ nm.

Fig. 6. Calibration curves for metal ions. (a) Titanium, (b) zirconium, (c) thorium. $[P] = 4 \cdot 10^{-4}$ *M*; $[Mo] = 2.4 \cdot 10^{-3}$ *M*; pH = 1; $\lambda = 350$ nm.

Accordingly, the absorbance of the aqueous phase after elimination of unreacted molybdophosphoric acid can be used for the determination of the trace metal. Calibration curves for titanium(IV), zirconium(IV), and thorium(IV) are given in Fig. 6. Beer's law is obeyed for metal ion concentrations of 1–7 p.p.m.

Chemical equilibrium of ternary heteropoly complexes

The formation of the ternary heteropoly complex depends strongly on the acidity of the solution (Fig. 1). The following discussion is limited to the low pH values; at higher pH, the system becomes very complicated because of metal hydrolysis reactions.

For molybdophosphoric acid an equilibrium of the following type:

$$[PO_4(MoO_3)_{12}]^{3-}+9H^+ \rightleftarrows PO_4H_3+6HMo_2O_6^+$$

was proposed by SOUCHAY[7]. BABKO AND SHKARAVSKII[3] who investigated the molybdotitanophosphate complex represented its dissociation as:

$$\mathrm{PTiMo}_{m\cdot n} \rightleftarrows \mathrm{P}_{\mathrm{free}}+\mathrm{Ti}_{\mathrm{free}}+n(\mathrm{Mo})_m$$

When a hydrogen ion term is supplied to the above equilibrium the following equilibrium is achieved for ternary heteropoly complexes:

$$(\mathrm{MePMo}_{b\cdot m})+a\ \mathrm{H}^+ \rightleftarrows \mathrm{Me}_{\mathrm{free}}+\mathrm{P}_{\mathrm{free}}+b\ (\mathrm{Mo})_m \tag{A}$$

where $\mathrm{MePMo}_{b\cdot m}$ is the ternary heteropoly complex, $\mathrm{Me}_{\mathrm{free}}$ the metal ion, $\mathrm{P}_{\mathrm{free}}$ the free phosphate, $(\mathrm{Mo})_m$ the molybdate polymerised "m" times. The relationship ($b\cdot m=12$) is considered to be established from the composition previously investigated.

The dissociation constant, K_{d}, is then given by the following expression:

$$K_{\mathrm{d}} = \frac{[\mathrm{Me}_{\mathrm{free}}][\mathrm{P}_{\mathrm{free}}][(\mathrm{Mo})_m]^b}{[(\mathrm{MePMo}_{b\cdot m})][\mathrm{H}^+]^a} \tag{1}$$

Measurable values of A_0 and A_{x} can be introduced; A_0 is absorbance obtained by forcing the reaction to completion with a large excess of molybdate, and A_{x} is the absorbance at the given molybdate concentration. Thus each term in eqn. (1) can be represented as follows:

$$[\mathrm{Me}_{\mathrm{free}}] = \frac{A_0-A_{\mathrm{x}}}{A_0}[\mathrm{Me}_{\mathrm{total}}]\ ;$$

$$[\mathrm{P}_{\mathrm{free}}] = \frac{A_0-A_{\mathrm{x}}}{A_0}[\mathrm{P}_{\mathrm{total}}]\ ;$$

$$[(\mathrm{Mo})_m] = \frac{1}{m}([\mathrm{Mo}_{\mathrm{total}}]-[\mathrm{Mo}_{\mathrm{comb}}])$$

$$= \frac{1}{m}\left([\mathrm{Mo}_{\mathrm{total}}]-12\frac{A_{\mathrm{x}}}{A_0}[\mathrm{P}_{\mathrm{total}}]\right)\ ;$$

$$[(\mathrm{MePMo}_{b\cdot m})] = \frac{A_{\mathrm{x}}}{A_0}[\mathrm{P}_{\mathrm{total}}]\ .$$

These are substituted into eqn. (1), which is arranged as follows:

$$K_{\mathrm{d}} = \frac{\dfrac{(A_0-A_{\mathrm{x}})^2}{A_0\cdot A_{\mathrm{x}}}[\mathrm{Me}_{\mathrm{total}}]\left(\dfrac{1}{m}\right)^b([\mathrm{Mo}_{\mathrm{total}}]-12\,\dfrac{A_{\mathrm{x}}}{A_0}[\mathrm{P}_{\mathrm{total}}])^b}{[\mathrm{H}^+]^a}$$

This equation becomes logarithmically:

$$\log\frac{A_0\cdot A_{\mathrm{x}}}{(A_0-A_{\mathrm{x}})^2[\mathrm{Me}_{\mathrm{total}}]} = b\log\frac{[\mathrm{Mo}_{\mathrm{total}}]-12\,\dfrac{A_{\mathrm{x}}}{A_0}[\mathrm{P}_{\mathrm{total}}]}{m} - \log K_{\mathrm{d}}-a\log[\mathrm{H}^+]$$

At a constant concentration of hydrogen ion (1 M), and on introduction of the formation constant, K_{f}, for K_{d}, this equation can be reduced to:

$$\log\frac{A_0\cdot A_{\mathrm{x}}}{(A_0-A_{\mathrm{x}})^2[\mathrm{Me}_{\mathrm{total}}]} = b\log\frac{[\mathrm{Mo}_{\mathrm{total}}]-12\,\dfrac{A_{\mathrm{x}}}{A_0}[\mathrm{P}_{\mathrm{total}}]}{m} + \log K_{\mathrm{f}} \tag{2}$$

When the values of the term on the left-hand side are plotted against those of the logarithmic term on the right-hand side, the values of b and $\log K_t$ can be obtained from the straight line drawn.

Spectrophotometric measurements of samples in 1 M perchloric acid solution were therefore carried out as a function of the concentration of molybdate, for constant concentrations of phosphate and metal ion. The results obtained (for $[\mathrm{Me}_{\mathrm{total}}] = [\mathrm{P}_{\mathrm{total}}] = 1 \cdot 10^{-3}\ M$) are shown in Fig. 7. The formation constants can be compared qualitatively by observing the shapes of the curves. If the formation constant of the ternary heteropoly complex were low, a gentle curve would be obtained over the higher concentrations of molybdate. Since the curve for the molybdozirconophosphate heteropoly complex is sharp, and has a prolonged horizontal section, this complex should have a greater formation constant.

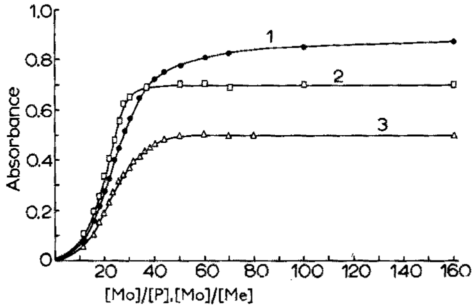

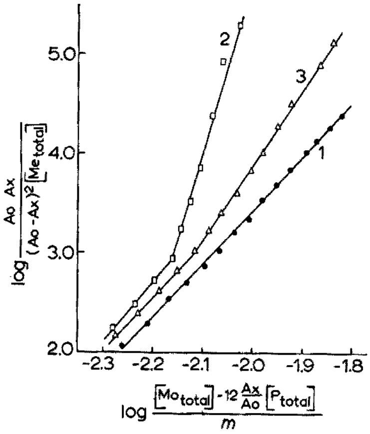

Fig. 7. Influence of molybdate concentration on the formation of ternary heteropoly complexes. (1) Molybdotitanophosphate, (2) molybdozirconophosphate, (3) molybdothorophosphate. $[\mathrm{P}] = [\mathrm{Me}] = 1 \cdot 10^{-3}\ M$; $[\mathrm{H}^+] = 1\ M$; $\lambda = 420$ nm.

Fig. 8. Determination of formation constant for ternary heteropoly complexes. (1) Molybdotitanophosphate, (2) molybdozirconophosphate, (3) molybdothorophosphate.

In accordance with eqn. (2), data obtained from these experiments were plotted in Fig. 8. In describing Fig. 8, the value m has to be given. Fortunately, evidence that the molybdenum species existing in 1 M acidic solution is a dimer has been given by many investigators[7–10], hence the value $m = 2$ was used. In Fig. 8 three lines are shown, but two of those have a break point. The values given in Table I were evaluated from

TABLE I

STOICHIOMETRIC COEFFICIENTS AND FORMATION CONSTANTS OBTAINED

Ternary heteropoly complex	*b*	*log K_t*
Molybdotitanophosphate	5.55	14.51
Molybdozirconophosphate	5.80	15.44
Molybdothorophosphate	5.60	14.92

this figure. Although two values of the slope were obtained for the molybdozirconophosphate and molybdothorophosphate complexes, the value nearer to six was chosen because of the stoichiometric evidence; if another value were adopted, an impossibly large value of the formation constant would be obtained which would not satisfy the stoichiometry ($b \cdot m = 12$). Various values of m other than 2 were applied to eqn. (2) by trial and error, but $m = 2$ was found to be most appropriate.

One of the reasons for the break points in the lines shown in Fig. 8 may be an inadequacy in the terms on the right side of equilibrium reaction (A), but no precise cause can be given. Nevertheless, it is clear that the formation constants of the ternary heteropoly complexes increase in the order of molybdotitanophosphate, molybdothorophosphate, and molybdozirconophosphate. In contrast, the order of the molar absorptivity is molybdothorophosphate, molybdozirconophosphate, and molybdotitanophosphate.

SUMMARY

Trace amounts of titanium(IV), zirconium(IV) and thorium(IV) ions were determined spectrophotometrically with molybdophosphoric acid solution. The method is based on the formation of the ternary heteropoly complex by reaction of the metal ion with molybdophosphoric acid, and the elimination of unreacted molybdophosphoric acid by extraction with *n*-butyl acetate. Beer's law was obeyed over the range 1–7 p.p.m. of metal ion. These ternary heteropoly complexes have the composition of Me:P:Mo = 1:1:12. The formation constants increase in the order, molybdotitanophosphate, molybdothorophosphate, and molybdozirconophosphate.

RÉSUMÉ

Des traces de titane(IV), de zirconium(IV) et de thorium(IV) ont pu être dosées spectrophotométriquement à l'aide d'acide molybdophosphorique. Cette méthode est basée sur la formation d'hétéropolycomplexe ternaire par réaction du métal avec l'acide molybdophosphorique et extraction de l'excès de réactif dans l'acétate de *n*-butyle. La loi de Beer s'applique aux concentrations de 1 à 7 p.p.m. du métal. Ces hétéropolycomplexes ternaires ont la composition suivante: Me:P:Mo = 1:1:12. Les constantes de formation croissent dans l'ordre: molybdotitanophosphate, molybdothorophosphate et molybdozirconophosphate.

ZUSAMMENFASSUNG

Es wurden Spuren von Titan(IV)-, Zirconium(IV)- und Thorium(IV)-Ionen spektralphotometrisch mit Molybdophosphorsäurelösung bestimmt. Die Methode berucht auf der Bildung eines ternären Heteropolykomplexes durch Reaktion der Metall-Ionen mit der Molybdophosphorsäure und auf der Eliminierung von nicht reagierter Molybdophosphorsäure durch Extraktion mit *n*-Butylacetat. Das Beersche Gesetz wird im Bereich von 1–7 p.p.m. Metallionen befolgt. Die ternären Heteropolykomplexe haben die Zusammensetzung Me:P:Mo = 1:1:12. Die Bildungskonstanten steigen in der Reihenfolge Molybdotitanophosphat, Molybdothorophosphat, Molybdozirconophosphat.

REFERENCES

1 R. M. Veitsman, *Zavodsk. Lab.*, 25 (1959) 408.
2 R. M. Veitsman, *Zavodsk. Lab.*, 26 (1960) 927.
3 A. K. Babko and Yu. F. Shkaravskii, *Zh. Neorgan. Khim.*, 6 (1961) 2091.
4 Yu. F. Shkaravskii, *Zh. Neorgan. Khim.*, 11 (1966) 120.
5 A. K. Babko, *Talanta*, 15 (1968) 721.
6 C. Wadelin and M. G. Mellon, *Anal. Chem.*, 25 (1953) 1668.
7 P. Souchay, *Pure Appl. Chem.*, 6 (1963) 61.
8 I. L. Jenkins and A. G. Wain, *J. Appl. Chem.*, 13 (1963) 561.
9 Y. Sasaki and L. G. Sillen, *Acta Chem. Scand.*, 18 (1964) 1014.
10 S. R. Crouch and H. V. Malmstadt, *Anal. Chem.*, 39 (1967) 1084.

Analytica Chimica Acta
Elsevier Publishing Company, Amsterdam
Printed in The Netherlands

EXTRACTION AND SPECTROPHOTOMETRIC DETERMINATION OF TIN, ARSENIC AND GERMANIUM AS THEIR IODIDES

KATU TANAKA AND NOBUYUKI TAKAGI
Industrial Research Institute of Kanagawa Prefecture, Yokohama (Japan)

(Received July 12th, 1969)

Several studies have been made on the extraction of tin(IV)[1,2], arsenic(III)[3,4] and germanium(IV)[2] as their iodides by benzene or carbon tetrachloride. The systems have been further examined with regard to selectivity, and have been utilized in analytical practice for the separation of tin from a number of metals[5,6], the determination of tin[7,8] and arsenic[9,10] in steels, tin in organic matters[11], and tin[12,13] and arsenic[9,14,15] in other samples. These methods depend on the facts that tin(IV) and arsenic(III) can be extracted selectively and quantitatively from a sulfuric or perchloric acid solution containing alkali iodide, and arsenic(III) from a hydrochloric acid solution containing alkali iodide.

In the course of studies on the solvent extraction of tin(IV)[2,8], arsenic(III)[4,9] and germanium(IV)[2] as their iodides, it was found that each iodide, extracted into carbon tetrachloride, *n*-hexane or cyclohexane, has a characteristic absorbance spectrum in the ultraviolet region between 260 and 400 nm. The present work was aimed at establishing a spectrophotometric procedure for the determination of tin, arsenic and germanium by measuring the ultraviolet absorbance of these iodides. Studies made with cyclohexane as an extractant, led to the conclusion that this extraction-spectrophotometric method was useful for the determination of these elements. In view of the similarities of these iodides in their extraction and absorbance behaviour, the methods for the three elements are discussed together. The utility of the methods is confirmed by examples, involving the determination of tin in juice, tin and arsenic in steel (simultaneously), and germanium in its concentrates.

EXPERIMENTAL

Reagents and apparatus

Sodium iodide solution (5.0 M) was prepared freshly each day.

Cyclohexane, analytical grade, was used without further purification.

A stock solution of tin(IV) (1.00 mg/ml) was prepared by dissolving tin metal in concentrated sulfuric acid, evaporating the acid almost to dryness, and dissolving the residue in *ca.* 0.07 *M* ammonium oxalate solution.

Stock solutions of arsenic(III) and germanium(IV) (1.00 mg/ml each) were prepared by dissolving arsenic trioxide and germanium dioxide in dilute sodium hydroxide solutions, respectively. All the stock solutions were diluted to the required concentrations with distilled water before use.

A Hitachi-Perkin-Elmer 139 Spectrophotometer with 1-cm quartz cells was used for the spectrophotometric measurements.

General method

An aqueous solution (10 ml) containing the required amounts of test solution, acid and sodium iodide was placed into a separatory funnel and shaken with exactly 10 ml of cyclohexane. After the phases had separated completely with no water droplets in the organic phase, the aqueous phase was discarded and the organic phase was transferred dropwise to a measuring cell. The absorbance of the extract was then measured against cyclohexane as a reference.

RESULTS AND DISCUSSION

Spectral characteristics

Figure 1 shows the absorbance spectra of the three iodides extracted into cyclohexane from sulfuric acid solution containing sodium iodide. Each iodide has two absorbance peaks between 260 and 400 nm; tin(IV) iodide has its absorbance peaks at 364 and 285 nm, arsenic(III) iodide at 282 and 380 nm, and germanium(IV) iodide at 360 and 283 nm, respectively. A small absorption at 520 nm in every case is clearly due to free iodine co-extracted. Tests showed that the free iodine had far smaller absorbance over the range 270–400 nm than that at 520 nm, and the blank absorbances (curve D) were always less than 0.02 at 282 nm and less than 0.01 at 360 nm, when a freshly prepared sodium iodide solution was used. The cyclohexane used showed an absorbance of 0.03 at 282 nm against distilled water, but the value was essentially constant after the solvent had been mixed with any aqueous solution used here. Spectrophotometric measurements of the extracts can therefore be made against cyclohexane, at the respective absorbance maximum: for tin at 364 nm, for arsenic at 282 nm, and for germanium at 360 nm. All the extracts underwent serious decreases in absorbance when the extracts came in contact with any moisture, including atmospheric humidity. The extracts, therefore, could not be filtered into the cell in the usual way, and the measurements had to be made as soon as the extracts were transferred to a cell. For rapid separation of the phases without turbidity in the organic phase, it was advantageous to keep the separatory funnel horizontal, and to make the volume of the aqueous phase larger than that of the organic phase.

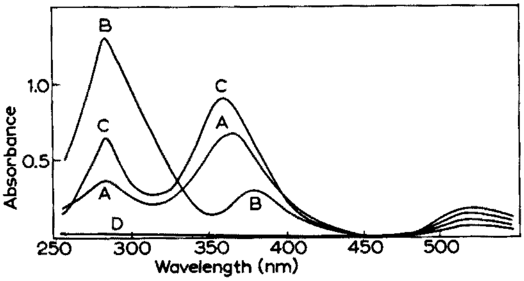

Fig. 1. Absorbance spectra for iodides of tin(IV), arsenic(III) and germanium(IV) in cyclohexane. (A) tin(IV) iodide; (B) arsenic(III) iodide; (C) germanium(IV) iodide; (D) blank in A or B. Aqueous phase: (A, B) 4 *M* H_2SO_4–1.0 *M* NaI; (C) 6 *M* H_2SO_4–0.50 *M* NaI. Element added: 100 μg.

Acidity and iodide concentration

The optimal composition of the aqueous phase for the extraction and determination of each element was studied. Figure 2 shows that, when the extraction was carried out from a sulfuric acid solution containing iodide, all the curves reached a plateau region as the concentration of sulfuric acid was increased. For extractions from hydrochloric acid solutions containing iodide, only arsenic(III) showed useful absorbance at 282 nm (Fig. 3). The species for arsenic(III) extracted in the latter case was shown, from the absorbance spectra, to be the same as that extracted from sulfuric acid solutions containing iodide. Moreover, it can be seen from Figs. 2 and 3 that the absorbance for arenic(III) was similar in the two types of extract; the real extractability of arsenic(III) exceeded 99% under appropriate conditions as described below. From these facts, it could be suggested that almost all arsenic(III) was extracted as the iodide from solutions of, for example, 5 *M* hydrochloric acid–1.0 *M* iodide or 6 *M* hydrochloric acid–0.5 *M* iodide. The extraction behaviour shown in Fig. 3 is useful for the determination of arsenic in the presence of tin and germanium. No tin(IV) species is significantly extracted under these experimental conditions[2], whereas germanium may be extracted into cyclohexane to a considerable extent as its chloride with a small amount of the iodide.

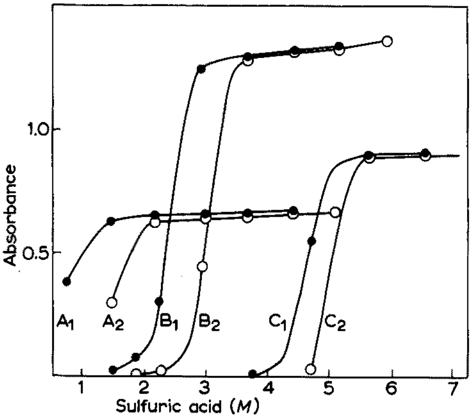

Fig. 2. Absorbance *vs.* the concentrations of sulfuric acid and sodium iodide. (A_1 and A_2) For tin(IV) at 364 nm; (B_1 and B_2) for arsenic(III) at 282 nm; (C_1 and C_2) for germanium(IV) at 360 nm. Sodium iodide: (A_1), (B_1) and (C_1), 1.0 *M*; (A_2), (B_2) and (C_2), 0.50 *M*. Element added: 100 μg.

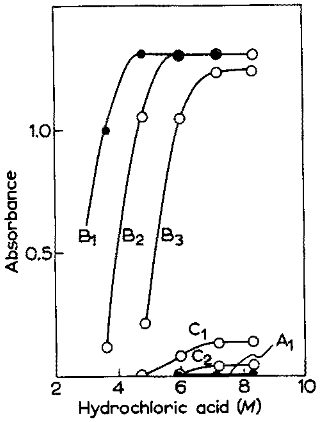

Fig. 3. Absorbance *vs.* the concentrations of hydrochloric acid and sodium iodide. (A_1) For tin(IV) at 364 nm; (B_1–B_3) for arsenic(III) at 282 nm; (C_1 and C_2) for germanium(IV) at 360 nm. Sodium iodide: (A_1), (B_1) and (C_1), 1.0 *M*; (B_2) and (C_2), 0.50 *M*; (B_3), 0.20 *M*. Element added: 100 μg.

Perchloric acid solutions containing iodide were found to give extractive and absorptive patterns for the three elements similar to those shown in Fig. 2. With iodide of 1.0 *M*, the absorbances for tin, arsenic and germanium became nearly constant when the concentrations of the perchloric acid were greater than 3, 4, and 6 *M* respectively.

Calibration graphs

Tin(IV) or arsenic(III) was extracted from the same solution containing 4 *M* sulfuric acid and 1.0 *M* sodium iodide, and germanium(IV) from a solution containing 6 *M* sulfuric acid and 0.5 *M* sodium iodide. Shaking was for 1 min in each case. The calibration graphs for the three elements showed good straight lines that passed almost through the origin (Table I); the molar absorptivities for tin at 364 nm, arsenic at 282 nm, and germanium at 360 nm were found to be 8700, 9700 and 6600, respectively. The technique for the simultaneous spectrophotometry of two components, originated by Knudson *et al.*[16], was used for the determination of tin and arsenic by means of the four absorptivities obtained above. The advantages will be shown later for steel analysis (pp. 362, 363 and 364).

TABLE I

CALIBRATION GRAPHS FOR TIN, ARSENIC AND GERMANIUM

Element present (μg)	*Absorbance*				
	Tin		*Arsenic*		*Germanium*
	A_{364}	A_{282}	A_{282}	A_{364}	A_{360}
0	0.003	0.014	0.014	0.003	0.004
20	0.151	0.082	0.262	0.040	0.190
40	0.291	0.160	0.541	0.077	0.371
60	0.440	0.232	0.790	0.121	0.536
80	0.572	0.290	1.07	0.168	0.708
100	0.721	0.371	1.32	0.200	0.895
Mean absorptivity ($-\log T$ in μg/ml)	0.073	0.0354[a]	0.130[a]	0.0200	0.091

[a] Blank absorbance, 0.014, was deducted.

For arsenic(III), another calibration graph was prepared by extracting from a solution of 5 *M* hydrochloric acid–1.0 *M* sodium iodide. The graph was again linear and the absorptivity was 0.130 at 282 nm, which agreed well with that obtained above.

Figure 2 shows that all the curves did not finally reach definite absorbances; the absorbances increased very gradually with the concentration of sulfuric acid, which is unfavourable for routine work. Tests showed that the blank absorbances at 282 and 364 nm were not greater than 0.03 and 0.01 respectively, even when the aqueous phase was composed of 6.5 *M* H_2SO_4–1.0 *M* NaI; the real extractability of tin was 99.2 and 99.6% with 2.2 *M* H_2SO_4–1.0 *M* NaI and 3.7 *M* H_2SO_4–1.0 *M* NaI, respectively, whereas the extractability of arsenic was 99.7 and 99.8% with 3.7 *M* H_2SO_4–1.0 *M* NaI and 5.15 *M* H_2SO_4–1.0 *M* NaI, respectively. The tendency to increased absorbances, therefore, was thought to be due to the extracted species themselves.

The extractabilities of tin(IV) and arsenic(III) were sufficiently high, hence it was possible to obtain a constant absorptivity by the following procedure. First, tin(IV) or arsenic(III) was completely extracted from a suitable solution, then the organic extract was shaken with 8 ml of 5 *M* sulfuric acid for a few seconds in order to hydrolyze the extract or return it partly into this acid phase, and, finally, 2 ml of 5.0 *M* sodium iodide was added and the phases were shaken for 1 min. With this procedure, the resultant absorbances for tin and arsenic at the wavelengths of 364 and 282 nm were in good agreement with those obtained by extracting the ions initially from a solution of 4 *M* H_2SO_4–1.0 *M* NaI. For germanium(IV), the procedure was less acceptable for obtaining a constant absorbance; shaking also caused a slight increase in absorbance. For practical purposes, shaking for 1 min was satisfactory.

Free iodine extracted gave an additive error in proportion to its amount, especially when the measurements were done at 282 nm. Therefore, it was indispensable to minimize the free iodine in the organic phase. The distribution of free iodine into inert solvents decreases greatly with increase of iodide in the aqueous phase, the iodine forming triiodide or polyiodide ion[17,18]; 1.0 *M* sodium iodide was therefore preferred for the determination of tin and arsenic. For germanium, 0.5 *M* sodium iodide with 6 *M* sulfuric acid was preferable, otherwise large amounts of sodium sulfate crystals were deposited in the separatory funnel. In the applications, some cases were found in which a large amount of free iodine appeared in the organic phase (Table II). But the iodine could be reduced or removed from the organic phase by washing with sulfuric acid solutions containing 1.0 *M* sodium iodide, as described above.

TABLE II

EFFECT OF DIVERSE IONS

(50 μg of required element added)

Diverse ion	*Added (mg)*	*Tin*[a]		*Arsenic*[a]		*Arsenic*[b]		*Germanium*[c]	
		A_{364}		A_{282}		A_{282}		A_{360}	
—	—	—	0.366	—	0.660	—	0.656	—	0.450
Cu(II)	5	0.377	0.366[d]	0.699	0.668[d]	0.682	0.658[d]	0.461	0.452[d]
Pb(II)	10	0.366		0.658		0.674		0.446	
Cd(II)	10	0.364		0.664		0.652		0.450	
Fe(III)	5	0.376	0.366[d]	0.697	0.662[d]	0.680	0.658[d]	0.458	0.449[d]
Bi(III)	10	0.365		0.662		0.658		0.447	
Hg(II)	10	0.364		0.668		0.662		0.447	
Sb(III)	10	0.418	0.364[d]	0.886	0.660[d]	0.721	0.656[d]	0.482	0.450[d]
Sn(IV)	10					0.699	0.656[d]		
Ge(IV)	1	0.362		0.664	(Ge 100 μg)	0.676	0.661[d]		
Mo(VI)	10	0.367	0.365[d]	0.678	0.665[d]	0.682	0.660[d]	0.468	0.456[d]
V(V)	10	0.379	0.366[d]	0.701	0.668[d]	0.699	0.661[d]	0.468	0.450[d]
Se(IV)	0.8		0.427[d]		0.739[d]	0.775	0.775[d]		0.520[d]
Se(IV)	0.1	0.408	0.408[d]	0.730	0.721[d]	0.678	0.672[d]	0.504	0.502[d]
Te(IV)	1.3	0.369		0.688	0.674[d]	0.668		0.466	
KNO_3	10	0.362		0.654		0.658		0.451	
$NaNO_2$[e]	10	0.355		0.665		0.54		0.446	
NaCl	(0.1 *M*)	0.366		0.660				0.440	
NaCl	(0.2 *M*)	0.366		0.662				0.401	

Aqueous phase: a = 4 *M* H_2SO_4–1.0 *M* NaI, b = 5 *M* HCl–1.0 *M* NaI and c = 6 *M* H_2SO_4–0.5 *M* NaI.

[d] Extract washed once. [e] $NaNO_2$ was decomposed with urea before the addition of solvent and NaI.

Stability of extracts

The absorbances of all the extracts were stable for at least 30 min after extraction, provided that the extracts were separated from the aqueous phase. When the aqueous phase was composed of sulfuric acid greater than 7.5 *M* and the temperature was above 25°, an oxidation–reduction reaction took place on standing between sulfuric acid and sodium iodide, generating considerable amounts of both iodine and hydrogen sulfide. In this case, a serious additive error occurred. For routine work, the concentration of sulfuric acid should not exceed greatly the required value, the temperature should be below 25°, and measurements should be made soon after the extraction.

Effects of diverse ions

Oxidants including iron(III), copper(II), molybdenum(VI), and vanadium(V) caused an additive error, giving free iodine (Table II); this iodine could be washed out as already described. Antimony(III) iodide has been reported to be extracted into benzene[4,19] from a sulfuric acid solution containing potassium iodide, the optimum iodide concentration being 0.01 *M*. Tests showed that antimony(III) iodide gave a sharp absorption peak at 286 nm, being extracted into cyclohexane also; however, with 0.5 or 1.0 *M* sodium iodide, the extractability was very low, antimony(III) forming the ionic iodocomplex. Washing removed any antimony(III) iodide extracted.

A small amount of nitrate did not interfere, but nitrite interfered seriously; this interference was easily avoided by preliminary addition of some urea. Compounds of tellurium and especially of selenium interfered in all amounts tested; these compounds may be extracted into cyclohexane, as elemental selenium[20] (benzene used) and elemental tellurium also, or as certain iodides of these elements, all of which may absorb ultraviolet light. Sulfite, thiosulfate and acetate interfered seriously. Other cations and anions were not tested. NEWMAN AND JONES[5] reported that small amounts of tin(IV) could be separated from a number of cations and anions by toluene extraction from a solution of 4.5 *M* sulfuric acid–0.5 *M* potassium iodide, and LUKE[13] obtained a clean separation of tin from metals and alloys by benzene extraction of tin(IV) iodide. These investigations suggest that other cations and anions not tested here may be allowable. However, the influence of other substances, especially of many organic materials, should be noted closely in routine practice.

APPLICATIONS

Determination of arsenic in the presence of tin and germanium

Figure 3 indicates the possibility of determining arsenic in the presence of tin and germanium. As shown in Table II, 50 μg of arsenic can be determined in the presence of 10 mg of tin or 1 mg of germanium.

Determination of tin in juice

Procedure. Weigh out 1–5 g of a homogeneous sample into a 100-ml conical beaker. Add 4.0 ml of concentrated sulfuric acid (above 95%), then heat gently and destroy the organic material with nitric acid added drop-wise until the solution becomes colourless. In this step the sulfuric acid must not fume strongly. To the solution, add a few ml of water and 0.1 g of urea and mix. Transfer the solution to a separatory funnel with a little water and make the volume about 15 ml with water. Allow to cool, add exactly 5 or 10 ml of cyclohexane and 3 ml of 50 *M* sodium iodide, and shake for 1 min. Measure the absorbance of the extract at 364 nm against cyclohexane.

Results. The results given in Table III were compared with those obtained by a spectrophotometric procedure with catechol violet[5,11].

Simultaneous determination of tin and arsenic in steel

Procedure. Dissolve 0.1–0.3 g of a sample in nitric acid (1:1) with or without hydrochloric acid (1:1). Add 4–5 ml of perchloric acid and heat until strong fumes of perchloric acid are evolved. To the residue add 15 ml of water and 0.6–0.7 g of hydrazine sulfate, and boil gently with a cover for 5–10 min. To this add 0.2 g of oxalic acid to prevent hydrolysis of tin(IV), and continue boiling for 3 min more. Transfer all the contents to a separatory funnel with 15 ml of sulfuric acid (1:1) and dilute to about 30 ml with water. Allow to cool, add exactly 10 ml of cyclohexane and 3 ml of 5.0 *M* sodium iodide, and shake for 1 min. Discard the aqueous layer and half of the organic layer also. To the organic layer add 8 ml of 5 *M* sulfuric acid, shake for 10 sec, then

TABLE III

DETERMINATION OF TIN IN ORANGE JUICE

(Solvent used: bottled juice, 5 ml; canned juice, 10 ml)

Sample	*Taken (g)*	*Tin added (μg)*	*Tin found (μg)*
Bottled juice	5.0	0	<0.5
	5.0	5.0	4.9
	5.0	10.0	9.9
	5.0	20.0	20.2
	5.0	30.0	29.5
	5.0	50.0	50.3
Canned juice[a]	1.00	0	88.0, 86.5, 86.0

[a] Catechol violet method: 87±2 μg of tin in 1 g.

TABLE IV

DETERMINATION OF TIN AND ARSENIC IN STEEL

Sample	*Taken (g)*	*Elements added (μg)*		*Absorbance*		*Elements found (μg) (%)*[a]	
		Tin	*Arsenic*	A_{282}	A_{364}	*Tin*	*Arsenic*
Pure iron	0.30	0	0	0.016^{b}	0.007^{b}		
	0.30	100	0	0.373^{b}	0.722^{b}		
	0.30	0	100	1.32^{b}	0.201^{b}		
	0.30	20	80	1.13	0.311	20.8	79.7
	0.30	40	80	1.19	0.458	41.4	78.3
	0.30	60	80	1.28	0.611	62.3	79.2
	0.30	80	80	1.35	0.750	81.6	79.1
	0.30	80	20	0.559	0.636	82.6	18.9
	0.30	80	40	0.807	0.661	80.7	38.2
	0.30	80	60	1.07	0.703	80.9	58.1
	0.30	80	80	1.32	0.730	79.3	77.5
B.C.S. No. 218/2^{c}	0.200			1.30	0.634	65.3 (0.033)	79.9 (0.040)
	0.100			0.658	0.319	32.8 (0.033)	40.5 (0.040)
	0.050 + pure iron 0.2 g			0.337	0.161	16.4 (0.033)	21.0 (0.042)
	0.050 + pure iron 0.2 g			0.658^{e}	0.325^{e}	16.8 (0.034)	20.1 (0.040)
B.C.S. No. 219/2^{d}	0.200			1.07	0.480	47.5 (0.024)	67.5 (0.034)
	0.100			0.561	0.254	25.3 (0.025)	35.3 (0.035)
	0.050 + pure iron 0.2 g			0.284	0.132	13.3 (0.027)	17.7 (0.035)
	0.050 + pure iron 0.2 g			0.556^{e}	0.260^{e}	12.6 (0.025)	17.3 (0.035)

[a] Calculation: C_{Sn} (μg in 10 ml) = 150 A_{364}–22.9 A_{282}; C_{As} (μg in 10 ml) = 82.2A_{282}–42.5A_{364}.
[b] Mean value of triplicate results.
[c] Tin, 0.035%; arsenic, 0.036%.
[d] Tin, 0.024%; arsenic, 0.034%.
[e] 5 ml Solvent was used.

add 2 ml of 5.0 *M* sodium iodide, and shake for 1 min. Measure the absorbance of the extract at 282 and 364 nm against cyclohexane. Calculate the amounts of tin and arsenic from equations prepared previously.

Results. The results are shown in Table IV. In this procedure special attention was given to the reduction of Fe(III), Cr(VI), Mo(VI) and V(V) to their lower valence states, and to minimizing the blank absorbance at the two wavelengths. The absorptivities of an element at the two wavelengths were determined by applying the entire procedure in the presence of 0.3 g of pure iron with, for convenience, 100 μg of tin or arsenic. As the blank absorbances at the two wavelengths were very small (Table IV), the values were neglected for the absorptivities and the absorbances actually measured, for the calculation of the amounts of the two elements. In this method, selenium and tellurium interfered. Large amounts of tungsten caused negative errors for tin and arsenic, tungstic acid being deposited during dissolution of sample, and the test elements being adsorbed on the acid. However, 10 mg of tungsten was allowable when the dissolution was done in the presence of 1–2 drops of phosphoric acid. Niobium and tantalum were not tested, but other common elements did not interfere.

Determination of germanium in its concentrates

The method consists in extracting germanium(IV) as its chloride in the usual way[21] into cyclohexane, converting the chloride into the iodide by shaking the organic extract with a solution of 6 *M* sulfuric acid–0.5 *M* iodide and measuring the absorbance at 360 nm.

Procedure. Decompose a sample (containing less than 120 μg of germanium) with hydrofluoric, nitric and 8 ml of concentrated sulfuric acids in a platinum dish. Evaporate the acids until fumes of sulfuric acid are gently evolved. If any organic matter is present, destroy it by adding some chromium trioxide during this step and reduce the excess of chromic acid with a little hydrogen peroxide solution. If any elemental sulfur or much lead sulfate is formed, dilute the solution with water, filter, and evaporate the filtrate to a small volume. Transfer the solution to a separatory funnel and dilute to 17–18 ml with water. Allow to cool, add exactly 10 ml of cyclohexane and 2 ml of concentrated hydrochloric acid, and shake for 2–3 min. After the layers have separated, discard the aqueous layer. Wash the organic layer with 10 ml of *ca.* 10 *M* hydrochloric acid, shaking for 1 min. Repeat the washing with 10 ml of 10 *M* hydrochloric acid containing a few mg of potassium bromate and discard the acid. Transfer half the organic layer with a pipette into another separatory funnel. To this add 9 ml of 6.5–7 *M* sulfuric acid and 0.1 g of finely powdered hydrazine sulfate, and shake to reduce co-extracted bromate to bromide. Add 1 ml of 5.0 *M* sodium iodide and shake for 1 min. Measure the absorbance of the extract at 360 nm against cyclohexane.

Results. The results for smelting dusts shown in Table V were compared with those obtained by the phenylfluorone method[22]. In this procedure, germanium(IV) could be extracted quantitatively into cyclohexane from the combined acids, greater than 6.5 *M* in sulfuric acid and 1.2 *M* in hydrochloric acid or greater than 5.5 *M* in sulfuric acid and 2.4 *M* in hydrochloric acid. The conversion of germanium(IV) chloride to its iodide was seen to take place rapidly, but hydrochloric acid present in the conversion system interfered. The absorbance at 360 nm decreased linearly with the concentration of hydrochloric acid; with 0.6 *M* hydrochloric acid, a 10% decrease

TABLE V

DETERMINATION OF GERMANIUM IN SMELTING DUSTS

Sample[a]	*Taken (g)*	*Germanium found (%)*[b]
A	0.113	0.038
	0.205	0.037
	0.326	0.037
B	0.0100[c]	0.503, 0.495
	0.0200[c]	0.490, 0.493
C	0.500	0.0058, 0.0056

[a] Constituents: A: Cu 33, Pb 4, Zn 3, As 0.3, Se 0.2%.
B: Cu 30, Pb 15, Zn 10, As 0.5, Se 0.005%.
C: Cd 55, Zn 4, As 0.22, Se 0.01%.

[b] Germanium present (phenylfluorone method): A 0.038, B 0.50, C 0.0058%.

[c] An aliquot of sample solution was taken.

in absorbance occurred. Therefore, half the extract of germanium(IV) chloride was transferred to another separatory funnel, so that the conversion could be made without interference from hydrochloric acid. The absorptivity for germanium at 360 nm thus obtained agreed well with that already given in Table I. Arsenic(III) chloride could be removed completely from the first extract by washing with potassium bromate solution. Selenium(IV) is extracted by benzene[23,24] to a small extent from hydrochloric acid. The element was found to be extracted into cyclohexane also in the first extraction and to cause a positive error. Therefore, selenium(IV) was removed from the first extract by washing with 10 *M* hydrochloric acid.

A simple spectrophotometric method for the determination of tin, arsenic and germanium has been presented. PAUL AND GIBSON[25] have developed a method for determining tin in tin-rich metals and alloys, which involves iodoethane extraction of tin(IV) from a solution 0.6 *M* in hydrochloric acid and 4 *M* in potassium iodide, and the measurement of the extract at 410–430 nm. Their method requires stricter control of the composition of the aqueous phase and in removal of co-extracted free iodine and tin(IV) is not quantitatively extracted. The method presented here is simple and selective, and useful for the determination of tin, arsenic and germanium in various samples.

SUMMARY

Tin(IV), arsenic(III) and germanium(IV) can be extracted quantitatively into cyclohexane from solutions containing sulfuric acid and sodium iodide. The extracted iodides have characteristic absorbance spectra in the ultraviolet region. When the measurements are made at 364 nm for tin, at 282 nm for arsenic and at 360 nm for germanium, the respective absorption maxima, the calibration graphs are linear and the molar absorptivities are 8700, 9700 and 6600, respectively. Arsenic(III) can be extracted mainly as its iodide from hydrochloric acid solutions containing sodium iodide, the molar absorptivity at 282 nm being also 9700. Recommended procedures are given for the determination of tin in juice, tin and arsenic in steels (simultaneously), and germanium in its concentrates.

RÉSUMÉ

L'étain(IV), l'arsenic(III) et le germanium(IV) peuvent être extraits quantitativement dans le cyclohexane renfermant acide sulfurique et iodure de sodium. Les iodures extraits présentent des spectres d'absorption caractéristiques dans l'ultraviolet. Lorsque les mesures sont faites à 364 nm pour l'étain, à 282 nm pour l'arsenic et à 360 nm pour le germanium, les courbes d'étalonnage sont linéaires; les coefficients d'extinction molaire sont respectivement 8700, 9700 et 6600. L'arsenic(III) peut être extrait comme iodure en solution acide chlorhydrique renfermant de l'iodure de sodium. Le coefficient d'extinction molaire à 282 nm est également de 9700. Des méthodes sont proposées pour le dosage de l'étain dans des jus, de l'étain et de l'arsenic dans des aciers (simultanément) et du germanium dans ses concentrés.

ZUSAMMENFASSUNG

Zinn(IV), Arsen(III) und Germanium(IV) können quantitativ mit Cyclohexan aus Lösungen extrahiert werden, die Schwefelsäure und Natriumjodid enthalten. Die extrahierten Jodide besitzen charakteristische Absorptionsspektren im u.v. Bei 364 nm für Zinn, 282 nm für Arsen und 360 nm für Germanium ergeben sich lineare Eichkurven und molare Extinktionen von 8700, 9700 bzw. 6600. Arsen(III) wird in der Hauptsache als Jodid aus salzsaurer Lösung, die Natriumjodid enthält, extrahiert. Die molare Extinktion bei 282 nm beträgt ebenfalls 9700. Verfahren werden angegeben zur Bestimmung von Zinn in Orangensaft, Zinn und Arsen in Stählen und Germanium in seinen Konzentraten.

REFERENCES

1 D. D. Gilbert and E. B. Sandell, *Microchem. J*,. 4 (1960) 491.
2 K. Tanaka, *Japan Analyst*, 11 (1962) 332.
3 G. O. Brink, P. Kafalas, R. A. Sharp, E. L. Weiss and J. W. Irvine, Jr., *J. Am. Chem. Soc.*, 79 (1957) 1303.
4 K. Tanaka, *Japan Analyst*, 9 (1960) 574; 10 (1961) 1087.
5 E. J. Newman and P. D. Jones, *Analyst*, 91 (1966) 406.
6 M. Malát, *Z. Anal. Chem.*, 187 (1962) 404.
7 H. Specker and G. Graffmann, *Z. Anal. Chem.*, 228 (1967) 401.
8 K. Tanaka, *Japan Analyst*, 13 (1964) 725.
9 K. Tanaka, *Japan Analyst*, 9 (1960) 700; 10 (1961) 612.
10 E. Migeon and J. Migeon, *Chim. Anal. (Paris)*, 43 (1961) 276.
11 Analytical Methods Committee, *Analyst*, 92 (1967) 320.
12 N. Košaric and G. Leliaert, *Mikrochim. Acta*, (1961) 806.
13 C. L. Luke, *Anal. Chim. Acta*, 39 (1967) 404.
14 D. Ishii and T. Takeuchi, *Japan Analyst*, 11 (1962) 118.
15 S. M. Milaev and K. P. Voroshnina, *Zavodsk. Lab.*, 29 (1963) 410.
16 H. W. Knudson, V. W. Meloche and C. Juday, *Ind. Eng. Chem., Anal. Ed.*, 12 (1940) 715.
17 J. S. Carter, *J. Chem. Soc.*, (1928) 2227.
18 M. Davies and E. Gwynne, *J. Am. Chem. Soc.*, 74 (1952) 2748.
19 R. W. Ramette, *Anal. Chem.*, 30 (1958) 1158.
20 A. A. Tumanov and N. M. Shakhverdi, *Zavodsk. Lab.*, 33 (1967) 20.
21 E. B. Sandell, *Colorimetric Determination of Traces of Metals*, 3rd Edn., Interscience, New York, 1959, p. 482.
22 K. Bansho and Y. Umezaki, *Japan Analyst*, 16 (1967) 715.
23 K. Tanaka, *Japan Analyst*, 18 (1969) 315.
24 K. Tanaka, N. Takagi and H. Tsuzimura, *Japan Analyst*, 18 (1969) 319.
25 A. D. Paul and J. A. Gibson, Jr., *Anal. Chem.*, 36 (1964) 2321.

Analytica Chimica Acta
Elsevier Publishing Company, Amsterdam
Printed in The Netherlands

MESURE DES FAIBLES ECARTS A LA STOECHIOMETRIE DU DIOXYDE D'URANIUM

J. C. VIGUIE ET J. P. CHABERT
Service de Physico-chimie des Combustibles, Centre d'Etudes Nucléaires de Grenoble, C.E.A., 38-Grenoble (France)

(Reçu le 21 juillet, 1969)

On sait que les qualités nucléaires du dioxyde d'uranium UO_{2+x} sont liées à la valeur x de la stoechiométrie.

D'autre part, les progrès en sensibilité apportés récemment à la mesure de x ont permis de constater que certaines propriétés physiques des oxydes frittés variaient de façon considérable à l'approche de la stoechiométrie. L'intérêt de ces phénomènes nous a conduit à rechercher une méthode d'analyse adaptée aux échantillons dont les écarts à la stoechiométrie sont inférieurs à 0.010. Les difficultés souvent citées du traitement de tels échantillons montrent en effet que ceux-ci ne peuvent être analysés de manière satisfaisante par simple extrapolation de techniques mises au point pour de plus fortes valeurs de x. Les choix que nous avons donc été amenés à faire dans les méthodes et le mode opératoire seront justifiés par l'évaluation de leur incidence sur la sensibilité du résultat x.

PRINCIPE DE LA MESURE

L'analyse en solution présente sur d'autres techniques l'avantage de donner une mesure absolue de x susceptible d'une grande sensibilité. Elle utilise l'hypothèse suivante: une attaque acide met en solution l'uranium aux valences IV et VI dans une proportion correspondant à l'état d'oxydation du métal dans le solide:

$$UO_{2+x} + 2(2-x)H^+ \rightarrow (1-x)U^{4+} + xUO_2^{2+} + (2-x)H_2O$$

Classiquement, x est obtenu à partir de la quantité d'uranium(VI) et de la masse de la prise d'essai. Nous avons déjà signalé[1] les avantages de la détermination de l'uranium(IV) en solution. Elle permet d'éviter la pesée; x étant donné par la relation:

$$\frac{x}{1-x} = \frac{\text{nb de moles de U(VI)}}{\text{nb de moles de U(IV)}}$$

Les différentes étapes de la détermination de x sont alors:
la mise en solution de l'oxyde,
le dosage de l'uranium(VI),
le dosage de l'uranium(IV).

La mise en solution de l'oxyde

Les échantillons proche de la stoechiométrie ont la particularité de ne se dissoudre que lentement en milieu acide. Si l'attaque dure trop longtemps, les ions U^{4+} en solution sont oxydés par l'oxygène atmosphérique[2]. On peut l'accélérer en broyant l'échantillon mais on risque alors une oxydation directe du solide[3].

Dans les deux cas, la mise en solution introduira une erreur par excès sur x.

L'acide phosphorique a été souvent retenu comme agent dissolvant à cause de la stabilité à l'air des solutions phosphoriques de l'uranium(IV). Les premiers auteurs ont tiré argument de cette stabilité pour effectuer l'attaque à l'air libre. Nous avons vérifié cependant qu'en milieu phosphorique concentré à 180°, l'oxydation par l'oxygène atmosphérique entraîne une erreur $\Delta x = 5 \cdot 10^{-4}$ unités par heure de chauffage. Cette erreur est réduite d'un facteur 20 quand l'attaque est faite sous argon.

Un inconvénient souvent mentionné de l'acide phosphorique est la précipitation de composés uraneux au moment de la dilution. Ce phénomène n'ayant jamais été clairement discuté, certaines remarques doivent être faites à son sujet. La précipitation se manifestant après que l'acide phosphorique ait été chauffé au-delà de sa température de déshydratation (environ 180°), nous admettrons que des ions condensés du type pyrophosphate sont à l'origine de ce phénomène (précipitation d'un composé non chargé du type pyrophosphate uraneux). A l'instant où le précipité se forme, il peut toujours être dissous en ajoutant de l'acide phosphorique concentré. On a ainsi la confirmation de l'existence de complexes phosphoriques solubles. Inversement, ces complexes sont dégradés en présence d'un acide fort; les solutions précipitent alors moins facilement. Nos dilutions seront donc faites avec une solution d'acide sulfurique 3.5 *N*.

On constate effectivement que la solution concentrée, chauffée une heure à 90° en présence de l'acide sulfurique 3.5 *N*, ne précipite plus à la dilution par suite de l'hydrolyse des ions pyrophosphates[4].

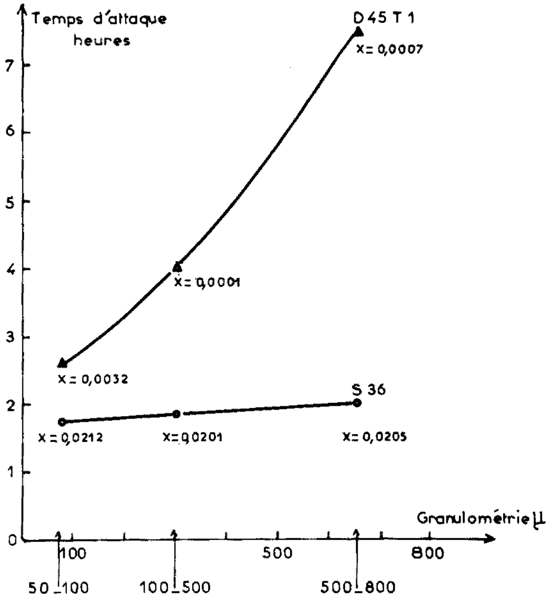

Fig. 1. L'influence de la durée de l'attaque et de la granulométrie.

L'influence de la durée de l'attaque et de la granulométrie est illustrée par la Fig. 1. On voit que pour un échantillon donné, la granulométrie 100–500 μ donne les valeurs de x les plus faibles, c'est-à-dire celles qui ont le plus de chances d'être correctes. Nous retiendrons ces dimensions. Nous avons par ailleurs mesuré l'oxydation superficielle de ces particules en effectuant deux attaques successives sur une même prise d'essai: la première solution d'attaque conduisant systématiquement à un résultat plus fort, nous ne retiendrons pour le calcul de x que la seconde. Cette façon de faire, qui elimine l'erreur induite par la fixation d'oxygène sur le solide (évaluée à $x = 3 \cdot 10^{-4}$ unités) est à la fois plus simple et plus sure que l'emploi d'une boite à gants[5].

Le dosage de l'uranium(VI)

Des méthodes décrites: polarographie[1,6,7], ampérométrie[8], coulométrie à tension contrôlée[9,10], la dernière paraît être à l'heure actuelle la plus sensible. L'uranium(VI) est réduit sur la cathode de mercure selon la réaction:

$$4\ H^+ + UO_2^{2+} + 2\ e \rightarrow U^{4+} + 2\ H_2O$$

Si Q est la quantité d'électricité nécessaire pour réduire la totalité de l'uranium(VI) présent dans la prise d'essai, on a: nombre de moles U(VI) $= Q/2F$.

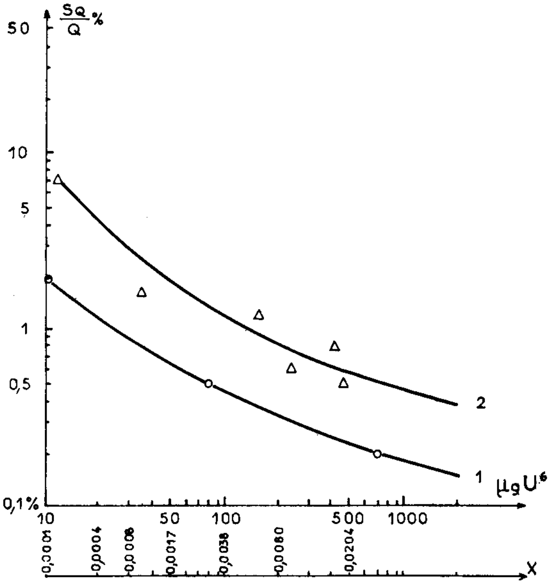

Fig. 2. Variation de la reproductibilité en fonction de la quantité d'uranium. ○ H_2SO_4 *N*; △ H_2SO_4 3.5 *N*–H_3PO_4 4.5 *N*–U^{4+} 3 mg/ml.

La Fig. 2 représente la variation de la reproductibilité, exprimée par l'écart quadratique moyen relatif S_Q/Q en fonction de la quantité d'uranium. L'échelle graduée en valeurs de x permet de voir que l'analyse d'un oxyde de formule $UO_{2.001}$ conduit à la détermination de 20 μg d'uranium(VI) en présence de 20 mg d'uranium(IV); la reproductibilité est comprise entre 5 et 10%.

Le dosage de l'uranium(IV)

Le dosage de 20 mg d'uranium(IV) relève de techniques classiques. Pour ne parler que des méthodes électrochimiques: la polarographie[6], la coulométrie[10], le titrage potentiométrique par le dichromate de potassium[1] ont été utilisées. Les trois dernières techniques sont susceptibles de donner une précision de quelques millièmes.

Nous avons retenu le titrage potentiométrique pour la simplicité de sa mise en oeuvre. Il utilise la réaction:

$$2\,H^+ + 3\,U^{4+} + Cr_2O_7^{2-} \rightarrow 3\,UO_2^{2+} + 2\,Cr^{3+} + H_2O$$

Si n est le volume utilisé de solution titrante et N sa normalité, on a: nombre de moles U(IV) $= n.N/2$.

Le choix des méthodes à appliquer à ces trois opérations ne sera judicieux que si l'incertitude apportée par chacune concourt de façon homogène à l'incertitude attachée au résultat x. Les deux seules opérations susceptibles de limiter la précision de la mesure dans le domaine de x que nous avons choisi sont la mise en solution, et le dosage de l'uranium(VI).

TECHNIQUE DE LA MESURE

L'attaque de l'échantillon

L'attaque est effectuée sous atmosphère d'argon (Fig. 3). Celui-ci est débar-

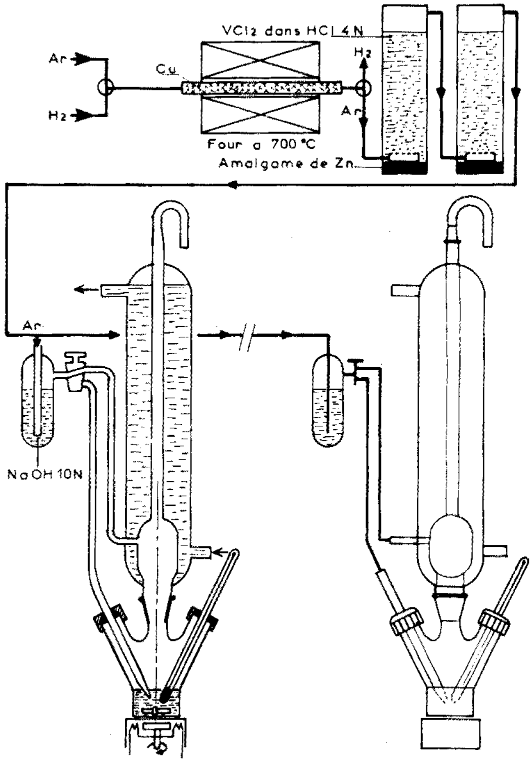

Fig. 3. L'ensemble pour l'attaque de l'échantillon.

rassé des traces d'oxygène par passage sur des copeaux de cuivre chauffés au rouge. Des barboteurs régénérant en permanence des ions vanadeux complètent la purification[11].

Le dosage de l'uranium(VI)

La cellule d'électrolyse, d'un type classique, est prévue pour recevoir 10 ml de solution. Les détails principaux sont portés sur la Fig. 4. Le corps de la cellule et les compartiments sont en verre Pyrex, le couvercle et l'agitateur en Plexiglass.

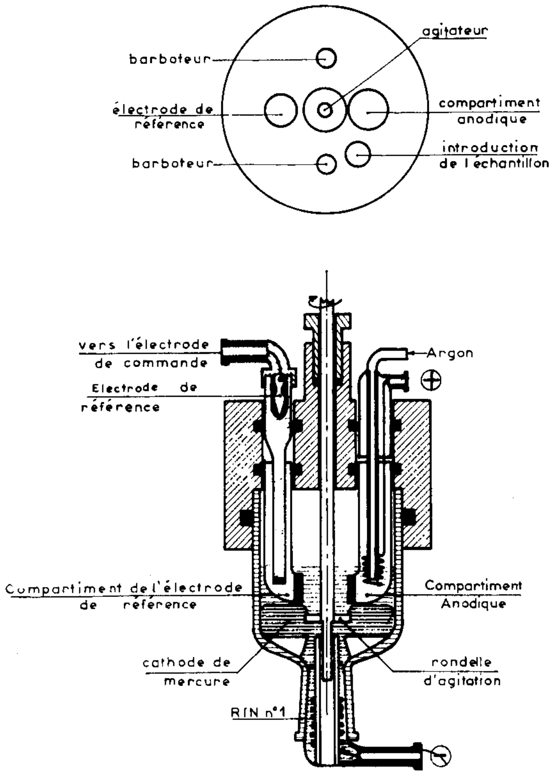

Fig. 4. La cellule d'électrolyse.

Des joints assurent l'étanchéité de l'ensemble. Deux tubes à extrémité capillaire font barboter de l'argon en permanence dans la solution. La cathode est constituée par 12 ml de mercure (99.99999%, Mercure et Industrie), dont la surface est brassée par une rondelle d'agitation tournant à 1900 r.p.m. Un moteur Brion Leroux type 2, muni d'une sortie tachimétrique permet d'ajuster la vitesse de façon très précise.

L'ensemble potentiostatique (Fig. 5) comprend: un potentiostat Tacussel type 40-1, un millivoltmètre Tacussel type S6R3 Z, un enregistreur de courant graphispot Sefram, et un intégrateur de courant Tacussel type IG 3 1000.

La gamme de mesures s'étend de 12 μg à 6 mg d'uranium; c'est-à-dire de 10 à 5000 mC. Les blancs dépendent à la fois de la tension de préréduction et de la tension de réduction; ils sont de l'ordre de 10 mC.

L'intensité peut atteindre pour les grandes quantités 30 mA en début d'électrolyse; dans tous les cas elle redescend à moins de 5 μA en fin d'électrolyse.

La durée de l'électrolyse varie, selon la quantité déterminée entre 15 et 30 min.

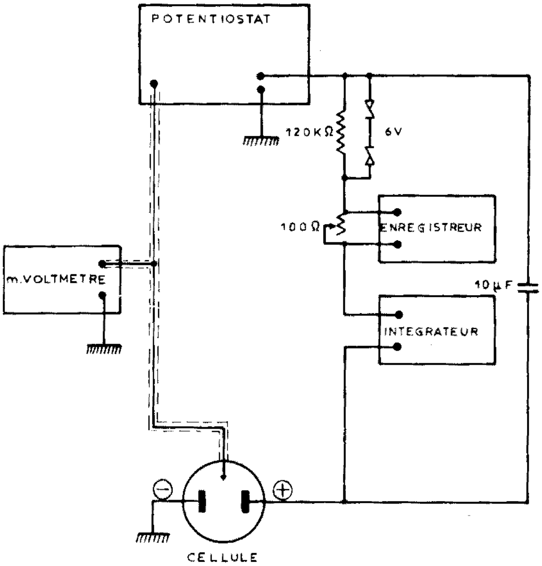

Fig. 5. L'ensemble potentiostatique.

Le dosage de l'uranium(IV)

L'oxydation des ions U^{4+} par une solution titrée de dichromate de potassium est suivie par potentiométrie à courant nul sur une électrode indicatrice de platine. Le potentiomètre enregistreur Metrohm E 336 assure la synchronisation entre l'avancée du papier et la montée du piston dans la burette.

Mode opératoire

L'échantillon de dioxyde d'uranium est d'abord broyé au mortier; la poudre est tamisée de manière à recueillir 150 mg environ de la fraction 100–500 μ. On ajoute 5 ml d'acide phosphorique concentré (Prolabo R.P.) dans le matras d'attaque. Après 10 min de dégazage par un courant d'argon, le chauffage est mis en route et l'arrivée d'argon dirigée vers l'ajutage supérieur. A l'apparition de la teinte verte, le chauffage est coupé, la solution refroidie est rejetée. On ajoute de nouveau 5 ml d'acide phosphorique concentré et, avec les mêmes précautions on amène la température à 180°. Quand la plus grosse partie du solide est passée dans la solution, celle-ci est refroidie, puis portée à l'aide d'une pipette dans 50 ml d'une solution de l'acide sulfurique 3.5 N dégazée et froide. Cette solution, diluée, mise dans un flacon à bouchon rodé peut se conserver au réfrigérateur indéfiniment.

Une partie aliquote v (normalement $v = 10$ ml) de la solution précédente est introduite dans la cellule d'électrolyse. La tension de préélectrolyse est choisie d'après le Tableau I.

Quand le courant de préélectrolyse est descendu en-dessous de 5 μA, on amène la tension de l'électrode de mercure à -380 mV/E.C.S. et on enclanche le comptage du coulomètre. Quand le courant est revenu à 5 μA, on note la quantité d'électricité (Q brut): cette valeur diminuée de la valeur du blanc donne la quantité d'électricité Q nécessaire pour réduire la totalité de l'uranium(VI) présent dans la prise d'essai.

TABLEAU I

CHOIX DE LA TENSION DE PRÉÉLECTROLYSE

Mesure prévue (Q mC)	*Tension préélect. (mV/E.C.S.)*
100 et moins	+ 60
1000	+ 80
2000	+ 100

Une deuxième partie aliquote V (normalement $V = 20$ ml) de la solution initiale est portée dans un becher, on ajoute 2 ml d'une solution de chlorure ferrique concentrée (30%, Prolabo), on complète à 50 ml par la solution d'acide sulfurique 3.5 N. Trois à quatre millilitres de solution de dichromate de potassium 0.1 N (Titrisol, Merck) sont nécessaires pour atteindre le saut de tension qui marque le point équivalent; soit n ml la quantité consommée.

Il peut arriver que des échantillons très proches de la stoechiométrie et particulièrement denses ne s'attaquent que très lentement. Si 3–4 h d'attaque à 180° ne parviennent pas à faire passer la majeure partie de l'échantillon en solution, on portera la température à 240–250°. Après dissolution, on ajoute 30 ml de l'acide sulfurique 3.5 N dégazée dans le matras à travers le réfrigérant[5]; on laisse 1 h environ à 90–100°. La solution refroidie est portée à 50 ml et conservée comme il est indiquée plus haut. Après ce traitement, la réduction coulométrique sera fixée à −250 mV/E.C.S.

La surstoechiométrie est calculée au moyen des formules:

$$\frac{x'}{1-x'} = \frac{1}{96520} \frac{V}{v} \frac{1}{N} \frac{Q}{n} \tag{1}$$

$$x = x' - \varepsilon \tag{2}$$

Avec les notations définies plus haut, Q est exprimé en mC (la valeur expérimentale étant naturellement corrigée du blanc analytique), n en ml, N en équivalents par litre. ε est la correction du blanc d'attaque. Pour le mode opératoire décrit, ε est évalué à 0.0004. La signification de cette correction sera discutée plus loin.

RÉSULTATS

Exemples de mesure

1. Echantillon S 23-1. Attaque à 180°.

Coulométrie (Fig. 6a): $v = 10$ ml

$$\left.\begin{array}{l} Q_1 = 11 \text{ mC} \\ Q_2 = 13 \text{ mC} \end{array}\right\} \text{moyenne } Q = 12 \text{ mC}$$

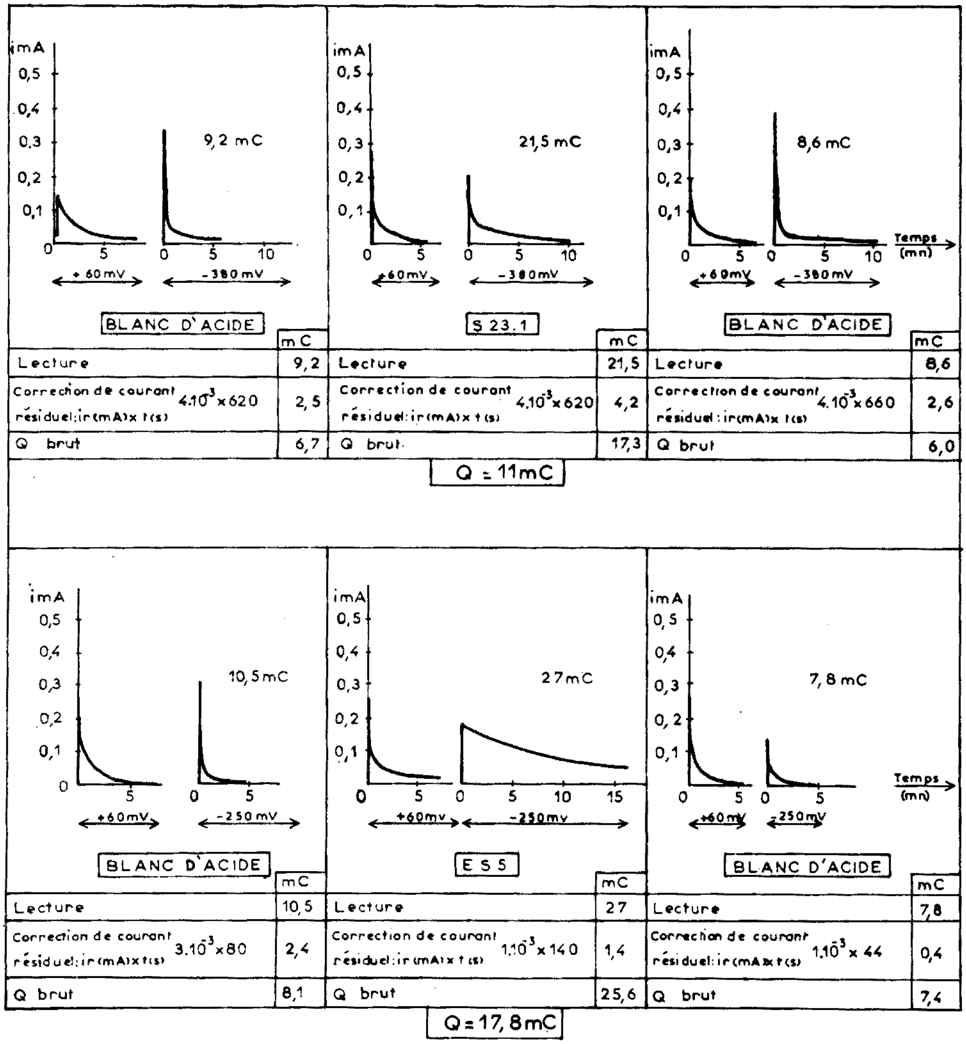

BLANC D'ACIDE	mC	S 23.1	mC	BLANC D'ACIDE	mC
Lecture	9,2	Lecture	21,5	Lecture	8,6
Correction de courant résiduel: ir(mA) x t(s) $4.10^{-3} \times 620$	2,5	Correction de courant résiduel: ir(mA) x t(s) $4.10^{-3} \times 620$	4,2	Correction de courant résiduel: ir(mA) x t(s) $4.10^{-3} \times 660$	2,6
Q brut	6,7	Q brut	17,3	Q brut	6,0

Q ≃ 11mC

BLANC D'ACIDE	mC	E S 5	mC	BLANC D'ACIDE	mC
Lecture	10,5	Lecture	27	Lecture	7,8
Correction de courant résiduel: ir(mA) x t(s) $3.10^{-3} \times 80$	2,4	Correction de courant résiduel: ir(mA) x t(s) $1.10^{-3} \times 140$	1,4	Correction de courant résiduel: ir(mA) x t(s) $1.10^{-3} \times 44$	0,4
Q brut	8,1	Q brut	25,6	Q brut	7,4

Q = 17,8mC

Fig. 6. Exemples des courbes coulométriques. (a) Premier échantillon (S 23-1), (b) deuxième échantillon (ES-5).

Potentiométrie: $V = 10$ ml
$n = 2.04$ ml

$$\frac{x'}{1-x'} = \frac{1}{96520} \cdot \frac{10}{10} \cdot \frac{1}{0.1} \cdot \frac{12}{2.04} = 0.0006$$

$$x' \simeq 0.0006$$

$$\varepsilon = 0.0004$$

$$x = 0.0002$$

2. Echantillon ES-5. Attaque à 250°.

Coulométrie (Fig. 6b): $v = 10$ ml

$$\left.\begin{matrix} Q_1 = 17 \text{ mC} \\ Q_2 = 17.8 \text{ mC} \end{matrix}\right\} \text{moyenne } Q = 17.4 \text{ mC}$$

Potentiométrie: $V = 20$ ml

$n = 3.76$ ml

$$\frac{x'}{1-x'} = \frac{1}{96520} \cdot \frac{20}{10} \cdot \frac{1}{0.1} \cdot \frac{17.4}{3.76} = 0.0010$$

$$x' \simeq 0.0010$$

$$\varepsilon = 0.0004$$

$$x = 0.0006$$

Reproductibilité

Les résultats de mesures répétées effectuées dans les conditions courantes de l'analyse, sont présentés dans le Tableau II. Ils permettent d'évaluer la variation de la reproductibilité en fonction du mode opératoire et de la valeur de x.

TABLEAU II

ANALYSE D'ENSEMBLE DES RÉSULTATS

	Mode op. no. 1 attaque 180° x	*Mode op. no. 2 attaque 240°* x	*Moyenne* $\bar{x}$	$\frac{S_x}{x}$ (%)	$\frac{S_Q}{Q}$ (%)
S 40	0.0184 0.0186 0.0194		0.0188	2.8	0.6
D 47-1	0.0076 0.0074 0.0075 0.0076 0.0074 (0.0099)[a] 0.0076		0.0075	1.3	0.9
S 42	0.0057 0.0063 0.0057		0.0059	5.9	1.1
D 44-6		(0.0019)[a] 0.0044 0.0041 0.0044 0.0031	0.0036	30	1.3
ES-5	0.0006 0.0002	0.0005 0.0006 0.0006 0.0004 (0.0013)[a]	0.0005	18	7

[a] Valeurs rejetées pour avoir une probabilité supérieure à 0.95, d'être incompatible (test de Grubbs) avec les autres résultats de la série.

Les résultats correspondant aux échantillons D 44-6 et ES-5, montrent que le mode opératoire no. 2 donne des résultats moins reproductibles. A 240°, en effet, plusieurs incidents risquent de compromettre la bonne marche de l'attaque:

Le temps de chauffe peut varier du simple au triple pour un même échantillon, dans la mesure où il dépend de la vitesse de déshydratation de l'acide phosphorique qui, elle-même, dépend de la géométrie de l'appareil, du rendement thermique, etc.

Quand l'acide phosphorique est déshydraté, sa température est difficile à stabiliser. Dans la pratique, certaines attaques présenteront des pointes de température de plusieurs dizaines de degrés.

L'opération de réhydrolyse de l'acide pyrophosphorique à 90° introduit un risque supplémentaire d'oxydation.

Enfin, les ions phosphates en se fixant sur le mercure augmentent le temps d'électrolyse, le courant résiduel, la valeur des blancs et nuisent ainsi à la qualité de la mesure coulométrique.

Pour toutes ces raisons, le mode opératoire no. 2 n'est utilisé que pour les échantillons proches de la stoechiométrie dont l'attaque, selon le mode no. 1, serait trop longue (plus de 10 h). Un temps de chauffage aussi long conduirait de toute manière aux mêmes inconvénients. L'analyse de l'échantillon ES-5 montre qu'il n'existe pas dans ce cas de différence importante entre les résultats des deux méthodes.

Des valeurs de S_Q/Q tirées de la Fig. 2 (courbe 2) sont portées en regard de S_x/x. L'écart est systématique; S_x/x est plus grand.

Le Tableau III permet de comparer pour un même échantillon les écarts quadratiques moyens S_Q/Q et S_x/x: faisons l'hypothèse (*H*) que la dispersion des valeurs x a pour unique origine l'incertitude des mesures entrant dans le calcul de x; on obtiendra l'expression analytique de la reproductibilité de x en différenciant l'expression (2), soit:

$$\frac{dx}{x} = \frac{x'}{x}\frac{dx'}{x'} - \frac{\varepsilon}{x}\frac{d\varepsilon}{\varepsilon} \tag{3}$$

de l'expression (1) on tire par ailleurs:

$$\frac{dx'}{x'} = \frac{dV}{V} - \frac{dv}{v} - \frac{dN}{N} - \frac{dn}{n} + \frac{dQ}{Q}$$

Pour des valeurs de x inférieures à 0.01, les quatre premiers termes sont négligeables; ils introduisent une erreur égale au plus à quelques millièmes. L'expression (3) devient alors:

$$\frac{dx}{x} \simeq \frac{x'}{x}\frac{dQ}{Q} - \frac{\varepsilon}{x}\frac{d\varepsilon}{\varepsilon}$$

En termes de variance:

$$\sigma_x{}^2 = \left(\frac{x'}{x}\right)^2 \sigma_Q{}^2 + \left(\frac{\varepsilon}{x}\right)^2 \sigma_\varepsilon{}^2$$

ε, étant une correction constante appliquée à l'ensemble des résultats du Tableau III, n'a pas d'influence sur la reproductibilité: $\sigma_\varepsilon{}^2 = 0$.

$$\sigma_x = \frac{x'}{x}\sigma_Q \quad \text{ou:} \quad \sigma_{x'} = \sigma_Q.$$

Cette égalité permettra de dire si l'hypothèse (*H*) est raisonnable ou si elle est à rejeter.

Echantillon S 40. La variance des six mesures de Q obtenues à partir des trois déterminations parallèles est:

$(S_Q/Q)^2 = 0.88$ avec trois degrés de liberté.

La variance des trois mesures de x' est:

$(S_{x'}/x')^2 = 7.62$ avec deux degrés de liberté.

Le test de comparaison des variances se résume par l'égalité:

$$\frac{(S_{x'}/x')^2}{(S_Q/Q)^2} = 8.66 = F_{0.94}{}^{(2,3)} \quad (F\text{: variable de Fischer–Snedecor}).$$

La probabilité d'avoir $\sigma_{x'}$, distinct de σ_Q (et supérieur) est 0.94.

Echantillon S 42.

$$\frac{(S_{x'}/x')^2}{(S_Q/Q)^2} = 27 = F_{0.995}{}^{(2,4)}$$

La probabilité d'avoir $\sigma_{x'} \neq \sigma_Q$ est cette fois 0.995.

TABLEAU III

ANALYSE DES VARIANCES S_x ET S_Q

Attaques	*n ml*	*Q mC*	*x*
S 40-1	3.68	340.5	0.0184
	3.70	340.9	
S 40-2	3.68	340	0.0186
	3.67	347.5	
S 40-3	4.08	395.8	0.0194
	4.08	398.5	
S 42-1	4.31	127.8	0.0057
		128	
		126.4	
S 42-2	4.10	132.1	0.0063
		133.5	
S 42-3	4.10	121.8	0.0057
		119	

Dans les deux cas il faut conclure que $\sigma_{x'}$ est supérieur à σ_Q de façon significative. L'hypothèse (*H*) doit être rejetée; la dispersion des valeurs de x a une autre origine que l'incertitude des mesures entrant dans le calcul de x. Il faut donc suspecter l'attaque d'être le facteur critique pour l'ensemble de l'analyse.

Si on compare les résultats du Tableau II avec les résultats des auteurs qui ont cherché à analyser des échantillons proches de la stoechiométrie par différentes méthodes: coulométrie[10], polarographie oscillographique différentielle[5] on voit que ces derniers ont des possibilités équivalentes au-dessus de $x = 0.004$. Il semble par contre que le mode opératoire décrit plus haut conduise à une meilleure reproductibilité pour les échantillons dont la surstoechiométrie est voisine de 0.001.

Justesse et sensibilité

Le Tableau IV rapproche nos résultats de ceux obtenus par gravimétrie, suivant les deux techniques classiques:

1. Grillage à l'air à 800° et pesée de U_3O_8.
2. Réduction sous hydrogène à 1250° et pesée de UO_2.

Les résultats obtenus par voie électrochimique sont systématiquement in-

TABLEAU IV

ÉVALUATION DE LA JUSTESSE

Echant.	*Grillage*	*Réduction*	*Déterminat. électrochim.*
44'-1	0.0080	0.0100	0.0071
44'-6	0.0080	0.0075	0.0055
47-1	0.0100	0.0150	0.0074
47-6	0.0065	0.0045	0.0048
		0.0030	

férieurs. STROMATT ET CONALLY[10] notent des écarts plus grands encore. L'erreur systématique de pesée liée à la fixation d'eau sur UO_2 peut expliquer ces différences[3,12]; 10 p.p.m. d'eau sur l'échantillon fait faire à la méthode gravimétrique une erreur de 0.0005 unités par excès.

La détermination de valeurs très faibles de x ne peut être abordée que dans la mesure où le mode opératoire conduit à un blanc d'attaque suffisamment bien défini.

Des copeaux d'uranium métallique, décapés, puis attaqués selon le mode 2 donnent une solution d'ions U^{4+} contenant un peu d'uranium(VI). Pour cette quantité, le calcul de x conduirait à la valeur 0.0004. Nous estimerons donc que cette valeur liée au mode opératoire décrit, constitue le blanc de l'analyse. Plus précisément, il est défini par les grandeurs suivantes:

Valeur moyenne: 0.0004
Variance : 0.0001

DISCUSSION DES RÉSULTATS

De gros efforts ont été faits ces dernières années pour améliorer le dosage de l'uranium(VI), dans la mesure où il semblait que lui seul limitait la détermination des petites valeurs de x. Par contre, très peu a été dit sur les conditions de dissolution de UO_2. Or, nous disposons maintenant d'une méthode de dosage de l'uranium(VI) d'une qualité suffisante pour que la précision et la sensibilité de la mesure ne soient plus limitées que par la seule irreproductibilité des conditions de l'attaque. Une amélioration de l'ensemble de la détermination est donc possible en agissant sur ce facteur. D'autre part, cette amélioration peut être suivie en comparant $(S_{x'}/x')^2$ et $(S_Q/Q)^2$.

Lorsque ces deux grandeurs prendront des valeurs suffisamment voisines d'après le test d'analyse des variances, on concluera que l'hypothèse (H) est vérifiée. Il n'y aura dès lors plus de progrès à faire.

Le principal facteur d'irreproductibilité se trouve certainement dans la variation de température de la solution pendant l'attaque. Si le chauffage était asservi à la température, la déshydratation de l'acide phosphorique et le temps d'attaque seraient beaucoup mieux définis.

Les impuretés susceptibles d'interférer avec le dosage de l'uranium(VI) sont Fe(III) et Mo(VI). Nous ferons l'hypothèse que la réduction effectuée au cours de la préparation de UO_2 les réduit au même titre que l'uranium à des valences inférieures qui n'interfèrent plus. Fer(III) contenu dans l'acide est réduit pendant la préélectrolyse.

La nécessité de corriger le résultat x' d'un blanc comptant pour l'ensemble de l'analyse s'impose quand on constate que les méthodes de dissolution n'ont jamais donné pour un échantillon des valeurs inférieures à $\varepsilon = 0.0004$. L'uranium métal, le dioxyde UO_2 soigneusement réduits conduisent l'un et l'autre à ce résultat. Nous faisons donc l'hypothèse que toute mise en solution entraîne une oxydation dont il importe de tenir compte pour corriger le résultat final.

Il est indispensable d'évaluer ε chaque fois qu'un nouveau mode opératoire est défini. On ne peut émettre que des hypothèses sur l'origine des corps oxydants responsables de ce blanc: impureté de l'argon, traces d'oxygène fixées sur les parois du récipient d'attaque, etc.

Le Tableau II montre l'existence de valeurs aberrantes dans les séries de mesure. Pour se mettre à l'abri d'erreurs accidentelles importantes, les analyses comporteront deux attaques. Si l'écart des deux résultats est compatible avec la valeur de S_x/x, on donnera la moyenne. Sinon, une troisième analyse devra être entreprise pour permettre d'écarter le résultat aberrant.

Il ressort de cette étude que la détermination des faibles écarts à la stoechiométrie n'est pas une opération exceptionnelle. Elle peut être effectuée dans une seule journée sans prendre plus que les précautions habituelles. Trois analyses peuvent être conduites simultanément. Le dosage de séries est facile à mettre en oeuvre.

RÉSUMÉ

La mesure de la surstoechiométrie x du dioxyde d'uranium UO_{2+x} a été étudiée dans le cas particulier des valeurs de x inférieures à 0.01. L'échantillon, mis en poudre, est dissout dans l'acide phosphorique concentré. L'uranium(VI) est dosé par réduction coulométrique à potentiel contrôlé, l'uranium(IV) est oxydé par une solution titrée de dichromate de potassium. Il est montré que l'incertitude sur x provient essentiellement du manque de reproductibilité des conditions de l'attaque. Pour le mode opératoire décrit, des valeurs de $x = 0.0005$ ont été déterminées avec une reproductibilité relative de 20%.

SUMMARY

The measurement of deviations from stoichiometry x of uranium dioxide UO_{2+x} has been investigated in the particular case of x less than 0.01. The powdered sample is dissolved in concentrated phosphoric acid. Uranium(VI) is measured by coulometric reduction at controlled potential; uranium(IV) is oxidised by a standard solution of potassium dichromate. It is shown that the uncertainty in x is essentially due to the lack of reproducibility of the initial dissolution. With the described operating method, values of x equal to 0.0005 have been determined with a relative reproducibility of 20%.

ZUSAMMENFASSUNG

Es wurden Untersuchungen zur Stöchiometrie des Urandioxids UO_{2+x} für den besonderen Fall durchgeführt, dass x kleiner als 0.01 ist. Dazu wird die gepulverte Probe in konzentriertem Phosphorsäure gelöst. Uran(VI) wird durch coulometrische

Reduktion mit kontrollierten Potentialen bestimmt; Uran(IV) mit einer Standardlösung von Kaliumdichromat oxidiert. Es konnte gezeigt werden, dass die Unsicherheit, mit der x bestimmt werden kann, im wesentlichen von der Reproduzierbarkeit der anfänglichen Auflösung abhängig ist. Mit der beschriebenen Methode konnten x-Werte von 0.0005 mit einer relativen Reproduzierbarkeit von 20% bestimmt werden.

BIBLIOGRAPHIE

1 J. C. VIGUIE ET G. UNY, *Rapport C.E.A. R 3029*, 1966.
2 J. HALPERN ET J. G. SMITH, *Can. J. Chem.*, 34 (1956) 1419.
3 H. NICKEL, *Nukleonik*, 8 (1966) 366.
4 P. PASCAL, *Traité de Chimie Minérale X-829*, 1956.
5 H. J. SHALGOSKY, R. C. SMART ET J. WATLING, *AERE R 4270*, 1964.
6 C. NENS, C. CANTON ET R. MOLINA, *Rapport C.E.A. R 3186*, 1967.
7 R. M. BURD ET G. W. GOWARD, *Rapport WAPD no. 205*, 1959.
8 J. J. ENGELSMAN, J. KNAAPE ET J. VISSER, *Talanta*, 15 (1968) 171.
9 H. C. JONES, W. D. SHULTS ET J. M. DALE, *Anal. Chem.*, 37 (1965) 680.
10 R. W. STROMATT ET R. E. CONALLY, *Anal. Chem.*, 33 (1961) 345.
11 A. G. STOMBERG ET Y. N. ZHIKHAREV, *Zavodsk. Lab.*, 31, 10 (1965) 1185.
12 E. A. SCHAEFFER ET J. O. HIBBITS, *Anal. Chem.*, 41 (1969) 254.

Analytica Chimica Acta
Elsevier Publishing Company, Amsterdam
Printed in The Netherlands

AUTOMATISCHE SCHNELLMETHODE ZUR KOHLENSTOFF- UND WASSERSTOFF-BESTIMMUNG*

WOLFGANG MERZ
Untersuchungslaboratorium der Badischen Anilin- u. Sodafabrik A.G., Ludwigshafen/Rhein (Deutschland)

(Eingegangen den 26. August, 1969)

Der Trend nach weitestgehender Automation analytischer Verfahren hat auch vor der organischen Mikroelementaranalyse nicht Halt gemacht. Für viele grössere Laboratorien ist die Automation und damit die Einsparung von Arbeitskräften sogar zu einer Existenzfrage geworden. Automation ist für uns heute kein Schlagwort mehr, sie ist zwingende Notwendigkeit. Die am häufigsten zu bestimmenden Elemente sind in den meisten Labors Kohlenstoff, Wasserstoff und Stickstoff. Eine Automation der Mikroelementaranalyse sollte demnach zweckmässigerweise hier einsetzen. Prinzipiell sind dabei zwei Möglichkeiten gegeben. Zum einen eine Methode, mit der die drei Elemente aus einer Einwaage erfasst werden, zum anderen ausgesprochene Schnellverfahren für jedes einzelne Element. Der erstere Weg, die gemeinsame Erfassung von Kohlenstoff, Wasserstoff und Stickstoff wurde bereits reichlich praktiziert. Es sind zahlreiche Verfahren bekannt und ebensoviele Geräte auf dem Markt, die als C, H, N-Automaten propagiert werden. In vielen Fällen wird dabei aber einer gefälligen Aufmachung mehr Interesse geschenkt, als der eigentlichen Automation, die meist nur eine Teilautomatisierung darstellt. Von selbsttätiger Arbeit des Gerätes über die gesamte Analysendauer, einschliesslich der Endbestimmung, kann kaum die Rede sein. Der Analytiker bleibt also weiterhin beschäftigt, sodass der Zeitgewinn nur aus der gemeinsamen Erfassung von C, H und N resultiert. Auch sind die meisten kommerziellen C,H,N-Geräte ausschliesslich im Ultramikrobereich, also mit Einwaagen unter 1 mg einsetzbar, ein Handicap, das einer universellen Automation zwangsläufig im Wege steht. Wir versuchten daher den anderen Weg zu beschreiten, nämlich für jedes Element ein Schnellverfahren auszuarbeiten, das zudem weitestgehend automatisierbar sein sollte. Eine wesentliche Voraussetzung war das Vorhandensein elektronischer Wägeeinheiten, wie sie beispielsweise Fa. Sartorius[1] liefert. Die Wägezeit ist hier gegenüber konventionellen Waagen stark verkürzt. Auch steht der Messwert codiert zur weiteren Datenverarbeitung zur Verfügung.

Unsere Schnellmethode zur Stickstoffbestimmung[2] durch explosionsartige Verbrennung der Substanz in reinem Sauerstoff in einem senkrecht angeordneten Quarzrohr und Überführung der Crackgase mit Kohlensäure in ein automatisch arbeitendes Azometer, hat sich bereits im Routinebetrieb bewährt. Der Analysenvorgang wird durch ein Programmschaltwerk über Zeitrelais gesteuert und das Stickstoffvolumen ausgedruckt. Die reine Analysenzeit beträgt 2.5 Min. In der Praxis sieht

---

* Vorgetragen auf dem International Symposium on Analytical Chemistry, Birmingham, Juli, 1969.

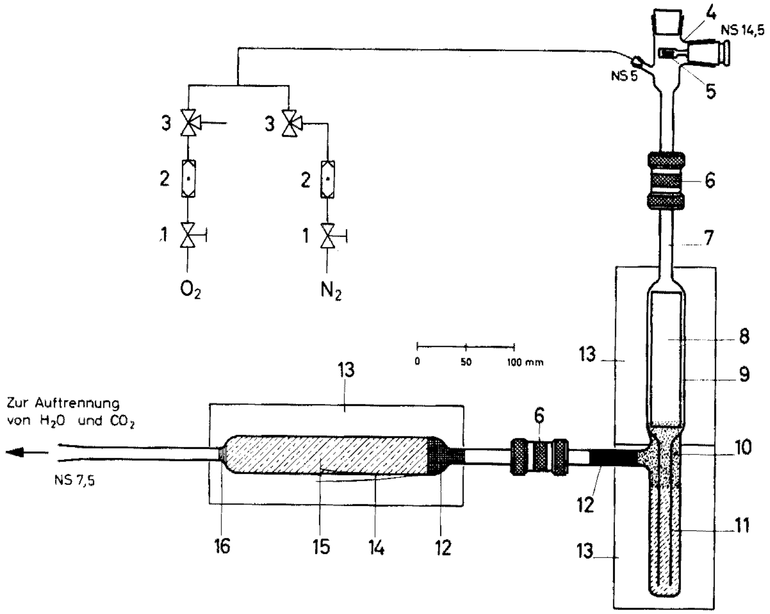

Abb. 1. Verbrennungsapparatur. (1) Feinregulierventil, (2) Strömungsmesser, (3) Magnetventil, (4) Probeneinschleussvorrichtung, (5) Aluminiumschiffchen mit Substanzeinwaage, (6) Schraubverbindung, (7) Verbrennungsrohr, (8) Verbrennungskammer, (9) Schutzhülse, (10) Quarzsplitter, (11) CuO, (12) Ag-wolle, (13) Ofen, (14) Reduktionsrohr, (15) Cu, (16) Cu-Drahtnetz.

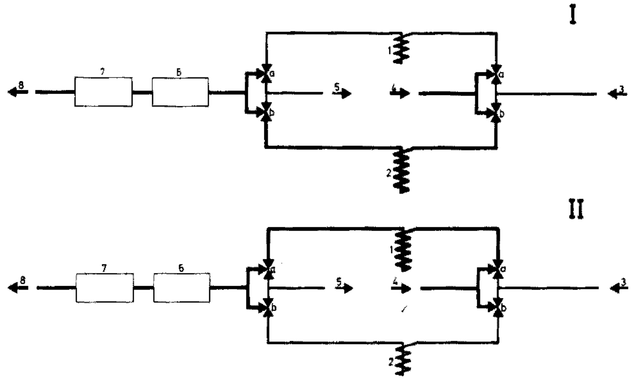

Abb. 2. Ventilsteuerung mit Heizung und Kühlung der Silberspiralen zur Auftrennung von H_2O und CO_2. (I) und (II) zeigen schematisch die beiden Analysenzyclen. Bei (I) ist die Spirale (1) gekühlt (−60 bis −80°), die Spirale (2) erwärmt (200–250°) und die Ventile (a) ein-, (b) ausgeschaltet. Im Zyclus (II) ist es umgekehrt. (1) und (2) Silberspiralen, (3) Eingang von CO_2 und H_2O mit N_2 als Treibgas (vom Verbrennungstrakt kommend), (4) separater N_2-Strom, (5) Ausgang zur CO_2-Titration (C), (6) Kohle (1120°), (7) CuO (550°), (8) Ausgang zur CO_2-Titration (H).

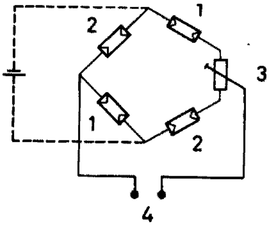

Abb. 3. Brückenschaltung des Titrators. Über den Fotowiderständen (1) und (2) sind die Interferenzfilter von 470 (1) und 610 nm (2) angeordnet. (3) Potentiometer zur Sollwerteinstellung des Farbtones, (4) Anschluss zum Steuergerät.

dies so aus, dass bei uns für den Routinebetrieb 2 Personen pro Automat eingesetzt sind, die abwechselnd einwiegen und die Apparatur bedienen. Unter diesen Bedingungen können im Mittel 100 Bestimmungen an einem Arbeitstag ausgeführt werden.

Der Erfolg dieser Methode war Anlass für uns, auch für die Elemente Kohlenstoff und Wasserstoff ein Schnellverfahren auszuarbeiten, zumal sich die oben erwähnte Verbrennungstechnik hierfür geradezu anbot. Auch garantierte die hohe Strömungsgeschwindigkeit eine entsprechend kurze Ausspülzeit. Das grosse Fragezeichen war aber die Endbestimmung sowohl bei Kohlenstoff als auch bei Wasserstoff. Wasserstoff aus getrennter Einwaage zu bestimmen, wäre in jedem Falle unrationell. Seine Miterfassung bei der Stickstoffbestimmung über Umsetzung des primär gebildeten Wassers mit Calciumcarbid oder -hydrid brachte nicht die erwarteten Ergebnisse. So blieb die Bestimmung von Kohlenstoff und Wasserstoff aus einer Einwaage die Methode der Wahl. Das messbare Endprodukt bei der Verbrennung des Kohlenstoffs ist Kohlendioxid. Neben der Leitfähigkeitsmessung[3,4] schien uns vor allem die Titration der Kohlensäure in nichtwässriger Phase besonders geeignet[5–7]. Das gleichzeitig anfallende Wasser kann nach Ausfrieren direkt[8,9] oder über entsprechende Umsetzungsprodukte indirekt bestimmt werden. Auf Grund der Ergebnisse zahlreicher Vorversuche entschieden wir uns schliesslich für ein Verfahren, das der Automation der C,H-Bestimmung sehr entgegenkam. Das Wasser wird im Stickstoffstrom über auf 1120° erhitzte Kohle geleitet, das gebildete Kohlenmonoxid zu Kohlendioxid oxidiert und dieses analog der C-Bestimmung titriert. Für beide Elemente ergibt sich somit dieselbe Endbestimmung, die zudem mittels kolorimetrischer Endpunktsindikation vollautomatisch ausgeführt werden kann.

EXPERIMENTELLER TEIL

*Aufbau des C,H-Automaten**

Der von uns entwickelte Automat besteht aus folgenden Teilen: 1. Der Verbrennungsapparatur einschliesslich der beiden Gasquellen Sauerstoff und Stickstoff, 2. dem Trennsystem für Kohlensäure und Wasser einschliesslich der Anlage zur Überführung des Wassers in Kohlensäure, 3. den beiden Titrierständen mit Motorkolbenbüretten und zentralen Vorratsgefässen für Absorptions- und Titrierlösung, 4. dem Steuerteil zur automatischen Titration und Programmschaltwerk für den gesamten Analysenzyklus, sowie 5. dem Drucker.

Die Verbrennungsapparatur (Abb. 1) besteht aus der Probeneinschleusvorrichtung, dem senkrecht angeordneten Verbrennungsrohr mit Verbrennungskammer, Oxidationsteil und seitlichem Abgang sowie dem Reduktionsrohr. Als Oxidationskatalysator verwenden wir Kupferoxid, das auf 800° erhitzt wird. Halogene und Schwefeldioxid werden an Silberwolle absorbiert, die auf 500–600° gehalten wird. Das Kupfer im Reduktionsrohr wird auf 500° erhitzt. Die Verbrennungskammer, in die zur Erhöhung der Lebensdauer des Rohres eine Quarzhülse eingesetzt ist, wird auf 950° erhitzt. Wegen dieser hohen Temperatur war es notwendig, die Kupferoxid schicht im Oxidationsteil tiefer beginnen zu lassen, um ein Sintern zu verhindern. Der entsprechende Raum bis zur eingesetzten Quarzhülse wurde mit Quarzsplitter ausgefüllt. Das System zur Auftrennung (Abb. 2) von Kohlensäure und Wasser besteht aus zwei Spiralen aus Silberrohr als Kühlfallen, die umschichtig (wechselseitig)

---

* Kann komplett von der Firma W. C. Heraeus, Hanau, bezogen werden.

aufgeheizt und gekühlt werden. Vier Magnetventile schalten abwechselnd die gekühlte Spiralfalle in den mit etwa 50 ml/min von der Verbrennungsapparatur kommenden Gasstrom ein, während gleichzeitig die aufgeheizte Falle von einem separaten Stickstoffstrom (90 ml/min) ausgespült wird. Das ausgetriebene Wasser wird durch Überleiten des Wasserdampfes über Kohle bei 1120° und Oxidation des gebildeten Kohlenmonoxides in einer nachgeschalteten Kupferoxidschicht in Kohlendioxid übergeführt.

Zur Endbestimmung verwenden wir den von BRODKORB UND SCHERER[10] beschriebenen Automaten zu kolorimetrischen Titration in einer stark vereinfachten Ausführung. Das Wesentliche an diesem Titrator ist das automatische Abstellen der Titration beim Erreichen eines bestimmten Farbtones. Wir wählten als Titrierlösung Tributylmethylammoniumhydroxid. Ebenfalls geeignet ist Tetrabutylammoniumhydroxyd. Als Indikator hat sich Thymolphthalein am besten bewährt. Die Steuerung (Abb. 3) erfolgt über vier in einer Brückenschaltung zusammengefassten lichtempfindlichen Widerständen, denen jeweils ein Filter zugeordnet ist, sodass beim Farbumschlag ein Spannungswechsel an den Endpunkten der Brücke auftritt. Die Filter sind paarweise angeordnet und entsprechen der Farbe der Lösung sowie deren Komplementärfarbe, bei Thymolphthalein Blau und Gelb. Das Gerät erlaubt demnach eine spezifische Messung der Farbänderung des Indikators und unterscheidet sich dadurch grundlegend von den üblichen Geräten zur photometrischen Titration.

Die verwendeten Titrierstände wurden speziell für diese kolorimetrische Titration der Kohlensäure entwickelt. Das Titriergefäss (Abb. 4) fasst etwa 20 ml Dimethylformamid, dem zur Erhöhung der Absorptionskraft geringe Mengen Monoäthanolamin zugesetzt sind. Ein Magnetrührer sorgt für ausreichende Durchmischung bei Absorption und Titration des CO_2.

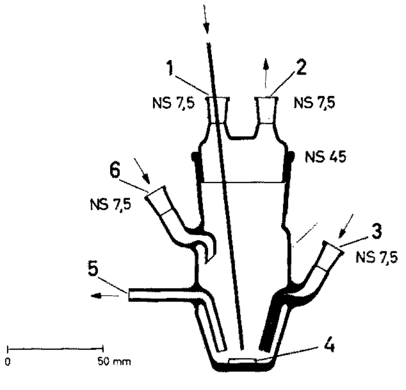

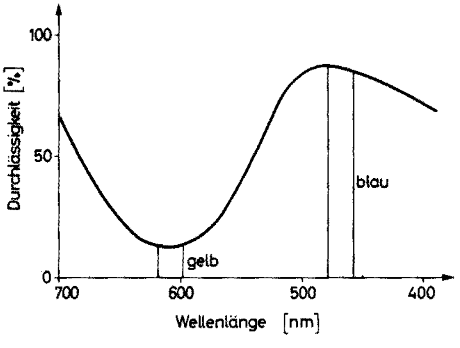

Abb. 4. Titriergefäss. (1) Zulauf der Titrierlösung, (2) Gasaustritt (N_2), (3) Gaseintritt ($CO_2 + N_2$), (4) Magnetrührer, (5) Absaugung von Absorption- und Titrierlösung mittels Unterdruck, (6) Zulauf der Absorptionslösung.

Abb. 5. Absorptionskurve von Thymolphthalein.

Die Bestimmung des Wirkwertes der Titrierlösung erfolgt durch Titration einer definierten Menge CO_2 aus einem Rezipienten bekannten Volumens. Die zur kolorimetrischen Titration notwendigen Filter und Fotowiderstände sind in eine Kunststoffhalterung eingesetzt, in die das Titriergefäss eingepasst wird. Auf diese Weise ist eine ausreichend grosse Schichtdicke der Lösung garantiert. Wir arbeiten mit vier Filtern und entsprechend vier Fotowiderständen. Als Filter verwenden wir Interferenzfilter, da diese eine besonders geringe Bandbreite aufweisen (Abb. 5). Bei farbloser Lösung, im sauren Bereich also, werden alle vier Fotowiderstände gleich belichtet. Im Äquivalenzpunkt wird die Lösung blau, was bedeutet, dass die beiden Fotowiderstände unter den Gelbfiltern von 610 nm plötzlich weniger Licht erhalten, als die Fotowiderstände unter den Blaufiltern von 470 nm. Dies führt naturgemäss zu einer Verstimmung der Brücke. Die dabei auftretende Diagonalspannung ist gleichzeitig Eingangssignal für das Steuergerät der Motorbürette. Die gesamte Anordnung ist von einem Schutzgehäuse umgeben, das auch die Lichtquelle für das notwendige diffuse Licht enthält. Der gesamte Analysenzyclus, einschliesslich der Endbestimmung, läuft automatisch ab. Das digital angezeigte Volumen der Titrierlösung kann ausgedruckt oder direkt einem Rechner zugeführt werden. Zu beachten ist dabei allerdings, dass der CO_2-Wert aus dem Wasser nicht von der laufenden Analyse, sondern von der vorhergegangenen Verbrennung stammt. Der Analysenzyklus ist also phasenverschoben.

Ein Zyklus dauert beim derzeitigen Stand der Automation 8 Min. Diese Zeit beinhaltet ausreichend Sicherheitsreserven für schwer verbrennbare Substanzen und umfasst auch die Vorbereitung der beiden Titrierzellen einschliesslich der Vortitration auf den eingestellten Blauwert, wozu 2 Min erforderlich sind. Im Routinebetrieb rechnen wir mit durchschnittlich 40 Analysen pro Arbeitstag, pro Automat und Person.

Reagenzien

Absorptionslösung. 150 Teile Dimethylformamid (destilliert), 1 Teil Monoäthanolamin und 1 Teil Thymolphthalein (0.2%ig in Äthylalkohol).

Titrierlösung. Etwa 0.02 *N* Tributylmethylammoniumhydroxid in *tert*-Butylalkohol, dem 5–10% Benzol zugesetzt sind. Tributylmethylammoniumhydroxid kann als 40%ige, wässrige Lösung von der Fa. Fluka A.G., Buchs (Schweiz) bezogen werden.

Ausführung der Bestimmung

Zur Ausführung der Analyse werden 3–5 mg Substanz in einem Schiffchen aus Aluminiumfolie eingewogen, mit etwa 50 mg Braunstein überschichtet und das Schiffchen anschliessend mit Hilfe einer Pinzette zusammengefaltet. Flüssigkeiten werden in dünnwandigen Kapillaren aus leicht schmelzbarem Phosphatglas* eingewogen. Braunstein hat gegenüber anderen Oxidationsmitteln den Vorteil, dass er nicht nur ein Sauerstoffdonator ist, sondern auch Halogene, Schwefelwasserstoff und Schwefeldioxid teilweise absorbiert. Auch verhindert Braunstein eine Karbonatbildung, wodurch weitere "saure" Zuschläge nicht mehr notwendig sind. Um den unvermeidbaren Wasserblindwert entsprechend niedrig zu halten, muss allerdings der käufliche, gefällte Braunstein durch Glühen bei 800° im Sauerstoffstrom vorbehandelt werden. Durch Drücken des Startknopfes 1 am Steuergerät erfolgt automatisch die Vorbereitung für die Titration (Abb. 6). Über Magnetventile fliessen aus dem zentralen Vorratsgefäss jeweils *ca.* 20 ml Absorptionslösung in die beiden Titrierzellen, wo sie auf schwache Blaufärbung vortitriert werden. Der gewünschte Farbton ist an der Brücke mit Hilfe eines Potentiometers einstellbar.

Die Titrierlösung wird dabei zunächst in rascher Folge zugegeben. Das Auf-

---

* Phosphatglas kann von der BASF bezogen werden.

treten der ersten blauen Schlieren verstimmt die Brücke und die anfallende Spannung schaltet automatisch den Tastgang ein. Die Zugabe der Titrierlösung erfolgt nun nicht mehr kontinuierlich, sondern in kleinen Portionen von jeweils 0.01 ml. Die Zeit bis zur nächsten Entfärbung der Lösung und damit gekoppelten Wiedereinschaltung der Bürette wird gegen Ende der Bestimmung grösser. Erreicht sie 20 Sec, so schaltet die Zudosierung automatisch ab. Die Titration ist beendet. Die Motorkolbenbüretten werden automatisch auf 0 gestellt und der eigentliche Analysenzyklus kann beginnen (Abb. 7).

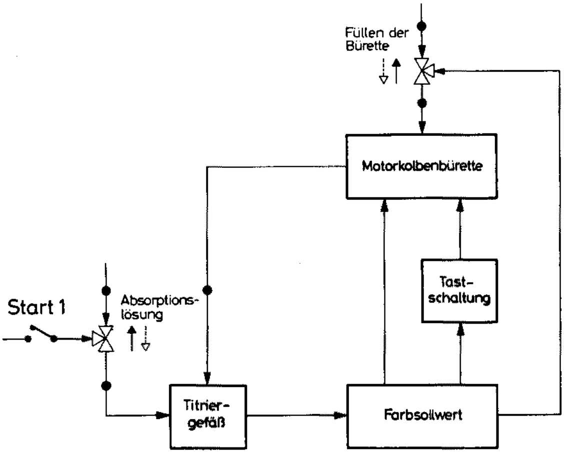

Abb. 6. Blockschaltbild der Vorbereitung der Titrationszellen (für C und H gleichzeitig).

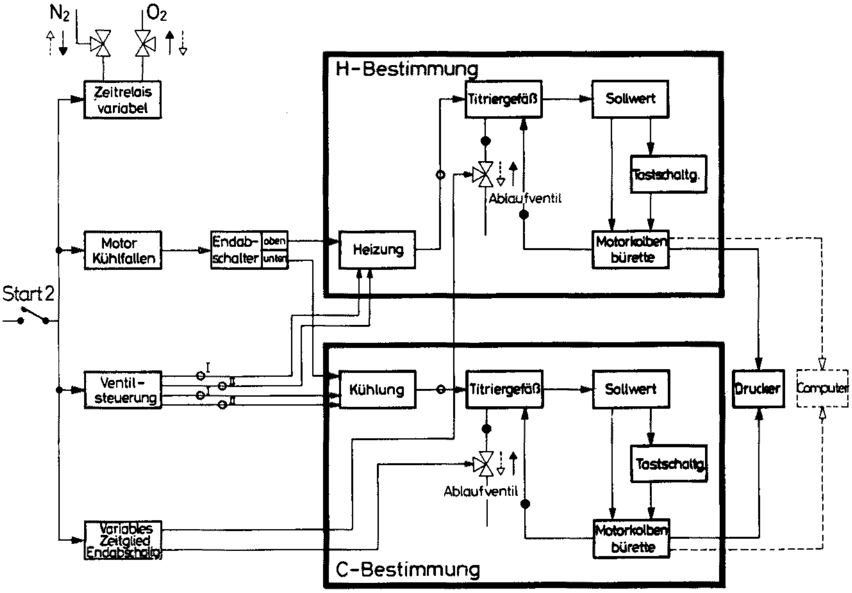

Abb. 7. Blockschaltbild des Analysenprogrammes. Der Block Ventilsteuerung (I und II) ist in Abb. 2 im Detail zu ersehen. Gasleitungen sind durch einen Kreis (o), Flüssigkeitsleitungen durch einen Punkt (●) symbolisiert.

Das Aluminiumschiffchen mit der Einwaage wird in den Napf der Einschleusvorrichtung gestellt und durch Drücken von Startknopf 2 der Gasstrom von Stickstoff auf Sauerstoff umgeschaltet. Gleichzeitig erfolgt auch die Umschaltung der Magnetventile für das Trennsystem Wasser und Kohlendioxid, sowie das Heben bzw. Senken der beiden Kühlfallen. Die Endabschaltung der Kühlfallen steuert schliesslich das Aufheizen der einen Silberspirale, die als Widerstand geschaltet ist. Mit dem separaten Stickstoffstrom wird das Wasser der vorangegangenen Analyse ausgetrieben, über Kohle und Kupferoxid in Kohlendioxid übergeführt und dieses schliesslich in der vorbereiteten Titrierzelle bestimmt. In der Zwischenzeit ist andererseits das Verbrennungsrohr mit Sauerstoff gefüllt, die Kontaktzone reaktiviert und die Probe wird durch Drehen des Napfes eingeworfen. Die Zeit in der Sauerstoff durch die Apparatur strömt, ist regelbar. Als zweckmässig erwiesen sich 1.5 Min. Anschliessend schaltet der Automat wieder auf Stickstoff um. Das Fallenlassen der Probe sollte 15–20 Sec nach Start 2 erfolgen. Nach Passieren der Silber- und Kupferschicht enthält das Treibgas nur noch Kohlendioxid und Wasser. Letzteres wird in der auf −60 bis −80° gekühlten Silberspirale kondensiert, während das CO_2 direkt in die zweite Titrierzelle gelangt und hier fortlaufend automatisch titriert wird. Die Automatik ist dabei so ausgelegt, dass auch nach Erreichen des Tastprogrammes bei erneutem Anfall von CO_2 die Titrierlösung wieder kontinuierlich zufliesst. Durch Fehlen der blauen Schlieren kommt die Brücke wieder in den abgeglichenen Zustand. Die Endabschaltung erfolgt in beiden Zellen gemeinsam.

Im Analysenprogramm wird also nicht auf eine 20 Sec lang bestehende Blaufärbung titriert, sondern aus Sicherheitsgründen generell eine Endzeit von 6 Min vorgegeben. Dies war notwendig, da bei der Titration des aus dem Wasser stammenden CO_2 anfallende Blindwerte ein automatisches Abschalten problematisch machen würden. Nach Ablauf dieser vorgegebener Zeit werden automatisch die Volumina der Titrierlösung ausgedruckt bzw. direkt einem Rechner zugeführt. Gleichzeitig werden beide Titriergefässe durch Anlegen von Unterdruck in ein Sammelgefäss entleert und sind damit für den nächsten Zyclus wieder einsatzbereit.

Berechnung

$$\%\,C(H) = \frac{(A-B)\cdot K\cdot 100}{E}$$

A = Gesamtverbrauch in ml
B = Blindwert in ml
E = Einwaage in mg
K = Konzentration der Titrierlösung entsprechend dem gegebenen Bürettenvolumen (zwischen 0.05 N und 0.02 N). 1 ml 0.05 N Tributylmethylammoniumhydroxidlösung entspricht 0.600 mg C (0.100 mg H); 1 ml 0.02 N entspricht 0.240 mg C (0.040 mg H).

ERGEBNISSE UND DISKUSSION

In der Tabelle (Tabelle I) sind Analysenwerte ausgewählter Testsubstanzen zusammengestellt, die die Zuverlässigkeit und Genauigkeit dieser Methode beweisen. Die angegebenen Werte sind jeweils Mittelwert aus 10 Verbrennungen. Die grösste

TABELLE I

ANALYSENWERTE AUSGEWÄHLTER TESTSUBSTANZEN

Substanz	*% C*		S^a	*% H*		S^a
	Berechnet	*Gefunden Mittelwert*		*Berechnet*	*Gefunden Mittelwert*	
Jodbenzoesäure	33.89	33.98	0.13	2.03	2.04	0.10
Kalium-biphthalat	47.05	47.07	0.15	2.47	2.57	0.15
Sulfaminsäure	0	0.11	0.15	3.11	3.13	0.16
Stearinsäure	76.00	76.02	0.15	12.76	12.60	0.21
Melamin	28.57	28.66	0.15	4.80	4.93	0.21
Harnstoff	20.00	20.12	0.20	6.71	6.63	0.18
Acetanilid	71.09	71.18	0.18	6.71	6.74	0.18
Kupferphthalocyanin	66.72	66.62	0.20	2.80	2.85	0.17
Pikrinsäure	31.45	31.54	0.15	1.32	1.44	0.14
2-Chlor-4-nitro-6- brom-anilin	28.66	28.63	0.19	1.60	1.79	0.21
p-Fluorbenzoesäure	60.02	59.99	0.12	3.57	3.61	0.13

[a] Standardabweichung.

Standardabweichung liegt sowohl bei Kohlenstoff als auch bei Wasserstoff nicht über 0.25%. Der grosse Vorteil der Methode ist vor allem aber der Zeitgewinn. Eine Beaufsichtigung des Automaten ist nicht notwendig, sodass lediglich die Einwaage und—augenblicklich noch—die Einschleusung der Probe manuell auszuführen sind. Dieser Vorgang der Probeneinführung kann selbstverständlich noch über eine Mehrkammereinrichtung automatisiert werden. Die Regelung erfolgt dabei über die zentrale Steuereinheit im Rahmen des normalen Analysenprogrammes. Damit ist aber gleichzeitig auch die Möglichkeit gegeben, die im Augenblick noch getrennt gestarteten Programme zu kombinieren. Nach Ablauf des Vorbereitungsprogrammes wird automatisch das Analysenprogramm gestartet und die Probe eingeschleust. Fasst die Mehrkammereinrichtung eine entsprechend grosse Anzahl Proben, so könnte man sogar daran denken, das Ende der Analyse, also das Entleeren der Titriergefässe, automatisch als Startsignal für den folgenden Zyclus zu benutzen. Vergleicht man abschliessend den Arbeitsaufwand unserer Schnellmethoden für C,H und N mit dem durchschnittlichen Aufwand der kommerziell erhältlichen C,H,N-Automaten, so ergibt sich im Augenblick folgendes Bild. Der Durchschnittswert pro Mann und Tag liegt bei uns bei 40 C,H oder 50 N-Bestimmungen. Auf C,H,N umgerechnet ergibt dies 20–25 Analysen. Nehmen wir an, dass die gleiche Zahl sich auch bei den C,H,N-Geräten erreichen lässt, was sicher nicht für alle gilt, so ergibt sich dennoch für unsere Arbeitsweise ein Plus aus den folgenden Gründen: 1. Grössere Einwaagen und damit eine geringere Anforderung an die Homogenität der Proben, was letzten Endes auch ein Zeitvorteil ist, 2. die Möglichkeit, jede Analyse zeitlich zu verfolgen und schliesslich, 3. vor allem aber die Unabhängigkeit von physikalischen Eichungen und damit die strenge Linearität zwischen Menge und Messwert.

ZUSAMMENFASSUNG

Es wird über eine Schnellmethode zur Mikrobestimmung von Kohlenstoff und Wasserstoff in organischen Substanzen berichtet. Die Methode arbeitet automatisch,

wobei der gesamte Analysenablauf durch ein Programmschaltwerk über Zeitrelais gesteuert wird. Die mit MnO_2 überschichtete Substanz wird in einem senkrecht angeordneten Quarzrohr im Sauerstoffstrom verbrannt. Zur vollständigen Oxidation werden die Verbrennungsgase über Kupferoxid geleitet. Das Ausspülen erfolgt im Stickstoffstrom. Wasser wird durch Ausfrieren abgetrennt und die Kohlensäure in die vorbereitete Titrierzelle geleitet. Zur Absorption wird eine aminhaltige Dimethylformamidlösung eingesetzt; die anschliessende Titration mit Tributylmethylammoniumhydroxid erfolgt automatisch mittels kolorimetrischer Endpunktsindikation. Der Verbrauch wird digital angezeigt und kann direkt ausgedruckt werden. Anschliessend wird das Wasser ausgeheizt, im Stickstoffstrom über Kohle geleitet und das gebildete Kohlenmonoxid durch Kupferoxid zu Kohlendioxid oxydiert. Die Endbestimmung erfolgt analog. Bei wechselseitiger Verwendung von zwei Gefrierfallen und zwei Titrationseinrichtungen kann die Wasserbestimmung parallel erfolgen. Die reine Analysenzeit für Kohlenstoff und Wasserstoff beträgt in diesem Falle acht Minuten.

SUMMARY

A fully automatic method for the rapid microdetermination of carbon and hydrogen is described. The sample is covered with manganese dioxide and burnt in a stream of oxygen in a vertical silica tube; the products of combustion are led over copper oxide to ensure complete oxidation. The apparatus is flushed with nitrogen; water is frozen out, and carbon dioxide is absorbed in a titration cell containing an amine in dimethylformamide. The carbon dioxide is titrated automatically with standard tributylmethylammonium hydroxide, with colorimetric end-point determination, the volume of titrant being displayed digitally and printed out. Water is vapourized in a stream of nitrogen and passed over carbon at 1120° to form carbon monoxide, which is then oxidized with copper oxide to carbon dioxide; this is absorbed and titrated as just described. The whole cycle is controlled automatically by time switches. By using duplicate freezing traps and titration cells, water from a previous combustion can be determined at the same time as carbon dioxide. The analysis time for both carbon and hydrogen is then 8 min.

RÉSUMÉ

On décrit une méthode rapide de micro-analyse du carbone et de l'hydrogène dans les substances organiques: méthode automatique avec programme et relais temporisés. La substance, recouverte d'une couche de MnO_2, est brûlée dans un courant d'oxygène, dans un tube de quartz vertical. Pour oxyder complètement les gaz de combustion, on les fait passer sur de l'oxyde de cuivre. Le rinçage a lieu dans un courant d'azote. L'eau est séparée par congélation et l'acide carbonique est introduit dans la cellule de titrage préparée. Pour l'absorption, on utilise une solution de diméthylformamide contenant une amine. CO_2 est titré automatiquement à l'aide d'hydroxyde de tributylméthylammonium avec indication du résultat en code digital. Ensuite l'eau chauffé est entraînée sur du charbon; l'oxyde de carbone formé est oxydé en gaz carbonique par l'oxyde de cuivre. La détermination finale a lieu de la même manière. En utilisant alternativement deux pièges à congélation et deux

dispositifs de titrage, on peut déterminer l'eau parallèlement. Le temps nécessaire à l'analyse proprement dite du carbone et de l'hydrogène est dans ce cas de 8 minutes.

LITERATUR

1 Fa. SARTORIUS GmbH, Göttingen (Deutschland); vgl. H. D. KREFT, *Glas-Instr.-Tech. Fachz. Labor*, 12 (1968) 292.
2 W. MERZ, *Z. Anal. Chem.*, 237 (1968) 272.
3 H. MALISSA, *Mikrochim. Acta*, (1957) 553; (1960) 127.
4 W. STUCK, *Mikrochim. Acta*, (1960) 421.
5 L. BLOM UND L. EDELHAUSEN, *Anal. Chim. Acta*, 13 (1955) 120.
6 P. BRAID, J. A. HUNTER, W. H. S. MASSIE, J. D. NICHOLSEN UND B. F. PEARCE, *Analyst*, 91 (1966) 439.
7 A. CAMPIGLIO, *Mikrochim. Acta*, (1968) 106.
8 F. A. KEIDEL, *Anal. Chem.*, 31 (1959) 2043.
9 F. SALZER, *Z. Anal. Chem.*, 205 (1964) 66.
10 E. BRODKORB UND H. SCHERER, *Ind. Chim. Belge*, Nr. Spezial I, 32 (1967) 137; *DBP 1279384*; *DBP 1291981*.

Analytica Chimica Acta
Elsevier Publishing Company, Amsterdam
Printed in The Netherlands

ULTRAVIOLET EMISSION AND ABSORPTION SPECTRA PRODUCED BY ORGANIC COMPOUNDS IN OXYHYDROGEN FLAMES[1]

PART I. EMISSION SPECTRA

V. J. SMITH AND J. W. ROBINSON
Chemistry Department, Louisiana State University, Baton Rouge, La. 70803 (U.S.A.)

(Received August 8th, 1969)

Emission and absorption spectra of flames containing organic materials have been studied for some time[2-7]. An attempt is made here to extend the information to analytical chemistry. The purpose of the present investigation is three-fold: (*a*) to indicate sources of spectral interferences in flame photometry and atomic absorption, (*b*) to add to the knowledge of physical and chemical processes in flames employed for analytical work, and (*c*) to study the development of analytical methods for the determination of organic compounds by flame spectroscopy. Some preliminary results have already been reported[8,9].

Spectral interferences in flame emission spectroscopy include those produced by emission from excited OH radicals in the determinations of bismuth[10-13], magnesium[10,11,14], copper[15], aluminum[11,16], molybdenum[11], and vanadium[11,16]; emission from CH radicals in determinations of chromium[14]; emission from C_2 radicals in determinations of beryllium[17]; emission from CH and C_2 radicals in determinations of lanthanum[14]; and emission from CN radicals in determinations of molybdenum[18].

The involved sequence of events which occurs in the flame after the sample has been introduced includes (*a*) solvent evaporation, (*b*) solute dissociation and vaporization, (*c*) excitation of the species of interest, (*d*) emission, and (*e*) absorption. Each step is dependent on the physical and chemical conditions in the flame[9,11,16,18-44]. KIRKBRIGHT AND WEST *et al.*[16,18,44] investigated flame processes by examining emission spectra produced in and by nitrous oxide–acetylene flames. They discussed spectral interferences produced. COWLEY *et al.*[33] investigated flame processes by examining atomic and molecular emission and absorption spectra produced in and by oxyacetylene flames.

Nonmetals can be determined analytically by measuring their flame emission spectra[20,45-54]. GILBERT[20] reported a sensitivity of 0.01% of an alcohol by measuring emission from CH and C_2 radicals in hydrogen flames. By measuring emission from molecular fragments DAGNALL *et al.*[45,46] and SYTY AND DEAN[47] observed detection limits in the p.p.m. range for compounds containing phosphorus and sulfur. MCCREA AND LIGHT[48], using the limited area flame spectrometry technique to observe reaction zones, investigated emission responses produced when hydrocarbon–methanol solutions were introduced into oxyhydrogen and air–hydrogen flames. In the

0.1–1.0 molal range they found a linear relationship between emission intensities at 4315 Å (CH) and 5165 Å (C_2) and the concentrations of a given hydrocarbon. PARSONS[54] showed that geometrical isomers can be distinguished by flame spectroscopy. He studied CH and C_2 emission produced by normal and branched alcohols in hydrogen-entrained air flames.

EXPERIMENTAL

Equipment

All data were obtained with a Beckman Atomic Absorption Assembly, consisting of the lamp power supply, gas regulator unit, model DB-G spectrophotometer, 10-in laboratory potentiometric linear-log recorder, scale expander, and a turbulent flow burner assembly with one small-bore Beckman total consumption burner in the central position. Hoke flowmeters (62222 AAL and 62222 AAD) were connected between the gas regulator unit and the burner, and standard oxygen and hydrogen flows were read directly in l/min.

Compounds studied

The compounds studied were cyclohexane, benzene, toluene, distilled water, ethanol, butanol, anisole, methyl isobutyl ketone, amyl acetate, acetic acid, butylamine, pyridine, nitroethane, nitropropane, ammonium hydroxide, tributyl phosphate, triethyl phosphate, phosphoric acid, ammonium dihydrogen phosphate, thiophene, dimethyl sulfoxide, chloroform, and butyl chloride (from U.S. Industrial Chemicals Co., Matheson Coleman and Bell, Mallinckrodt, Allied Chemical, J. T. Baker Chemical Co., Fisher Scientific Co., and Eastman Organic Chemicals). In general the solvents were reagent grade, containing 0.002% or less residue after evaporation. Anisole, methyl isobutyl ketone, amyl acetate, butylamine, nitroethane, nitropropane, tributyl phosphate, triethyl phosphate, thiophene, and butyl chloride were practical grade. The compounds were not purified before use.

Procedure

Gas flow rates were 3.5 l/min of oxygen and 10 l/min of hydrogen.

Unless specified otherwise, solutions were aspirated into the flame with oxygen. For aspiration with hydrogen the oxygen and hydrogen gas lines were switched at the burner.

Desired flame heights were obtained by positioning the burner so that the beam from a lamp focused on the lens leading to the monochromator would pass through the vertical axis of the flame at known distances above the tip of the burner.

The flame emission profiles were obtained with an aperture having a 1.8 × 0.6-cm horizontal slit between the flame and the lens leading to the monochromator.

For scanning over extended time periods of several minutes, organic solvents were contained in a cylindrical glass tube approximately 30 cm long and 70 ml in capacity with a small hole for the burner capillary in one end and a larger hole in the other end for sample introduction. For smaller periods of time, 5- or 10-ml glass beakers, covered with aluminum foil into which a hole was punctured for the capillary, were used.

The spectral region between 2000–6500 Å was investigated.

RESULTS AND DISCUSSION

Wavelengths of band maxima and identification of the species emitting

The prominent emission bands that were observed are listed in Table I by wavelength and species emitting.

Spectra from the oxyhydrogen flame exhibited bands of the 3064 Å OH system[19,55]. When organic solvents were aspirated into the flame, the emission intensity of the flame was generally increased and spectra in the visible and ultraviolet regions exhibited bands produced by excited fragments formed in the flame from the flame gases and organic compounds (Figs. 1–11).

When solvents containing carbon, hydrogen, and/or oxygen atoms were aspirated into the flame, in addition to OH bands, the 3900 Å CH, the 4300 Å CH, and the Swan C_2 systems were observed[19,33,54,55], as shown in Fig. 4.

When organic solvents containing nitrogen atoms were aspirated into the flame,

TABLE I

EMISSION BANDS PRODUCED BY OXYHYDROGEN FLAMES INTO WHICH ORGANIC COMPOUNDS WERE INTRODUCED

Wavelength of band maxima (Å)[a]	*Emitting species*	*Wavelength of band maxima (Å)*[a]	*Emitting species*
2140	CN, NO	3590	CN
2250	CN, NO	3640	Hg
2300	PO	3850	CN
2360	CN, NO	3870	CN
2370	PO	3870	CH
2460	PO	3890	CH
2470	CN, NO	4040	Hg
2530	PO	4160	CN
2580	CN, NO	4180	CN
2580	CCl	4200	CN
2580	CS	4220	CN
2600	CS	4310	CH
2620	OH	4360	Hg
2690	OH	4500	NH
2830	OH	4680	C_2
2890	OH	4700	C_2
2950	OH	4720	C_2
3070	OH	4740	C_2
3090	OH	5130	C_2
3240	SH	5160	C_2
3250	PO	5460	C_2
3260	PO	5470	Hg
3270	PO	5500	C_2
3280	SH	5540	C_2
3360	NH	5580	C_2
3370	NH	5640	C_2
3400	PH	5900	Na
3430	OH	9300	H_2O
3480	OH	9700	H_2O

[a] Wavelengths were measured to ±30 Å.

in addition to emission from excited OH, CH, and C_2 fragments, bands in the 2000–2700 Å region, probably due to NO and/or CN fragments[16,20,55,56], the 3360 Å NH system[19,55], the violet CN system[19,55,57], and a band at 4500 Å, probably due to NH[55], were observed (Figs. 1 and 5). Nitroethane and concentrated ammonium hydroxide produced NH emission.

In addition to OH, CH, and C_2 bands, when tributyl or triethyl phosphate was

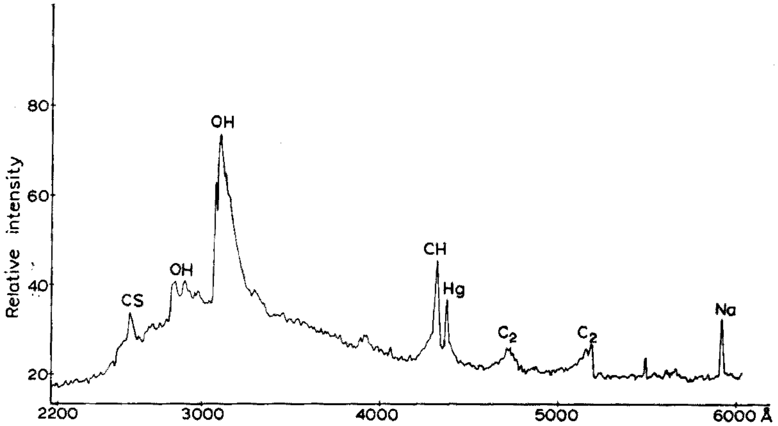

Fig. 1. Emission bands produced by excited NO and CN fragments. Pyridine was sprayed into the flame. Flame height 0.75 cm.

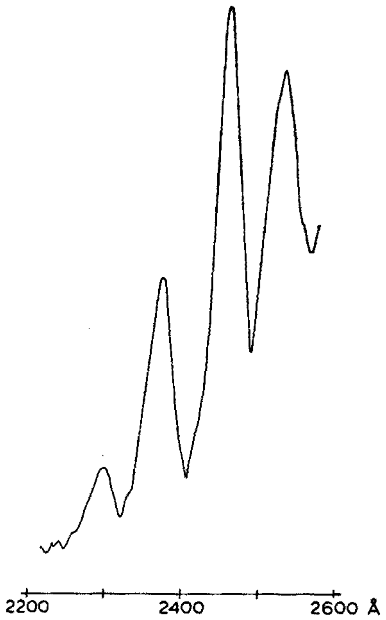

Fig. 2. Emission bands produced by excited PO fragments. Triethyl phosphate was sprayed into the flame. Flame height 0.75 cm.

Fig. 3. Emission produced by excited CCl fragments. Chloroform was sprayed into the flame. Flame height 0.75 cm.

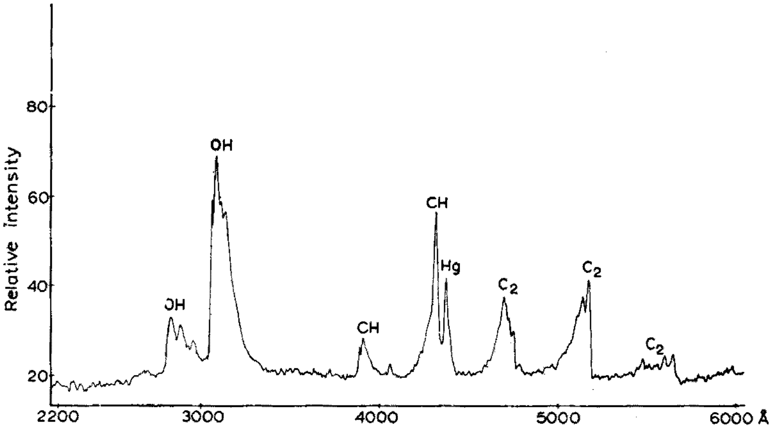

Fig. 4. Flame emission spectrum of benzene 0.75 cm above the burner. Slit 0.30 mm. Gain 7.5. Oxygen 3.5 l/min. Hydrogen 10 l/min.

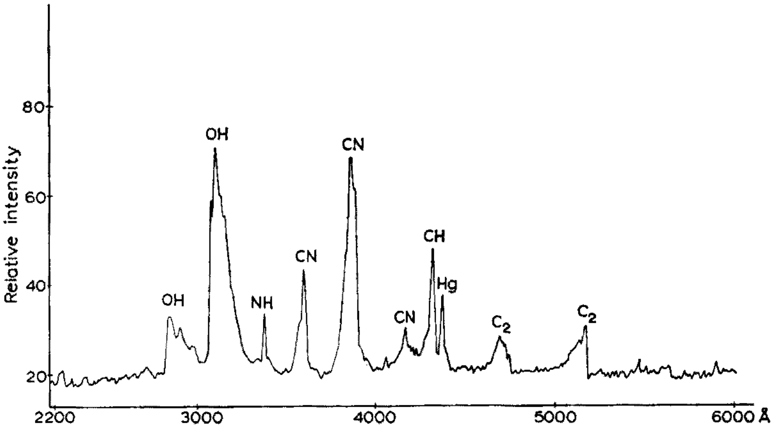

Fig. 5. Flame emission spectrum of pyridine 0.75 cm above the burner. Slit 0.30 mm. Gain 7.5. Oxygen 3.5 l/min. Hydrogen 10 l/min.

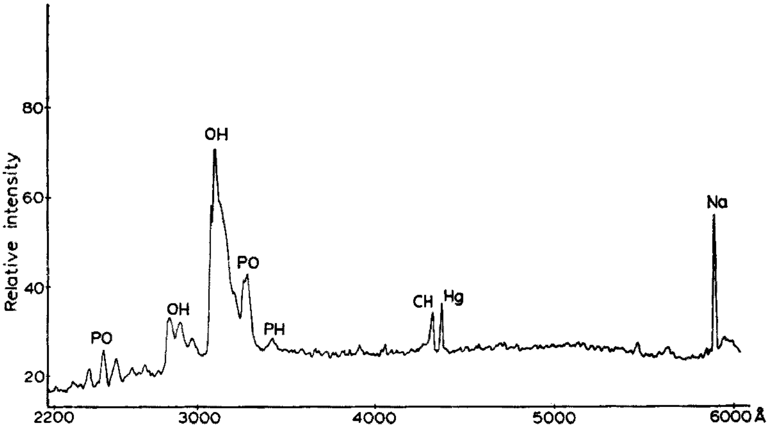

Fig. 6. Flame emission spectrum of tributyl phosphate 0.75 cm above the burner. Slit 0.30 mm. Gain 7.5. Oxygen 3.5 l/min. Hydrogen 10 l/min.

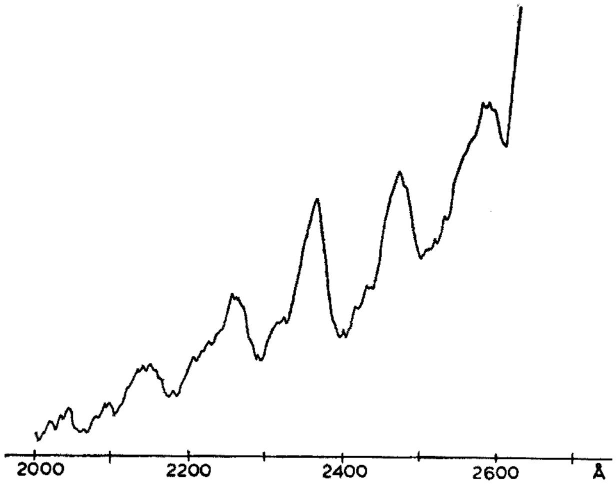

Fig. 7. Flame emission spectrum of thiophene 0.75 cm above the burner. Slit 0.30 mm. Gain 7.5. Oxygen 3.5 l/min. Hydrogen 10 l/min.

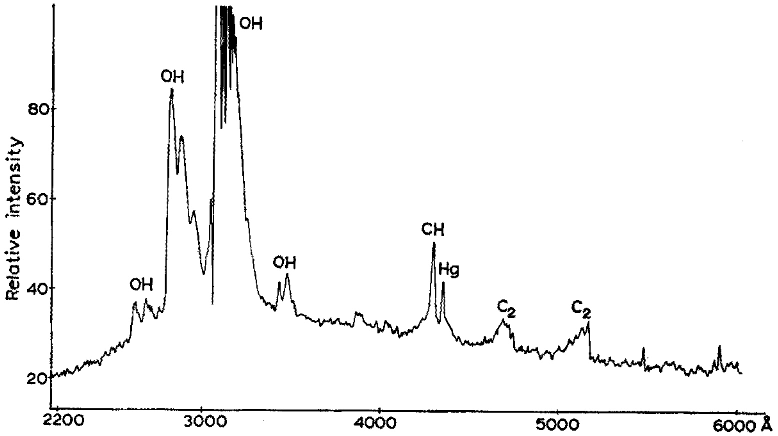

Fig. 8. Flame emission spectrum of benzene 2 cm above the burner. Slit 0.30 mm. Gain 7.5. Oxygen 3.5 l/min. Hydrogen 10 l/min.

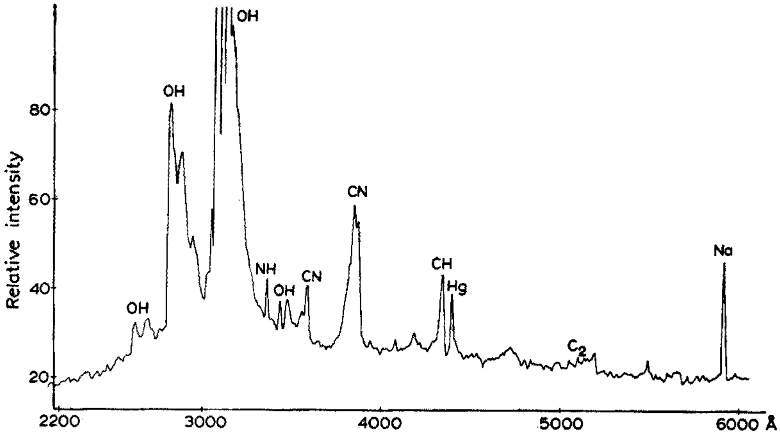

Fig. 9. Flame emission spectrum of pyridine 2 cm above the burner. Slit 0.30 mm. Gain 7.5. Oxygen 3.5 l/min. Hydrogen 10 l/min.

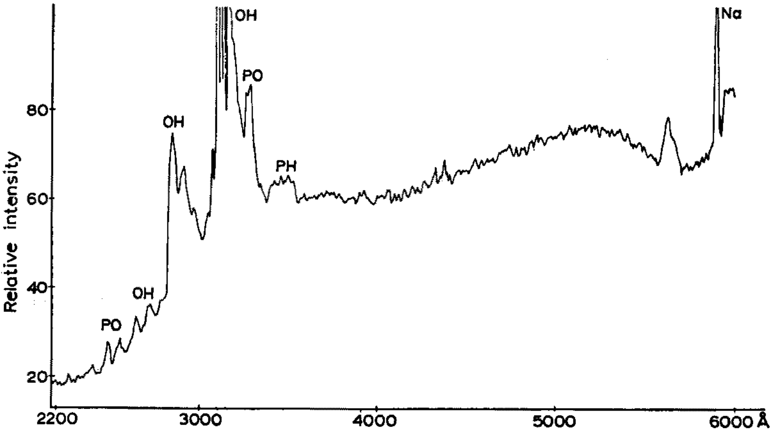

Fig. 10. Flame emission spectrum of tributyl phosphate 2 cm above the burner. Slit 0.30 mm. Gain 7.5. Oxygen 3.5 l/min. Hydrogen 10 l/min.

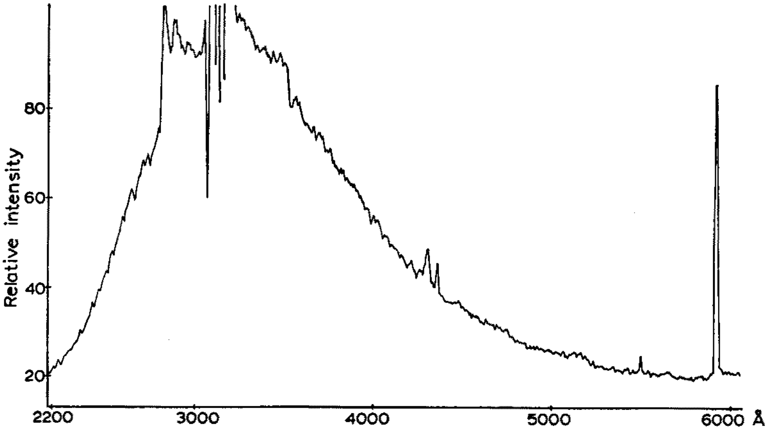

Fig. 11. Flame emission spectrum of thiophene 2 cm above the burner. Slit 0.30 mm. Gain 7.5. Oxygen 3.5 l/min. Hydrogen 10 l/min.

sprayed into the flame, the β and γ PO and the 3400 Å PH (some emission from PO may also have been detected at this wavelength) systems were observed[51,55] (Figs. 2 and 6). Concentrated phosphoric acid and a 15% aqueous solution of ammonium dihydrogen phosphate also produced PO emission.

When dimethyl sulfoxide or thiophene was sprayed into the flame, CS bands[20,55] and the 3237 Å SH system[55] were observed (Fig. 7). Several weak bands were also observed between 3000 and 4500 Å indicating the formation in the flame of other excited molecular fragments containing sulfur, *e.g.* SO and S_2[45,51,55].

Solvents containing chlorine produced a band at 2580 Å, probably caused by excited CCl fragments[55] (Fig. 3).

Emission produced by C_2 fragments when chloroform was aspirated into the flame, and emission produced by NH fragments when nitroethane was introduced into the flame, were evidence of the involved chemical reactions occurring in the flame.

An emission band at 5900 Å caused by sodium impurity[14,58] was frequently observed.

Lines at 3640, 4040, 4360, and 5470 Å, which also appeared when the region was scanned without the flame were produced by emission from mercury in the fluorescent lights in the laboratory[58].

Comparisons between emission spectra produced by different compounds

Figures 4 through 11 show emission spectra at flame heights of 0.75 and 2.0 cm, respectively, produced when benzene, pyridine, tributyl phosphate, and thiophene were introduced into the flame.

Variations in the aspiration rates (Table II) and in the chemical and physical processes in the flames produced differences between spectra obtained from different solvents.

TABLE II

SOLVENT ASPIRATION RATES

(Gas flow rates: oxygen (aspirating) 3.5 l/min, hydrogen 10.0 l/min)

Solvent	*ml aspirated into the flame per min*	*Solvent*	*ml aspirated into the flame per min*
Benzene	1.3	Pyridine	1.0
Cyclohexane	1.1	Nitroethane	1.2
Distilled water	1.0	Tributyl phosphate	0.3
Butanol	0.5	Triethyl phosphate	0.6
Amyl acetate	1.0	Thiophene	1.3
Methyl isobutyl ketone	1.4	Dimethyl sulfoxide	0.5
Anisole	0.9	Chloroform	1.1
Acetic acid	0.7	Butyl chloride	1.7
Butylamine	1.5		

The total consumption burner produces a turbulent diffusion flame[2,19,20,41,59], in which there is more intermixing of the flame zones and an effectively larger reaction zone than in a premixed flame. Results[59] indicate that for oxyhydrogen flames the region of non-equilibrium is restricted to the reaction zone in the immediate vicinity of the burner. The sizes of the sample drops reaching the flame vary and a significant number of drops passes through the flame without being completely evaporated.

The sizes, shapes, and structures of the flames varied for different solvents. The flame by itself was visible to a height of 6 cm and had a maximum diameter of about 1 cm, approximately 4 cm above the tip of the burner. When relatively non-combustible solvents such as ethanol or dimethyl sulfoxide were introduced, the size of the flame was increased slightly. When very combustible solvents such as benzene or pyridine were introduced, the flame became visible to a height of 8 cm and had a maximum diameter of about 2 cm at a distance of 5–6 cm above the tip of the burner. For all solvents the blue cone generally extended from 0.1 cm above the tip of the burner, where the flame began, to 1.5–2.0 cm above the burner.

As shown in Figures 4 through 11, the relative intensities of the bands produced by excited organic fragments are highest in the spectra from the blue reaction zone (at a flame height of 0.75 cm). Emission from OH and PO radicals is intense above the reaction zone. In addition to bands, emission observed over wide spectral regions was especially intense for solvents containing phosphorus and sulfur. Compounds containing phosphorus produce a strong continuum in flames in the visible region due to PO[2,47,60,61]. The high background emission produced by compounds containing sulfur can be attributed to the presence of SO_2, which produces a strong continuous emission and also a violet or blue color in the flame[2].

Emission profiles

Flame emission profiles were obtained at several wavelengths by measuring emission intensities at selected heights above the base of the flame (Figs. 12–16). In order to obtain the data shown in Figs. 13–16, the signal from the flame was subtracted from signals obtained when solvents were sprayed into the flame. A flame height of zero corresponds to the top of the burner, or the base of the flame.

At 3090 Å the emission was most intense between flame heights of 2.0 and 4.0 cm (Fig. 12). Emission at this wavelength was produced by excited OH radicals.

Profiles at 4310 Å (emission produced by excited CH radicals), 4680 Å (C_2), 3860 Å (CN), and 3360 Å (NH), are similar (Figs. 13 and 14). Maximum emission was produced in the reaction zone.

The emission profiles of OH, CH, C_2, CN and NH fragments agree with the scans obtained at different flame heights as shown in Figs. 4–11. They also agree in general with reports in the literature[23,41,48].

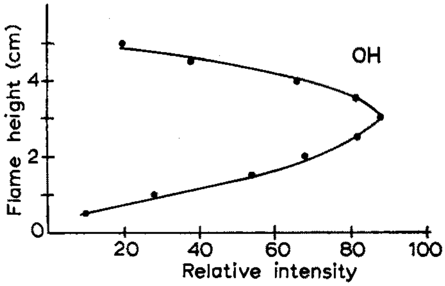

Fig. 12. Flame emission profile at 3090 Å. No solvent. Slit 0.25 mm. Gain 6.1.

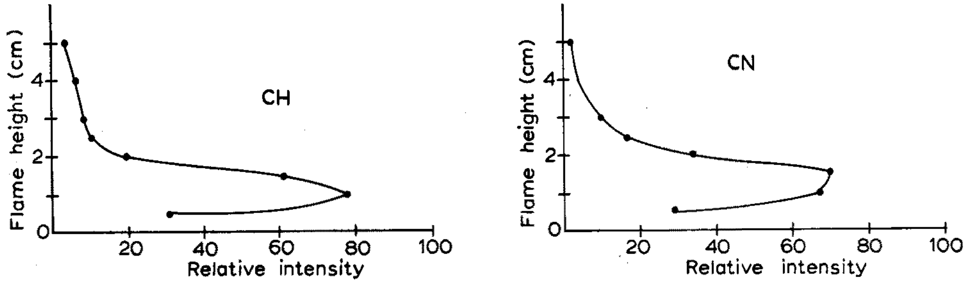

Fig. 13. Flame emission profile at 4310 Å. Benzene was sprayed into the flame. Slit 0.25 mm. Gain 6.8.

Fig. 14. Flame emission profile at 3860 Å. Pyridine was sprayed into the flame. Slit 0.20 mm. Gain 6.8.

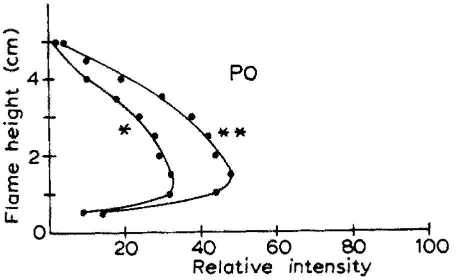

Fig. 15. Flame emission profile at 2460 Å. Tributyl phosphate (*) and triethyl phosphate (**) were sprayed into the flame. Slit 0.25 mm. Gain 7.7.

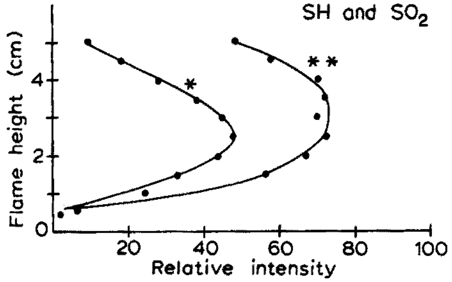

Fig. 16. Flame emission profile at 3280 Å. Dimethyl sulfoxide (*) and thiophene (**) were sprayed into the flame. Slit 0.25 mm. Gain 6.9.

Profiles obtained for tributyl and triethyl phosphates at 2460 Å (PO) show maximum emission intensities between flame heights of 0.5 and 2.0 cm and intense emission above the reaction zone (Fig. 15). Profiles obtained for the same compounds at 3270 Å (PO) show maximum emission intensity between flame heights of 1.5 and 3.5 cm. Profiles for PO fragments agree with spectra shown in Figs. 6 and 10.

The emission profile obtained for thiophene at 2590 Å (CS and SO_2) shows maximum emission intensity in the reaction zone and intense emission above the reaction zone. Profiles obtained for emission produced by dimethyl sulfoxide and thiophene at 3280 Å (SH and SO_2) show maximum intensities between flame heights of 1.5 and 4.5 cm (Fig. 16). The profiles agree with scans obtained at different flame heights (Figs. 7 and 11).

Continuous background emission produced by solvents containing phosphorus and sulfur probably contributes significantly to intensity measurements recorded in the flame profile studies.

The emission profile produced by chloroform at 2580 Å shows that maximum emission intensity from CCl fragments comes from the reaction zone.

Sensitivity estimates obtained by measuring emission intensities of NH and CH radicals

It was found that solutions of organic compounds produced emission bands characteristic of each component. Estimates of sensitivity for pyridine in ethanol solutions and ethanol in water solutions were obtained at flame heights of 0.75 cm and flow rates of 3.5 l/min of oxygen and 10 l/min of hydrogen.

For pyridine–ethanol solutions at 3360 Å, where emission from the NH fragment was observed, a concentration of $\geq 2\%$ pyridine was required to produce an emission signal significantly greater than that produced when ethanol was aspirated into the flame. For ethanol–water solutions at 4310 Å, where emission from the CH fragment was observed, a concentration of $\geq 5\%$ ethanol was required to produce an emission signal significantly greater than that produced when water was aspirated into the flame.

Effects of hydrogen–oxygen concentrations in the flame on emission spectra

Emission spectra were recorded from flames in which the hydrogen to oxygen gas ratios were 1:3.5 and 5:3.5. These were compared to the spectra recorded at a ratio of 10:3.5 shown in Figs. 4–11.

The sizes of the flames were drastically decreased at the lower hydrogen flow rates. The spectra obtained reflected the differences in the sizes of the flames. For example, emission produced in the oxyhydrogen flame by OH radicals was most intense 3 cm above the burner for a hydrogen flow rate of 10 l/min, 2 cm above the burner for a flow rate of 5 l/min, and 1 cm above the burner for a flow rate of 1 l/min.

Aspiration of the solution into the flame with hydrogen instead of oxygen should produce a more reducing atmosphere for the sample. The effect of aspirating with hydrogen on emission spectra obtained from several solvents was studied by switching the hydrogen and oxygen gas lines at the burner. Gas flow rates were 3.5 and 10 l/min of oxygen and hydrogen, respectively. The flame by itself was visibly 11 cm high with a diameter of 1.5 cm at a flame height of 8–9 cm. The introduction of benzene, pyridine, butyl alcohol, dimethyl sulfoxide, or tributyl phosphate increased the size of the flame only slightly due to relatively low aspiration rates: benzene 0.4 ml/min, pyridine 0.2 ml/min and the other solvents 0.1 ml/min.

No marked differences were observed in spectra obtained from flames in which hydrogen was the aspirating gas and spectra obtained from flames into which oxygen aspirated the compounds, indicating that excited species produced in both instances were the same.

SUMMARY

Ultraviolet emission spectra produced by aspirating organic compounds into oxyhydrogen flames have been investigated. Spectra are presented and compared. The prominent bands observed are listed by wavelength and species emitting. Flame emission profiles for organic and inorganic fragments are presented. Maximum emission by organic fragments occurred in the reaction zone of the flame. Emission by OH and fragments containing phosphorus or sulfur was intense above and within the reaction zone of the flame. Spectra obtained by varying the hydrogen-to-oxygen ratio in the flame and by aspirating with hydrogen instead of oxygen reflected the different sizes of the resulting flames. The bands observed were similar. Estimates of detection limits obtained for pyridine and ethanol by measuring the intensities of emission from NH and CH fragments were $\geq 2\%$ pyridine in ethanol and $\geq 5\%$ ethanol in water.

RÉSUMÉ

On examine les spectres d'émission ultraviolets produits en aspirant les composés organiques dans des flammes oxyhydrogène. Les spectres sont présentés et comparés. Les limites de détection obtenues pour la pyridine et l'éthanol sont estimées en mesurant les intensités d'émission des fragments NH et CH soit: $\geqq 2\%$ pour la pyridine dans l'éthanol et $\geqq 5\%$ pour l'éthanol dans l'eau.

ZUSAMMENFASSUNG

Es wurden u.v.-Emissionsspektren, welche beim Versprühen organischer

Verbindungen in einer Sauerstoff–Wasserstoff-Flamme entstehen, untersucht. Die Spektren werden angegeben und verglichen. Die beobachteten Hauptbanden werden nach Wellenlängen und Spezies tabelliert. Flammenemissionsprofile für organische und anorganische Fragmente werden angegeben. Die maximale Emission durch organische Fragmente tritt in der Reaktionszone der Flamme auf. Eine Emission durch OH und Fragmente, die Phosphor oder Schwefel enthalten, war besonders intensiv oberhalb und innerhalb der Reaktionszone der Flamme. Spektren, die durch ein Variieren des Wasserstoff–Sauerstoff-Verhältnisses und durch Versprühen von Wasserstoff anstelle von Sauerstoff erhalten wurden, spiegeln die unterschiedlichen Grössen der resultierenden Flammen wieder. Die beobachteten Banden waren jedoch ähnlich. Abschätzungen der Nachweisgrenzen für Pyridin und Äthanol durch Messung der Intensitäten der Emission von NH- und CH-Fragmenten ergaben etwa 2% für Pyridin in Äthanol und etwa 5% für Äthanol in Wasser.

REFERENCES

1 Taken in part from the *Ph.D. Dissertation* of V. J. SMITH, Louisiana State University, Baton Rouge, 1969.
2 A. G. GAYDON, *The Spectroscopy of Flames*, J. Wiley and Sons, New York, 1957.
3 A. G. GAYDON, *Advan. Spectry.*, 2 (1961) 23.
4 R. BLEEKRODE AND W. C. NIEUWPOORT, *J. Chem. Phys.*, 43 (1965) 3680.
5 K. H. BECKER AND K. D. BAYES, *J. Chem. Phys.*, 48 (1968) 653.
6 P. F. JESSEN AND A. G. GAYDON, *Combust. Flame*, 11 (1967) 11.
7 E. M. BULEWICZ, *Combust. Flame*, 11 (1967) 297.
8 J. W. ROBINSON AND V. SMITH, *Anal. Chim. Acta*, 36 (1966) 489.
9 J. W. ROBINSON, *Atomic Absorption Spectroscopy*, Marcel Dekker, New York, 1966.
10 K. RUDIGER, B. GUTSCHE, H. KIRCHHOF AND R. HERRMANN, *Analyst*, 94 (1969) 204.
11 G. F. KIRKBRIGHT AND T. S. WEST, *Appl. Opt.*, 7 (1968) 1305.
12 R. M. DAGNALL, D. C. THOMPSON AND T. S. WEST, *Talanta*, 14 (1967) 1467.
13 R. S. HOBBS, G. F. KIRKBRIGHT, M. SARGENT AND T. S. WEST, *Talanta*, 15 (1968) 997.
14 J. A. DEAN, *Flame Photometry*, McGraw-Hill, New York, 1960.
15 J. B. WILLIS, in *Methods of Biochemical Analysis*, Vol. 11, Interscience, New York, 1963, p. 1.
16 G. F. KIRKBRIGHT, M. K. PETERS AND T. S. WEST, *Talanta*, 14 (1967) 789.
17 H. C. ESHELMAN AND J. ARMENTOR, *Develop. Appl. Spectry.*, 3 (1964) 190.
18 G. F. KIRKBRIGHT, A. SEMB AND T. S. WEST, *Talanta*, 15 (1968) 441.
19 R. MAVRODINEANU AND H. BOITEUX, *Flame Spectroscopy*, J. Wiley and Sons, New York, 1965.
20 P. T. GILBERT, *Colloq. Spectros. Intern., 10th, University of Maryland, 1962*, Spartan Books, Washington, D.C., 1963, p. 171.
21 C. T. J. ALKEMADE, *Colloq. Spectros. Intern., 10th, University of Maryland, 1962*, Spartan Books, Washington, D.C., 1963, p. 143.
22 D. G. MITCHELL, *Lab. Pract.*, 16 (1967) 587.
23 B. E. BUELL, *Anal. Chem.*, 35 (1963) 372.
24 M. MARGOSHES, *Colloq. Spectros. Intern., 12th, Exeter, 1965*, Hilger and Watts, London, 1965, p. 26.
25 S. P. SINGHAL AND C. L. CHAKRABARTI, *Colloq. Spectros. Intern., 13th, Ottawa, 1967*, Adam Hilger, London, 1968, p. 286.
26 G. M. HIEFTJE AND H. V. MALMSTADT, *Anal. Chem.*, 40 (1968) 1860.
27 J. A. DEAN AND J. E. ADKINS, *Analyst*, 91 (1966) 709.
28 I. RUBESKA AND B. MOLDAN, *Analyst*, 93 (1968) 148.
29 C. T. J. ALKEMADE, *Anal. Chem.*, 38 (1966) 1252.
30 C. S. RANN AND A. N. HAMBLY, *Anal. Chem.*, 37 (1965) 879.
31 D. C. MANNING AND L. CAPACHO-DELGADO, *Anal. Chim. Acta*, 36 (1966) 312.
32 G. F. KIRKBRIGHT, *Lab. Pract.*, 17 (1968) 906.
33 T. G. COWLEY, V. A. FASSEL AND R. N. KNISELEY, *Spectrochim. Acta*, 23B (1968) 771.
34 J. B. WILLIS, *Appl. Opt.*, 7 (1968) 1295.
35 J. W. ROBINSON, *Anal. Chim. Acta*, 24 (1961) 254.
36 J. W. ROBINSON, *Anal. Chim. Acta*, 23 (1960) 479.
37 J. A. DEAN, *Develop. Appl. Spectry.*, 3 (1964) 207.

38 J. A. DEAN, *Develop. Appl. Spectry.*, 4 (1965) 443.
39 J. A. DEAN, *Develop. Appl. Spectry.*, 5 (1966) 317.
40 E. PUNGOR, *Flame Photometry Theory*, D. Van Nostrand, London, 1967.
41 D. J. HALLS AND E. PUNGOR, *Anal. Chim. Acta*, 44 (1969) 40.
42 J. RAMIREZ-MUNOZ, *Atomic-Absorption Spectroscopy*, Elsevier, Amsterdam, 1968.
43 S. R. KOIRTYOHANN AND E. E. PICKETT, *Anal. Chem.*, 40 (1968) 2068.
44 G. F. KIRKBRIGHT, M. SARGENT AND T. S. WEST, *Talanta*, 16 (1969) 245.
45 R. M. DAGNALL, K. C. THOMPSON AND T. S. WEST, *Analyst*, 92 (1967) 506.
46 R. M. DAGNALL, K. C. THOMPSON AND T. S. WEST, *Analyst*, 93 (1968) 72.
47 A. SYTY AND J. A. DEAN, *Appl. Opt.*, 7 (1968) 1331.
48 P. F. McCREA AND T. S. LIGHT, *Anal. Chem.*, 39 (1967) 1731.
49 M. BEROZA AND M. C. BOWMAN, *Environ. Sci. Technol.*, 2 (1968) 450.
50 D. A. LEATHARD AND B. C. SHURLOCK, *Advan. Anal. Chem. Instr.*, 6 (1968) 1.
51 A. J. McCORMACK, *M.S. Thesis*, Cornell University, 1963.
52 R. S. BRAMAN, *Anal. Chem.*, 38 (1966) 734.
53 W. L. CRIDER, *Anal. Chem.*, 41 (1969) 534.
54 M. L. PARSONS, *Analytical Letters*, 2 (1969) 229.
55 R. W. B. PEARSE AND A. G. GAYDON, *The Identification of Molecular Spectra*, 3rd Edn., Chapman and Hall, London, 1963.
56 K. H. BECKER AND K. D. BAYES, *J. Phys. Chem.*, 71 (1967) 371.
57 B. E. BUELL, *Anal. Chem.*, 34 (1962) 635.
58 W. R. BRODE, *Chemical Spectroscopy*, J. Wiley and Sons, New York, 1939.
59 L. DE GALAN AND J. D. WINEFORDNER, *J. Quant. Spectry. Radiative Transfer*, 7 (1967) 703.
60 R. HERRMANN AND C. T. J. ALKEMADE, *Chemical Analysis by Flame Photometry*, 2nd rev. Edn., Translated by P. T. GILBERT, Interscience, New York, 1963.
61 R. K. SKOGERBOE, A. S. GRAVATT AND G. H. MORRISON, *Anal. Chem.*, 39 (1967) 1602.

Analytica Chimica Acta
Elsevier Publishing Company, Amsterdam
Printed in The Netherlands

AN ANALYSIS OF THE THERMAL DECOMPOSITION OF TETRAETHOXYSILANE BY GAS CHROMATOGRAPHY

GEORGE W. HEUNISCH*
Electronic Components Laboratory, U.S. Army Electronics Command, Fort Monmouth, N.J. (U.S.A.)
(Received July 28th, 1969)

Thin insulating films are used by the semiconductor electronics industry for isolation purposes and for device fabrication. The film most commonly used for this purpose is silicon dioxide. In the special case of silicon devices, direct thermal oxidation at 1150° is entirely adequate. However, when substrates other than silicon are to be coated or a lower temperature is desirable, a deposition method must be used.

Deposition of silicon dioxide is often accomplished[1,2] by thermal decomposition of silane compounds. Tetraethoxysilane has received special emphasis because of its high oxygen content. A study of the tetraethoxysilane decomposition reaction should lead to better control and be useful in predicting the decompositions of other analogous compounds.

EXPERIMENTAL

The decomposition apparatus used is similar to that described by JORDAN[1] and used by the electronics industry. A flow diagram is shown in Fig. 1.

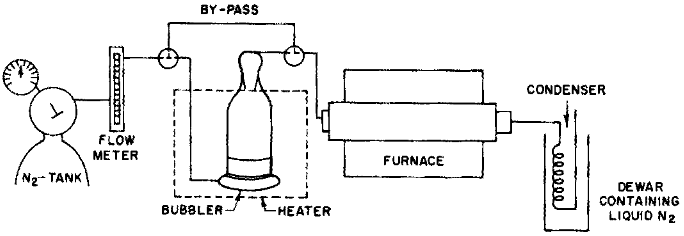

Fig. 1. Flow diagram of reaction apparatus.

Nitrogen carrier gas passes through the liquid tetraethoxysilane in the bubbler and carries the vapors into the heated furnace. Ordinarily, a substrate is placed in the furnace and coated with silicon dioxide produced by the vapor decomposition. The reaction products are collected in a spiral collection tube immersed in liquid nitrogen. Nitrogen carrier gas is allowed to flow, via the bypass, through the collection tube during immersion to prevent water vapor from entering the low pressure area produced. The bubbler is thermostatted with a water bath at 100°. The volumetric flow rate of carrier gas is monitored by a flow meter calibrated with a bubble counter similar to that used with gas chromatography. The furnace temperature is determined

---

* Present address: Continental Oil Company, Ponca City, Okla., U.S.A.

by measuring the EMF produced by a platinum–10% rhodium thermocouple. The temperature recorded is the maximum temperature in the furnace profile and is maintained to ±2°.

The products were analyzed with a Perkin-Elmer Model 154 D Vapor Fractometer equipped with a thermal conductivity detector. A 1-m, stainless steel (0.25″ o.d.) column packed with 4.14% polypropylene glycol on sieved 45/60 mesh Chromosorb P, which had been treated with dimethyldichlorosilane, was used for all separations. Approximately 0.1-μl samples were injected into a heated injection port. A column temperature of 40° was used throughout this investigation and was maintained by the heater assembly in the chromatograph. Helium was the carrier gas, and for convenience the flow rate was always adjusted to *ca.* 100 ml/min.

An injection signal was obtained by momentarily shorting the thermistor output. The signal was produced when the syringe plunger was depressed and in contact with the grounded injection block. In this way retention times could be measured to within 1%.

The partition ratio, the ratio of adjusted retention time to the time of elution for an air peak, was calculated. Partition ratios are independent of flow rate, column length, and sample size for ideal samples producing symmetrical peaks.

RESULTS AND DISCUSSION

Useful films have been deposited at 617°, and the furnace was initially set at that temperature. With the nitrogen flow rate at 246.0 ml/min, the reaction products were collected. After 5 h of collection about 1 ml was produced.

A chromatogram of the products is shown in Fig. 2. Peak 6, having the largest partition ratio ($k=165$), is unreacted tetraethoxysilane. It gives a symmetrical peak, and partition ratios are identical with the pure material.

Distillation of the sample yields a pure fraction (b.p. 79–80°), giving a positive iodoform test. Comparison of infrared spectra confirms the presence of ethanol. Comparison of partition ratios shows that peak 5 in Fig. 2 is ethanol.

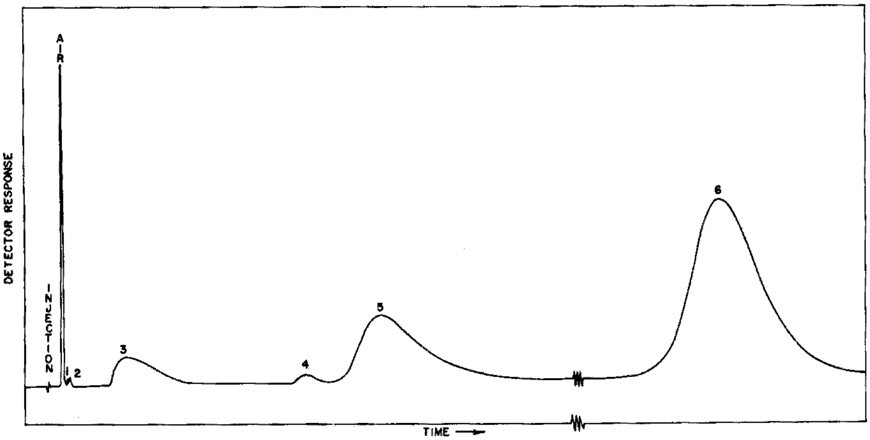

Fig. 2. Chromatogram of tetraethoxysilane decomposition products at 600°.

Peak 3 is unsymmetrical, indicating a slightly polar component. Because diethyl ether decomposes at 600° to generate acetaldehyde as well as other products$^{3-5}$, it was thought that tetraethoxysilane, being an ethyl ether, might also decompose to acetaldehyde. A solution of 2,4-dinitrophenylhydrazine may be added directly to the reaction mixture after removal of the highly volatile components, 1 and 2. The precipitate, recrystallized from ethanol, gives the yellow hydrazine of acetaldehyde melting at 156–157°.

The small, minor peak 4 can be determined entirely from gas chromatograms. In neutral or basic solution ethanol and acetaldehyde react to form acetal. Acetal was prepared in basic sodium hydroxide solution by the addition of excess of ethanol to acetaldehyde. The chromatogram obtained was identical to the combination of peaks 4 and 5 in Fig. 2. Addition of more ethanol enhanced the peak corresponding to peak 5, identifying that peak. The partition ratio ($k=15.9$) of peak 4 was identical with that of the acetal peak ($k=15.6$). Addition of hydrochloric acid cleaves the acetal causing the acetal peak to disappear and generating the acetaldehyde peak. Addition of hydrochloric acid to the reaction mixture caused peak 4 to disappear and enhanced peaks 3 and 5, showing peak 4 to be acetal.

An interesting sequence was observed during the acetal analysis. Acetal, being an ideal or symmetrical peak, remains at a fixed retention time for all sample sizes. The unsymmetrical ethanol peak, on the other hand, shows a decrease in retention time with increasing sample size. A ten-fold change in sample volume causes the ethanol peak (B) to pass through the acetal peak (A) inverting the elution order as shown in Fig. 3.

Tetraethoxysilane thermally decomposes at 600° into the same products as those found in the decomposition of diethyl ether by a static method$^{3-5}$. To establish (a) if diethyl ether is formed during the decomposition of the silane and (b) if it is

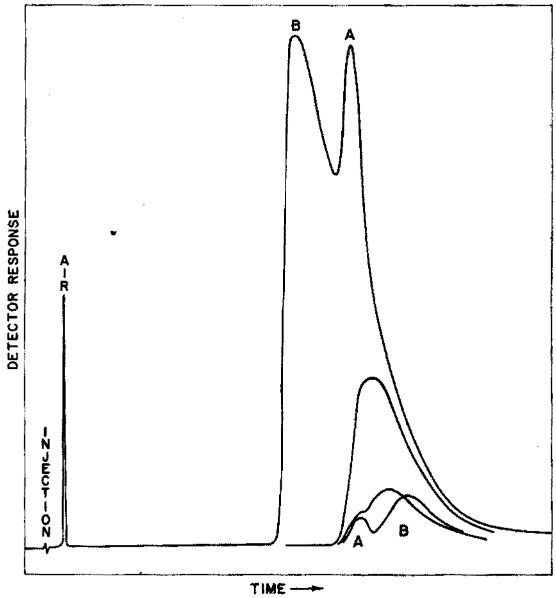

Fig. 3. Peak elution time inversion as a function of sample size.

significantly decomposed by the flowing process, furnace temperature and flow rate changes were made, and diethyl ether was introduced into the furnace at 600°. The tetraethoxysilane was replaced by diethyl ether in the bubbler and allowed to pass into the furnace for 15 min at a flow rate of 105.0 ml/min. The bubbler temperature was held at 28°. The ether decomposed as shown by the chromatogram given in Fig. 4.

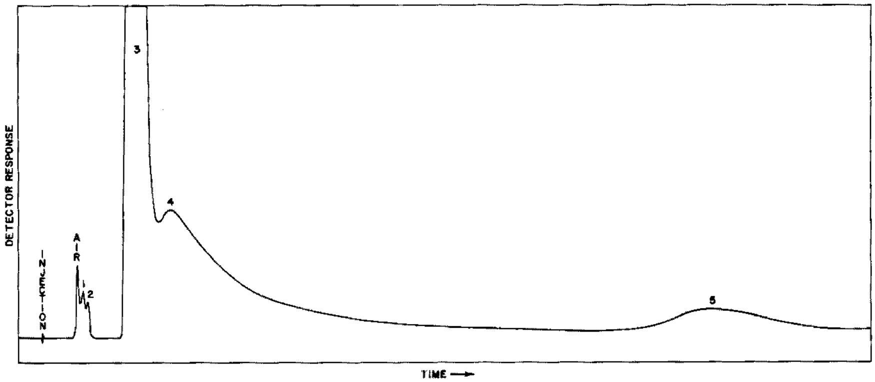

Fig. 4. Chromatogram of diethyl ether decomposition products at 600°.

Peak 3 is unreacted ether. Peak 4 is acetaldehyde and was determined by its 2,4-dinitrophenylhydrazine derivative. It is, then, reasonable to assume that peaks 1 (k=0.21), 2 (k=0.31), and 5 are ethane, ethylene, and ethanol, respectively[3-5]. The relatively small amount of ethanol with respect to acetaldehyde is also reported by DANBY AND FREEMAN[3]. Peaks 1 (k=0.34), and 2 (k=0.41), Fig. 2, are probably smaller quantities of ethane and ethylene.

If diethyl ether is present in the silane decomposition, a fast carrier flow rate and a reduction of the furnace temperature should produce a diethyl ether peak in the chromatogram; however, no ether peak is formed by either an increase in flow rate to 600.0 ml/min or a temperature reduction to 24°. It is interesting that decomposition occurs as low as 100°, although to a greatly reduced extent.

Possible mechanisms are given below:

(a)

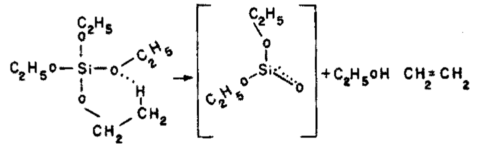

(b)

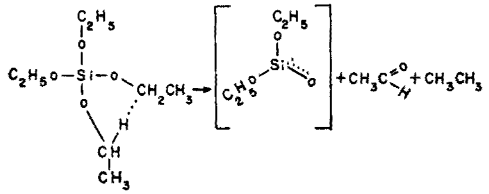

Further breakdown of the intermediate leads to silicon dioxide.

It should be noted that increasing the furnace temperature to 840° causes charring. No analysis was made at that temperature, because the dark deposits render this temperature impractical for depositing clear silicon dioxide films.

SUMMARY

The principle products of the thermal decomposition of tetraethoxysilane in a flowing system are acetaldehyde, ethanol, ethylene, and ethane. Acetal is found as a secondary reaction product formed by the addition of collected ethanol to acetaldehyde. Although the same products are produced by the thermal decomposition of diethyl ether at the same temperature, no ether has been found in the reaction products of the silane compound. The products are probably derived directly from the silane molecule.

RÉSUMÉ

Les produits de décomposition thermique du tétraéthoxysilane sont: acétaldéhyde, éthanol, éthylène et éthane. L'acétal est un produit de réaction secondaire formé par l'addition de l'éthanol à l'acétaldéhyde. Bien que les mêmes produits soient formés par la décomposition thermique du diéthyléther à la même température, on ne retrouve pas d'éther dans les produits de réaction du composé silane. Les produits sont probablement dérivés directement de la molécule silane.

ZUSAMMENFASSUNG

Die Grundprodukte der thermischen Zersetzung von Tetraäthoxysilan in einem fliessenden System sind Acetaldehyd, Äthanol, Äthylen und Äthan. Acetal wurde als sekundäres Reaktionsprodukt aus Äthanol und Acetaldehyd gebildet. Obwohl die gleichen Produkte bei der thermischen Zersetzung von Diäthyläther bei derselben Temperatur gebildet werden, wurde kein Äther als Reaktionsprodukt der Silanverbindung gefunden. Die Stoffe leiten sich wahrscheinlich direkt vom Silanmolekül ab.

REFERENCES

1 E. L. Jordan, *J. Electrochem. Soc.*, 108 (1961) 478.
2 J. Klerer, *J. Electrochem. Soc.*, 108 (1961) 1070; 112 (1965) 503.
3 C. J. Danby and G. R. Freeman, *Proc. Roy. Soc.*, A 245 (1958) 40.
4 G. R. Freeman, *Proc. Roy. Soc.*, A 245 (1958) 75.
5 K. J. Laidler and D. J. McKenney, *Proc. Roy. Soc.*, A 278 (1964) 505, 517.

Analytica Chimica Acta
Elsevier Publishing Company, Amsterdam
Printed in The Netherlands

MODIFIED WINKLER DETERMINATION OF OXYGEN IN DIMETHYLFORMAMIDE: OXYGEN SOLUBILITY AS A FUNCTION OF PARTIAL PRESSURE

HELEN J. JAMES AND R. F. BROMAN
Department of Chemistry, The University of Nebraska, Lincoln, Nebr. 68508 (U.S.A.)

(Received July 2nd, 1969)

Present studies of analytical applications for superoxide ion produced by the one-electron reduction of oxygen in aprotic solvents has made necessary the routine determination of the concentration of dissolved oxygen in such solvents. Modified Winkler and polarographic methods are available for oxygen determination in aqueous solutions, and modified Winkler methods have been reported for the determination of dissolved oxygen in dimethylsulfoxide[1] and formamide[2]. To establish the validity of a polarographic analysis in an aprotic solvent the concentration of dissolved oxygen as a linear function of the partial pressure of oxygen in the gaseous phase in equilibrium with the solution must be established[3]. To verify this statement of Henry's law, absolute values of the dissolved oxygen concentrations can be determined by modifications of the Winkler method reported here. These modifications allow smaller nonaqueous samples than previously reported methods[1,2].

The Winkler method for the determination of oxygen concentrations depends upon a quantitative oxidation of iodide to iodine[4]. An alkaline solution of potassium or sodium iodide is added to a known quantity of water followed by the addition of a manganese(II) salt solution which is used as a quantitative carrier of the oxygen. A precipitation of this carrier, an oxidized form of manganese, immediately occurs. After the precipitate settles, a strong acid is added which allows the precipitate to react to form iodine in an amount equal to twice the number of moles of dissolved oxygen. The iodine is titrated with a standard thiosulfate solution, or an excess of added thiosulfate is back-titrated with an iodate solution[5].

POTTER AND WHITE[6] modified the original Winkler method to include a correction for the amount of oxygen dissolved in the reagents and also for the amount of interfering substances present. By doubling the reagent size a determination of the amount of oxygen dissolved in the reagent is made. To determine if interferences are present, the order of the reagent additions is changed so that the solution is first made basic, then acidic, and finally the manganese(II) solution is added. A titration of liberated iodine indicates the amount of interferences under both basic and acidic conditions. BARGH[7] used a potentiometric end-point detection for the determination of microamounts of dissolved oxygen. RALLO AND RAMPAZZO[2] determined the concentration of dissolved oxygen in formamide by displacing a known amount of water with formamide and titrating the iodine liberated. The difference between the quantity of iodine titrated with and without formamide indicated the concentration of the oxygen in the formamide. POMEROY AND KIRSCHMAN[8] indicated that a greater concentration of iodine sharpened the end-point. These modifications of the original

Winkler method needed to be incorporated into a systematic analysis of dissolved oxygen in aqueous and nonaqeous solutions. The method described in this paper uses no specially prepared apparatus and can be performed on relatively small samples.

Numerous methods for determining oxygen concentrations in aqueous solutions rely upon a polarographic reduction of oxygen. HOARE[3] has reviewed several of the more recent polarographic techniques. In aqueous or protic solutions the reduction of oxygen is a two-electron transition to peroxide; however in aprotic solvents a superoxide intermediate is stable. In dimethylformamide (DMF) with tetrabutylammonium perchlorate (TBAP) as a supporting electrolyte, a one-electron transition to superoxide has been reported[9,10]. PEOVER AND WHITE[9] determined that the half-wave potential of the oxygen–superoxide couple was -0.97 V *vs.* a saturated calomel electrode (S.C.E.). Because the diffusion coefficient of oxygen in DMF has not previously been reported, a polarographic analysis for oxygen in this solvent necessitates an absolute means for determining oxygen concentrations, such as the Winkler method. Oxygen determinations which employ a polarographic reduction to superoxide should be less tedious than the Winkler method for routine analysis.

EXPERIMENTAL

Polarographic determination of oxygen

For the polarographic determination of the diffusion currents of oxygen in DMF, a 0.1 *F* tetraethylammonium perchlorate (TEAP) solution was added to a three-compartment electrochemical cell. Sintered-glass disks separated the three compartments which held a dropping mercury electrode, a S.C.E., and a platinum electrode as the working, reference, and auxiliary electrodes, respectively. The solution in the working electrode compartment was then saturated with a gas mixture from an H. Wosthoff o.H.G. Model G18/3F piston-driven gas-mixing pump (Calibrated Instruments, Inc., 17 West 60th St., New York 10023), which delivered a mixture of oxygen and nitrogen having ratios from 10:90 to 90:10. The stated relative accuracy of these mixtures is 0.05%. The DMF (Fisher Certified Reagent) was used as received, and the TEAP (tetraethylammonium perchlorate; Southwestern Analytical Chemicals) was dried over phosphorus pentoxide in a vacuum desiccator. Solutions were deoxygenated with nitrogen to obtain background current values and were saturated with oxygen to obtain maximum diffusion current values. (In the remainder of this discussion the oxygen:nitrogen ratios will be replaced by the mole fraction of oxygen in the gas mixture. Thus if the oxygen:nitrogen ratio is 30:70, the mole fraction of oxygen is 0.3.) To confirm the one-electron transition to superoxide under these conditions, analysis was carried out on a polarogram of a 0.1 *F* TEAP solution in DMF which has been saturated by a gas mixture containing 0.2 mole fraction of oxygen. A plot of log $((i_d - i)/i)$ *versus* potential gave a slope of 0.068 with an $E_{\frac{1}{2}}$ of -0.86 V *vs.* S.C.E. which verified the superoxide formation[10]. To ensure that a measured diffusion current was not on a polarographic maximum, all subsequent diffusion current measurements were made at -1.2 V *vs.* S.C.E.

Winkler determination of oxygen

Solutions. Aqueous 70% (w/v) potassium hydroxide, 15% (w/v) potassium iodide and 50% (w/v) manganese(II) sulfate monohydrate were prepared from reagent-grade chemicals. A standard 0.02 F solution of potassium iodate was prepared by weighing the dried reagent. An aliquot of this iodate standard was diluted daily to $8 \cdot 10^{-5}$ F. A stock 0.1 F thiosulfate solution was diluted to about 0.03 F and standardized against the diluted iodate solution each day.

Procedure. A small Erlenmeyer weighing bottle of about 16-ml capacity was filled to overflowing with water, and the ground-glass stopper was carefully placed on it so that no air was trapped. The exact amount of water contained was determined by weighing. With hypodermic syringes, 0.2 ml of the alkaline iodide solution and 0.1 ml of the manganese(II) solution were added. The stopper was replaced, the bottle shaken, the precipitate was allowed to settle, and then 0.2 ml of concentrated sulfuric acid was added with a pipette. By making all the additions to the bottom of the bottle, no reagent was lost when the stopper was replaced. The bottle was again shaken to dissolve the precipitate, and the contents of the bottle were washed into a beaker containing 1.0 ml of the diluted thiosulfate solution. A little solid potassium iodide was added to sharpen the end-point and the solution was titrated with the diluted iodate standard solution potentiometrically with a platinum electrode as the indicator electrode and a S.C.E. as the reference electrode. The reverse reagent procedure was used to determine the amount of interfering substances; however, only 0.25 ml of the thiosulfate solution was added to the beaker before titration.

For the Winkler determinations in DMF, solutions containing 0.1 F TEAP were bubbled with gas mixtures as described previously. Samples of the DMF solutions ranging from 2.0 to 0.5 ml, depending on oxygen partial pressures, were withdrawn with a syringe filled with a curved needle so as to allow introduction of the sample into the Erlenmeyer bottle which had been filled with water and inverted into a beaker of water. Since the density of DMF is less than that of water, the sample was carefully injected from the syringe into the bottle so that the DMF formed a separate layer displacing the water from the flask. The stopper was replaced, the bottle removed from the beaker and shaken to dissolve the DMF. The oxygen content of the solution was then determined as described above. The DMF samples were also analyzed for interfering substances by the reverse reagent method.

The values for dissolved oxygen concentrations in DMF were calculated from the following equation:

$$\text{millimoles of } O_2 = (V_t C_t - 6 V_i C_i)/4 = D$$

where V_t = volume of thiosulfate solution in ml, V_i = volume of iodate solution in ml, C_t = formality of thiosulfate solution, and C_i = formality of iodate solution.

Thus the concentration of oxygen in DMF, C, is given by

$$C = \frac{D-W}{V_d} + \frac{W}{V_w - V_r}$$

where W = millimoles of oxygen in water minus the millimoles of interferences in the water, D = millimoles of oxygen found minus the millimoles of interferences in DMF, V_w = volume of water in ml contained in the bottle, V_d = volume in ml of the DMF sample, and V_r = volume of the alkaline iodide and manganese(II) solutions (*i.e.*, 0.2 ml).

No attempt was made to control the total pressure and temperature of the samples.

RESULTS AND DISCUSSION

For the modified Winkler method the double reagent method indicated that relatively little, if any, oxygen is dissolved in the reagents and thus the sample size contained in the bottle needed to be reduced by the amount of reagent added. Also, analytical results on DMF samples containing 0.1 *F* tetrabutylammonium perchlorate were difficult to reproduce, and the reverse reagent method indicated a large degree of interference. This interference was not apparent for samples containing 0.1 *F* tetraethylammonium perchlorate, hence TEAP was used as the supporting electrolyte. A possible explanation for the interference due to TBAP is that this modified Winkler method is performed in an aqueous solution and TBAP is only slightly soluble in water. Since TEAP is quite soluble in water, it apparently does not interfere with the method. A plot of oxygen molarity in DMF determined by the Winkler method *vs.* the mole fraction of oxygen in the gaseous phase (Fig. 1) was found to be linear over the range 0.0–0.8 units of a mole fraction. Any determinations in which a mole fraction higher than 0.8 was used, gave erratic and irreproducible results which may indicate difficulty in introducing into the syringe a reproducible sample containing a large amount of dissolved gas. The linear correlation coefficient for the plot of oxygen concentration in DMF *vs.* the oxygen mole fraction in the gaseous phase is 0.997 indicating that Henry's law is obeyed over this range. The least squares fit of the straight line gives $C = 3.11$ (mole fraction) $+ 0.034$, where C is expressed in mM.

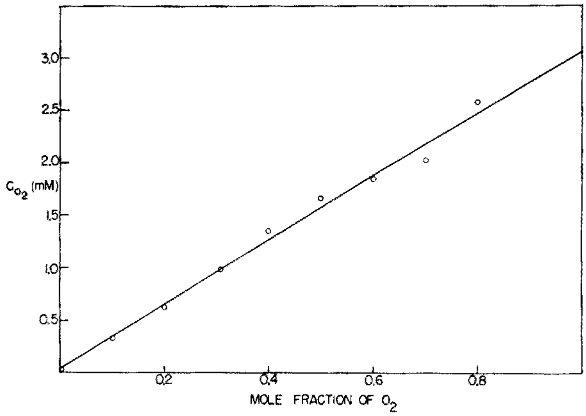

Fig. 1. Oxygen concentration in DMF containing 0.1 *F* TEAP as a function of the mole fraction of oxygen in the gaseous phase.

All Winkler determinations were repeated until there was a relative deviation of less than 1%. The fact that the intercept of the line is not zero can be attributed to small amounts of oxygen present in the nitrogen used and to fluctuations of the ambient temperature. However, the reproducibility of the results indicates that for ordinary temperature fluctuations this method can be used without temperature control.

To determine if there were a linear correlation between the diffusion current of oxygen in DMF and the mole fraction of oxygen in the gaseous phase, a plot relating these two factors was drawn for the typical set of data in Table I. The linear correlation coefficient for this line was found to be 0.989, indicating that Henry's law

TABLE I

DIFFUSION CURRENTS OF OXYGEN REDUCTION IN DMF CONTAINING 0.1 *F* TEAP AT −1.2 V *vs.* S.C.E.

Mole fraction of O_2	i_d *(μA)*[a]	*Concn. (mM)*[b]	*Mole fraction of* O_2	i_d *(μA)*[a]	*Concn. (mM)*[b]
0.1	4.7	0.339	0.6	24.1	1.89
0.2	8.3	0.650	0.7	28.1	2.21
0.3	12.0	0.961	0.8	32.0	2.52
0.4	15.0	1.27	0.9	35.5	2.83
0.5	18.6	1.58	1.0	41.2	3.14

[a] Diffusion current corrected for residual current.

[b] Concentration calculated from $C = 3.11$ (mole fraction) $+0.034$.

is obeyed for all partial pressures of oxygen and also that the diffusion currents can be used for the analytical determination of oxygen. The equation for this line is given by:

$$i_d = 40.2 \text{ (mole fraction)} - 0.167$$

The standard deviation of the slope is 2.1 and of the intercept is 1.3. Thus it seems practicable to relate the concentration of oxygen in DMF directly to the polarographic diffusion current over the entire range of mole fractions of oxygen from zero to one.

A plot of the experimentally determined diffusion currents *vs.* the calculated oxygen concentrations (Table I) can be used to determine the diffusion-current constant, *I* (Fig. 2). The linear correlation coefficient is 0.998 and the equation is

$$i_d = 12.9 \text{ (conc)} - 0.500$$

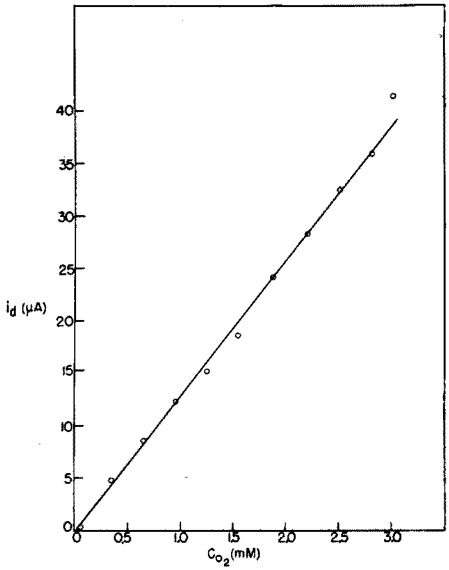

Fig. 2. Diffusion current of oxygen reduction in DMF containing 0.1 *F* TEAP measured at −1.2 V *vs.* S.C.E. as a function of the concentration of oxygen calculated from $C = 3.11$ (mole fraction) $+0.034$.

The standard deviation of the slope is 0.258 and of the intercept is 0.504. Thus although the intercept is negative, the deviation indicates that the theoretical intercept of zero is attained within experimental error. The diffusion-current constant is given by the equation, $I = i_d/(Cm^{2/3}t^{1/6})$. From the slope of the line in Fig. 2, and the capillary characteristics of 4.20-sec drop-time and 1.27-mg/sec delivery rate, the diffusion-current constant is calculated to be 8.54 μA mmole^{-1} l mg$^{-2/3}$ sec$^{-1/2}$. This value corresponds to a diffusion coefficient of oxygen in DMF of $1.4 \cdot 10^{-4}$ cm^2 sec^{-1}. (This value is obtained assuming a one-electron reduction of oxygen, which is apparently confirmed by a doubling of the current and anodic wave shift upon addition of excess of phenol to the solution[10]. The diffusion coefficient reported here is abnormally large, compared to a value of about $3 \cdot 10^{-5}$ cm^2 sec^{-1} in dimethylsulfoxide[1]. The high value may possibly be due to exaltation of the wave caused by impurities in solution[11].)

The work described indicates that one can determine oxygen concentrations in aprotic solvents in a manner similar to the polarographic determinations in aqueous solution; however, a one-electron transition to superoxide gives rise to the measured current rather than a two-electron change to peroxide. Thus, determinations in such solvents as pyridine, acetonitrile and dimethylsulfoxide could be performed routinely by measuring diffusion currents rather than by a lengthy Winkler method. However, it must first be established whether the current is linearly related to the mole fraction of oxygen in the gaseous phase through the entire range of mole fractions from zero to one. A nonlinearity could mean a deviation from Henry's law or a polarographic maximum at the potential used to measure the diffusion current.

This work was supported by funds from the Research Council of the University of Nebraska and from the National Science Foundation (traineeship for H.J.J.).

SUMMARY

Dissolved oxygen concentrations in dimethylformamide were determined by a modified Winkler method with small sample sizes and no special control of ambient temperature and pressure. The concentrations measured covered a range 0.008–2.59 mM with a relative deviation of less than 1%. Both the oxygen concentrations determined by this method and polarographic diffusion currents were linear functions of the mole fraction of oxygen; therefore a polarographic reduction of oxygen can be used for rapid determination of oxygen in this solvent.

RÉSUMÉ

On propose une méthode de Winkler modifiée pour le dosage de l'oxygène dissous dans la diméthylformamide. On peut utiliser de petits prélèvements d'échantillons; aucun contrôle spécial de température et de pression n'est nécessaire. La marge des concentrations mesurées est de 0.008 à 2.59 mM, avec une déviation relative de moins de 1%. La concentration en oxygène déterminée par cette méthode et les courants de diffusion polarographique sont des fonctions linéaires de la fraction molaire de l'oxygène; la réduction polarographique peut par conséquent être utilisée pour le dosage rapide de l'oxygène dans ce solvant.

ZUSAMMENFASSUNG

Die Konzentrationen von in Dimethylformamid gelöstem Sauerstoff wurden nach einer modifizierten Winklerschen Methode mit kleinen Proben und ohne besondere Kontrolle der Temperatur und des Druckes bestimmt. Die gemessenen Konzentrationen lagen in einem Bereich von 0.008–2.59 mM und konnten mit einer relativen Abweichung von weniger als 1% bestimmt werden. Sowohl die Sauerstoffkonzentrationen, die nach dieser Methode bestimmt wurden, als auch die polarographischen Diffusionsströme waren lineare Funktionen des Molenbruchs vom Sauerstoff. Deshalb kann die polarographische Reduktion des Sauerstoffs zur schnellen Bestimmung desselben in diesem Lösungsmittel verwendet werden.

REFERENCES

1 E. L. Johnson, K. H. Pool and R. E. Hamm, *Anal. Chem.*, 38 (1966) 183.
2 F. Rallo and L. Rampazzo, *J. Electroanal. Chem.*, 16 (1968) 61.
3 J. P. Hoare, *The Electrochemistry of Oxygen*, Interscience, New York, 1968, pp. 167–168.
4 L. W. Winkler, *Ber.*, 21 (1888) 2843.
5 N. H. Furman (Editor), *Standard Methods of Chemical Analysis*, 6th Edn., Vol. I, D. Van Nostrand, New York, 1962, p. 784.
6 E. C. Potter and J. F. White, *J. Appl. Chem.*, 7 (1957) 285, 459.
7 J. Bargh, *Chem. Ind. (London)*, (1959) 1307.
8 R. Pomeroy and H. D. Kirschman, *Ind. Eng. Chem., Anal. Ed.*, 17 (1945) 715.
9 M. E. Peover and E. S. White, *Chem. Commun.*, 10 (1965) 183.
10 D. L. Maricle and W. G. Hodgson, *Anal. Chem.*, 37 (1965) 1562.
11 J. P. Hoare, *The Electrochemistry of Oxygen*, Interscience, New York, 1968, p. 186.

Analytica Chimica Acta
Elsevier Publishing Company, Amsterdam
Printed in The Netherlands

SHORT COMMUNICATIONS

A rapid method for the analysis of total and organic carbon in shale with a high-frequency combustion furnace

In a geological survey, one analysis which is very important is that for organic carbon concentration present in the rocks studied. If the survey is to be extensive, analysis time becomes a factor. Thus, a method which gives fast and reliable results is useful when thousands of samples are to be studied. Such a method was developed and is described in this paper.

Several workers have reported methods for organic carbon in soil and ore samples[1–15]. The basic idea is always to eliminate inorganic carbon from the sample by acid treatment and to analyze the residue for organic carbon; the time-consuming step is the acid treatment of the sample. The work reported here describes an efficient method of acid treatment coupled with a rapid combustion technique which saves considerable time; 40–50 samples per day can be analyzed.

Experimental

Apparatus. The instrument used for burning the samples was a Leco (Laboratory Equipment Co.) Model No. 572-100 gasometric carbon analyzer.

Procedure. Samples are weighed into Leco combustion crucibles (No. 528-11). If the approximate carbon content is unknown, a sample size of 80–100 mg is taken. The samples are then wetted with 1:4 hydrochloric acid dropwise until all CO_2 evolution ceases; high carbonate samples may require several additions of acid. After acid treatment the crucibles containing the samples are dried at 100° for 30 min to remove excess acid. After removal from the oven, 2 scoops of iron powder (Leco No. 501-78) followed by one scoop of tin metal accelerator (Leco No. 501-76) are added to each crucible on top of the sample. The scoop used (Leco No. 503-32) holds about 1 g of iron powder. The samples are then burned as usual in the induction furnace of the Leco instrument. A "blank" crucible is carried through the same procedure as the samples. Naturally, if total carbon is sought, the acid treatment is omitted.

Calculations. The information required to calculate percent carbon in a sample is the atmospheric pressure, the temperature in the volumetric apparatus of the Leco carbon analyzer, the sample weight and the volumes of the CO_2 formed from burning the sample and the blank. The manufacturer's chart provides the appropriate factor for various temperatures and pressures. The volumetric apparatus contains two scales. The scale varying from 0.00–1.50 is used for the calculation.

$$\% \text{ Carbon} = \text{factor } [\text{vol. } CO_2 \text{ (sample)} - \text{vol. } CO_2 \text{ (blank)}]/(\text{sample weight in g}).$$

Results and discussion

The principle of the Leco apparatus is simple. The sample is burned in a stream of pure oxygen at about 1400°, and the carbon dioxide formed is measured, so that the amount of carbon present can be calculated. Probably the most critical point in the method is ensuring that the sample burns completely. The Leco instrument is used primarily for carbon in steel samples, which owing to their high conductance in the induction furnace, burn quite readily. This is not true for samples containing significant concentrations of non- or low-conducting substances, which therefore require the addition of some material of high conductance.

The first experiments were designed to determine the optimal type and amount of conducting material. With pure sodium carbonate and potassium hydrogen phthalate as sources of carbon, the results obtained with one scoop of iron and one scoop of tin added to the sample were within 0.06% of the theoretical values, whereas results obtained after addition of two scoops of tin were very low. However, occasionally a sample would not burn properly even under the former conditions, and it was decided to use two scoops of iron and one scoop of tin on top of the samples. With this combination, little or no evidence of incomplete burning has been found.

Several synthetic standards and some pure compounds were analyzed for total carbon (Table I). Standards 1–4 were prepared by weighing the ingredients into small bottles and then grinding the total contents in a Bleuler mill. The results for the pure compounds are more accurate than those for the mixtures. This could mean that the mixtures were not completely homogeneous even after grinding.

Table II contains data for percent organic carbon. Standards 5–12 were prepared

TABLE I

TOTAL CARBON DATA

Standard	*% Composition*			*% Carbon sought*	*% Carbon found*	*% Error*
	Na_2CO_3	*$KHC_8H_4O_4$*	*Al_2O_3*			
1	22.30	22.30	55.40	13.02	13.58	+ 4.3
2	13.09	17.48	69.43	9.71	9.61	− 1.0
3	5.04	4.96	90.00	2.91	2.74	− 5.8
4	65.34	34.66	0.0	23.71	23.20	− 2.2
$Na_2C_2O_4$				17.92	18.00	+ 0.4
$Na_3C_6H_5O_7 \cdot 2H_2O$				24.50	24.55	+ 0.2
$KHC_8H_4O_4$				47.05	46.89	− 0.3
C_6H_5COOH				66.84	66.53	− 0.5

TABLE II

ORGANIC CARBON DATA

Standard	*% Composition*			*% Carbon sought*	*% Carbon found*	*% Error*
	$Na_2C_2O_4$	*Na_2CO_3*	*$CaCO_3$*			
1[a]	—	—	—	10.49	10.38	− 1.0
2[a]	—	—	—	8.23	7.97	− 3.2
3[a]	—	—	—	2.34	2.33	− 0.4
4[a]	—	—	—	16.31	15.57	− 4.5
5	66.30	33.70	—	11.88	12.00	+ 1.0
6	47.57	52.43	—	8.52	8.49	− 0.4
7	63.90	36.10	—	11.45	11.22	− 2.0
8	36.98	63.02	—	6.63	6.65	+ 0.3
9	33.26	—	66.74	5.96	6.00	+ 0.7
10	51.62	—	48.38	9.25	9.13	− 1.3
11	67.58	—	32.42	12.11	11.93	− 1.5
12	89.29	—	10.71	16.00	15.41	− 3.7

[a] See Table I for composition of standards.

by weighing the relevant salts directly into the crucible and then acidifying to eliminate the carbonate; this avoids the possibility of sample inhomogeneity. The results generally tend to be low, possibly because CO_2 evolution carries small quantities of the organic carbon out of the crucibles. Since the data are generally quite good, no investigations were conducted concerning these errors.

A brief study of the effect of sample size was conducted (Table III). The data show that sample sizes up to 1 g can be successfully burned in the induction furnace. All the data are quite good except for a 0.48% result on sample No. 1892-74-1, which should probably have been rejected.

TABLE III

EFFECT OF SAMPLE SIZE

Range of sample weights (g)	*% Organic carbon*[a]	U_{50}	U_{99}
Sample no. 2549-61 (Shale)			
0.1003–0.1021	1.45 ± 0.03	1.45 ± 0.02	1.45 ± 0.24
0.2082–0.2168	1.41 ± 0.01	1.41 ± 0.005	1.41 ± 0.06
0.4011–0.4077	1.40 ± 0.003	1.40 ± 0.003	1.40 ± 0.04
0.6065–0.6134	1.41 ± 0.01	1.41 ± 0.006	1.41 ± 0.07
Sample no. 1892-74-1			
0.5265–0.5662	0.44 ± 0.03	0.44 ± 0.04	0.44 ± 0.49
1.0350–1.0865	0.41 ± 0.01	0.41 ± 0.01	0.41 ± 0.13

[a] Each result is the average of 3 determinations.

TABLE IV

ANALYSIS OF SHALES

Sample no.	*% Total C*		*% Org C*		*% Inorg C*		*Standard CO_2 anal*
	Leco	*F&M*	*Leco*	*F&M*	*Leco*	*F&M*	
73	3.10	3.12	0.61	0.87	2.49	2.25	2.24
74	2.46	2.43	0.21	0.57	2.25	1.86	2.26
78	1.45	1.44	0.06	0.12	1.39	1.32	1.41
80	3.43	3.43	0.30	0.16	3.13	3.27	3.26
82	3.76	3.98	0.16	0.26	3.60	3.72	3.78

Although the method was developed specifically for determining organic carbon, it can also be used to determine inorganic carbon. Table IV shows results obtained on five shale samples analyzed by the present method, a similar method with the F & M Scientific Corp. CHN analyzer, and the standard CO_2 method, *i.e.*, acid evolution and absorption in Ascarite. There would be no advantage in analyzing for inorganic carbon by the Leco or F & M methods because two analyses must be run to obtain the inorganic carbon result. However, the data show that the method is applicable if required.

The only acid tested other than hydrochloric acid was nitric acid; 1 : 4 nitric acid was used to eliminate inorganic carbon. The results obtained for standards similar in composition to standards 5–8 in Table II were similar to those obtained when hydrochloric acid was used; no advantage was found and hydrochloric acid was therefore preferred in order to avoid possible errors from oxidation of certain types of organic carbon by nitric acid.

The precision of the method was determined on a shale sample which was analyzed repeatedly over a period of several weeks by 3 different analysts. For 16 analyses, an average value of 17.68% carbon was found with an average deviation of ±0.24% ($U_{50}=17.68\pm0.04$; $U_{99}=17.68\pm0.18$).

Experiments were carried out to determine the effect of Dolomite ($CaCO_3$–$MgCO_3$) in samples. Bremner[8] reports that Dolomite is difficult to decompose by acid treatment; this was confirmed for the procedure outlined above. This disadvantage was overcome by immersing the sample in 1:4 hydrochloric acid in an aluminum container inserted in the combustion crucible; after immersion for *ca.* 30 min, all of the Dolomite decomposed. The excess of acid was then evaporated before combustion of the sample in the induction furnace as described above. Table V shows the results obtained for some standards containing Dolomite as the inorganic portion. The aluminum containers were made from ordinary aluminum foil in a simple mold. Acid stronger than 1:4 should be avoided to prevent destruction of the aluminum.

TABLE V

ANALYSES OF SAMPLES CONTAINING DOLOMITE

Standard	*Composition*		*% Org C sought*	*% Org C found*	*% Error*
	$Na_2C_2O_4$	*Dolomite*			
1	58.43	41.57	10.47	10.51	+ 0.4
2	51.56	48.44	9.24	9.21	− 0.3
3	0	100	0	− 0.08[a]	—

[a] The blank gave a slightly higher reading than this sample.

The method described is adequate for determining organic carbon. Good results can be expected provided that all inorganic carbon is removed in the acidulation procedure and that the sample burns completely. Samples containing Dolomite must be treated initially with acid in an aluminum cup inserted in the combustion crucible, in order to decompose the Dolomite.

Analytical Section,
Continental Oil Company,
P. O. Drawer 1267,
Ponca City, Okla. 74601 (U.S.A.)

Jerry W. Wimberley

1 *J. Assoc. Offic. Agr. Chemists,* I (1915) 411.
2 J. W. Reed, *J. Ind. Eng. Chem.,* 13 (1921) 305.
3 L. V. DeNardo, *Giorn. Chim. Ind. Applicata,* 10 (1928) 233.
4 L. E. Allison, *Soil Sci.,* 40 (1935) 311.
5 E. M. Crowther *et al., Trans. 3rd Intern. Congr. Soil Sci., Oxford,* 1 (1935) 114.
6 E. R. Pruvis and G. E. Higson, *Ind. Eng. Chem., Anal. Ed.,* 11 (1939) 19.
7 J. M. Alfareda and A. S. Ruiz, *Anales fis. y quim. (Madrid),* 41 (1945) 1332.
8 J. M. Bremner, *Analyst,* 74 (1949) 492.
9 B. A. Vavis and K. V. Bal'yan, *Zavodsk. Lab.,* 25 (1959) 418.

10 L. E. ALLISON, *Soil Sci. Soc. Am. Proc.*, 24 (1960) 36.
11 E. D. GIMPELEVICH AND E. Y. SIMONOVA, *Tr. Vses. Nauchm. Issled. Geologorazved. Inst.*, 11 (1958) 278.
12 I. C. FROST, *U.S. Geol. Surv., Profess. Paper No. 400-B*, p. 217.
13 N. P. DATTA, M. S. KHERA AND T. R. SAINI, *J. Indian Soc. Soil Sci.*, 10 (1962) 67.
14 J. L. ELLINGBOE AND L. E. WILSON, *Anal. Chem.*, 36 (1964) 434.
15 *Agronomy*, 9(2) (1968) 1367.

(Received August 8th, 1969)

Anal. Chim. Acta, 48 (1969) 419–423

The determination of free alcohols in alcohol ethoxylates by programmed-temperature gas chromatography

The literature contains few references to the analysis of alcohol ethoxylates[1–3], probably because of the complexity of these systems. When an alcohol or a mixture of alcohols is ethoxylated, not all of the alcohol reacts. One criterion for determining the extent of reaction is the concentration of free alcohols that remain after the ethoxylation reaction.

Free alcohols cannot be estimated directly by means of gas chromatography with a thermal conductivity detector, owing to the complexity of the products. Compounds of widely varying molecular weights also have widely varying thermal conductivities, and alcohols of relatively low molecular weight would give much more response in the thermal conductivity detector than the ethylene oxide adducts of these alcohols. Even the use of calibration factors is useless for a full range analysis, since a change in the ethoxylation level would cause a change in these factors. Even if the factors remained constant, pure ethoxylates would be required in order to determine these factors, and these are most difficult to prepare and purify.

A direct analysis would also be difficult with other types of detectors, because some of the products are so involatile that they are probably never eluted from the GC column. Therefore, the analysis must be done by use of internal standards regardless of the type of detector employed.

Experimental

The instrument used for this work was an F&M Model 500 programmed-temperature chromatograph. The samples were resolved on a column consisting of 3′ × 0.18″ i.d. aluminum tubing packed with 15% SE-31 (General Electric silicone rubber) on 70–80 mesh Anakrom A.B.S. (Analabs Inc.). The column was stabilized by heating to 325° for 4 h. The instrument conditions were as follows:

Injection port temperature — 300°
Block temperature — 325°
Initial column temperature — 100°
Program rate — 5.6°/min until the desired components have eluted, then manually turned to 325° to elute rapidly the higher-molecular-weight compounds
He carrier gas flow rate — 65 ml/min
Sample size — 3–5 μl
Bridge current — 175 mA
Recorder — Brown 1 mV
Chart speed — 1/2 in/min

Materials. 1. Pure samples of C_6–C_{18} even-carboned alcohols or samples for which the alcohol compositions are known.

2. Ethoxylates which are free from alcohols.

3. Some pure odd-carboned alcohols or paraffins for use as internal standards.

The internal standard used depends on the sample to be analyzed. It is desirable to use an internal standard whose thermal conductivity is not very different from the alcohols to be determined. The internal standards used in this work were Phillips pure nonane for ethoxylates prepared from C_6, C_8, and C_{10} alcohols and *n*-tridecanol for ethoxylates prepared from C_{12}, C_{14}, C_{16}, and C_{18} alcohols. The sample was prepared for analysis by simply weighing into a bottle and adding internal standard to give an appropriate concentration. A concentration of 10–15% of internal standard gave good results in this work.

The percent free alcohol is calculated from:

$$\%\ \text{alcohol} = \frac{(Gi)(K)(Aa)(100)}{(Gs)(Ai)}$$

where Gi = g of internal standard, Aa = area of alcohol peaks, Gs = g of sample, Ai = area of internal standard peak, and K = (response of internal standard per unit weight)/(response of alcohol per unit weight).

Results and discussion

Chromatograms of an ethoxylate prepared from a mixture of C_6, C_8, and C_{10} alcohols with *n*-nonane weighed into the sample as the internal standard, and of an ethoxylate prepared from a mixture of C_{12}, C_{14}, and C_{16} alcohols with nC_{13} alcohol as the internal standard were run. In both cases, K was approximately equal to 1. Many compounds would be suitable for use as an internal standard provided that K is known, and the compound elutes in an open spot on the chromatogram. Table I shows the accuracy found for these synthetic standards prepared from pure alcohols, pure internal standards, and alcohol-free ethoxylates. These data resulted from single runs of the standards, the average percentage error being 3.4%.

TABLE I

ACCURACY DATA

Sample no.	*Alcohol*	*Composition weight*	*Area % found*	*% Error*
A	C_6	2.40	2.48	3.3
	C_8	3.52	3.64	3.4
(nC_9 internal standard)	C_{10}	4.99	4.89	2.0
B	C_{12}	4.14	4.25	2.7
	C_{14}	4.61	4.57	1.1
	C_{16}	1.62	1.57	3.1
(nC_{13} alcohol internal standard)	C_{18}	0.72	0.67	6.9
C	C_{12}	3.62	3.69	1.9
	C_{14}	10.14	10.58	4.3
	C_{16}	3.55	3.52	0.8
(nC_{13} alcohol internal standard)	C_{18}	1.58	1.46	7.6

Standards A and B plus an actual reaction mixture were run 6 times each in order to determine the precision of the method. These data are shown in Table II.

From the accuracy and precision data, it can be seen that the value of K is not 1.0 for all of the alcohols analyzed. For example, with a value of 1.08 for K in the case of the C_{18} alcohol, the accuracy would increase significantly for that particular alcohol. However, in this work the interest was in the analysis for total unreacted alcohol rather than the analysis for individual alcohols. Therefore, if one determines the error for total alcohols in Table I the errors become 0.9, 0.3, and 1.9 percent for samples A, B, and C. The magnitude of these errors appears quite acceptable.

TABLE II

PRECISION DATA

Sample no.	*Alcohol*	*Average % found*	*Average % deviation*
A	C_6	2.48 ± 0.03	1.2
	C_8	3.65 ± 0.01	0.3
	C_{10}	4.93 ± 0.07	1.4
B	C_{12}	4.24 ± 0.06	1.4
	C_{14}	4.56 ± 0.06	1.3
	C_{16}	1.57 ± 0.02	1.3
	C_{18}	0.67 ± 0.02	3.0
Reaction sample	C_{10}	0.82 ± 0.01	1.2
	C_{12}	3.28 ± 0.04	1.2
	C_{14}	3.15 ± 0.04	1.3
	C_{16}	0.68 ± 0.02	2.9

Research and Development Department,
Continental Oil Company,
Ponca City, Okla. 74601 (U.S.A.)

JERRY W. WIMBERLEY

1 L. GILDENBERG AND J. R. TROWBRIDGE, *J. Am. Oil Chemists' Soc.*, 40 (Sept. 1963) 23.
2 R. CELADES AND C. PAQUOT, *Rev. Franc. Corps Gras*, 9 (1962) 145.
3 J. TORNQUIST, *Acta Chem. Scand.*, 20 (1966) 572.

(Received August 8th, 1969)

Anal. Chim. Acta, 48 (1969) 423–425

The spectrophotometric determination of cerium with methylene blue

GOTO AND KAKITA[1] have described a method for the determination of cerium(IV) referred to by BELCHER AND WILSON[2] as the extractive determination of cerium from methylene blue in weakly basic solution. This presupposes that a cerium(IV)–methylene blue complex, extractable into benzene, is formed. Upon investigation with a radioactive tracer, cerium-141, it was found that under no conditions of pH or concentration of reagents could cerium be extracted into benzene. In the presence of cerium(IV), however, the benzene layer assumes a red colour with maximum absorbance at 510 nm, the intensity of which is proportional to the cerium present as shown by GOTO AND KAKITA. Consequently, the mechanism of the reaction has been studied in an attempt to furnish an explanation and also to extend the scope to the determination of cerium(III), the form in which cerium usually occurs in samples.

Equipment

Spectra were obtained with a Unicam SP 800. Precise absorbance measurements at 510 nm, required for the calibration curve and for recoveries, were obtained with a Unicam SP 500 spectrophotometer.

Preparation of the calibration curve

To 25 ml of distilled water in a separating funnel add 2 ml of 2 N sulphuric acid, 1 ml of an aqueous 0.1% (w/v) methylene blue solution and x ml of $0.666 \cdot 10^{-3}$ M cerium(IV) sulphate (x to be in the range 0–10 ml; 1 ml contains 93.4 μg of cerium(IV)). Swirl to mix the contents and add 2 ml of buffer solution (10 g of ammonium chloride and 57 ml of 0.88 ammonia diluted to 100 ml with distilled water) followed by 10.0 ml of benzene. Shake for 1 min. After separation, transfer the benzene layer to a stoppered bottle containing 0.1 g of anhydrous sodium sulphate and shake to remove moisture. Determine the absorbance of the benzene solution at 510 nm in a 1-cm cell against a reagent blank. The calibration curve obtained is linear over the range 0–10 ml and has a slope of 0.00146 absorbance units per μg of cerium.

The determination of cerium(III)

Evaporate to dryness an aliquot of sample solution containing 0–1 mg of cerium. Dissolve the residue in 2 ml of 8 N nitric acid and add 50 mg of potassium bromate. Swirl to effect solution and transfer quantitatively to a 100-ml separating funnel containing 25 ml of distilled water. Add 1 ml of the above methylene blue solution, and proceed as for the preparation of the calibration curve.

Discussion

Microgram quantities of cerium may be determined by the method with an accuracy of $\pm 2.5\%$. Persulphate, permanganate and chromate give rise to interference by oxidation of the methylene blue. Iron(II) interferes because of its reducing action on cerium(IV). No interference was observed with a 100-fold excess of iron(III), but large amounts of iron precipitate on the addition of the alkaline buffer which hinders the subsequent separation step. Nitrates and bromates have no effect on methylene blue, hence bromate was chosen to oxidize cerium(III).

The reaction between cerium(IV) and methylene blue appears to be an oxidation of the latter under mildly acidic conditions. It is essential to add the methylene blue solution to an acidic cerium solution. When the alkaline buffer was added before the methylene blue, it was found that the absorbance at 510 nm was not related to the cerium content of the sample. A molar ratio plot between cerium(IV) and methylene blue was obtained by adding aliquots of cerium(IV) to a methylene blue solution and determining the absorbance at 340 nm, where the absorbances of methylene blue and cerium(III) are small but that of cerium(IV) is high. A molar ratio of 2:1 for cerium-

(IV) to methylene blue (tetramethylthionine chloride dihydrate) was obtained, which suggests that the material responsible for the absorbance peak at 510 nm in benzene is trimethylthionine quaternary base. Potentiometric studies in non-aqueous media have confirmed the fact that the oxidation product is a strong base.

The proposed reaction scheme outlined below is a modification of the oxidation scheme suggested by MACNEAL AND KILLIAN[3].

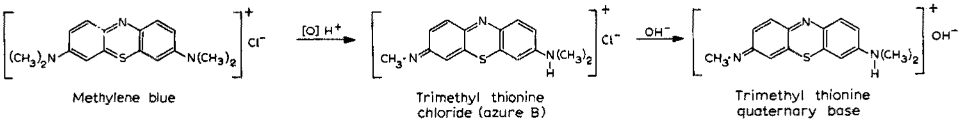

Mass spectrometry of the benzene extract has shown the presence of a parent ion of mass 270 consistent with the trimethyl thionine cation.

Department of Chemistry,
Sheffield Polytechnic,
Pond Street,
Sheffield S1-1WB (England)

F. VERNON

1 H. GOTO AND Y. KAKITA, *J. Chem. Soc. Japan*, 79 (1958) 1524.
2 R. BELCHER AND C. L. WILSON, *New Methods of Analytical Chemistry*, Chapman and Hall, London, 1964, p. 267.
3 W. J. MACNEAL AND J. A. KILLIAN, *J. Am. Chem. Soc.*, 48 (1926) 740.

(Received July 19th, 1969)

Rapid polarography of uranium in 1 *M* hydrofluoric acid with a vertical-orifice polytetrafluoroethylene dropping-mercury electrode*

Hydrofluoric acid is becoming increasingly important in the analytical chemistry of uranium-containing materials. It is a component of numerous media used for dissolutions, separations, and the study of corrosion. The uranium–hydrofluoric acid system is of particular importance in nuclear science and in reactor technology. The polarography of uranium in numerous supporting media has been studied extensively[1–7]. The catalytic effect on the polarographic reduction of nitrate in acid solution by uranium[1,8] has been investigated.

The development of the polytetrafluoroethylene (Teflon) D.M.E.[9] made possible polarography in hydrofluoric acid media. TAYLOR[10] has demonstrated that the Teflon D.M.E. can be made reproducibly; he used the electrode to study the polarographic behavior of a number of metal ions in aqueous hydrofluoric acid. With a Teflon D.M.E., HEADRIDGE *et al.*[11] investigated the polarographic behavior of some 28 elements in 0.1 *M* hydrofluoric acid–0.1 *M* ammonium fluoride. Later HEADRIDGE

---

* Research sponsored by the U. S. Atomic Energy Commission under contract with the Union Carbide Corporation.

AND HUBBARD[12] determined molybdenum in niobium-base alloys by polarographic reduction in 0.5 *M* hydrofluoric acid–0.5 *M* sulfuric acid.

A polarographic wave of good form for uranyl ion in aqueous hydrofluoric acid was observed earlier[9]. Uranium(VI) was among the cations studied by HEADRIDGE *et al.*[11]; they found that in 0.1 *M* hydrofluoric acid–0.1 *M* ammonium fluoride a broad curve ($E_{\frac{1}{4}}-E_{\frac{3}{4}}=270$ mV) occurs at $E_{\frac{1}{2}}=-0.51$ V *vs.* S.C.E. but give no other information about the polarographic behavior of uranium(VI) in aqueous hydrofluoric acid.

With the vertical-orifice D.M.E. of Teflon, the polarographic characteristics of uranium in 1 *M* hydrofluoric acid have now been studied in some detail.

Experimental

Polarograph. The ORNL Model Q-1988FES polarograph[13] was used in its three-electrode function. The fast-scan circuit permitted a maximum drop time (t) of 1 sec.

Electrodes and cell. The controlled electrode was a vertical-orifice Teflon D.M.E.[9]. The orifice diameter of the Teflon segment was 72 μ; that of the 98-mm-long glass segment was 70 μ. The characteristics of the D.M.E. in 1.22 m*M* uranyl nitrate–1 *M* hydrofluoric acid at a potential of −1.000 V *vs.* S.C.E. and $h=118$ cm were: $t=0.517$ sec; $m=3.983$ mg/sec; and $w=2.059$ mg.

The reference electrode was an S.C.E. at 25.0° ± 0.2°. The S.C.E. was bridged to the test solution through 0.1 *M* potassium chloride–1 m*M* hydrochloric acid. The counter electrode was a length of pyrolytic-graphite-coated spectrographic graphite (diameter ~1/16-in).

The polarographic cell and associated apparatus were made of HF-resistant materials.

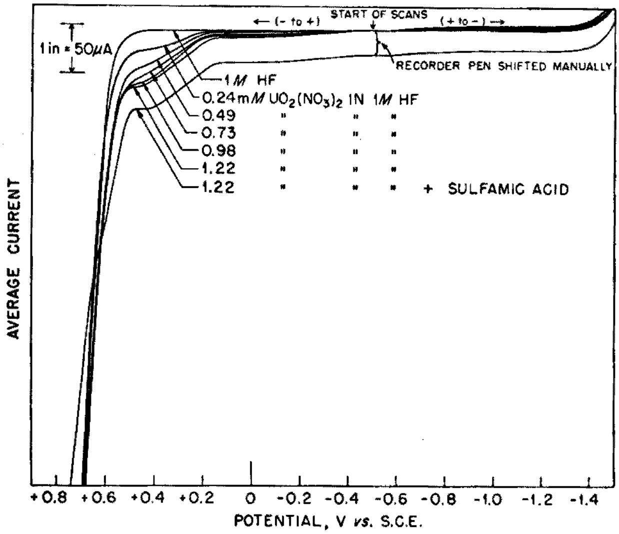

Fig. 1. Average-current regular polarograms that indicate two waves for uranium in 1 *M* hydrofluoric acid. Scan rate, 3 V/min.

Reagents. The stock solution of uranyl nitrate was 0.04 *M* in uranium and 0.06 *N* in nitric acid.

The 1 *M* hydrofluoric acid was prepared by diluting electrolytic grade 49% hydrofluoric acid (General Chemical Co.) with triple-distilled water.

Test solutions. Test solutions that were 0.24–1.22 m*M* in uranium were prepared by diluting aliquots of the stock solution of uranyl nitrate with 1 *M* hydrofluoric acid. All the test solutions were deaerated with purified nitrogen before they were analyzed.

Results and discussion

Search for polarographic waves of uranium. The search for polarographic waves of uranium was made by recording polarograms of the above-mentioned test solutions over the range of potential from +0.6 to −1.5 V *vs.* S.C.E. The polarograms (Fig. 1) indicate the existence of two waves, the wave at the more positive potential being very much larger than the other.

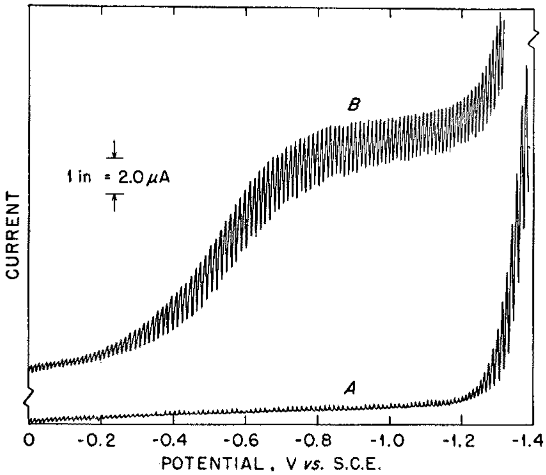

Fig. 2. Undamped regular polarogram of uranyl ion in 1 *M* hydrofluoric acid. Test solutions: (*A*) 1 *M* HF; (*B*) 1.22 m*M* $UO_2(NO_3)_2$–1 *M* HF. Scan rate, 1.5 V/min.

Wave at $E_{\frac{1}{2}} \cong -0.55$ *V vs. S.C.E.* The more negative polarographic wave was studied at sensitivities much greater than that used for the recording of the polarograms shown in Fig. 1. Figure 2 presents undamped regular polarograms of 1 *M* HF and 1.22 m*M* $UO_2(NO_3)_2-1$ *M* HF. Average-current regular and first-derivative polarograms were also recorded for the solutions. None of these three types of polarograms indicated the appearance of maxima, although no maximum suppressor was present in the solutions.

The $E_{\frac{1}{2}}$ value for the more negative wave was determined to be about −0.55 V *vs.* S.C.E. This value is an average value determined from average-current polarograms recorded by scanning the voltage in both the (+ to −) and (− to +) directions at three scan rates (0.3, 1.5, 3.0 V/min), and from measurements of the potentials at which the peak heights of first-derivative polarograms are maximal. Change in uranium concentration (*C*) in the range 0.24–1.22 m*M* did not cause the $E_{\frac{1}{2}}$ value to change. HEADRIDGE *et al.*[11] report the value −0.51 V *vs.* S.C.E. as the $E_{\frac{1}{2}}$ of uranium(VI) in 0.1 M HF–0.1 M NH_4F.

The recording of superimposed, replicate, average-current polarograms (both regular and first-derivative) showed that the reproducibility of this polarographic wave was excellent.

The relation of C to both $\bar{\imath}_d$ and $(d\bar{\imath}/dt)_{max}$ was perfectly linear over the range of C studied. In both cases the linear plot passed through the origin. This wave is therefore quantitatively as well as qualitatively useful. Asymmetry in the first-derivative peak of the wave suggests that the reduction is irreversible.

Wave at $E_{\frac{1}{2}} \cong +0.3$ *V vs. S.C.E.* The wave at $E_{\frac{1}{2}} \cong +0.3$ V *vs.* S.C.E. is of particular interest because of its magnitude and because a polarographic wave of positive $E_{\frac{1}{2}}$ does not seem to have been reported for uranium[6,7]. The wave height seems to be a function of the uranyl nitrate concentration of the test solution, although it appears that the C *vs.* $\bar{\imath}_d$ relation is not linear. Also, the wave apparently does not result from the dissolution of mercury, since it is not present on the polarogram for 1 M hydrofluoric acid. The addition to the test solution of sulfamic acid, which destroys nitrite by reducing it to nitrogen, did not affect the wave except to shift it to a slightly more negative position. It is known that the reduction of nitrate in acid solution is catalyzed by uranium[1,8]. It seems very likely that this more positive wave is catalytic. Further study will be required to determine its cause and the extent of its analytical usefulness.

This work was carried out under the supervision of P. F. THOMASON AND W. D. SHULTS, with whom many helpful discussions were held.

Analytical Methodology Group,
Analytical Chemistry Division,
Oak Ridge National Laboratory,
Oak Ridge, Tenn. 37830 (U.S.A.)

H. P. RAAEN

1 W. E. HARRIS AND I. M. KOLTHOFF, *J. Am. Chem. Soc.*, 69 (1947) 446.
2 H. I. SHALGOSKY, *Analyst*, 81 (1956) 512.
3 D. J. FISHER AND P. F. THOMASON, *Anal. Chem.*, 28 (1956) 1285.
4 C. AUERBACH AND G. KISSEL, *U. S. At. Energy Comm. Rept. BNL-800*, May 1963.
5 W. U. MALIK, H. O. GUPTA AND C. L. SHERMAN, *J. Electroanal. Chem.*, 14 (1967) 239.
6 L. MEITES, *Polarographic Techniques*, 2nd Edn., Interscience, New York, 1965, Apx. B.
7 J. HEYROVSKY AND J. KUTA, *Principles of Polarography*, Academic Press, New York, 1966, p. 546.
8 J. T. STOCK, *Amperometric Titrations*, Interscience, New York, 1965, p. 651.
9 H. P. RAAEN, *Anal. Chem.*, 34 (1962) 1714; 36 (1964) 2420; 37 (1965) 677, 1355; *Chem. Instrum.*, 1 (1969) 287.
10 M. S. TAYLOR, *Polarography in Acid Fluoride Solution*, Ph.D. Thesis, University of Sheffield, Sheffield, England (October 1963).
11 J. B. HEADRIDGE, A. G. HAMZA, D. P. HUBBARD AND M. S. TAYLOR, in G. J. HILLS, *Polarography 1964*, Vol. 1, Macmillan, London, 1966, pp. 625–633.
12 J. B. HEADRIDGE AND D. P. HUBBARD, *Analyst*, 90 (1965) 173.
13 D. J. FISHER, W. L. BELEW AND M. T. KELLEY, *Chem. Instrum.*, 1 (1968) 181.

(Received July 15th, 1969)

The spectrophotometric determination of copper in sea water with quinoline-2-aldehyde-2-quinolylhydrazone

Much of the early classical work on the determination of copper in sea water has been stated to be unreliable because of faulty analytical techniques and contamination[1]. A recent method[2] for the determination of copper in saline waters requires concentration from a relatively large volume before determination. Quinoline-2-aldehyde-2-quinolylhydrazone (QAQH) reacts with copper to give a red complex, readily extractable by benzene, with a molecular extinction coefficient of $5.8 \cdot 10^4$ $l mole^{-1} cm^{-1}$; since the few metal ions that react with QAQH can be masked, a highly selective determination of copper is possible[3]. QAQH permits the direct determination of copper in sea water; comparatively small volumes (200 ml) of sea water are required and the determination can be done in less than 1 h.

Apparatus, reagents and solutions

A Unicam SP 500 spectrophotometer and 10-cm cells were used for absorption measurements at 555 nm.

QAQH was prepared as previously described[3]. Reagent solutions (0.05%) were freshly prepared in water containing 1 ml of concentrated hydrochloric acid per 100 ml of solution.

The phosphate buffer was a 0.2 *F* disodium hydrogen phosphate solution.

Copper standards were obtained by dilution of 0.01 *F* stock solutions prepared from primary standard copper wire.

Artificial sea water (ASW) was prepared by the recipe of LYMAN AND FLEMING[4]; traces of copper were removed by reaction with QAQH and extraction. Atlantic sea water samples were provided by the Atlantic Oceanographic Laboratory, Bedford Institute, Dartmouth, N.S., Canada. One sample (SW I), collection station and depth unknown, had been millipore-filtered and treated with hydrochloric acid as a preservative. The second sample (SW II) was a homogeneous mixture of sea waters collected at depths of 100, 500, 1800, 2800, 3800 and 4800 m from one station at 37° 31′0″ N and 60°18′0″ W; this solution had been neither filtered nor treated with preservative.

Procedure

To 200 ml of aqueous solution containing copper, add 20 ml of 2.5% sodium fluoride, 4 ml of 0.05% QAQH solution and 20 ml of phosphate buffer (final pH should be between 6.9–7.4). Extract after 15–20 min with 20 ml of benzene. Extract again with 5 ml of benzene and collect the extracts in a 25-ml volumetric flask. Dilute to the mark with benzene and determine absorbance within 1 h against a blank carried through the same procedure. Measure at 555 nm in a 10-cm cell.

The procedure previously described[3] was found to be unsatisfactory when applied to the determination of less than 10 p.p.b. of copper; recovery of copper was incomplete and the results were not reproducible. However, the above procedure gave excellent results in the 0–10 p.p.b. concentration range; similar results were obtained for the same amount of copper extracted from 50 ml or 200 ml of solution.

Calibration curves and results

A typical calibration curve is a straight line through the origin, showing an absorbance of *ca.* 0.600 for 8 p.p.b. of copper. Identical straight-line calibration curves were obtained for copper extracted from 200 ml of distilled water or 200 ml of artificial sea water. For 2.0 p.p.b. of copper added to artificial sea water, the result obtained on the analysis of six samples was 2.0 ± 0.1 p.p.b.

TABLE I

ANALYSIS OF SEA WATER SAMPLES[a]

Sample	*Absorbance expected*	*Absorbance found*	*Amount of copper found (p.p.b.)*	*Amount of copper in sea water (p.p.b.)*
SW I + 1.8 p.p.b. of copper; SW I blank	0.132	0.133 ± 0.003	1.8	—
SW I + 3.3 p.p.b. of copper; SW I blank	0.246	0.238 ± 0.004	3.2	—
SW I + 1.8 p.p.b. of copper; distilled water blank	—	0.372 ± 0.005	5.0	3.2
SW I + 3.3 p.p.b. of copper; distilled water blank	—	0.469 ± 0.009	6.4	3.1
SW I; distilled water blank	—	0.230 ± 0.010	3.1	3.1
SW I; ASW blank	—	0.234 ± 0.010	3.2	3.2
SW II + 1.8 p.p.b. of copper; SW II blank	0.132	0.133 ± 0.002	1.8	—
SW II + 3.3 p.p.b. of copper; SW II blank	0.246	0.240 ± 0.010	3.2	—
SW II + 1.8 p.p.b. of copper; distilled water blank	—	0.315 ± 0.010	4.3	2.5
SW II + 3.3 p.p.b. of copper; distilled water blank	—	0.410 ± 0.010	5.6	2.3
SW II; distilled water blank	—	0.177 ± 0.003	2.4	2.4
SW II; ASW blank	—	0.180 ± 0.003	2.5	2.5

[a] Each result is the average of 3 determinations.

Table I shows the results obtained for copper added to sea waters and for the sea waters alone; results for spiked copper samples are essentially the same for measurements made against distilled water, artificial sea water or sea water blanks. The copper content for sea water I is 3.2 ± 0.1 p.p.b. (15 determinations) and for sea water II is 2.4±0.1 p.p.b. No difference was found for sea waters that had been treated with nitric and sulphuric acids to destroy organic matter.

This work was supported by grants from the Defence Research Board and National Research Council.

Department of Chemistry,
Dalhousie University,
Halifax, Nova Scotia (Canada)

J. ABRAHAM
M. WINPE
D. E. RYAN

1 J. P. RILEY, *Chemical Oceanography*, Vol. 2, Academic Press, New York, 1965, p. 292–424.
2 R. R. BROOKS, B. J. PRESLEY AND I. R. KAPLAN, *Anal. Chim. Acta*, 38 (1967) 321.
3 G. G. SIMS AND D. E. RYAN, *Anal. Chim. Acta*, 44 (1969) 139.
4 J. LYMAN AND R. H. FLEMING, *J. Marine Res.*, 3 (1940) 134.

(Received July 2nd, 1969)

A new reference electrode for electrochemistry in pyridine

Numerous reference electrodes are available for aqueous electrochemistry, whereas very few examples have been reported for use in individual nonaqueous systems[1]. In pyridine, the choice is restricted to the Ag|$AgNO_3$ (1.0 M) electrode (NAgE)[2,3], Zn(Hg)|$ZnCl_2$(s) electrode[4], or various types of aqueous reference electrodes combined with an aqueous–nonaqueous liquid junction. Use of the latter electrodes often contaminates anhydrous solutions with water.

The potential of a freshly prepared NAgE *vs.* an aqueous saturated calomel electrode (S.C.E.) has recently been shown[5] to be 70 ± 10 mV, which value is slightly smaller than the 90 mV previously reported[3]. Study of several NAgE electrodes showed that an aging process (probably loss of silver nitrate) causes the potential to decrease slowly, *e.g.*, after *ca.* 4 months the potential is −3 mV *vs.* S.C.E. Because of the scatter of the NAgE potential, a new reference electrode was sought.

In an investigation of the kinetics of the electrochemical reduction of copper(II) in pyridine, BOCHKOV AND GORBACHEV[6] suggested that the redox couple Cu(I)/Cu(II) in pyridine might serve as a reference electrode. Four reference electrodes involving this couple have been evaluated; the most stable and reproducible example is described.

Experimental

The reference electrode solution is a pyridine solution of 2.5 mM copper(I) chloride, 25 mM copper(II) chloride and 0.1 M tetraethylammonium chloride, prepared from anhydrous salts. This solution is separated from the working electrode compartment by a glass frit and a plug of 0.1 M tetraethylammonium perchlorate–pyridine–6% methyl cellulose gel. The electrode is a 2-cm^2 platinum sheet.

Equilibrium potentials of the electrode were measured by a Leeds & Northrup pH meter and polarograms were recorded with a Leeds & Northrup Type E Electro-Chemograph equipped with an operational amplifier-based IR-compensator[7].

Results and discussion

Potential measurements on the copper reference electrode *vs.* S.C.E. over a period of 5 days showed no drift and only small experimental scatter; the mean value and range were 3 ± 2 mV. After 5 days, a very slow drift to more negative potential occurred, probably owing to loss of copper salts through the plug and frit. The potential of this electrode should, however, be less dependent on loss of electrolyte than the NAgE because the potential is determined by the ratio of the redox constituents, which is likely to remain relatively constant during diffusive concentration depletion. Nevertheless, for accurate work, the solution in the reference electrode compartment should be replenished at least once a week.

Microscale polarization experiments showed that, after 30 sec of polarization at 20 μA cm^{-1}, the equilibrium potential is regained in 60 sec. Consequently, when the electrode is used in a three-electrode configuration[8] with IR compensation, no significant polarization will occur.

A polarogram of 1.2 mM sodium perchlorate in 0.1 M tetraethylammonium perchlorate had an $E_{\frac{1}{2}}$ value of -1.842 V with the potential scale referred to the Cu(I)/Cu(II) redox potential, compared with -1.889 V *vs.* NAgE, a shift of 47 mV. Computation of the potential shift from the values of the two reference electrode potentials *vs.* S.C.E. suggests that the difference should be 67 mV. However, this calculation ignores liquid junction potentials; for direct correlation of reference potentials, the salt-bridge connection should be made with the polarographic solution used in the half-wave potential measurements[9]. With this intermediate salt-bridge, the experimental potential difference is 47 mV, which agrees with the difference in $E_{\frac{1}{2}}$ value.

In conclusion, the pyridine Cu(I)/Cu(II) reference electrode is a stable, reproducible reference electrode with a potential (liquid junction potential included) close to that of the aqueous S.C.E.

The authors thank the National Science Foundation and Petroleum Research Fund of the American Chemical Society, which helped support the work described.

Department of Chemistry,
University of Michigan,
Ann Arbor, Mich. 48104 (U.S.A.)

JOHN BROADHEAD
PHILIP J. ELVING

1 D. J. G. IVES AND G. J. JANZ (Editors), *Reference Electrodes: Theory and Practice*, Academic Press, New York, 1961.
2 U. BERTOCCI, *Z. Elektrochem.*, 61 (1957) 431.
3 A. CISAK AND P. J. ELVING, *J. Electrochem. Soc.*, 110 (1963) 160.
4 L. M. MUKHERJEE AND J. J. KELLY, *J. Phys. Chem.*, 71 (1967) 2348.
5 J. BROADHEAD AND P. J. ELVING, *Anal. Chem.*, in press.
6 Y. G. BOCHKOV AND S. V. GORBACHEV, *Russian J. Phys. Chem.*, 40 (1966) 393.
7 R. ANNINO AND K. J. HAGLER, *Anal. Chem.*, 35 (1963) 1555.
8 J. E. HICKEY, M. S. SPRITZER AND P. J. ELVING, *Anal. Chim. Acta*, 35 (1966) 277.
9 K. TSUJI AND P. J. ELVING, *Anal. Chem.*, 41 (1969) 216.

(Received August 28th, 1969)

Errors in the use of volumetric flasks for extraction in atomic absorption spectroscopy

Extraction of metals as their complexes into organic solvents as a means of sensitivity enhancement has been widely adopted in atomic absorption spectroscopy. In many laboratories where routine trace element analyses are to be carried out, it has become a common practice, in order to facilitate extractions, to put the aqueous sample (100–150 ml) in a volumetric flask (200–250 ml) or in a Babcock bottle[1,2] with the organic solvent and chelating agent and to carry out the extraction in these containers. When the extraction is finished, distilled water is added to these vessels to bring the organic phase to the narrow necks thus enabling direct and convenient aspiration without using a separatory funnel to separate the organic phase.

However, if *ca.* 100 ml of distilled water passes through the organic layer which has already attained equilibrium with its underlying aqueous layer, then one or both of the following effects may be expected. (*1*) Some organic solvent can dissolve in the scouring water resulting in a concentration effect on the metal complex in the organic phase. (2) The metal complex can be back-extracted (or carried along with the organic solvent) into the aqueous phase resulting in a lowering of the concentration of complex in the organic layer.

Experiments were carried out to investigate the net effect on the concentration of the extract of several common trace elements with the ammonium pyrrolidine dithiocarbamate/methyl isobutyl ketone (APDC/MIBK) system.

Instrumentation

A Jarrell-Ash atomic absorption spectrophotometer model 82-528 was used for the investigation. The resonance sources were hollow cathode lamps (Westinghouse). Operating conditions were determined empirically for each element. Air–acetylene flames were used with a 10-cm laminar burner for most of the elements except for molybdenum. The instrument was operated in the concentration mode to present the absorption signals on a linear percentage scale proportional to concentrations.

Reagents

Pure analytical-grade reagents were used throughout the work. Methyl isobutyl ketone was distilled.

Procedure

The extraction of the following elements was investigated: Cr(VI), Pb, Co(II), Zn, Cu(II), Fe(III), Mo(VI), Mn(II), Cd(II), Ni, Bi(III) and Sb(III).

Two 100-ml aliquots of membrane-filtered lake water were spiked with 3 μg of a trace element, and the solutions were adjusted to a suitable pH with dilute hydrochloric acid or ammonia. One was placed in a 250-ml volumetric flask and the other was placed in a 150-ml separatory funnel. After addition of 7 ml of 1% APDC and 10 ml of MIBK, these two containers were shaken for 10 min in a mechanical shaker. Distilled water was added carefully along the wall of the volumetric flask without violent disturbance of the organic phase, to bring the organic layer to the neck of the flask for convenient atomic absorption aspiration. The organic layer in the separatory funnel was separated in a small container. The absorption of the metal in these two organic extracts was determined and compared.

The following were the extraction conditions for each element:

Pb, Co(II), Zn, Cu(II), Fe(III), Ni at pH 3–5[3].

Mn(II) at pH 6–9.

Mo(VI) at pH 2 extracted with 10 ml 1% oxine in MIBK[4], nitrous oxide–acetylene flame was used for atomic absorption. The spike was 4 μg.

Cd(II) at pH 6–7[5].

Sb(III) at pH 3.5[6]. The spike was 100 μg.

Bi(III) at pH 3.6. The spike was 100 μg.

Results and discussion

The results (Table I) showed that the practice of carrying out extraction in a volumetric flask and adding distilled water to raise the organic layer to the narrow neck caused serious errors for most of the complexes studied. For some complexes, such as Cr(VI), Zn, Cu(II), Fe(III) and Mn(II), loss in complex concentration occurred. It is likely that these complexes were back-extracted into the aqueous phase by the scouring water running through the organic layer. The most serious loss occurred for manganese(II) and zinc, amounting to 44% and 41% respectively. For other complexes such as Co(II), Mo(VI), Cd(II), Sb(III) and Bi(III), concentration effects resulted. It is evident that these complexes were not carried over to the aqueous phase while the organic solvent was dissolving in it. In the third class as demonstrated by lead and nickel complexes, no change in concentration was observed. For these complexes, apparently the solvent had carried an equivalent amount of the metal over to the aqueous layer.

TABLE I

COMPARISON OF ABSORPTION INTENSITY OF TWO EXTRACTION TECHNIQUES

Element	*Scale expansion*	*Absorbance intensity (%)*		*Effect on concentration*[c]
		Volumetric flask[a]	*Separatory funnel*[b]	
Cr(VI)	5×	38	48	−21
Pb	5×	24	25	n.c.
Co(II)	5×	48	45	+ 8
Zn	5×	19	32	−41
Cu(II)	5×	21	29	−28
Fe(III)	5×	23	28	−18
Mo(VI)	10×	26	23	+13
Mn(II)	5×	19	34	−44
Cd(II)	1×	29	26	+12
Sb(III)	1×	36	32	+13
Ni	5×	18	19	n.c.
Bi(III)	1×	42	34	+24

[a] Volumetric flask: extraction done in volumetric flask without separation, distilled water added to raise the organic phase to the neck.

[b] Separatory funnel: extraction carried out in a separatory funnel in the normal way; organic phase separated.

[c] The effect is estimated with reference to the separatory funnel method as the standard technique. (+) (−) indicate the apparent gain or loss (%) in concentration of complex in the organic extract by using the volumetric flask method. n.c. means no change.

These effects were reproducible, but their magnitudes were not. The scatters of error for duplicate analyses were from ±5% (for Co and Mo) to ±20% (for Zn and Mn) depending on the manner in which the distilled water was introduced into the volumetric flask. For the separatory funnel technique, the scatter of error was well within ±3% for most of the elements studied. It is readily conceivable that certain effects must occur when a fresh component phase is introduced to a system already in equilibrium.

Canada Centre for Inland Waters,
Burlington, Ontario
(Canada)

Y. K. CHAU
K. LUM-SHUE-CHAN

1 M. E. MORGAN, *Atomic Absorption Newsletter*, 3 (1964) 43.
2 T. JOYNER AND J. S. FINLEY, *Atomic Absorption Newsletter*, 5 (1966) 4.
3 R. R. BROOKS, B. J. PRESLEY AND I. R. KAPLAN, *Talanta*, 14 (1967) 809.

4 Y. K. CHAU AND K. LUM-SHUE-CHAN, *Anal. Chim. Acta*, 48 (1969) 205.
5 J. STARÝ, *The Solvent Extraction of Metal Chelates*, Pergamon, New York, 1964, pp. 160–166.
6 R. A. MOSTYN AND A. F. CUNNINGHAM, *Anal. Chem.*, 39 (1967) 433.

(Received July 28th, 1969)

Anal. Chim. Acta, 48 (1969) 434–437

Solvents for low-temperature phosphorimetry of nylon

Two rather extensive lists of solvent behavior at low temperatures[1,2] have proven extremely valuable to those engaged in phosphorimetry. However, for those interested in investigation of the phosphorescence of synthetic polymers, or impurities therein, this type of information has been very meager indeed. Although the present work was concerned primarily with nylon solvents, some of the solvents will obiously be applicable to other polymers.

Apparatus

The quartz phosphorescence tubes and the clear liquid nitrogen dewar were standard American Instrument Co. equipment.

Reagents

All solvents tested were reagent-grade chemicals, and were used without further purification. For a given application, such purification might well be necessary. The ethanol was 95% rather than "absolute".

Method

A small sample of each solvent was placed in each of three standard quartz phosphorescence tubes. Each of the tubes was plunged into a clear dewar containing liquid nitrogen, and subsequent behavior was observed. In all cases, the triplicate samples reacted identically.

Results

The ideal solvent, in this case, should dissolve nylon in reasonable quantities at room temperature, and form a clear glass upon rapid cooling to 77°K. Of all solvents listed in the references cited, only sulfuric acid and phosphoric acid appeared very promising, and these had been tested in the 193°–213°K range rather than at the more generally useful liquid nitrogen temperature of 77°K. These two were included in the present work along with several other powerful polymer solvents.

The results of the experiments are shown in Table I. It is evident from these data that the only solvents tested which are suitable for low-temperature phosphorimetry are phosphoric acid and formic acid–ethanol. All formic acid–ethanol mixtures listed are capable of room-temperature dissolution of reasonable amounts of nylon.

Frozen phosphoric acid solutions containing 10 g/l of nylon 66 exhibited slightly different phosphorescence behavior from frozen nylon fibers or films. Activation spectra in the two media were quite similar, but emission occurred at slightly shorter wavelengths in the glass, and the mean radiative lifetime was extended by about 30% over that for frozen fibers or films. It is not surprising that such effects were produced by the transition from a solid nylon environment to a highly acidic and relatively dilute frozen solution. Similar effects were observed for the formic acid–ethanol mixtures. This behavior causes no difficulty as long as its existence is borne in mind and no attempts are made to compare directly data measured from two different media.

TABLE I

SOLVENT BEHAVIOR AT 77°K

Solvent system	*Frozen state (77°K)*
Conc. sulfuric acid	Snow
Conc. phosphoric acid	Clear glass, slightly cracked
Hexafluoroisopropanol	Snow
Trifluoroacetic acid	Snow
Dichloroacetic acid	Snow
Formic acid, 98%	Snow
Formic acid: ethanol, 2:1 mixture	Clear glass, slightly cracked
Formic acid: ethanol, 3:1 mixture	Clear glass, slightly cracked
Formic acid: ethanol, 4:1 mixture	Clear glass, slightly cracked
Formic acid: ethanol, 5:1 mixture	Snow
Formic acid: ethanol, 6:1 mixture	Snow

Conclusions

This investigation has shown that concentrated phosphoric acid and several mixtures of formic acid and ethanol are satisfactory solvents for low-temperature phosphorimetry of nylon. Several other common polymer solvents have been found unsatisfactory.

Chemstrand Research Center,
P. O. Box 731,
Durham, N. C. 27702 (U.S.A)

L. D. JOHNSON

1 F. J. SMITH, J. K. SMITH AND S. P. MCGLYNN, *Rev. Sci. Instr.*, 33 (1962) 1370.
2 J. D. WINEFORDNER AND P. A. ST. JOHN, *Anal. Chem.*, 35 (1963) 2211.

(Received July 21st, 1969)

Selectivity in the synergetic extraction of cobalt(II) and nickel(II) with a mixture of 2-thenoyltrifluoroacetone and pyridine bases

Synergetic effects of neutral ligands (B) in the extraction of cobalt(II) and nickel(II) with 2-thenoyltrifluoroacetone (TTA) have already been investigated by several workers[1–3]. The authors have also suggested that the synergic extraction system is valid for the improvement of the spectrophotometric sensitivity in the determination of these ions with TTA[4–6]. However, as far as the selectivity is concerned, the TTA methods for cobalt(II)[4,5] and nickel(II)[6] are still inadequate.

Since the synergic effect is generally explained by the formation of an adduct $M(TTA)_2B_x$[1–3], the selectivity may be determined by the difference in stabilities of the resulting adducts. In the present communication the effects of pyridine bases on the selectivity in the cobalt(II) and nickel(II)–TTA extraction systems are described.

Reagents

TTA (Wako Pure Chemical Inc.) was used without purification. Pyridine and all other bases used were obtained from Tokyo Kasei Kogyo Co.

Benzene solution of the extractants. A 0.1 *M* pyridine base solution was prepared by dissolving a weighed amount of the reagent in benzene. Equal volumes of the base and 0.04 *M* TTA–benzene solution were mixed before the extraction experiments.

Cobalt(II) or nickel(II) solution. These solutions (1.00 g/l) were prepared by dissolving the nitrate or sulfate, respectively, in water.

Method

An aqueous solution (5 ml) containing 0.1 *M* sodium chloride and 1 mg of cobalt(II) or nickel(II) was transferred to a separatory funnel and 5 ml of benzene solution of the extractants was added. Then the mixture was shaken vigorously for 5 min and the phases were allowed to separate. The absorbance of the organic phase was measured at 430 nm against benzene with a Hitachi EPO type photoelectric photometer. The pH of the aqueous phase was measured with a Hitachi-Horiba F-5 type pH meter and a glass electrode.

Results and discussion

As can be seen in Fig. 1, the absorbance (A) increases with the increase in pH and finally reaches a constant value (A_c) at higher pH regions where each cation is extracted quantitatively into benzene[3,7]. Since there is a great difference in the A_c value between the two cations, the results are shown by using the ratio of A to A_c as a measure of extractability. In the case of pyridine, the extraction curve for nickel(II) agrees with that for cobalt(II) (Fig. 2 a). The curves for these metals with isoquinoline and 4-benzoylpyridine as additives show that cobalt(II) is more readily extracted than nickel(II) (Fig. 2 b and c). However, when picolines (Fig. 2 d–f), lutidines (Fig. 2 g, h), 3-aminopyridine, piperidine and aniline (Fig. 2 i–k) are employed, favorable extraction conditions for nickel(II) are attained.

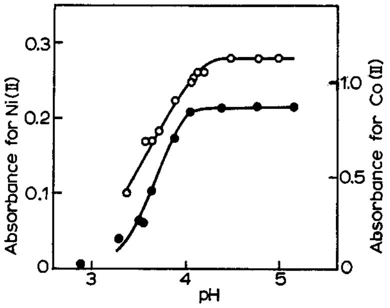

Fig. 1. Effect of pH on the extraction of Ni(II) and Co(II). (○) Ni(II), (●) Co(II); TTA = $2.0 \cdot 10^{-2}$ *M*, pyridine = $5.0 \cdot 10^{-2}$ *M*.

The above trend of the selectivity may be determined by the properties of the resulting adduct. From the results reported by IRVING[2] and the authors[3], synergic extraction with a mixture of TTA and pyridine bases is expected to proceed according to the equation:

$$M^{2+} + 2HT_{org} + xB_{org} = MT_2B_{x,org} + 2H^+,$$

where HT represents TTA and subscript org refers to the organic phase. A constant for the above reaction is defined by

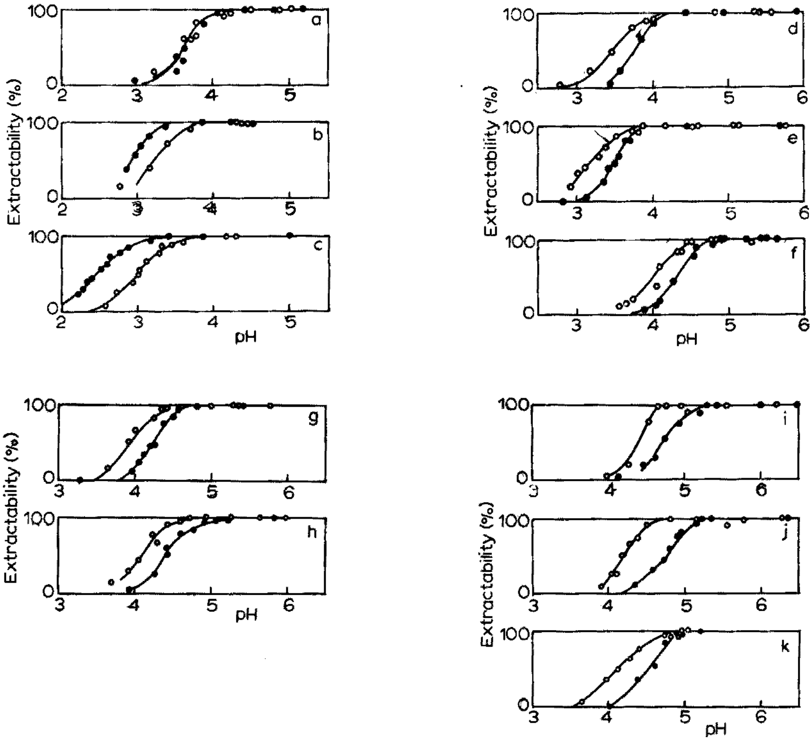

Fig. 2. Extraction curves for Ni(II) (○) and Co(II) (●) with (a) pyridine, (b) isoquinoline, (c) 4-benzoylpyridine, (d) γ-picoline, (e) β-picoline, (f) α-picoline, (g) 2,4-lutidine, (h) 2,6-lutidine, (i) piperidine, (j) 3-aminopyridine and (k) aniline as additive.

$$K_{e,x} = [MT_2B_x]_{org}[H^+]^2/[M^{2+}][HT]^2_{org}[B]^x_{org}.$$

With the formation constant

$$K_x = [MT_2B_x]_{org}/[MT_2]_{org}[B]^x_{org}$$

$K_{e,x} = K_{e,0}\,K_x$ can be derived. Since $K_{e,0}$ corresponds to an extraction constant in the absence of pyridine bases, the selectivity of the synergic extraction may be attributed to the degree of difference in K_x value for the resulting adduct.

Considering the mesomeric effect of substituted pyridines, a possible explanation for the above trend of selectivity is proposed. The electron-attracting benzoyl group decreases the charge density in the pyridine ring, therefore the π-acceptor capacity of 4-benzoylpyridine may be greater than that of pyridine. Similarly, isoquinoline is considered to exceed pyridine in π-acceptor capacity. By assuming that the degree of metal–ligand π-bonding decreases in the order Co(II) > Ni(II)[8], the above trend of selectivity is explained as follows. The synergic effect of a base acting as a π-acceptor may be helpful to the extraction of $Co(TTA)_2$ into the organic phase. In contrast, pyridine bases which contain electron-donating substituents such as methyl and amino groups should have less tendency to accept π-electrons than pyridine. Piperidine and aniline cannot accept π-electrons. The above considerations lead to the conclusion that nickel(II) is extracted preferentially to cobalt(II) by the synergic effect of a base which has a poor π-acceptor capacity.

The mesomeric effects of substituted pyridines on the apparent selectivities as observed above may assist in the analytical applications of synergic extractions, by a better choice of adduct-forming agent.

College of Technology,
Gunma University,
Kiriu, Gunma (Japan)

HIDEO AKAIWA
HIROSHI KAWAMOTO

1 H. M. N. H. IRVING AND D. N. EDGINGTON, *J. Inorg. & Nucl. Chem.*, 27 (1965) 1359.
2 H. M. N. H. IRVING, *Solvent Extraction Chemistry*, North-Holland Publishing Co., Amsterdam, 1967, p. 91.
3 H. KAWAMOTO AND H. AKAIWA, *J. Inorg. & Nucl. Chem.*, 31 (1969) 1141.
4 H. KAWAMOTO, *Japan Analyst*, 17 (1968) 1139.
5 H. KAWAMOTO AND H. AKAIWA, *Japan Analyst*, 18 (1969) 261.
6 H. AKAIWA, H. KAWAMOTO AND M. HARA, *Japan Analyst*, 17 (1968) 1139.
7 H. KAWAMOTO, *Radioisotopes*, 17 (1968) 388.
8 M. A. ROBINSON AND D. H. BUSCH, *Inorg. Chem.*, 2 (1963) 1171.

(Received July 22nd, 1969)

ERRATA

D. E. CAMPBELL, Determination of silicon in aluminum alloys by atomic absorption spectroscopy, *Anal. Chim. Acta*, 46 (1969) 31–36.

In the part describing the *Standard preparation* (p. 32) some clarification is required to accord with the subsequent discussion. Aluminum and sodium hydroxide should be added to the standard solutions in amounts corresponding to the amounts contained in sample aliquots.

For the determination of silicon in alloys, optimal results are obtained when the aliquots taken for analysis contain about 100 p.p.m. of silicon.

Anal. Chim. Acta, 48 (1969) 442

R. B. HESLOP AND A. C. RAMSEY, The Solvent Extraction of Vanadomolybdophosphoric acid as the Basis of a Substoichiometric Method for the Determination of Phosphorus, *Anal. Chim. Acta*, 47 (1969) 305–314.

On p. 312 of the above paper, the sentence starting on the 15th line from the foot of the page, should read:

Furthermore, the count-rates showed that phosphate had *not* been lost in the fuming-off.

Anal. Chim. Acta, 48 (1969) 442

Analytica Chimica Acta
Elsevier Publishing Company, Amsterdam
Printed in The Netherlands

BOOK REVIEWS

D. DYRSSEN, D. JAGNER AND F. WENGELIN, *Computer Calculation of Ionic Equilibria and Titration Procedures with specific Reference to Analytical Chemistry*, Almqvist and Wiksell, Stockholm, 1968, 250 pp., price 85 s.

For decades, students and practising chemists who wished to describe and understand even relatively simple chemical equilibria were forced to undertake almost interminable calculations. Moreover, they were often obliged to make assumptions and simplifications of unproven validity in order to obtain any results at all. The recent rapid proliferation of computers has swept away this drudgery and it is now possible to treat very complex equilibria, even those involving multiple phases, with relative ease, and without making unjustified assumptions.

The present text is an admirable presentation of just how powerful computer techniques can be in this respect. Using two, comprehensive, published programs and a number of smaller ones, the authors show how complex formation, solvent extraction, solubility phenomena, indicator equilibria (including those used in EDTA titrations) and potentiometric titrations can be completely evaluated with published physical constants and computer programs. It is stressed, however, that the physical constants used should be chosen carefully.

The book is written for chemists who already have a good grounding in writing computer programs in Algol. There is, however, an initial brief revision of the basic concepts used in the rest of the text. As well as including numerous examples, each chapter contains several problems to be solved by the reader.

J. P. DIXON, *Modern Methods in Organic Microanalysis*, Van Nostrand Series in Analytical Chemistry, D. Van Nostrand, London, 1968, xv+301 pp., price 70 s.

The stated purpose of this book is "to provide analytical chemists, their assistants, and their students with the basic principles of quantitative organic microanalysis". Against the background of a microchemical service laboratory, the author presents her practices and recommendations for those determinations commonly requested of the microanalyst.

The treatment is arranged in logical order. Chapter 1 deals with the operational practices of the laboratory, Chapter 2 with the design and equipment required in the laboratory, and Chapter 3 with sample handling procedures and weighing techniques. The succeeding chapters are concerned with the determination of carbon and hydrogen, nitrogen, oxygen, sulfur, the halogens, phosphorus, boron, the metals, functionality by non-aqueous titration, and miscellaneous functional groups. Separate chapters are devoted to the use of thin-layer chromatography, automatic analyzers, and a discussion of accuracy and errors.

While the number of determinative procedures presented is large, the quality of the treatment is very uneven. Only in a few cases is sufficient detail given so that a relatively untutored person could carry out the procedure. For example: in the chapter on carbon and hydrogen determination several methods are discussed, but only one method is presented in great detail, the Ingram flame ignition method. Even here the original reference should be consulted before any attempt is made to employ this excellent method. No method is included for the removal of fluorine if contained in the sample. The analysis of fluorine-containing materials is certainly a requirement, if not common practice, in the modern analytical laboratory.

In the chapter on the determination of the halogens, and after much discussion of methods, no actual procedure for the determination of fluorine is given or recommended.

The chapter on the determination of nitrogen contains three procedures that heretofore have not been fully appreciated: the use of the Ter Meulen determination, the determination of nitrogen in basic nitrogen compounds by non-aqueous titrimetry, and the use of the concentration procedure followed by Kjeldahlization for the determination of traces of nitrogen containing compounds in hydrocarbons.

The rather casual use of references makes it difficult to determine whether the author is reporting the results of her own work or discussing the findings of others. Some of the omissions are disconcerting. For example: in the section on the use of the oxygen flask combustion, only one citation is given to W. SCHÖNIGER and none to the comprehensive reviews on this method. In the chapter on the determination of carbon and hydrogen no credit is given for the early use of manganese dioxide for the removal of nitrogen oxides (BELCHER AND INGRAM) nor to the recent work (KAINZ) on the same material. The use of tungstic oxide as an additive in the combustion boat is given similar treatment. On page 157, in the chapter on the determination of phosphorus the statement is made that "both BELCHER AND MACDONALD (23) and KIRSTEN AND CARLSSON (24) have confirmed the author's confidence in this solution" (*no reference*). What discoveries one might make by using this style of phraseology.

The title of the book would imply a treatise on modern methods and equipment. In this aspect it is disappointing if not amazing. At no place in the book is mention made of the single-pan balance! Also, in the section on laboratory design the critical topic of environmental conditions is passed over with the advice that the balance room should be suitable for being air-conditioned, and that fans may be used to provide comfortable working conditions in the summer! No mention is made of the various ion-specific electrodes that have been available for a number of years. The section on instrumental equipment for the automation of analysis is of very little value, being merely a rehash of existing information without the benefit of critical evaluation or recommendation based on first-hand experience.

The book is illustrated with simple line drawings—in some cases too simple for use in duplicating the equipment being described. Also, the illustrations are not consistent. Either they do not agree with themselves or the details do not agree with the text. The most outstanding typographical (?) error is in the use, throughout the book, of adsorption for absorption.

This book certainly cannot be recommended as a guide to the novice, and I would be hard pressed to find adequate justification to recommend its purchase or perusal by the advanced worker.

L. A. HADDOCK, *Analysis in the Chemical Industry*, Pergamon Press, Oxford, 1968, xi+220 pp., price 35 s (Flexicover 25 s).

The undisputed significance of analytical sciences to chemical industry is highlighted in this publication which is part of a relatively new series of monographs on the U.K. Chemical Industry. These monographs are intended to provide teaching manuals for senior students, but *Analysis in the Chemical Industry* should also be read by anyone thinking of analytical chemistry as a career, and junior personnel with potential as the senior analysts of tomorrow. It is not intended that the series should be recognised as reference or text books; even so, this book could be read with profit by anyone wishing to make a broad assessment of the wide ramifications of the subject. The author has modestly left undisclosed his unquestionable qualification to present this highly condensed view of the profession.

The eight chapters appear under such headings as: Samples and Sampling, Laboratory Instruments, and Associated Techniques, Automatic and On-Line or Stream Analysis, and Works' Ancillary Problems. Each chapter is supported by adequate references that direct the reader to more detailed information. The book fulfils its main objective, and its price is reasonable.

Methods of Biochemical Analysis, Edited by DAVID GLICK, Vol. 16, Interscience Publishers–J. Wiley & Son, Inc., New York, 1968, viii+446 pp., price 155 s.

More than half of this latest volume in this most useful series is taken up by two long articles. The first of these, by J. K. WHITEHEAD AND H. G. DEAN, is concerned with the isotope derivative method in biochemical analysis. This review deals with general principles, factors affecting accuracy, methods, labelled materials and separation techniques and with applications of the method, chiefly to amino acids, proteins and peptides and to steroids. It is pointed out that the method could be more widely applied with advantage.

In the second long article, B. L. STREHLER considers the principles and practice of bioluminescence assay. Methodology is first dealt with, followed by a description of the properties of luminescent reactions and the application of bioluminescence to specific systems, *e.g.* assay of ATP and other substances with the firefly enzyme, and of nucleotide coenzymes with the bacterial luciferin–luciferase system.

There are five shorter chapters. M. K. SCHWARTZ AND O. BODANSKY contribute a review on the utilization of automation for studies of enzyme kinetics, a field of much topical interest. G. V. VAHOUNY AND C. R. TREADWELL deal with the enzymatic synthesis and hydrolysis of cholesterol esters. R. W. SCHAYER reviews methods for the determination of histidine decarboxylase activity. H. WEIL-MALHERBE considers the estimation of total (free+conjugated) catecholamines and some catecholamine metabolites in human urine. A. A. BOULTON describes the automated analysis of absorbent and fluorescent substances separated on paper strips.

E. V. EGOROV AND P. D. NOVIKOV, *Action of Ionizing Radiation on Ion-Exchange Materials*, Translated by J. SCHMORAK, Israel Program for Scientific Translations, Jerusalem, 1967, x+251 pp., price 140 s.

The degradation of ion-exchange resins under the action of ionizing radiation is important wherever they are used to separate highly-radioactive materials or in the active circuits of nuclear reactors. This book summarizes the diverse and scattered literature, much of it in Russian journals, up to 1965, and Western readers are fortunate in having the present translation.

Two introductory chapters on ion-exchange materials and on some aspects of radiation chemistry are followed by three chapters devoted to cation-exchange resins, anion-exchange resins and other miscellaneous exchangers. A final chapter considers possible reaction mechanisms. The book is well provided with tables and figures.

The first two chapters give sufficient detail about their respective subjects without burdening the reader with too many facts about either. The determination of resin properties and the problem of dosimetry are treated at length, and valuable information is given on the origins and properties of Russian and Eastern European resins. The next three chapters describe extensive experimental work on resins of all types under all conceivable conditions, with succinct summaries at the end of each section. The scientific merit of this work varies widely; critical comment is interspersed wherever possible, but frequently the wide range of possible variables does not permit it. The final chapter attempts to draw together the data to form a coherent picture, and some underlying principles are extracted, but—as the authors point out—much of this is speculation. There is clearly a need for a definitive study on a few important types of resin and on model compounds under carefully-chosen conditions. Only in this way will we disentagle the effects of matrix and of functional groups, of water content and degree of cross-linking, of cation (or anion) type, etc.

The book is rather long-winded in style, and much unnecessary repetition could have been eliminated in translation. At times the smallness of the print is tiring to the eye, and the Lilliputian type used for those sections in small print may have been responsible for some of the errors which have escaped proof-reading, such as the incorrect or incomplete formulae for the radicals on pp. 179, 189, 190, the disappearing positive charge in the first two reactions on p. 212, and the ion Tl^{4+} on p. 96. The careful reader whose eye is fresh will spot other examples of this kind. A more serious error, which must have been present in the original Russian version, is the suggestion on p. 74 that the reaction $RH+H^{\cdot}\rightarrow R^{\cdot}+H_2$ could be followed by the reverse reaction $R^{\cdot}+H_2\rightarrow RH+H^{\cdot}$.

These are small blemishes in an otherwise excellent account, in which the authors have made an honest attempt to draw together the threads without losing sight of the difficulties. It can be warmly recommended to all those interested in this topic.

G. H. SCHENK, *Organic Functional Group Analysis: Theory and Development*, Pergamon Press Ltd., Oxford, x+297 pp., price: Flexicover 30/–, Hard cover 40/–.

This is a book for students: it is one of the first in a new Series *Selected Readings in Analytical Chemistry* edited by Professor R. J. MAGEE, La Trobe University. One of the main objects of this Series is to delineate the way in which each particular branch of analytical chemistry began and then developed; in lectures to students nowadays there is an unfortunate but inevitable tendency for important, interesting background material to be progressively curtailed in order that the most recent developments can be discussed—often to little purpose since the essential foundations are inadequate. The novel feature of this Series is the inclusion of reproductions of carefully selected original papers which either describe the early classical methods, or show how these methods came to be extended or improved in terms of increased sensitivity, selectivity, or speed.

This text attempts to portray how some aspects of organic functional group analysis have progressed slowly but steadily through the efforts of many workers. To keep the book a reasonable size, SCHENK has elected to indicate the progress made in only seven different functional group analyses, the chapters involved extending to 96 pages. Reproductions of the more essential portions of 31 original papers, bridging the period from 1909 to 1966, occupy the remaining 196 pages.

The seven chapters deal with the carbonyl group, enolic-type compounds, the hydroxyl and amino groups, hydroxyl groups and alkoxysilanes, the epoxide group, 1,3-dienes, and, finally, electron-rich compounds.

Each chapter begins with a discussion of the early method of analysis and the theory, kinetics, and mechanism involved; the more modern methods are then described, and most of the chapters conclude by outlining a modern instrumental method of analysis.

At first sight it appears that a more classical and more conventional range of functional group analyses might have been selected to form the basis of an introductory student's text; when a selection has to be made, however, personal bias is usually involved and SCHENK admits to choosing those methods in which he is most interested. SCHENK also indicates that he intends this text to be "a valuable supplement" to FRITZ AND HAMMOND'S *Quantitative Organic Analysis* but the reviewer does not consider that a text such as this should have been written for such a purpose. Nevertheless SCHENK'S choice of topics is certainly justified for the way in which they enable the pattern of progress, from classical chemical to modern instrumental methods, to be displayed.

The success of this Series will depend, at least to some extent, on the way in which the reprints of the original literature can be integrated uniformly with the main text. The format used here is not entirely successful in this respect, but this book forms an interesting addition to the range of analytical literature that can be recommended to students.

ANALYTICA CHIMICA ACTA, VOL. 48 (1969)

AUTHOR INDEX

ANALYTICA CHIMICA ACTA, VOL. 48 (1969)

SUBJECT INDEX

CONTENTS

(continued on page 4 of cover)

(contents, continued from page 3 of cover)

Short Communications

PRINTED IN THE NETHERLANDS